The Moestroff Cave

A Study on the Geology and Climate of Luxembourg's Largest Maze Cave

Francis MASSEN, Editor

Contributing Authors:

Claude BOES
Camille EK
Sonja FABER
Antoine KIES
Francis MASSEN
Guy SCHINTGEN
Ed SINNER
Guy WARINGO

CENTRE DE RECHERCHE PUBLIC
CENTRE UNIVERSITAIRE

The Moestroff Cave

A Study on the Geology and Climate of Luxembourg's Largest Maze Cave

Francis Massen, Editor

CRP-CU

Centre de Recherche Public - Centre Universitaire

ISBN 2 - 919900-00-5

Centre de Recherche Public - Centre Universitaire Luxembourg, 1977

Production Editor: Francis Massen

Design and Layout: Colette Massen-Heirendt

Final Proof-Reading: Ed Sinner

Printed by rapidpress, 29-31 rue du puits, L-2355 Luxembourg

Disclaimer

The editor makes no warranty, expressed or implied, and assumes no legal liablity or responsability for the accuracy, correctness or usefulness of any information, apparatus, product or process disclosed. Reference herein to any specific commercial product, process or service by trade name, trademark, manufacturer or otherwise, does not necessarily constitute or imply its endorsement, recommendation or favoring by the editor. The view and opinions expressed by the authors do not necessarily state or reflect those of the editor.

Contents

Part 4: Appendices

Preface

Fernand Reinig

The project "Study of the physical parameters in the Moestroff cave" (PHYMOES) was launched in autumn 1990 as part of the CRP-CU's research unit "Metrology", after the Board of Directors of the Centre de Recherche Public - Centre Universitaire and the R&D department of the Ministry of Education had given their consent to financially support it.

The project's strong points that attracted the attention of the decision-makers were the multidisciplinary approach, the scientific co-operation envisaged with Belgian and German institutes, the subject of the study (the Moestroff cave is one of the longest caves in the Benelux countries) and ... the modest budget. With regard to this latter point, we would like to stress that the whole budget passed by the CRP-CU has been invested in the acquisition and maintenance of the scientific equipment needed to carry out the project since the intervening parties' contribution to the project was made on a voluntary basis. Thus, the actual costs of the project exceed by far the amounts granted by the public authorities.

At the time, nobody could know that the team under project leader Francis Massen would set about their task with so much enthusiasm that the initially set objectives were not only reached but surpassed. The publication of this 200-page final report constitutes one of the tangible proofs of the project's successful conclusion. There are a number of reasons for this success: the project leader's exemplary project management, a methodology adapted to a multidisciplinary and international team, a technically innovative approach in the field of "metrology" and scientific accuracy in the modelling of the observed phenomena.

The interesting and sometimes spectacular results were well received by the international scientific community. In this context, we could mention the organisation of the "International Meeting on Karstology" in Luxembourg, attended by scientists from the United States, Australia, Canada, Poland, the Czech Republic, Russia and the Ukraine, contributions to scientific colloquiums in Frabosa Soprana (Italy) and Besançon (France) and a number of international publications.

Moreover, the project was very successful with the media - a situation not very common for research work in Luxembourg. On several occasions, newspapers and magazines, the national television and radio station obviously took great delight in describing the adventures of the "caveman"

and his “activities uniting sport and science”. And how often do we see a minister of education, whose responsibilities also include scientific research, climb a steep ladder to check whether progress has been made concerning the setting up of scientific equipment in a cave as part of a research project. One event I particularly enjoy remembering is a tour in the cave organised on the occasion of the inauguration of the first “computer centre”, set up in the cavern with the help of a large French computer company.

The positive results obtained within the framework of the PHYMOES project allow us once more to tone down the assertions of a certain number of people who - sometimes peremptorily - maintain that it is very difficult, if not impossible, to obtain interesting results from research work done in Luxembourg in the field of science or applied sciences.

By way of conclusion, I would like to congratulate the project leader Francis Massen and his scientific and technical staff for their work in the interest of scientific research, as well as all other participants for their contributions, small or large, to the enormous success of this research project.

Fernand REINIG
managing director of the CRP-CU

Foreword

Camille Ek

Cave Climate is a difficult field of investigation, due to the obvious interference of the researcher with his object of study. This is particularly true for small caves, where the observer changes the atmosphere of the cave significantly.

Cave air is, however, of fundamental importance in biospeleology; besides, its composition and physical parameters reveal the ways and causes of its exchanges with external air through the underground passage-ways, the fissures, the pores of the rock, sometimes through seeping water.

The content of radio-active elements (radon a.o.) provides information about the exchanges between cave air and bedrock: this is an important sanitary topic, but it is also relevant to the forecasting of earthquakes and landslides. It was thus of paramount importance to include the variations of radon concentration in a climatological study of the Moestroff Cave.

The Phymoes Project represents a unique attempt by a group of re-searchers to develop a global and integrated study of cave climate. Air temperature, humidity, air flow dynamics, level of carbon dioxide, radon variations were all analyzed simultaneously, allowing the identification of correlations, but also the identification of causal relationships between the various parameters. The project deserved and included experts in physics, chemistry, geophysics, geology, but also in computing, mechanics and electronics. This enabled the team to launch a project that was not only scientifically sound, but also of a high technological standard.

The **Moestroff Cave** is the third longest cave in the Benelux countries (over 4 km in total length). It is as narrow as it is long: in most of the passages, it is difficult to pass each other and impossible to stand up. The exiguity of the passage-ways required thus a complete automation of the measurements. this could be achieved only thanks to the technological skill of some of the team members.

Thanks to the clear perception and kindness of Mr. Fernand Reinig, the generous support of the *Centre de Recherche Public - Centre Universitaire de Luxembourg* (CRP-CU) boosted the development of the project. After two years of hard work, the success was established with the *International Meeting on Karstology* in Luxembourg, where fourty specialists gathered to visit the cave and discuss the program and its first results. This meeting, mainly made up of members of the *Committee on Karts Physics and Chemistry* of the *International Union of Speleology*, led to a 195 page volume of *Proceedings*, edited by the *Service Géologique de Luxembourg*.

In 1994, the expertise of the team led to a request of the Flemish Water Company (VMW) for a quantitative study of a blowing cave in Tournai (Belgium). In 1995, the results of the project were presented in Fabrosa-

Soprana (Italy), and the project leader delivered a lecture in London on his data analysis methodology.

It can therefore be concluded that the Phymoes Project stands out as a major event in the current research on cave climatology.

Prof. Camille Ek

Département de Géographie Physique

Université de Liège, Belgium

Acknowledgments

The editor and the Phymoes members would like to express their gratitude for continuous support, help and sympathy to the following persons, organizations and companies:

- Centre de Recherche Public - Centre Universitaire de Luxembourg (CRP-CU) and its director Fernand Reinig
- Centre Universitaire de Luxembourg (CU) and its directeur Pierre Seck
- Ministère de l'Education Nationale (MEN), its minister Marc Fischbach and deputy director Georges Alff
- Recherche et Développement (R & D) du MEN and its directors Paul Lehnert and Pierre Decker
- Service Géologique du Luxembourg and its directors Jacques Bintz and Robert Maquil
- Division de la Radioprotection and its chief of department Michel Feider
- Lycée Classique de Diekirch (LCD) and its directors Roger Brachmond and Robert Bohnert
- BULL SA , Luxembourg
- PHOENIX Contact sàrl, Luxembourg
- Banque Générale du Luxembourg

Part 1

Introduction to the Moestroff Cave

Part 1: Introduction to the Moestroff Cave

1.1 STRUCTURAL GEOLOGY OF THE MOESTROFF CAVE

Sonja Faber, Camille Ek

1.1.1. Regional Geological Setting and Tectonical Structure

Luxembourg is characterized by two main regions which differ in its geological and morphological setting (fig.1.1.1):

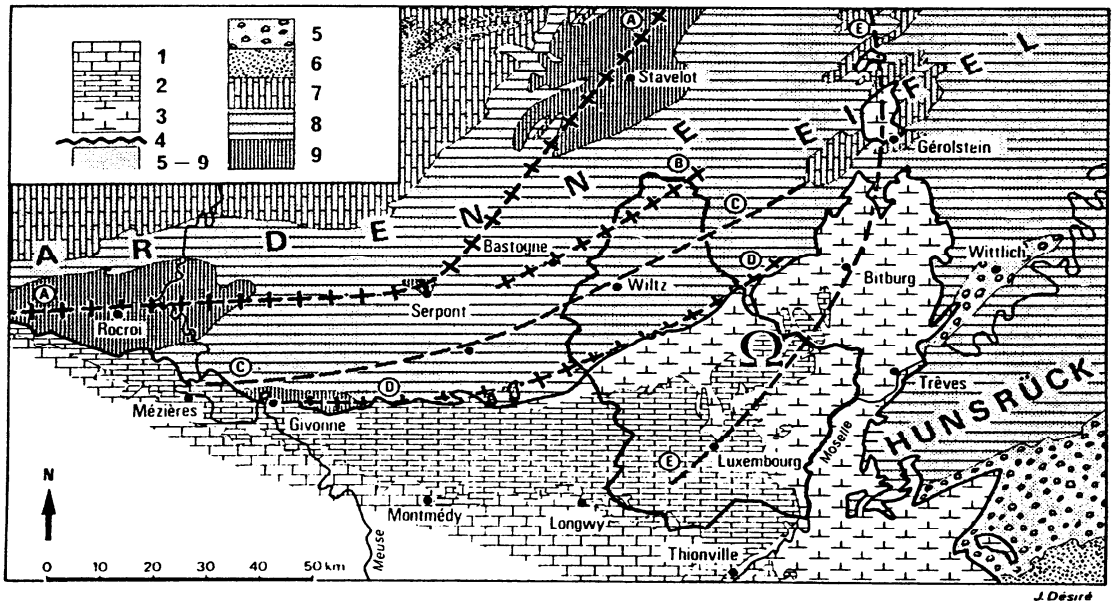

Fig.1.1.1. Regional geotectonic framework of Luxembourg [Maquil et al., 1994]
1,2=Jurassic formations; 3=Trias; 5-9=Paleozoic formations; 8=lower Devonian
D=anticlinorium of Givonne; E="Bay of Luxembourg" or Eifel trough. Ω = cave.

1. The northern region (so-called Oesling) represents the luxembourgean part of the Ardennes Mountains belonging tectonically to the Rhenish Shield complex. The outcropping basement consists mainly of Devonian rocks which have been strongly folded during the Hercynian orogeny followed by some low-rate uplift and a subsequent sedimentation period in Triassic times. In the younger geological history (Upper Tertiary and Quaternary) the Rhenish Massif has been subjected to some 300 m of plateau uplift, uplift movements are still going on at present times; erosion has removed the Triassic sedimentary cover, leaving exposed the folded Devonian basement (fig.1.1.2).
2. In the southern region (so-called Gutland) the Paleozoic rocks are entirely covered by Mesozoic sediments. With a thickness of approximately 800 m this sedimentary cover comprises essentially Triassic and Jurassic forma-

tions (fig.1.1.2). The Moestroff Cave is located at the northern rim of these Mesozoic sediments in a dolomitic layer of the Upper Muschelkalk inbetween the river Sauer to the south and the river Our to the northeast (see geological map of Luxembourg on the back cover).

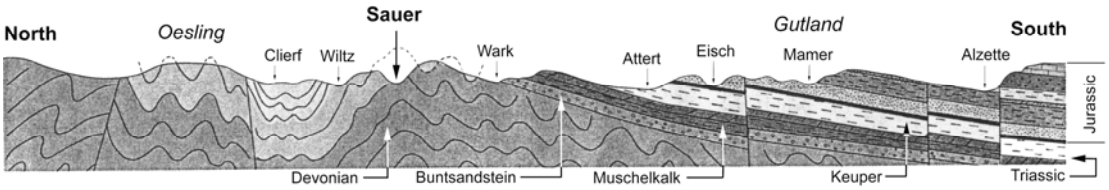

Fig. 1.1.2. Geological cross section through Luxembourg [Maquil et al., 1994]

Tectonic features within the western European area between the Alps and the North Sea are controlled by the following essential factors (fig.1.1.3):

- the present-day stress field, a uniform NW to NNW orientation of maximum compressive horizontal stress (S_{Hmax}) with a mean value of N145°E+/-26° [Liu, 1985; Müller et al., 1993]. The present-day stress field in Western Europe is largely controlled by plate driving forces acting on its boundaries, namely the ridge push from the Mid-Oceanic rift zone in the North-Atlantic towards the southeast, and the relative motion of Europe and Africa due to the collision between the Eurasian plate and the African plate in the Mediterranean region. A paleo-stress field with a S_{Hmax} orientation of NNE-SSW (N20°E) is supposed to have controlled tectonic movements in Late Eocene to Early Oligocene [Ahorner, 1975]
- the post-Hercynian block mosaic and the existence of deep reaching fault structures which form distinct zones of crustal weakness, one major fault system being the Rhine Rift System.

Dittrich [Dittrich, 1989] investigated the pattern of fracture zones and geological structures within the region of Trier/Luxembourg. The analysed data fit to 95% into three characteristic directions (fig.1.1.4):

1. Structures with a predominant **55°-70°** strike. The most prominent element of this type is the fracture zone which controls the slope of the Ardennes towards the Mesozoic layers in the south.
2. Structures with a **40°-55°** strike. Fracture zones with this direction represent the most dominent structural elements of the investigated area.
3. Structures with a **0°-20°** strike. The most important elements associated with these directions concentrate in the eastern part of the present region; their origin is supposed to be connected to that one of the NNE-SSW oriented Eifel trough (see fig.1.1.1). This direction is identical to the strike of the Upper Rhine Graben.

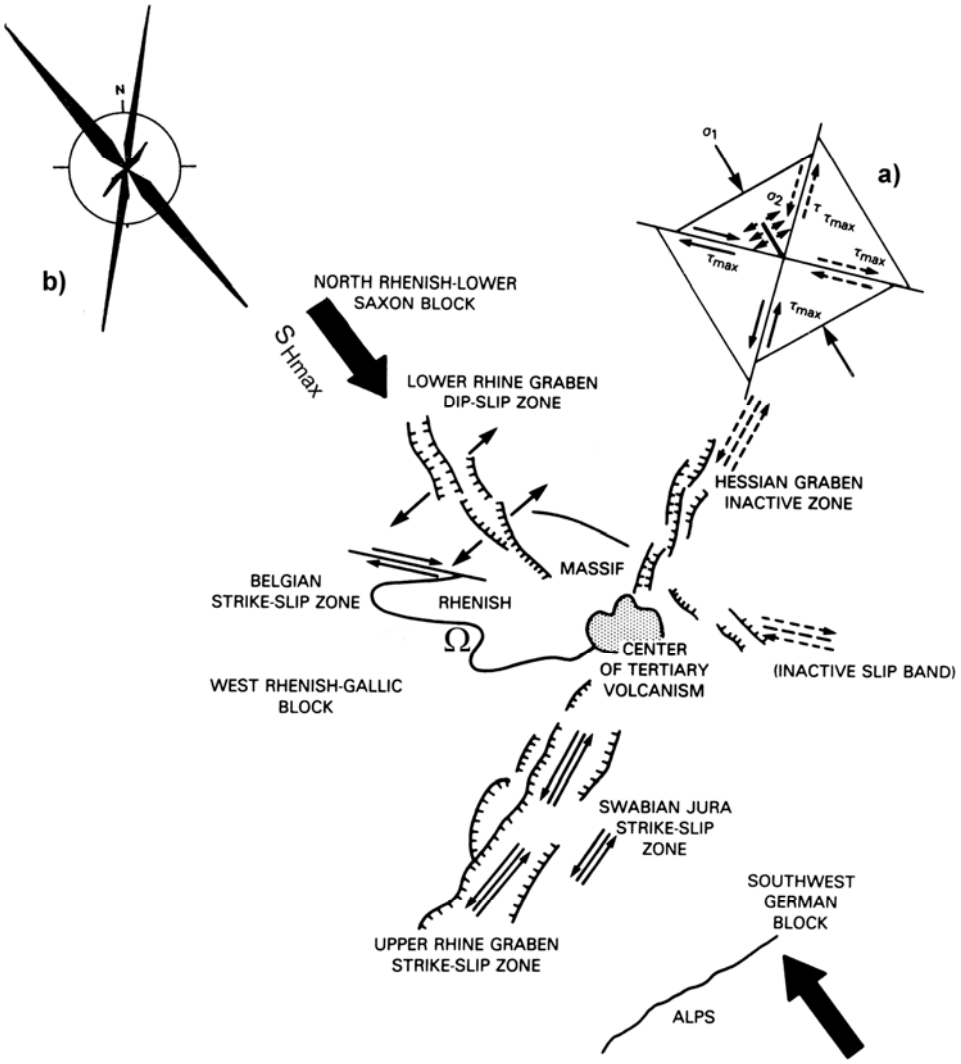

Fig.1.1.3. Seismotectonic scheme of the Rhine Graben rift system with calculated crustal stress components and block movements [Liu, 1985]. S_{Hmax}=maximum compressive horizontal stress: a) shear and tensional stress in a fractured crystal under compression b) orientation pattern of the cave galleries. Ω =location of the Moestroff cave

Comparable directions of strike have been presented by Berg [Berg, 1965] in a study on fractures and lineaments in the Paleozoic and Mesozoic elements of Luxembourg and of the Western Eifel. The two major strike directions in Mesozoic layers are found to be oriented NE and SE, while in

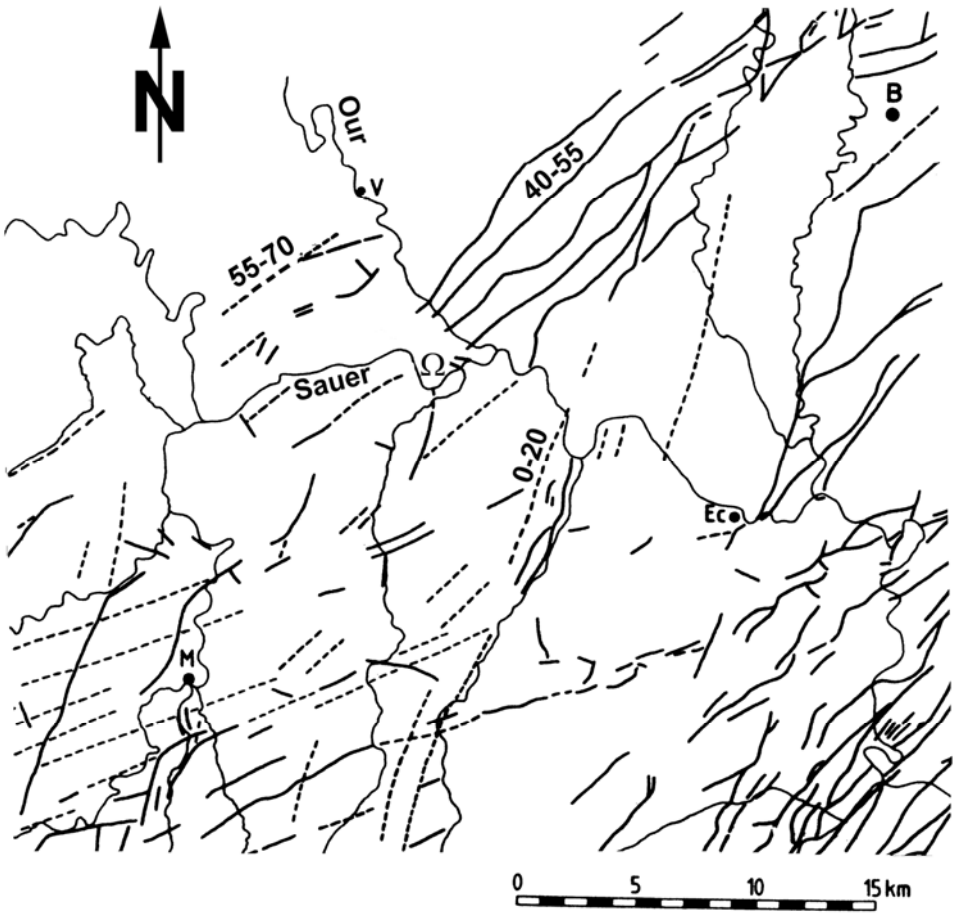

Fig.1.1.4. Directions of fracture zones and of tectonical structures [Dittrich, 1989]; B=Bitburg, Ec=Echternach, M=Mersch, V=Vianden, Ω = cave location

the vicinity of Moestroff and east of it the NNE direction is prevailing (fig.1.1.5a). Berg also points out a connection between this NNE orientation and the proximity of the Eifel trough striking in the same direction.

1.1.2. The Moestroff Cave - Actual Situation

The cave system of Moestroff represents a labyrinth of intersecting passages of rather uniform character (see fig. 1.1.5b). The orientation of this nearly horizontal maze pattern coincides closely with two of the directions of fractures and lineaments of the Mesozoic rocks in the region of Moestroff [Berg, 1965].

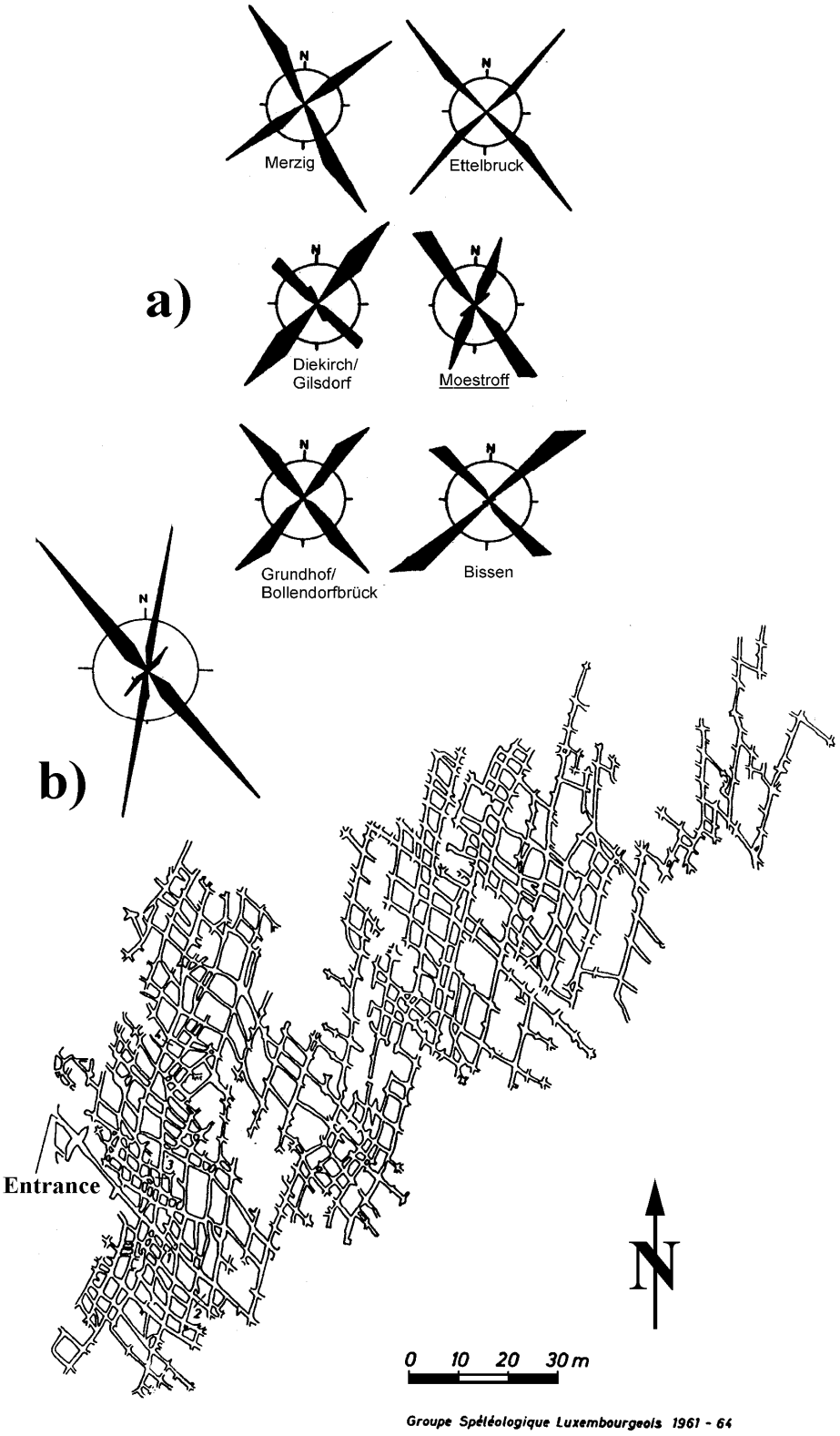

Fig.1.1.5. a) Orientation diagrams showing strike directions of facture zones in Triassic formations of Luxembourg [Berg, 1965]. b) Map of cave with orientation diagram of galleries.

The cave develops in the dolomitic layers of the Upper Muschelkalk. Figure 1.1.6 shows a schematic cross section through the geological sequences embedding the cave system. The main entrance to the cave is located at a height of 258 m above sea level in a cliff formed of dolomites, marly dolomites and marls. The vertical plane of the rock face with a nearly N-S extent of about 100 m has been exposed by a number of land slides, the most recent ones occuring in 1951 and 1965. In addition to the entrance to the accessible level of the cave system, two other levels of openings can be found in the rock face (fig.1.1.7). These openings of smaller dimensions, mostly filled with clay, are located several meters beneath the first one; their forms of contours are identical to those of the main cave level.

The level of the cave system coincides with a former terrace of the river Sauer [Neumann-Redlin, 1971], which actually flows approximately 100 m beneath. The direction of water flow within the Muschelkalk of this area has been investigated using Uranine as a tracer [Neumann-Redlin, 1971]. This experiment was carried out at a distance of nearly 1 km to the NE of

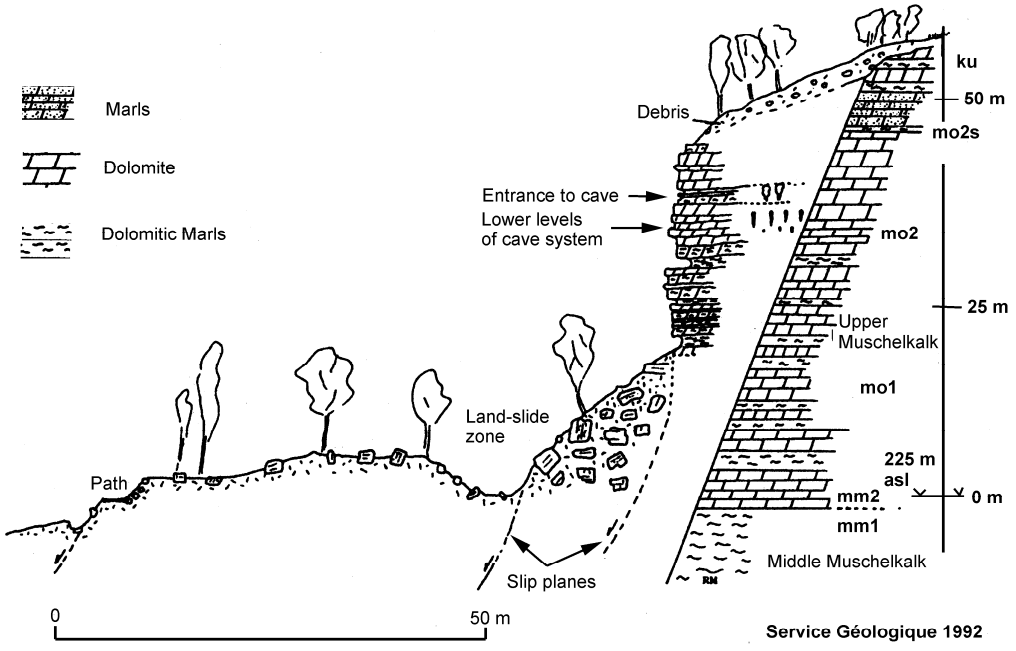

Fig.1.1.6. Schematic geological section of the hill side embedding the entrance to the Moestroff cave [Maquil et al, 1994]

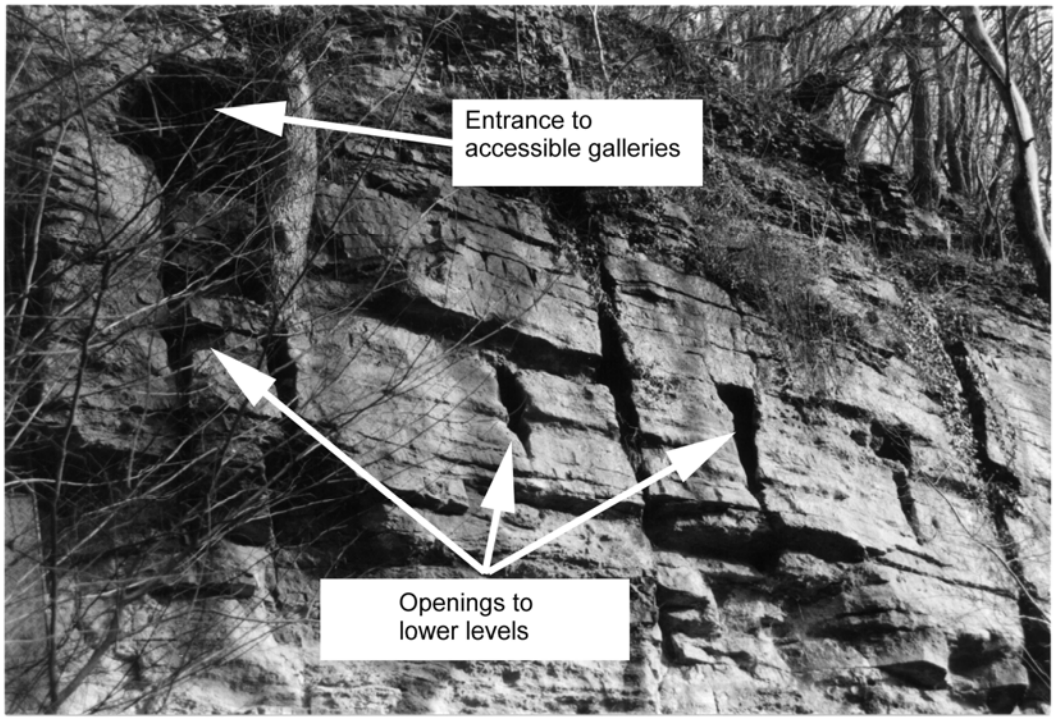

Fig.1.1.7. Rock face with entrance to the accessible galleries and with openings to the lower levels of the cave system

the location of the cave system (fig. 1.1.8). The resulting direction of flow is clearly orientated NW-SE and coincides with one major direction of the fracture zones in this region, and with one of the two main directions of the network pattern of the cave (fig. 1.1.5). At present times there exists no more water flow at the level of the cave, the active aquifer being located far below. Infiltration from above the cave system is very poor, mainly due to the existence of nearly impermeable layers of Keuper covering the Upper Muschelkalk.

The typical contour form of the corridors inside the cave can be seen in Figure 1.1.9. Their height rarely exceeds 1 meter. The bottom of the galleries is mostly covered with clay. Typical fissures at the ceiling can be observed throughout the cave, their downward continuation at the bottom of the galleries is exposed at places where the filling of clay is missing. These cracks seem to continue to one or several levels of corridors below the first one. As mentioned above, small openings to further presumed networks of the cave can be observed from outside in the rock face several meters beneath the entrance to the accessible cave system.

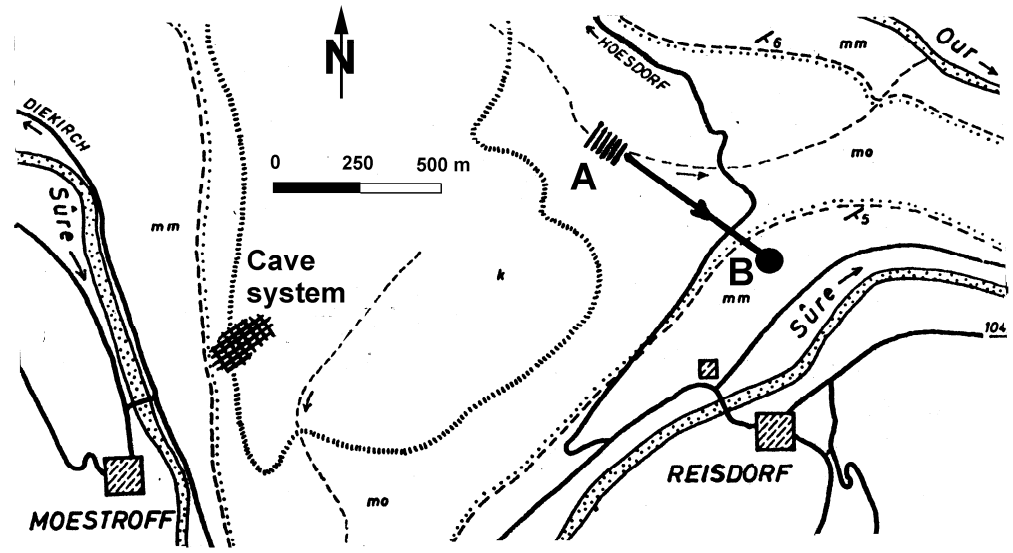

Fig.1.1.8. Location of the Moestroff cave system and of the tracer test area with indication of the drainage direction from the seepage zone A to the source B [Neumann-Redlin,1971].

1.1.3. Development of the Moestroff Cave

Subsequent to the sedimentation phase, the Mesozoic block was subjected to deformation processes. As already mentioned above, the pattern of tectonic block movements is controlled by the wide-spread regional stress field, in the earth's crust and by the pre-existing block mosaic within the Paleozoic basement. Under the influence of the large-scale tectonic stress field characteristic movements occur along the pre-existing fracture zones. The maze pattern of the Moestroff cave coincides perfectly with the directions of large-scale seismotectonic block movements (fig.1.1.3). This leads to the assumption that the formation of the initial fissure pattern predating the cave system was controlled by the same factors as the large-scale seismotectonic scheme of Central Europe.

The initial fissures were widened by the interaction of water being present for a certain time at the level of the cave system. The essential process creating the typical gallery form of the Moestroff cave is not yet defined. Seepage water from the surface may have widened the initial fissures somewhat, but certainly was passing too quickly through the cracks to create their present diameters exceeding occasionally 1 meter. As the level of the cave coincides with that one of a former terrace of the river Sauer, the assumption that the cave system was formed by an aquifer related to this level is obvious. It is not yet clear whether the water activity was limited to the chemical dissolution effect of stagnating water and/or

Fig.1.1.9. Typical form of galleries in the Moestroff cave

wether a mechanical action of circulating waters played a major role. The direction of a small-scale flow could have been orientated from NW to SE parallel to the present-day flow direction within the Muschelkalk (fig.1.1.8) and parallel to one direction of the cave network representing sort of a short-cut of the river Sauer through the plateau. A participation of the river Our in the assumed aquifer system can be imagened as well, leading to a possible flow direction from NNE to SSW. If the origin of the cave were to date back to the period of the former terraces of the Sauer and Our, its age would not exceed approximately 200 000 years.

1.1.4. Conclusions

The directional pattern of the Moestroff cave system as well as the fracture scheme of the Mesozoic formations in its vicinity fit well into the general seismotectonic scheme of Central Europe. This leads to the assumption that the development of the initial crack system was controlled by the same general stress regime as the large-scale tectonic units [fig.1.1.3.]. The initial fractures were enlarged by water infiltration and its chemical dissolution or/and its mechanical action. The most likely explanation for the existence of the cave system at the present level is that it was created by an aquifer related to the river Sauer; a former terrace of this river coincides with the level of the actual cave.

References

AHORNER, L. - Present-day stress field and seismotectonic block movements along major fault zones in Central Europe, Tectonophysics 29, 233-249, 1975.

BERG, D. - Die Klüfte im Paläozoikum und Mesozoikum von Luxemburg und der westlichen Eifel. Ihre Beziehungen zur allgemeinen Tektonik und ihr Einfluß auf das Gewässernetz, Service Géologique du Luxembourg publications, Vol. XVI, 1965.

DITTRICH, D. - Beckenanalyse der Oberen Trias der Trier-Luxemburger Bucht. Revision der stratigraphischen Gliederung und Rekonstruktion der Paläogeographie, Service Géologique du Luxembourg publications, Vol. XXVI, 1989.

LIU, H.S. - Satellite-determined stresses in the crust of Europe, in Seismic activity in Western Europe, P. Melchior (ed.), NATO ASI Series C, Vol. 144, 1985.

MAQUIL, R., EK, C. and FABER, A. - Le Muschelkalk Supérieur: Stratigraphie et Hydrogéologie de la région de Diekirch-Moestroff, in Comptes Rendus du Colloque International de Karstologie à Luxembourg, R. Maquil and F. Massen (eds.), Publications du Service Géologique du Luxembourg, Vol. XXVII, 29-43, 1994.

MÜLLER, B., ZOBACK, M.L., FUCHS, K., MASTIN, L., GREGERSEN, S., PAVONI, N., STEPHANSSON, O. and LJUNGGREN Ch. - Regional pattern of tectonic stress in Europe, SFB 108 Berichtsband 1990-1992, 725-767, Universität Karlsruhe, 1993.

NEUMANN-REDLIN, Ch. - Hydrogeologische und hydrochemische Untersuchungen im Oberen Muschelkalk und Keuper Luxemburgs, Service Géologique duLuxembourg publications, Vol. XXII, 1971.

1.2. Exploration and Mapping of the Moestroff Cave

Ed Sinner

1.2.1. Introduction

This article retraces the exploration and mapping of the Moestroff cave by the “Groupe Spéléologique Luxembourgeois “ (GSL), which translates into “Luxembourg Cave Exploration Group “. This group was created in 1959 by Roger Jacques under the auspices of the Luxembourg Youth Hostel Association, with the aim to provide sporty and scientific opportunities through cave exploration to young people.

Within two years, the group had grown from a handful of enthusiastic founding members [1] to a strong, highly motivated and well organized association, which undertook the systematic exploration of the Luxembourg underworld. Many important discoveries were made throughout the sixties in all major cave regions of the country. The comprehensive exploration of the Moestroff cave was one of the major achievements of this most interesting and prolific period in the group’s life.

Throughout the seventies and eighties, the emphasis drifted gradually away from Luxembourg caves towards large caves abroad, which offered naturally more sporty and demanding exploration opportunities. In 1989 however, some old-timers who had participated 25 years earlier in the exploration of the Moestroff cave, felt that their old love had not yet given away all its secrets, and decided to undertake a major research project about this most extensive and fascinating cave of Luxembourg. This was to become the PHYMOES project.

With hindsight, it can be stated that the “Groupe Spéléologique Luxembourgeois “ (GSL) was the first organization to introduce scientific cave exploration in Luxembourg. It has been one of the major contributors to underground discoveries in this country for nearly forty years. The exploration of the Moestroff cave and the PHYMOES project are among the most significant highlights of its activity, which will be described in this book.

Numbers in brackets refer to notes at the end.

1.2.2. The Early Days

Although the inhabitants of the village of Moestroff appear to have known for immemorial times the existence of a mysterious cave in the hills “op Kapendall” to the east of their village, it never had a name of its own, unlike most caves in other places. When talking about this cave, people referred only to its location, a place called “an der Lee”, meaning “in the Cave” in Luxembourgish language. Neither does the Moestroff cave appear in any of the old legends which abound for many other caves in Luxembourg, nor have the names of the first explorers or descriptions of early discoveries been recorded. Some old stories which survive are not supported by evidence: old villagers mentioned an unnamed professor of a nearby high school (Lycée Classique de Diekirch - LCD) who is said to have visited the cave with his students around World War I. There is also the saga of some english speleologists who explored the cave in very ancient times and are said to have emerged on the other side of the mountain in the Our valley near the village of Hoesdorf, after an underground journey of several days.

After World War II, the Moestroff cave received increasing attention by young people, who were attracted by its fascinating maze. Erny Schmit, Julot Faber, François Müller, Roger Jacques (the later founder of the GSL), Nelly Moia, Georges Als [28], Constant Useldinger and Pol Schneider are a few names of these pioneers. The latter is the author of the only published article about the Moestroff cave from these early days. [Schneider, 1957].

1.2.3. The First Encounter

The first encounter of the GSL with the Moestroff cave took place on 28 May 1961. It was a short visit [2], which immediately conveyed the impression that the exploration of this amazing labyrinth would be quite different from what the group had undertaken up to then, and that it would definitely be quite challenging and dangerous to explore.

As a result of this visit, it was decided to organize a five day summer camp in July 1961, with the aim to probe more deeply into the cave and to gain experience with the main obstacles of its exploration, such as:

- the difficult access to the entrance
- the extensive length and restricted dimensions of the corridors
- the high humidity and rather low temperature
- the orientation difficulties in the labyrinth
- the logistic support to the exploration team
- the safety and rescue possibilities.

This first exploration camp took place in Moestroff from 22nd to 26th July 1961, with 14 participants [3]. The equipment for the base camp and the exploration (approximately 300 kg) was brought by railway to the Moestroff station, and transported onwards by truck to the base camp installed in the forest, a few hundred meters from the cave entrance. Ten field telephones loaned by the Luxembourg Army proved to be most useful for communicating with the exploration teams, and the telephone wires provided an easy reference for orientation and mapping. Within three days, 465 meters of corridors had been mapped [4]. Stalactites [5], calcite crystals in half-domes [6] and several types of fossils were discovered [7].

With hindsight, it is interesting to note that temperature measurements were already included in this very first exploration programme of the Moestroff cave. These were performed with a mercury thermometer with a resolution of 0.5°C, recording temperature minima and maxima , and it was soon found out that the presence of an explorer taking the readings disturbed the temperature indications significantly. This difficulty would be overcome only thirty years later through the use of electronic sensors and automatic dataloggers within the PHYMOES project.

Several important conclusions were drawn from this first encounter of the GSL with the Moestroff cave ([Sinner, 1961]:

- The sheer size of the labyrinth would require significant exploration and surveying efforts
- Logistic support would be of critical importance for success
- Reliable communications with the exploration teams were an essential prerequisite to safety
- Some kind of a coordinate system would be required to facilitate orientation and mapping
- The existence of a practicable underground junction of the Sûre and Our valleys through the Moestroff cave was most unlikely.

It is interesting to note that these preliminary conclusions were confirmed by the subsequent explorations.

1.2.4. Summer 1962

Based on the experience gained in 1961, it was decided to organize a second exploration camp in summer 1962 . It would be of longer duration, involve more exploration teams, and benefit from improved logistic support.

The base camp - comprising seven tents- was installed on a small platform at the end of a narrow forest road, approximately 100 meters from the cave

entrance. The boys slept in the tents, whereas the girls lodged in a large mill building down in the village, as mixed dormitories were neither readily accepted by the parents of the youngsters nor by the village community in those days. Besides the smaller camping tents, a large army tent was set up as refectory and briefing room. Another mid-sized tent served as telecommunications center and drawing office, where the results from the exploration and surveying teams were immediately recorded and plotted.

The access to the cave presented a real problem, as the steep ascent from the camp to the bottom of the cliff through a steep slope of rock debris, clay and gravel was exhausting and partially dangerous. Therefore, a forest track with roughly hewn stairs was constructed by workers of the local city council (Administration Communale de Bettendorf) upon the initiative of its members Jos. Brebsom and Batty Meisch, who enthusisastically supported the exploration project with word and deed. The remaining 10 meters from the bottom of the cliff to the cave entrance had still to be overcome with a steel-rope ladder with aluminum rungs, then widely used by speleologists; the fixed ladder described in Part 1, Chapter 2 of this book would be installed in 1991 only for the Phymoes project.

Water supply was another serious problem, as there was no spring or stream close by. A wheeled water-tank of 800 l capacity was eventually obtained on loan from a government organization (Administration des Ponts & Chaussées).

750 hot meals had to be prepared in 10 days [8]; a local refrigerator manufacturing company (SIVIA) was approached for sponsoring, and it loaned a small camping refrigerator running on kerosene, which proved to be most useful for conservation of meat and dairy products in those hot summer days. A local dairy company contributed half a liter of fresh milk per day for each team member.

The Luxembourg Army loaned 13 field telephones and 1000 m of two-wire telephone cable. A number of these telephones were light-weight sound-powered models, which proved to be quite handy and useful in the narrow corridors of the labyrinth.

All in all, the materiel for the 1962 camp totalled 1500 kg, which was carried by truck to the village of Moestroff, and from there by hand and agricultural tractors over the forest road to the base camp.

The coordination and administration of all these preparation efforts - which extended over several months before the camp - was planned and executed in an outstanding manner by Ed Nicolay, the managing director of the Luxembourg Youth Hostel Association. His personal interest in scientific research, his vast experience in organization and his extraordinary skills in dealing with young people as well as with senior governe-

Fig. 1.3.1. Two members of the GSL discuss with Jacques Bintz, director of the Service Géologique du Luxembourg (center of the photo) at the 2nd relay in 1962 (photo Ed Sinner). Protection helmets are tank-crew helmets from surplus army supplies.

ment officials provided an essential contribution to the success of the project.

The camp took place from 20 to 31 July 1962, with 19 full-time exploration team members, 16 part-time participants and four guest scientists [9,10].

The rather high number of part-time participants resulted from the fact that some members were seconded to a nearby archeological exploration camp, to assist the excavations of a roman villa “op Uresbierg” near Bigelbach under the direction of Professor P. Jost from the Lycée Classique de Diekirch (LCD). As a matter of fact, Professor Jost was not only a distinguished archeologist, he also had a keen scientific interest in the exploration of the Moestroff cave, and provided substantial assistance in securing logistic support for our camp through his excellent relationships with government administrations. Therefore, a close cooperation between the two exploration camps was quite natural, and with hindsight, it turned out to be a most rewarding exercise of scientific cross-fertilization for many of us.

The intensive preparation efforts yielded substantial results: 1200 m of corridors were surveyed in 10 days, bringing the total length of the cave at the end of the 1962 camp to 1600 m [11]; several types of concretions [12], calcite basins populated by minuscule cave insects [13] and large banks of fossils [14] were discovered; strange places were found, such as a corridor exceeding 2 m of height (quite unusual at Moestroff) [15], or a crevice covered with a fine slimy clay resembling molten chocolate, which would later become a famous milestone deep inside the mountain known as “chocolate crevice” [16] to insiders.

New cave entrances were also discovered during this camp [17], but unfortunately they were so narrow that they could only be passed by very slim and fit young people, and turned out to be of no practical use for later explorations.

During the 1962 camp, a much-needed coordinate system was introduced, to provide firm references for the explorers and surveyors. It was based on the idea to use the main corridors as grid references. The gallery proceeding from the main entrance to the inside of the mountain was labeled “00” (zero-zero). All corridors situated to its right (south-west) were labeled R1, R2, R3 etc..., whereas those to its left (north-east) were labeled L1, L2, L3, etc... The intersecting galleries with a north-east / south-west direction were labeled K, L, M, etc... when moving into the mountain (eastwards), and J, I, H, etc... as one moved towards the cliff (westwards). By convention, the intersection at the First Relay was designated “K-00”. When the end of the alphabet was reached, a new labeling cycle with indexed letters A’, B’, C’,...X', Y', Z', A’’, B’’, C’’, etc... would start.

This system proved to be simple, although not fully reliable. While there is some regularity in the maze pattern, anomalies are not uncommon, and those lead to ambiguities in the numbering system. To avoid misinterpretations, the main intersections were therefore identified with small number plates nailed to the rock, which provided unambiguous reference points to the explorers and surveyors.

The 1962 expedition received wide publicity in the media: major newspapers covered the event [Mey, 1962], and the magazine “Revue” dedicated two extensive articles with many photographs to the Moestroff expedition and the excavations of the roman villa at Bigelbach. Three of our ladies [18] even made it to cover girls on the front page of two issues of that magazine [Nilles & Krier, 1962].

1.2.5. Interlude

The harvest of results from the ’62 expedition, specifically the large quantity of surveying notes, took a while to exploit, and many “holes” called for follow-ups. Moreover, experience had shown that thorough planning was essential to success. It was therefore decided to delay the next large expedition by one year, and to use the intervening time for an in-depth review of the 1962 results, and for detailed planning of the 1964 exploration camp.

From November 1962 to July 1964, seven descents were made into the cave [19], totaling 39 participants and 500 exploration man-hours [GSL, 1963; Zeyen, 1966; GSL, 1966]. Significant results from these sorties were the precise location of the “Chocolate Crevice” [16], discovery of the “Birthday Maze” [20] and the “Adrienne Maze” [21], a deep penetration

into the mountain up to coordinate G'-L50, where many cave insects were found, discovery of a small cascade with a waterflow of approximately 0.5 l/s at coordinate P-L24.5, discovery of the "4th Relay" [22] which would become an important milestone and rest point deep in the mountain for the next exploration teams, and the surveying of more than 1000 m of corridors. On the eve of the '64 expedition, 2497 m of the cave had thus been mapped.

1.2.6. Summer 1964

1964 was the fifth anniversary year of the GSL, and by then the group had reached maturity. It had more than 40 members, many of whom were quite experienced; it could count on the support of local and government administrations for support; its activities were well perceived by the public and the media, and most teething problems experienced during the first two expeditions at Moestroff had been ironed out. After a thorough preparation period of two years, the stage was set for what would become the largest ever expedition at Moestroff.

It took place from 8th to 22nd August 1964 with 19 participants and three guest scientists [23, 24]. The experience gained in '61 and '62 had led to further improvements in logistics. Six large tents and lightweight communications equipment was loaned by the Luxembourg Army. The camp platform and access track had been further improved and the access stairs to the cliff had been refurbished by the local city council.

From the operational point of view, the most significant improvement was a much larger headquarters tent with windows loaned by the Army. It provided the much needed space for the drawing boards and plotting tables, and housed also the telephone switchboard. This was connected to a small self-made transistorized amplifier (a rarity in those days), which provided hands-free monitoring of all telephone traffic with and among the exploration teams working deep inside the mountain. This was not only most useful for the direction and control in real-time of exploration operations, it provided also an important psychological comfort to the teams fighting the darkness and unknown in the fantastic maze, and was an essential contribution to safety. With this system, no team ever lost its way.

As a matter of fact, the only significant safety incident ever to happen at Moestroff occurred outside: during a daylight exploration of crevices at the foot of the cliff, while looking for a possible new entrance, a 20 kg stone fell from a height of approximately one meter above right on top of the helmet of a team member [25]. Apart from the psychological shock of the impact and a crack in the helmet, he suffered no injury, which was confirmed by an immediate medical examination.

A detailed account of the 1964 operations at Moestroff is given in (GSL, 1966).

When the camp closed down on 22nd August 1964, 3980 meters of the cave had been surveyed [26], but the deep penetrations into the mountain had confirmed earlier suppositions that it was not possible to traverse the mountain under ground and emerge in the Our or Sûre river valleys. The farthest point reached was at coordinate L'-L56, but the deeper one penetrated into the maze, the more clay and silt were filling the corridors, up to the point where even our slimmest explorers could not progress any further.

A number of interesting features were nevertheless discovered during those runs probing deep into the mountain: well developed calcite and ferrous silicate deposits around L'-L50; calcite crystallized in prismatic shapes at W-L23 ; small cave insects living in clay cones at W-L26 ; a stalagmite and an eccentric stalactite at U-L22 ; a major fossil embedded in the rock at T-L27, etc....

Although the maze appears to be mainly horizontal at approximately 250 m above sea level [Maquil & Massen, 1994], a detailed survey with a high precision clinometer from the main entrance to the "4th Relay" [22] revealed that the corridors from N-L5 to V-L14 lie approximately 70 cm deeper than the main entrance (fig. 1.3.2); a correlation of those findings with geological features on the surface could however not be established.

Temperature and humidity measurements were performed again, but yielded no reliable results because of disturbances caused to the measured values by the presence of an operator.

With hindsight, it is interesting to note that measurements of air conductivity and radioactivity had also been envisaged, but could not be implemented for lack of suitable battery-powered instruments of adequate sensivity.

A number of clay and silt samples were analyzed for pollen contents [Coûteaux, 1965] in an attempt to establish an approximate date for the formation of the maze, but quite surprisingly no trace of pollen was found. It was intended to carry out another series of palynological tests to substantiate or invalidate these preliminary results, but for a variety of reasons this was never done.

The media covered the 1964 exploration camp extensively, partly because it was a most welcome subject for reporters in the otherwise very quiet midsummer period, and partly because the press had been invited and briefed beforehand. RTL (Radio Luxembourg) and TV Saarbrücken (Germany) broadcast reports about the explorations; further accounts can be found in the following press articles of that period: Républicain Lorrain [RL, 1964], France Journal [FJ, 1964], Luxemburger Wort [LW, 1964] and Letzebuerger Land [Krieps, 1964; Hemmer, 1964].

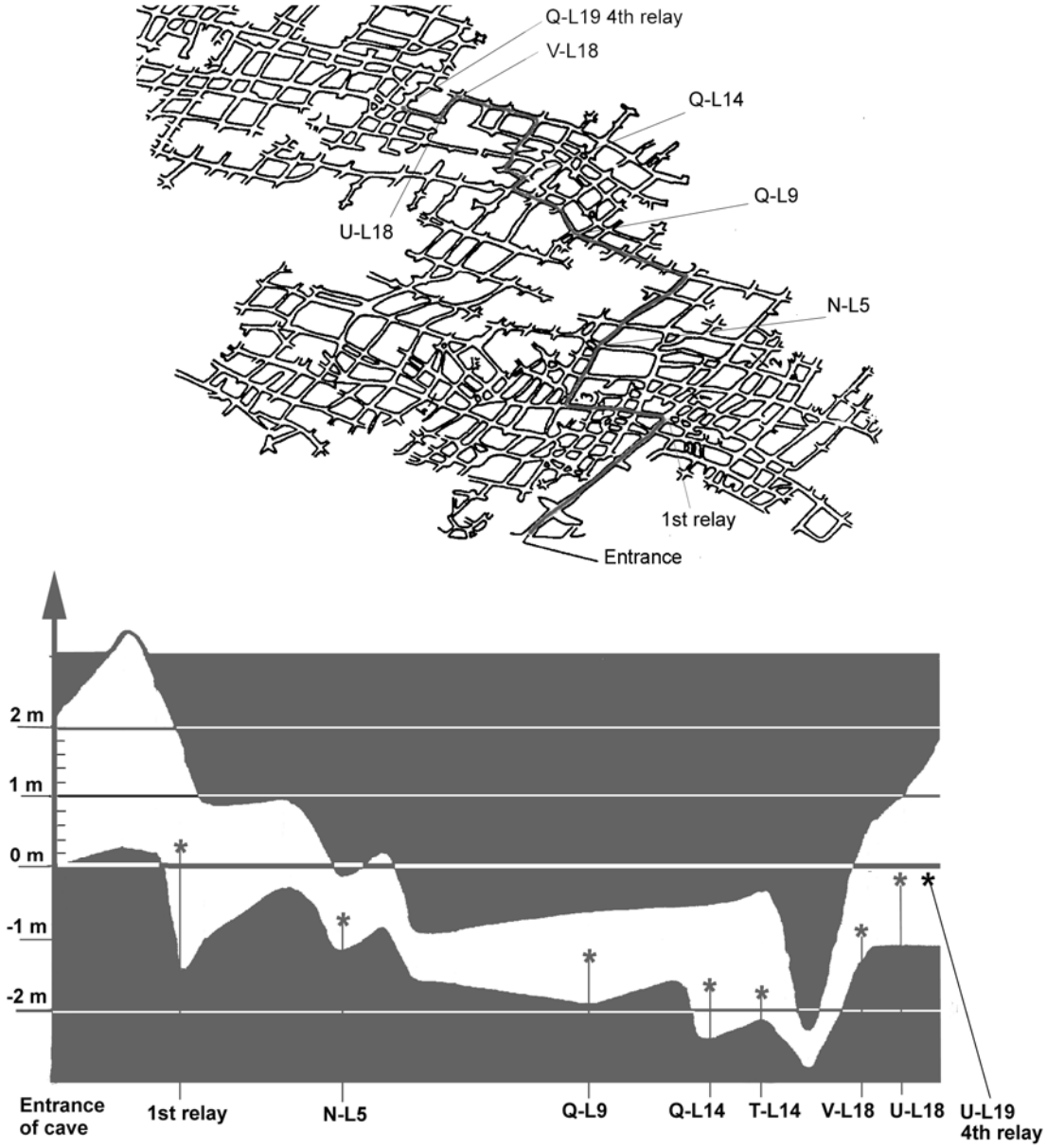

Fig.1.3.2. Profile with horizontal levels from entrance through the 4th relay (U-L19)

1.2.7. The Ebb

After the August ’64 expedition, the Moestroff cave had in no way given away all its secrets yet. Although the survey of the corridors could be considered as nearly complete in all areas where human beings could penetrate, many questions about the creation and development of this extraordinary maze pattern remained to be answered.

In the following years, a few more descents were made [27], but none yielded significant new findings. The main reason was not so much a lack

of things to be found, but rather the shift of interest to an entirely new area, the "Schnellert" region near Berdorf, where spectacular new discoveries were made in 1965 and 1966.

These would absorb most of the energy of the group in the years to come, and the Moestroff cave would slowly drift out of focus for more than twenty five years.

1.2.8. The Revival

In October 1989, some "old-timers" who had participated in the fascinating explorations of the early sixties met again at the Moestroff cave for a what was supposed to be a leisurely guided tour for a foreign geologist. His name was Professor Camille Ek, and his scientific competence and his outstanding personality left a lasting impression. He gave the old-timers plenty of food for thought about their old love, and thus the Phymoes Research Project was borne. Within three years, it would become another significant milestone in the scientific exploration of that fascinating labyrinth: the Moestroff Cave.

Notes

[1] Founding Members of the Groupe Spéléologique Luxembourgeois (GSL) : FAUTSCH Georgy, HEMMEN Georges, HEMMER Carlo, JACQUES Roger, JOST Jacques, KAISER Jeanny, KLEIN Alice, LUDWIG Fred, SINNER Ed, SINNER Jean-Marie (24 - 25 October 1959).

[2] Participants at the first visit of the GSL to the Moestroff cave on 28th May 19961 were BARTHEL Fränz, SINNER Ed, SINNER Jean-Marie, WILDGEN François; they penetrated into the south-western part of the maze up to a point which would later be assigned the coordinate grid reference M-R9.

[3] Participants at the 1st Exploration Camp at Moestroff (22 - 26 July 1961): BETZ Jean-Jacques, FOLSCHEID René, GROST Ole (part time)**,** JOST Jacques (part time), GRÜNEWALD Michel (part time), KIRSCHTEN Norbert, KOLLMESCH Norbert, LUDWIG Paulette, SCHINTGEN Claude, SCHINTGEN Guy, SINNER Ed, SINNER Maryse, STEINBACH Paul (part time), WINTER Michel (part time).

[4] At the end of the 1st Exploration Camp on 26th July 19961, the area delimited by the corridors L16 to R9 and M to I had been surveyed.

[5] At M-R6

[6] At J1-L13

[7] Encrinus Liliformis, Holopellae, Soleniscus, Murchisonia Turbiata.

[8] It is interesting to note that the total cost charged to each participant of the 1962 summer camp for three meals a day during 10 days was only 450.-LUF; the cost of 25 kg of carbide used for lighting during the expedition was 325.-LUF, whereas the cost of 80 electrical batteries consumed was 1.070.-LUF.

[9] Participants at the 2rd Exploration Camp at Moestroff (20 - 31 July 1962):
BARTHEL Fränz, BARTHEL Marianne (part time), BETZ Jean-Jacques,
BIRGÉ Adrienne, ELSEN Paul, DIEDELING Lony (part time), FOLSCHEID René,
GINTER Paul, GROST Ole, GRÜNEWALD Michel,
JAANS Marie-Jeanne (part time), KAYL Mariette , KIRSCHTEN Norbert,
KISCH Robert, KISCH Victor, KOELLER Rich (part time),
KOLLMESCH Norbert (part time), LUTGEN Renée (part time),
MAMER Blanche (part time), MATGEN Henri, NICOLAY Jacques (part time),
PHILIPPE Lydie (part time), PIRSCH Suzette (part time),
SCHINTGEN Claude, SCHINTGEN Guy, SCHOLTES Jos (part time),
SINNER Ed , SINNER Jean-Marie,
STREVELER Nicole (part time), VIEUXTEMPS Louis (part time), WINTER Michel (Fip), WIRTZ Emile, ZEIHEN Jean (part time).

[10] Apart from the GSL participants, four guest scientists participated part-time in the explorations of 1962: J. BINTZ from the Service Géologique, Administration des Ponts&Chaussées, Luxembourg; A. GALLES from the Administration du Cadastre et de la Topographie, Luxembourg; H. GYZEN, a dutch geologist; D. BERG from the Geological Institue of the University of Köln, Germany.

[11] At the end of the 2nd Exploration Camp on 31st July 19962, the area delimited by the following coordinate grid reference points had been surveyed: Entrance Nr 2, G-L5, J1-L16, M-L16, O-L5, Q-L5, Q-00, .M-R9, H-R11; in addition, corridor Q from intersection L5 to intersection L18, and corridor L14 from intersection Q to intersection W.

[12] White calcite crystals in granular form at coordinates M-L12 and M-L13; a half-dome (géode) with prismatic calcite crystals at M-L12; brick-red calcite layer at M-L13; the "Crystal intersection" at J1-L12 was discovered by FOLSCHEID René and SINNER Jean-Marie on 23rd July 19962.

[13] During the exploration run on 28th July 1962 by SCHINTGEN Claude, KISCH Rob and MATGEN Henri, half a dozen of calcite basins (gours) with cave insects were discovered at Q-L15; this location was called "Midnight Hall" (SCHINTGEN, SINNER, 1963).

[14] Large banks of fossils (approximately 30 cm high) were found at I-L8 and J-L5.

[15] The corridor exceeding 2m of height is located at coordinate point G-L4.

[16] The "Chocolate Crevice" was discovered on 28th July 1962 by SCHINTGEN Claude, KISCH Rob and MATGEN Henri after a very tough exploration run of 12 hours; it is located at coordinate point P-L25; this coordinate was however not yet identified when the 1962 Exploration Camp closed; it was surveyed in July 1963 only. During the same run in 1962, half a dozen of calcite basins with cave insects

were discovered at Q-L15, and this was called "Midnight Hall" (SCHINTGEN, SINNER, 1963).

[17] Entrance Nr 2 is located to the north of the main entrance; it was discovered on 22nd July 19962 by KISCH Robert and WINTER Michel (Fip), leading to a wide array limited by corridors I to A and L1 to L12. Entrance Nr 3 is located to the south of the main entrance; it was discovered on 25 July 19962 by GINTER Paul and WIRTZ Emile. It was used as a cable duct for the outside weather station during the PHYMOES project.

[18] Streveler Nicole and Diedling Lony were shown on the cover page of the magazine "Revue - Letzebuerger Illustre'ert" Nr 32 dated 11 August 19962; Adrienne Birgé appeared on the cover page of the same magazine in issue Nr 33 dated 18 August 19962.

[19] Explorations in preparation of the 1964 expedition took place on 3 November 1962, 20-22 July 1963, 5-6 October 1963, 24 November 1963, 2 February 1964, 4-5 April 1964, 11-12 July 1964, 25-26 July 1964.

[20] The "Birthday Maze" (so called because its discovery coincided with the 21st birthday of SCHINTGEN Guy, one of the most prominent leaders of the group) was discovered on 5-6 October 1963 and comprises the area limited by corridors P-L25 to T-L32, X-L38 and Y-L42. During this run, more red clay infiltrations were discovered at R-L27, and more cave insects at T-L29 and T-L31. The wide intersection at Y-L39 was called "Birthday Hall".

[21] The "Adrienne Maze" was discovered on 2nd February 1964, and was named after an outstanding team member, BIRGE Adrienne. Its discovery provided a much easier way to the "Birthday Maze", shortcutting the difficult route from Q-L15 to P-L25.

[22] The "4th Relay" was discovered on 4-5 April 1964; it is situated at coordinates U-L19. The normal route from the main entrance to the "4th Relay" passes through the following intersections: K-00 (1st Relay), K-L5.5, Q-L5, Q-L14, V-L14, V-L17, U-L17.

[23] Participants at the 3rd Exploration Camp at Moestroff (8 - 22 August 1964): BETZ Jean-Jacques, BILLARD Josette (CSAJ, Grenoble), BILLARD Robert (CSAJ, Grenoble), BIRGÉ Adrienne, DECKER Marianne, FABER Sonja, GINTER Marie-Paule, GINTER Paul, GLESENER Carlo, GRÜNEWALD Michel, HEIRENDT Colette, MASSEN Juliette, SCHINTGEN Claude, SCHINTGEN Guy, SINNER Ed, SINNER Jean-Marie, THOLL Jeannot, ZEYEN Claude, ZEYEN Roland.

[24] M. Verhoeven, a dutch geologist; Friedrich Kupsch and Wolfgang Irrlitz, two german geologists doing research work on the limestone structures of the Sûre valley.

[25] Claude Zeyen

[26] The progress of the surveying efforts at the 3rd Exploration Camp at Moestroff (8 - 22 August 1964) was quite impressive, as evidenced by the following figures: 8th August: 2497m; 13th August: 3168 m; 14th August: 3661 m; 22nd August: 3980 m.

GINTER Paul and his team surveyed 1014 m in 5 days, which was an outstanding achievement.

[27] Explorations after the 1964 expedition took place on 22 November 1964 (discovery of an ascending crevice with water intrusion at E'-L28), 18-19 September 1965, 15 May 1966, 29 December 1967, 9 February 1969.

[28] Nelly Moia and georges Als visited the cave in autumn 1956 or 1957.

References

COÛTEAUX, M. - Letter to J. Bintz dated 1. 3. 1965.

France-Journal - 3. Expedition der luxemburgischen Höhlenforschergruppe. France-Journal, 7. 8. 1964.

France-Journal - " Groupe Spéléologique Luxembourgeois " feierte fünfjähriges Bestehen. France-Journal, 19. 8. 1964.

GSL (Groupe Spéléologique Luxembourgeois) - Rapport du IIe camp spéléologique à Moestroff (22. -26. 7. 1961). La Vie Souterraine, 2, Luxembourg, Sept. 1961, p. 4-6.

GSL (Groupe Spéléologique Luxembourgeois) , - Rapport d'activités. La Vie Souterraine, 7, Luxembourg, Oct. 1963, p.12-14.

GSL (Groupe Spéléologique Luxembourgeois) - Rapport d'activités. La Vie Souterraine, 8, Luxembourg, Aug. 1964, p. 11-13

GSL (Groupe Spéléologique Luxembourgeois) - Rapport sur la IVe expédition d'été du GSL à Moestroff, du 8 au 22 juillet 1964. La Vie Souterraine, 9, Luxembourg, Sept. 1966, p. 27-35.

HEMMER, C. - Notizblock. Letzebuerger Land, 35, 28. 8. 1964.

KRIEPS, R. - Die Höhlenforscher von Moestroff. Letzebuerger Land, 34, 21. 8. 1964

Luxemburger Wort - Höhlenforschung in Moestroff. Luxemburger Wort, 14. 8. 1964

MAQUIL, R., MASSEN, F. (editors) - Comptes Rendus du Colloque International de Karstologie ä Luxembourg 25-26 Août 1992. Publications du Service Géologique du Luxembourg, Vol. XXVII, 1994.

MEY, T. - Junge Speläologen und Geschichtsforscher " op Kâpendall" und auf dem "Uresbierg". Letzebuerger Journal, 169, Luxemburg, 26. Juli 1962, p.4.

NILLES, L.N., KRIER, T. - Villa Rustica " op dem Haischen ". Revue Letzebuerger Illustre'ert, 32, Luxembourg 11. Aug. 1962, p. 10-18.

NILLES, L.N., KRIER, T. - Höhlenforschung op Kâpendall. Revue Letzebuerger Illustre'ert, 33, Luxembourg 18. Aug. 1962, p. 28-29.

SCHINTGEN, G., SINNER, E. - Rapport sur le IIIe camp d'été du GSL à Moestroff du 20 au 31 juillet 1962 (1ère partie). La Vie Souterraine, 6, Luxembourg, Fév. 1963, p. 8-13.

SCHINTGEN, G., SINNER, E. - Rapport sur le IIIe camp d'été du GSL à Moestroff du 20 au 31 juillet 1962 (2e partie). La Vie Souterraine, 7, Luxembourg, Oct. 1963, p 4-8.

SCHNEIDER, P. - Scout (Bulletin de la FNEL), 1957.

Républicain Lorrain - La plus grande caverne du Grand-Duché livre ses secrets. Le Républicain Lorrain, Luxembourg, 27 Juillet 1962.

Républicain Lorrain - 3e expédition du groupe spéléologique qui poursuivra l'exploration de la caverne. Républicain Lorrain, 6. 8. 1964.

Républicain Lorrain - 3e expédition à la caverne de Moestroff: les spéléologues veulent porter la longueur du couloir exploré à 4000 mètres. Républicain Lorrain, 13. 8. 1964.

Républicain Lorrain - Joyeux anniversaire pour les spéléologues qui fêtaient la cinquième année d'existence de leur groupe. Républicain Lorrain, 18. 8. 1964.

ZEYEN, C. - La découverte du réseau Adrienne. La Vie Souterraine, 9, Luxembourg, Sept. 1966, p. 6-7.

Part 2

The Phymoes Research Project

Part 2: The Phymoes Research Project

2.1. The Genesis of Project Phymoes

Francis Massen, Antoine Kies

« *Well, what do you know about that cave ?* »

This embarassing question asked by Camille EK started project Phymoes.

In automn 1989, Camille EK, professor at the University of Liège (Belgium) and at the Centre Universitaire of Luxembourg, was invited by the Luxembourg Cave Exploration Group (GSL, Groupe Spéléologique Luxembourgeois) to give a conference about his expedition to Chinese caves. Prior to his exposé, Camille EK wanted to visit the largest cave of Luxembourg, the Moestroff Cave. He was truly amazed by this extraordinary anastomozed gallery system, and so quite innocently asked the above question. All the members of the GSL present (many of whom had participated actively in the exploration of the cave 25 years ago) had to admit that except for a reasonably good topography, not much was known about the Moestroff Cave. One or two temperature measurements had shown that the cave temperature was about 10 degrees Celsius, but that was it. We knew nothing about wind movements, gaz concentrations, water inflow, humidity and temperature variations, and so on...

A quite cheerfull discussion started and concluded after a short time that a serious scientific study of the cave was long overdue and should be started as soon as possible. A group of 8 people, all members of the GSL, decided to participate actively to the research project; these were:

BOES Claude	*Diplomchemiker preparing a doctorate at the University of Münster, Germany*
FABER Sonja	*Dr. in geophysics, researcher at the University of Karlsruhe, Germany*
KAYSER Pit	*Ing.dipl., professor at the Institut Supérieur de Technologie, Luxembourg*
HEIRENDT Colette	*Math. and physics professor at the Lycée Technique Hôtelier, Diekirch, Luxembourg*
MASSEN Francis	*Physics professor at the Lycée Classique, Diekirch, Luxembourg*
SCHINTGEN Guy	*Ing.technicien, technical manager of CITO Benelux (later PHOENIX Contact), Luxembourg*
SINNER Ed	*Dr. Ing., Namsa, Luxembourg*
WARINGO Guy	*Ing.dipl., professor at the Institut Supérieur de Technologie, Luxembourg*

Several months later, Colette Heirendt resigned from the group and was replaced by

KIES Antoine	*Physics professor, Centre Universitaire, Luxembourg*

These people agreed that Francis MASSEN should be the project leader and take all the necessary steps to start a research project under the authority of the Centre de Recherche Public, Centre Universitaire de Luxembourg (CRP-CU), which is the independently run research institution attached to the Centre Universitaire. Camille EK should assume a tutoring role for the whole project.

The researchers of this team had a rather unusual profile:

1. All but Boes Claude and Kayser Pit were well over 40 years old.
2. All but Boes Claude had full time jobs.
3. The professional qualifications and expertise of individual team members was very broadly distributed, covering physics, informatics, geology, chemistry, topology, metal working, industrial electronic connecting and housing technology.
4. The team members decided that they would do their work free of charge, and that all financial resources should be used in buying, building and maintaining the scientific and ancillary equipment.

As the researchers could not work 8 hours a day on the project, it was obvious that a lot of automatic instruments would be used.

A cave has many interesting aspects which justify a research project, but we decided to put the emphasis on underground climatology. Underground climatology is not any more a new revolutionary subject in speleology, but still a research topic of primary interest. Pratically all great scientific speleologists have done some underground climate research, and Andrieux [Andrieux, 1965] for instance published a rather detailed manual on the subject.

It was decided to do a several years long, continuous monitoring of the most important climatic parameters in representative parts of the cave. We wanted to use the newest technology available for a fully automatic measuring network. This had not been done in any cave to our knowledge. Automatic measurements were mandatory for two obvious reasons:

1. The Moestroff Cave is such a confined environment that the presence of an operator changes parameters like temperature, air movement, CO_2 concentration and so on drmatically. Fig.2.1.1. for instance shows how an operator working for about half an hour at station 3 provokes a rise of about 2 degrees in local temperature. The operator then left for station 4, and came back after some exhausting work to leave the cave. His higher thermal output shows clearly up in the increased temperature peak when he passes station 3 again on his way out.
2. The team member's professional duties did not allow them to spend the same amount of time on this project as would be the case for full time researchers.

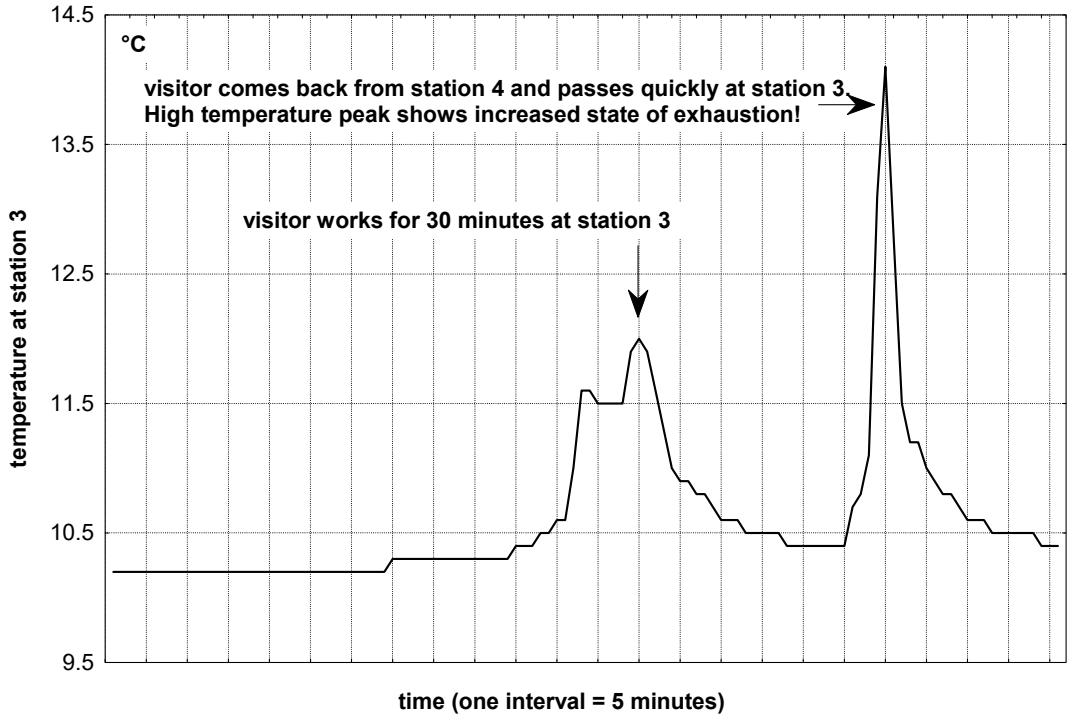

Fig.2.1.1: Influence of a visitor on local cave temperature at station 3. Temperature profile recorded during a fast sampling campaign in February 1992.

A lot of preliminary work started soon after Camille Ek's exposé. On June 22th 1990, a meeting with Fernand REINIG, administrator of the CRP-CU, Francis Massen and Colette Heirendt cleared all funding problems and baptized the project as « PHY-MOES » (PHY meaning "PHYSICS" and MOE "MOESTROFF"), which we quickly simplified into PHYMOES.

Starting date of the project was 1st October 1990, and it should run for 3 years. Later on, the project duration was extended to 4 years, so that the official dates are: start of Phymoes: October 1990, end of Phymoes: September 1994.

The relationship with the CRP-CU was always an extremely good one, based on full trust and absolute minimal bureaucracy. Many important decisions could be taken by the project leader urgently without tedious administrative procedures; whenever authorizations for large investments were necessary, these were obtained very quickly. The project leader can not overemphasize the positive aspect of this fine unbureaucratic collaboration on the PHYMOES project.

Understandably the Moestroff Cave, which had always been open to visitors, had to be closed to protect the scientific equipment against intruders, and to avoid any disturbance of ongoing measurements. The

necessary authorization was given by the Ministère des Eaux et Forêts, with the restriction that the unique cave entrance should be closed by a wide-meshed iron door, which would not hinder the movements of bats or other animals. As one of the parameters to be measured was air movement, we had to use wide-meshed grating anyway.

All preliminary work like building the protective hardware, choosing, ordering, testing and installing the scientific instruments, dataloggers, computing software, power-supplies and electronic controlling equipment was finished before the 1st August 1991. From that date on, the equipment was running continuously up to the 30th September 1994, and for a subset, even up to December 1994.

Two private sponsors gave Phymoes a most welcome and important aid:

BULL Luxembourg SA donated a portable miniHD ZDS computer, which was heavily used during the first two years, and despite extremely rough treatment in the cave, it never failed to work. On Sunday 16th June 1991, M. Petesch, Director of BULL Luxembourg SA, donated this computer to the project leader during a meeting at the cave entrance.

PHOENIX Contact (Luxembourg; technical manager G. Schintgen) constructed, free of charge, in its factory all the necessary water-proof enclosures with the electronic controlling and switching devices, and all the heavy cables to run from the central station to the different dataloggers and instruments.

The **Ministry of Education** (MM. Paul LENERT and Georges ALFF) of Luxembourg helped many times with supplementary subsidies, which were used to buy either special software, or to cover unplanned important expenditures.

References

ANDRIEUX, Claude - Sur la Mesure Précise des Charactéristiques Météoclimatiques Souterraines. Annales de Spéléologie, XX, fasc.3, p. 319-340. 1965.

2.2. Access and Protection Measures

Guy Waringo, Ed Sinner

The only practicable access to the extensive maze of the Moestroff cave is located approximately in the middle of a partially overhanging cliff, the height of which ranges from 15 to 20 m. The rather difficult natural configuration required a number of preparatory works and installations, whose aim was:

1. Ensure an easy and safe access to participants of the research project
2. Prevent access by unauthorised persons
3. Provide a hoist for moving heavy goods to and from the cave entrance.

The solutions which were developed to meet these interrelated and partially conflicting requirements will be described hereafter.

2.2.1. Access to the Cave

From the early days of the exploration of the Moestroff cave up to the preparation phase for the PHYMOES project, the only way for explorers to reach the entrance of the cave was by abseiling from the top edge of the cliff. This procedure was not only cumbersome, it was also dangerous because the edge of the cliff does not appear as a clean limestone fracture, but rather as an increasingly steep slope of slippery clay scattered with gravel and rocks. In view of the requirement to install heavy scientific equipment and the necessity to visit the cave every few days over a period of several years, it was therefore essential to create a safer and easier way to reach the cave entrance. The access route from the bottom was finally chosen, among others because there is an unpaved country road nearby, from where a forest track leads to the cliff. A steep slope (45 degrees) of rock debris, gravel and clay had to be overcome by excavating stairs reinforced with wooden planks, before the foot of the cliff was finally reached. From here, a rigid aluminium ladder of 8 meters leads to the cave entrance itself. This ladder is inclined at an angle of approximately 85 degrees from the horizontal, which is a compromise between the conflicting requirements of having a convenient climbing position and non-interference with the lifting equipment (described hereafter). As the cliff has an irregular surface, the distance from the ladder to the rock varies from approximately one meter at the bottom (where the cliff overhangs) to 5 cm in the upper third.

The ladder is attached to the rock at three points (bottom, middle, top) with flat steel bars, which are fastened on one side to a threaded bar

inserted through a ladder rung, and on the other side to short steel anchors inserted into the rock and secured with fast-setting cement. All bolts are secured with locknuts. The lower attachment point absorbs the vertical load forces and is therefore made of double steel bars on both sides, which constitute a rigid support frame. The middle and top steel bars operate - from a static point of view - as floating attachments. This type of construction was rather simple to install, and was easily fitted on the spot to the irregularities of the rock surface. It would obviously have been more appropriate to select the upper attachment as the fixed point of the design, but this would have complicated the installation significantly. The eight anchors were prepared prior to installation in the workshop of the Lycée Classique de Diekirch (LCD), but the flat steel bars had to be cut to length and drilled on the spot. This required a column drilling machine, an abrasive cutting machine and a power generator, which was also feeding the electro-pneumatic drill used for drilling the anchor bores.

In order to prevent corrosion, all nuts, bolts and threaded bars were made of brass. All steel parts were cold-galvanised on the spot. Finally, the entire construction was coated with an olive-drab military paint. This provides a good blending of the construction with the environment and limited camouflage, in order not to attract unauthorised visitors. Without this coating, the aluminium ladder would be visible in wintertime over a distance of several miles.

As a matter of fact, the ladder does not terminate at the cave entrance itself, but at a small rock platform about three meters to the west. From this point the entrance is reached over a narrow strip of rock. In order to overcome this passage safely under slippery or icy conditions with heavy loads, a steel cable was laid from the top of the ladder to the cave entrance, and was secured with several pitons to the rock. It can either be used as a guiding handrail, or in combination with a carabiner and a safety harness for heavy lifting or installation works.

2.2.2. Securing the Entrance

In view of the anticipated duration of the project of several years, it was essential to restrict the access to the cave, in order to prevent theft or destruction of expensive measuring and data logging equipment, totalling an amount of several million LUF. Uncontrolled visits proceeding from mere curiosity had to be prevented too, as each penetration into the cave would cause significant disturbances to the variables under measurement. Therefore, access was limited for data collection and maintenance tasks only; and the duration was restricted to minimum essential requirements. Each visit had to be registered in a log book, for subsequent correlation with measured parameters. On the other hand, the interdiction of the cave to humans and large animals should not affect in any way free airflow to

and from the cave. Therefore, a door made of steel bars arranged in a grid pattern was retained to meet these requirements.

The location of this door was chosen at the end of the entrance tunnel, at a distance of approximately five meters from the outside, before reaching a large chamber where the power, control and data logging equipment would be installed. The door has a size of 1.4 x 0.8 meters. It is made of 16 mm round steel bars spaced 15 cm apart. These are held in place every 28 cm by heavy (20 x 30 mm) flat steel sections, which form also the frame of the door grid. All steel sections are fillet-welded to each other. The door frame is made of sturdy angle steel sections (L50 x 50 x 6 mm) which fully enclose the door. The door hinges were welded in place in such a way that it is impossible to lift or remove the door when closed. The door is locked with a padlock protected by heavy steel reinforcements so that the shackle cannot be reached with a metal saw, a file or a bolt clipper. The door hinges are similarly protected against attempts to cut the bearing pins with a saw or a file. The metal works for the door construction were performed conveniently in the workshops of the Lycée Classique de Diekirch (LCD) and of the author respectively. The installation was however much more difficult. Steel anchors (cross section 30 x 4 mm) had to be inserted every 20 cm around the door frame into holes drilled into the rock, and were glued in place with fast-setting cement. After the cement had hardened, the steel bars were bent in place and fixed to the door frame with screw clamps. After welding, the clamps were removed and the excessive length was cut off. Gas welding equipment was used for bending and welding of the steel sections. The large number of steel anchors provides additional security against unauthorised access, and enabled us to secure a loose rock in the ceiling by the same token. The uneven floor was filled with stones and concrete to close flush with the door step.

Despite these precautions, it seemed appropriate to prevent the access of unauthorised persons to the security door altogether. Therefore, the lower part of the ladder was covered over a length of 2.5 meters with a plate of sheet metal, which makes it impossible for anyone to climb up the ladder. This sheet metal plate is also secured in place with a padlock.

During the whole project, not a single attempt was made to break into the cave. With hindsight, it is however difficult to say if this success was achieved through the psychological deterrence of the security measures described above, or through the strength of their implementation.

2.2.3. Material Transport

Besides the installation of the basic equipment required for the project, such as cables, sensors, computers, data loggers, lighting, control and distribution panels, there was a requirement to bring a freshly charged

lead-acid battery into the cave at bi-weekly intervals, and to remove the depleted battery on the same occasion. All horizontal movements of heavy goods, including the escalation of the 45° slope at the foot of the cliff, are possible by hand, with backpacks or load carriers. A better and safer solution had however to be found for climbing the ladder, especially since the heavy lead-acid battery (30 kg) induced a potentially hazardous shift of the centre of gravity while ascending the ladder with a load carrier pack. This led to the following specifications :

1. It must be capable to lift, hold or lower loads from a safe position (small platform) at the top of the ladder.
2. It must be useable by a single operator.
3. It must be operated manually for obvious reasons of energy conservation.
4. It must be easily installed or removed without tools, and must be stowable in the secure area of the cave.

The main component of this special lifting device was a small manually-operated winch with a ratchet wheel, of the type used for hauling sailing boats out of the water. The commercial crank was replaced by a longer one, and the standard stranded steel cable was replaced by a thinner and much longer one of stainless steel. This hoist is positioned at the top of the ladder into a frame made from two U-shaped steel profiles which are inserted from above into the last and penultimate rung of the ladder. Lateral rigidity is provided by clamps surrounding the ladder upsides, which absorb pressure forces resulting from lateral torque. The vertical section of the frame forms a barrel in which the boom of the crane can move around over an angle of 180°. The modified winch is attached to the bottom of the barrel, and the crank plane is parallel to the ladder for easy operation. In order to compensate for the ladder slope (85°), the upper barrel fixation is connected to the upper U-shaped steel profile by a reinforced sheet metal spacer.

The boom consists of a rotating tube arranged vertically in such a way that loads with a vertical dimension of 80 cm can be lowered safely to the platform. This tube is welded to the boom itself, which is made of rectangular steel profile. It is fitted with two pulleys, one at the boom end and the other one close to the rotating tube. The width of these pulleys is such that they snugly fit into the rectangular steel profile, in order to avoid that the steel cable slips off the pulley and jams the hoist. The load end of the cable is fitted with a roller-bearing twist compensator; its weight provides enough cable tension even under no-load conditions to ensure proper winding of the cable on the winch reel. The load is connected to the cable by a carabiner with screw-on safety. The hoist is rated for load of 500 daN (recommended maximum). The heaviest loads used during the project, i.e. the lead acid batteries, are inserted into a transport frame fitted with a carrying handle and a lifting eye.

The hoist can be folded into stowing position for carrying it to and from the cave. In this position, the boom engages into a notch of the frame, and the eyelet at the end of the tensioned cable is hooked to the boom, so that the entire hoist becomes flat and rigid, and can be carried safely with one hand over the narrow rock strip from the platform at the top of the ladder to the cave entrance. The weight of the folded hoist is approximately 7 daN. **Photo H** shows the hoist mounted on top of the ladder.

With this device, the exchange of the lead-acid batteries can be performed by a single person in the following sequence :

1. Carry the battery by hand or with a load carrier pack to the bottom of the cliff.
2. Climb the ladder (without load).
3. Remove the hoist from the cave and mount it on the top of the ladder.
4. Lower the cable end to the bottom of the ladder.
5. Climb down the ladder.
6. Connect the load to the cable.
7. Climb the ladder.
8. Lift the load and carry it into the cave.

After battery exchange, the above sequence is performed in reverse order to bring down the depleted battery.

2.2.4. Conclusions

At the start of the research project, preliminary works were required in order to ensure a safe and convenient access to the cave at all times. A ladder to the cave entrance was installed in the lower part of the overhanging cliff. A small portable hoist was designed for moving heavy loads to and from the cave. The entrance was secured by a heavy steel door. Approximately 150 man-hours were spent on these preparations.

We can conclude that the design of the installations described above was adequate, as no maintenance actions or improvement modifications were required over several years. It would however be difficult to extrapolate the design details to other situations, as our solutions were tailored to the specific situation prevailing at the Moestroff cave.

2.3. Scientific Installation and Measurement Strategies

Francis Massen, Antoine Kies

2.3.1. Instruments Suitable for the Long-Time Underground Operation

In order to measure the underground climate, two most restrictive conditions are to be met:

1. Electronic instruments must be precise and accurate enough to record with adequate resolution very small changes in climatic parameters like temperature and humidity.
2. Electronic instruments must work reliably for long periods, even at relative humidity levels close to 100%.

The readings of the instruments were stored in electronic dataloggers. These loggers needed a very high resolution in order to sense even slight changes in the signals.

The Moestroff Cave is far away from a conventional domestic power supply. Therefor all equipment had to run from rechargeable batteries. As a consequence, absolute minimal electric power requirements were mandatory for the instruments, clocks and dataloggers. This very tough requirement was met by careful selection of the instruments, and by modifying some electrical devices.

Let us review in greater detail the different sensors and other equipment used; more details will be given in the relevant chapters, and full references to the equipment manufacturers can be found in appendix B.

2.3.2. Dataloggers

We needed dataloggers having at least a 12bit A/D converter, fully programmable channels adequate for voltage and current signals, power-saving sleep mode, possibility of an additional external power supply, serial connection to a personal computer and easy-to-use programming software.

We found only one type of datalogger meeting all these constraints: the Mikromec dataloggers of TECHNETICS (Germany) had 8 fully programmable input channels, a 14 bit A/D converter, a large memory for storing up to 64000 data-points and a very low power consumption due to its clever use of sleeping modes; a supplementary extremely important feature was that the loggers could run concurrently up to 9 independant programs.

To increase autonomy, the main 12V lead-acid accumulator driving the whole installation was connected in parallel to the internal 12V battery, enabling to continue logging for at least one week if by bad luck the main battery became exhausted. An additional internal lithium battery would retain the stored data even in case of complete failure of all 12V batteries; this actually gave us a twofold operational redundancy and an absolute insurance against accidental loss of data.

The loggers were driven by a RS232 serial connection line, extending to about 50 m for the most distant device. We used a communication speed of 4800 bit/s without any problems, and without resorting to additional signal amplifiers. The maximum logging period was about three months; as this represented a considerable data volume, and consequently a long time to download the data into the computer, we added a small amplified loudspeaker to the serial line. This gave an audible feedback of the ongoing downloading and allowed to do other jobs in the meantime.

Two modifications had to be done on the original logger:

1. The logger had no external RESET button, as the manufacturer were convinced this should never be needed. Actually, this was not the case, and we experienced some rare system blockages, which could only be solved by a hardware reset of the microprocessor. We added an external connector allowing this emergency hardware reset.
2. The logger could not start a serial communication when in sleep mode. As this was the normal situation, we had to wake up the logger by manually pushing its ON/OFF button. To enable this by remote action, we added a connector parallel to the ON/OFF switch, and a relay which simply closed two contacts to toggle the logger from sleep to wake and again from wake to sleep mode. This relay could be activated from the main central station at the caves entrance, so there was no need to physically approach the logger when downloading data or when reprogramming was needed. A glance on the main amperemeter was a good clue to see if the logger was awake or not.

Two loggers where constantly running in the cave, a third being used as spare.

The Mikromec logger is housed in an IP65 enclosure; in our opinion this was not a sufficient protection against constant 100% humidity levels and extremely muddy cave environment. Phoenix Contact enclosed the logger with its ancillary equipment as connecting bridges, relays and clocks in absolute waterproof ROSE casings, using watertight Heavycon connectors for power and signal cables (see chapter 2.4. for details).

A generous mass of dessicant (about 0.5kg) was enough to ensure a humidity level which never exceeded 40% in the enclosures (this level was

controlled by very cheep mechanic hygrometers from Conrad Electronics, Germany).

2.3.3. Thermometers and Hygrometers

The manufacturer of the the datalogger could deliver some ready to use sensors, whose characteristics were memorized in the EPROM of the logger. The combined thermometer/hygrometer CT-100 (from the Swiss manufacturer ROTRONIC) seemed adequate for our usage: temperature accuracy is 0.1 °C, humidity 1% and most important, the hygrometer is specified to work up to 100% relative humidity.

Some researchers follow extreme tough guidelines concerning temperature measurements in caves, rejecting all instruments which do not guarantee a resolution of at least 0.01°C; often they use selfbuilt NTC sensors, which, being analog devices, offer a theoretical unlimited resolution, but a dubious accuracy if not properly calibrated and recalibrated. Distinguishing temperature variations of 0.01°C may be mandatory in studying temperature gradients at the air-rock interface, or in the first mm of the rock material; but in our opinion, it is an overkill when all you want to monitor is air temperature. The natural variations caused by convection are very often of a magnitude of some degrees; even the practically stable deep cave air temperature measurement does not need to be done with a 0.01°C resolution to get a picture of its small seasonal variations. As we could not afford to pour the whole money available into ultra-precise temperature measurements, we decided that the Rotronic sensor would be adequate.

The CT-100 sensors quickly showed extremely bad misbehaviour in the humidity readings. The high humidity levels together with low air movements (mean air velocity lower than 20 cm/s) in he cave drove the capacitive humidity sensing element into saturation, and the instruments showed frequently impossible levels exceeding 100% after some days, without coming back to normal readings**.** This was not the case with the sensor mounted in the open air outside the cave. Another sensor which was mounted at 12 m from entrance (station 2), often exposed to air movements, also behaved much better.

As a first remedial, we exchanged the CT-100 model against a so called « meteorological » model YA-100, which according to the manufacturer should have a better behaviour for humidity measurements. We found that this was only partially true; over the whole duration of the project, we had at least **6** major breakdowns and consequently as many repairs and recalibrations to be done on the Rotronic sensors.

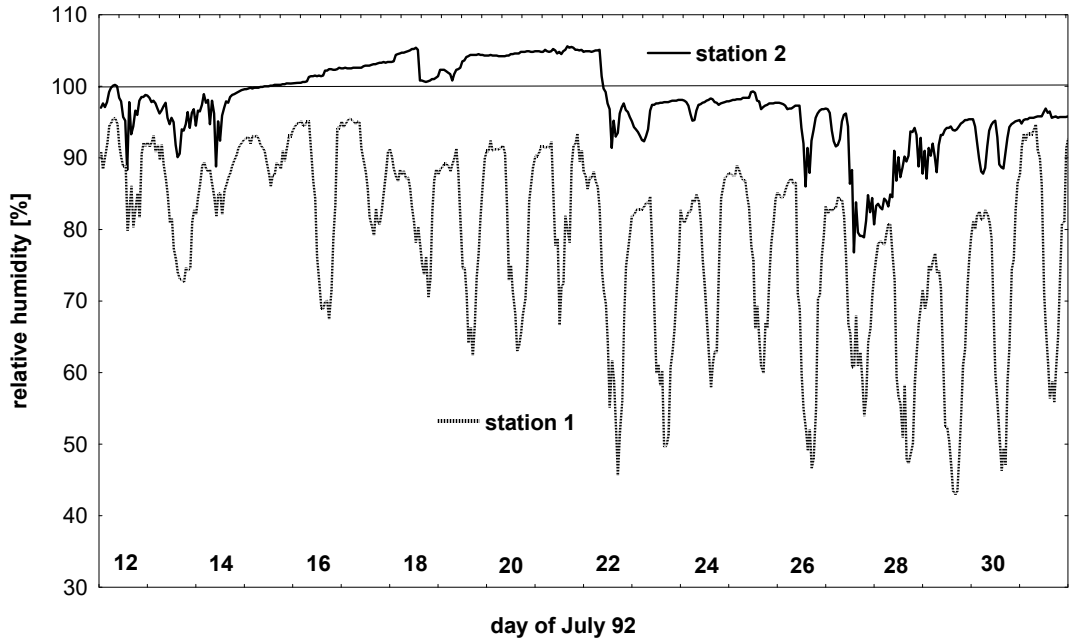

Fig. 2.3.1. Relative humidity recorded at station 1 (outside) and station 2 (x=12m) by Rotronic sensors; upper curve shows sensor misbehaviour.

Finally we gave up humidity measurement at station 3 where the air was constantly saturated. For the other two important stations we bought 2 dew-point sensors from KRONEIS (Austria). Compared to the Rotronics, these sensors were a big improvement, even if we had two break-downs, one caused by water seeping into the sensor-head and the other caused by a bad NTC device.

Actually we did quite a lot of research to find the good humidity sensor: we tested sensors from TESTOTERM (handheld devices and temperature/humidity T/H logger), ISEDD, PH. SCHENK (dual logger), most of which are based on capacitive or ceramic sensors. Neither of them was usable for long time monitoring in the cave; neither could meet the specifications of the manufacturer concerning humidity.

Besides air movement monitoring, humidity measurements gave us the most trouble; most gaps in our data-files are due to misbehaviour or hygrometers missing when being out for repair. Neither the resistive- nor the capacitive-type sensors are adequate for use in a cave; the only reliable instrument to measure very high humidity over long time levels actually remains the dew-point sensor.

We needed to know the relative humidity levels to be able to precisely compute the density of the moist cave air. Hints on how to compute this air density from temperature, air pressure and relative humidity can be found in Andrieux [Andrieux, 1970], the CRC Handbook of Chemistry and Physics [CRC 67th edition, 1986] , in Choppy [Choppy, 1990] and in

Recknagel [Recknagel, 1992]; one has to be careful because some authors (like Andrieux) are not very clear in their use of units. To compute the saturated water pressure, we used an expression derived from Choppy, based on an second order polynomial approximation of the water-pressure table which is quite good for the range of temperatures usually found in caves:

$$p_{sat} = \frac{H}{3600} * \left[(T+6)^2 + 180 \right] \qquad \textit{[eq.2.3.1]}$$

where:

T air temperature [°C]

p air pressure [mbar, Hpa]

H relative humidity of air [%]

In order to have some redundancy in our temperature measurements, we added two specialized HAMSTER dataloggers from Ph. Schenk (Austria; manufacturer EBRO, Switzerland). These are stand-alone watertight devices which can monitor temperature (Hamster) or temperature and humidity (Dual Hamster); besides the fact that the humidity data were practically useless (the logger going quickly into saturation), these small loggers are really switch-on-and-forget devices and enabled us a continuous control of the Rotronic or other devices; their temperature resolution is only 0.2 °C, but they proved extremely stable in over two years of continuous operation.

Measuring the temperature profile for air, surface and soil temperature along the main gallery was done several times a year by hand with three Testoterm probes for air, soil and contact temperatures with an accuracy of 0.1°C.

2.3.4. Air Pressure Sensors

We used 4 air pressure sensors adapted to the Mikromec logger and based on Sensortechnic's SCX15AN chip; these sensors are accurate up to 1 hPa. We had to build waterproof enclosures to protect them against humidity; using four sensors gave us a good redundancy. Two of these sensors became unserviceable during the 3 years underground operation, but we always had one in good working condition. The limited accuracy of 1 hPa means that these sensors cannot be used to measure pressure differences between entrance and deep cave locations, but are useful for atmospheric pressure recording only.

2.3.5. Anemometers and Detection of Airflow Direction

The Moestroff Cave has extremely narrow galleries, with a mean cross-section well below 1 m^2; as a consequence, resistance to air movements is high and air velocities are very low. Some preliminary measurements showed us that the range of wind velocities in the cave does not exceed a maximum of 2 m/s near the entrance, and drops to a few cm/s at a distance of 30 m from the entrance. This means that we could not use mechanical anemometers but had to install very sensitive hot-wire devices. Again the main problem was to find a hot-wire instrument which would reliably work at constant high humidity levels, have low power requirements and an analog output to transfer data into the datalogger. We choose the TA-2 handheld anemometer from Airflow (Germany); this instrument did not consume currents more than 80mA at the highest velocities (power consumption drops with decreasing air velocity) and had an analog output. Nevertheless there remained some serious problems to be solved before the instruments could be used in the cave.

The handheld anemometers had first to be mounted in a waterproof enclosure. Secondly they were build to work on 6VDC provided by 4 AA cells, so we had to find a solution to adapt them to our 12V power supply. And thirdly we found that the analog signal ground had to be separated from the power ground (a feature not documented by the manufacturer); in the Mikromec logger all signal grounds are common with the power ground. We solved both the 6VDC and galvanic decoupling by using for every anemometer a solid-state 3 Watt DC/DC converter built into the waterproof enclosure; this converter gives a regulated output of 5V from an input of 12V, and we found that the anemometer still worked fine with 5VDC.

The TA-2 anemometers are pure analog devices; zero offsetting had to be done manually at regular intervals. Actually the problem of zero-drift was not easy to tackle; figure 2.3.2. shows an extreme zero-drift during operation in August 92. By good luck, the zero-drift was usually either linear or a sudden step of the zero point, and as such could easily be corrected later on when the stored data were analysed.

Many experiments with lighted incense-sticks showed that the air movement over the whole gallery section was uni-directional: there were for instance no convective Rayleigh cells with air flowing in at the bottom and flowing out at the ceiling. So we installed the sensor at the midpoint of the gallery section; it was mechanically fixed on a two axis Cardan mount, so that a visitor would not damage the delicate sensor head inadvertantly.

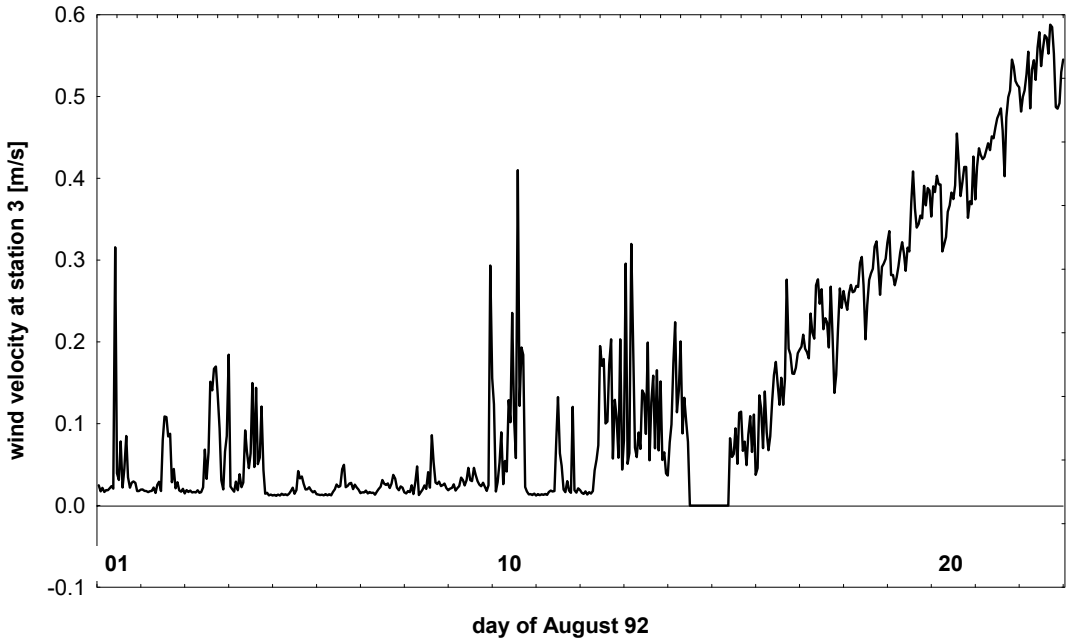

Fig. 2.3.2. Record shows slight zero offset and severe linear drift of hotwire anemometer readings in August 92.

On one sensor we had the problem that waterdrops running down the sensor mount completely immerged the tiny hot-wire during a very humid period; changing the sensor positiondis from vertical to oblique solved this.

The TA-2 anemometers, despite their careful watertight enclosures, remained delicate instruments to use in the harsh underground environment; we experienced a lot of instrument failures over the 3 years, but nevertheless were able to gather enough data to study seasonal, as well as daily or even extremely short time wind patterns.

A hot-wire anemometer can only monitor the absolute value of windspeed, and not the direction of air movements: this is a big handicap, as the knowledge of in- and outflow periods is of utmost importance.

In order to solve this problem we tried several solutions:

The first one was to use a second anemometer with a slitted cylinder covering the sensor (fig. 2.3.3)**.** Our idea was that the wind touching the sensor through the slit in the cylinder would give a higher reading than the wind blowing on the concave side of the cylinder; comparing the « slitted-cylinder » signal against the normal signal should allow to find the flow direction. This device worked reasonably well at the higher (>1 m/s) wind velocities; at low velocities, the « slitted-cylinder » signal was often noisy and ambiguous.

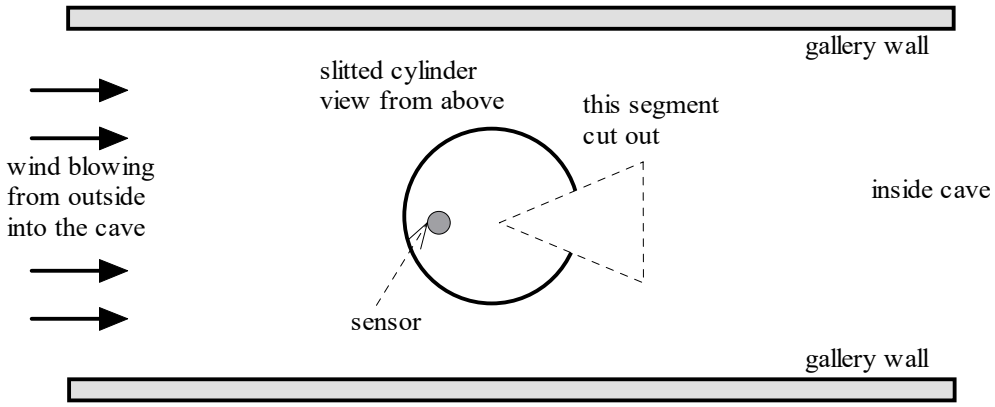

Fig.2.3.3: Slitted cylinder cover used to detect changes in wind velocity according to flow direction

In a second step we tried to build a complete new sensor using a sensor (AWM microbridge) from Honeywell; this was actually a solid-state electronic flow-meter used in medical equipments, which could detect as well air flow as flow direction (fig. 2.3.4). The prototype instrument worked fine during laboratory tests in an air tunnel where wind velocities were higher than approximately 50 cm/s. When we installed the sensor in the cave, we very often had no useful signal due to the low local velocities. Even if this sensor proved inadequate in the Moestroff Cave, it could be useful at places where wind velocities are usually higher, such as in some blowing holes.

Finally we installed an extremely precise SETRA differential manometer from GENERAL ELECTRIC CO., with plastic tubing extending to the entrance and to the last station at 50m distance from the entrance. We used a sensor with an output-swing of 2.5V corresponding to a differential pressure of 2.5mm water column; considering the 14bit resolution of the loggers, we were able to detect pressure changes as small as 0.01 Pa! Many manual checks with incense-sticks showed that this sensor reacted quickly to changes of the flow direction; the only serious problem was a potential zero-drift of the analogue sensor. We regularly checked the zero-offset in the cave and could correct a possible zero-shift either on the spot or by guessed interpolation, as will be seen later.

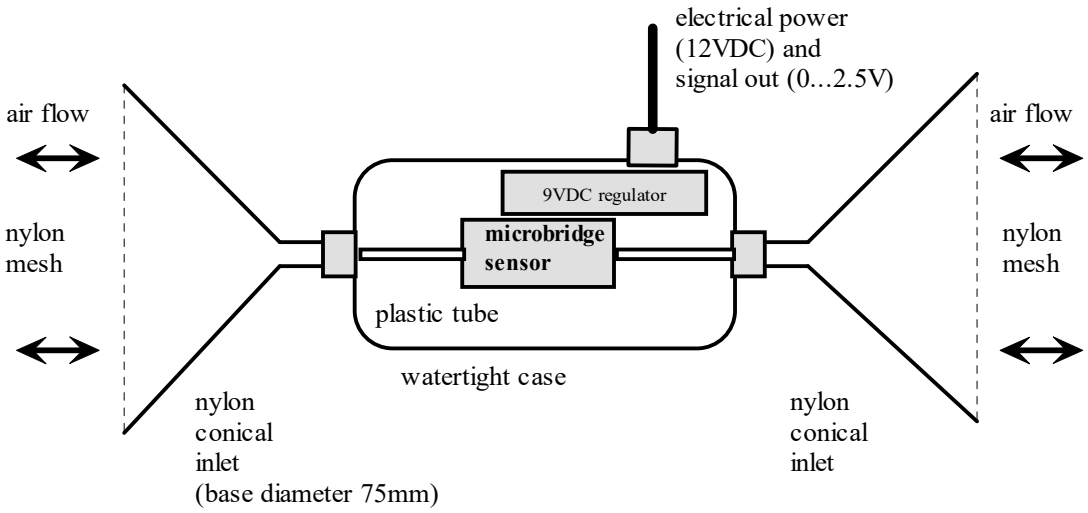

Fig.2.3.4. Calibration curves of the Phymoes-built AWM sensor to measure airflow and flow direction.

2.3.6. CO_2 Sensors

Some preliminary measurements using a GASTEC pump with CO_2 reactive capsules (akin to the well known Draeger instrument) showed that even at the most confined locations, CO_2 concentrations were rather low, lying somewhere between 500 ppm in the galleries up to 2000 ppm in the rock fissures.The Moestroff Cave is definitively not a foul air cave, and all earlier visitors never reported problems due to bad air.

The requirements to be met by a CO_2 sensor in the cave are extraordinarily high:

1. low power consumption
2. high precision and long-time stability
3. unaffected by extremely high humidity levels

We found a first ready-to-use instrument in Germany (ISEDD): the Canadian-made VALTRONICS CO_2 sensor. This is a NDIR device, measuring CO_2 concentrations by the absorption of an infrared light-beam. The Valtronic uses a sensor head working by pure diffusion, has voltage and current outputs and rather low (ca. 100mA) power requirements.

Alas, when exposed to constant high humidity levels near or at 100%, condensation occurred on the sensor optics and the instrument reported impossible high CO_2 concentrations due to absorption of the IR beam by the waterfilm covering the optics. The Valtronics could definitively not be used in the cave, and later we installed it as a reference station at the outside. Even there, rainy periods drove the instrument mad, but with dry weather conditions it usually reverted to correct operation.

As no suitable ready-to-use commercial instrument was available, we bought an OEM board called GASCARD 3000 manufactured by EDINBURGH SENSORS from Edinburgh (UK, Scotland). The Gascard 3000, based on a Motorola 68000-type microprocessor, is a pumped, very precise (3%) dual-beam NDIR sensor, specified for working up to 100% humidity (non-condensing!). After some discussions with the manufacturer, we decided to keep condensation out by sucking the air through a water-trap. As the instrument works on 24VDC, we used a heavy-power step-up DC/DC converter to transform the 12V input voltage to the required 24V. The power requirements of the board (300mA) together with those of the DC/DC converter (300mA) amount to a total of about 600mA, much too high to allow continuous operation. We solved this problem by switching the CO_2 sensor on only every two hours for about six minutes; in the water-proof enclosure we added an electronic fall-back timer which cut the power-supply automatically off after 10 minutes, so that even in the event of a failure of the master switching clock the main

power-supply batteries would not be drained by a continuously running CO_2 sensor (fig. 2.3.5).

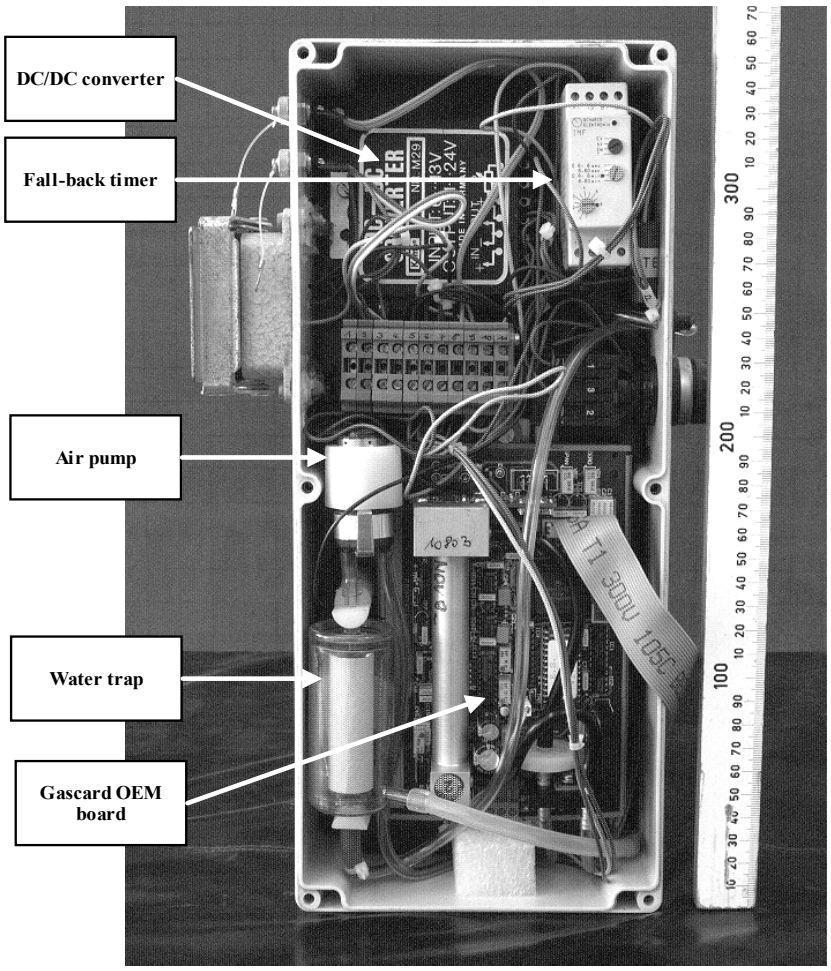

Fig.2.3.5. CO_2 sensor built from OEM Garscard board; scale in mm.

We built two of these sensors, and both worked extremely well for over two years in the cave, with one single breakdown of one Gascard board; the combination of pump & watertrap proved adequate to stop all problems related to condensation, even at 100% constant humidity levels.

At the end of the project, a supplementary portable CO_2 sensor, the ECO2 from Edinburgh Sensors, was used to do some spot sampling in the roof fissures of the galleries.

2.3.7. Radon Sensors

As these sensors will be described in more detail in chapter 3.6. concerning Radon measurements, a short overview only is provided hereafter.

We used three type of sensors: passive nuclear etch track and Eperm devices for long-time (usually 3 weeks) integrating measurements, Lucas cells for grap measurements and active electronic instruments (some with built-in datalogger) for spot measurements of the working level and hourly

measurements extending over days, weeks or even months for the radon concentration. None of these instruments were connected to the Mikromec loggers.

The Moestroff Cave was at times a sort of proving ground to test radon sensors for their suitability in a high humidity environment. Let us say briefly here that the nuclear etch track devices (« Karlsruher Modell ») behaved very well, and that electronic devices should not be left for extended periods in a very humid cave.

2.3.8. External Weatherstation

After the first year of operation, we saw that air movements in the cave were heavily influenced by external wind blowing at the outside. To monitor this wind activity, we installed an autonomous electronic weatherstation (Weathermonitor II, DAVIS Corp. USA) at the entrance of the cave. This weatherstation has its own datalogger and was driven by a separate battery, to avoid a potential disaster to the main equipment if a lightning would touch the external weatherstation sensors. Wind speed was the most useful of the registered parameters, as it allowed us to differentiate the periods with and withoutout external wind. This rather cheap weatherstation worked fine without any failure.

2.3.9. Overall Installation

As the Moestroff Cave is such a complex and extensive maze of galleries, it was out of question to distribute the measuring instruments randomly over the whole cave. We decided to concentrate on the main gallery (called 00) which penetrates practically perpendicularly to the outside cliff into the Muschelkalk layer. We chose four locations:

1. Station 1 at the outside (x=0m): reference station for external climate
2. Station 2 at x=12m
3. Station 3 at x=31m
4. Station 4 at x=50m

Station 2 is typical of a location still heavily influenced by the external climate; station 3 lies at the limit where air movements can be measured, and station 4 represents the situation valid for all other similar or even more deeply situated locations: no measurable air movements, practically constant temperature but nevertheless gaz concentrations which vary remarkably at a daily and seasonal time-scale.

The main electronic hardware and power-supplies were located at the Salle Loubens, situated 6m after the entrance, and the only location of the cave

high enough to allow an upright standing position. One of the two loggers was situated at salle Loubens, and collected the data from stations 1 and 2; the second one was postioned midway between stations 3 and 4 to read the corresponding sensors (fig.2.3.6)

.

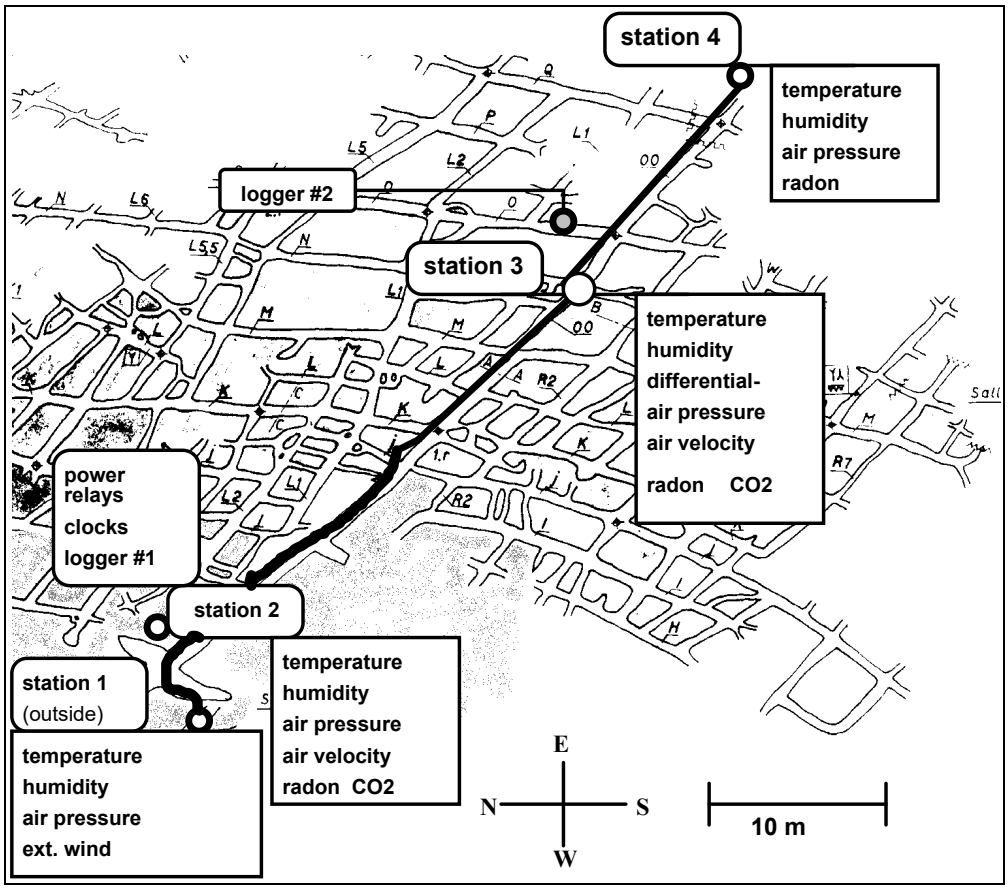

Fig.2.3.6. Phymoes installation

A battery driven DCF77 clock was used to manually synchronize the different independant clocks (loggers and CO_2-sensor). The sensors were switched on only every hour for about 20 minutes; this was achieved by inserting a clock and solidstate relay (SSR) into the main power cable. We looked very hard to find a suitable (possibly DCF77 driven) electronic clock to do this simple switching; but alas, all commercially available clocks were either mains driven, needed 24V supply and/or consumed for their own operation much more current than could be saved by switching the anemometers and dew-point sensors off for most of the time.

Finally we transformed an old EPSON PX8 portable computer to work as a switching clock; this computer can be programmed in BASIC to wake up

at certain times for a certain duration; passed this time, it fslls back into sleep mode needing practically no current. A signal fetched from the computer's motherboard was amplified to drive a SSR (solid-state relay) via a CMOS amplifier; this device proved extremely reliable and had a very low power consumption (about 4mA in sleep mode, needed by the CMOS amplifier and SSR). Later on we simplified this somewhat picturesque equipment (which worked without any flaw for practically two years) and built a dual clock device from CONRAD ELECTRONIC (Germany) modules (2 channel module, one module used for even and one for odd hours); removing the original mechanical relays and driving the main SSR directly by the outputs of the amplifier transistors enabled an overall power consumption for the whole installation of 4mA in sleep mode, 100 to 200mA in normal wake-up mode without the CO_2 sensors running, and 1.4A when all sensors were active.

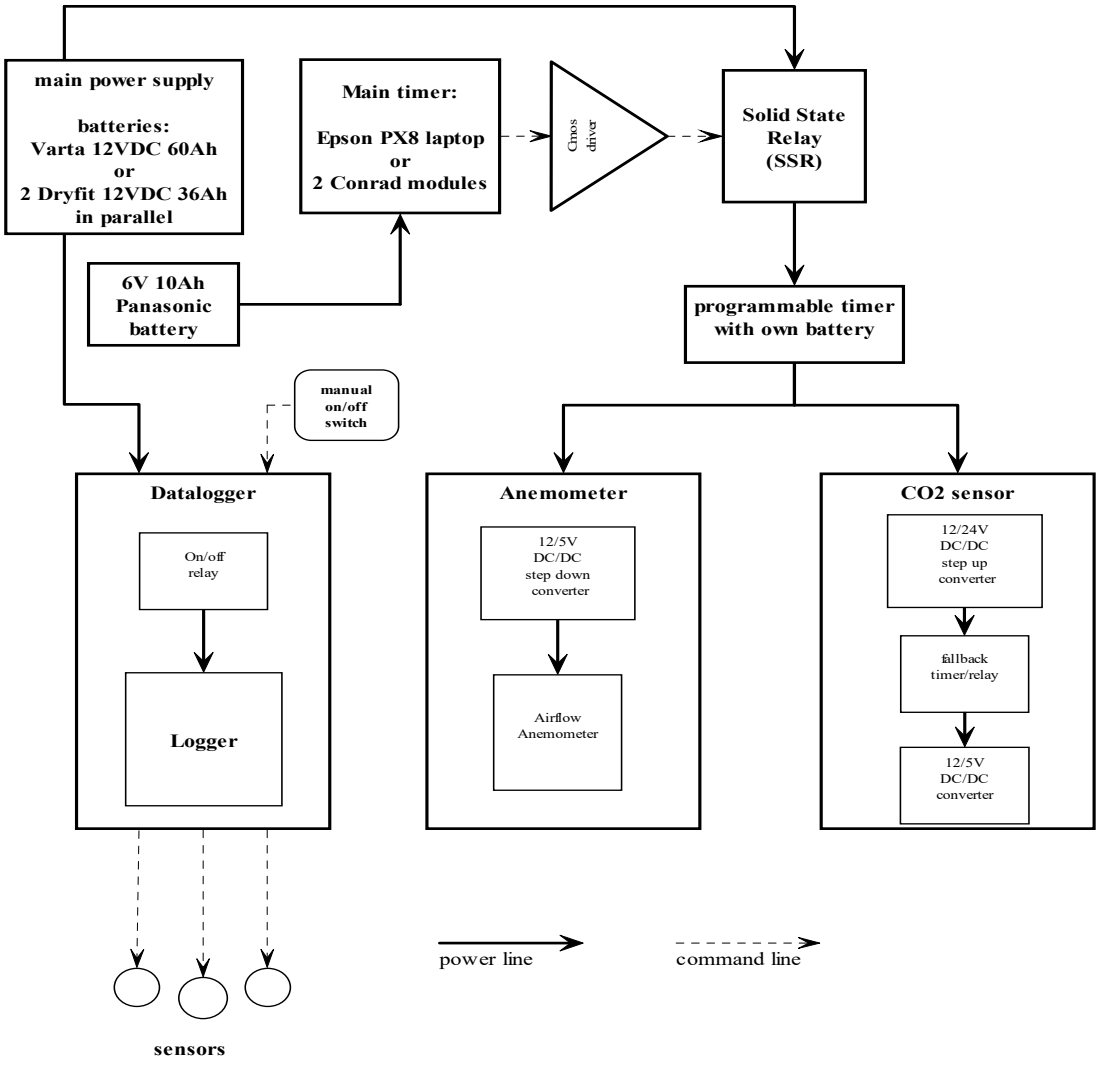

Fig.2.3.7. Overall power distribution

Figure 2.3.7. summerizes the general power distribution. The main 12VDC lead-acid batteries had to have an extremely low self-discharge rate, as our loggers usually stopped working when the supply voltage fell below 10.8V. We finally choose two special VARTA (type VSB 12506) 12V/60Ah batteries, which are completely sealed, can be operated in any position and have a discharge close to zero. These batteries behaved extremely well, and showed no degradation with time. Alas, they weighed over 25kp and put a heavy strain on the spinal column of the person who had to carry them on his back. After some near-accidents and increasingly severe back problems, we replaced these batteries in the last year by 12V Dryfit A500 "Solar" batteries from CONRAD Electronic (36Ah nominal charge) connected in parallel. These batteries were much lighter (12kp) but showed considerable self-discharge and ageing, and could not achieve the perfect operation of the original VARTA types.

2.3.10. Measurement Strategies

The measurement strategy had to meet to two opposite constraints:

1. Make many measurements to allow a sufficiently precise monitoring of the climatic parameters.
2. Switch on the whole equipment as little as possible to conserve electrical power.

As temperature, humidity and atmospheric pressure vary relatively slowly, one measurement per hour of these parameters seemed adequate. CO_2 concentrations experience rapid changes due to varying air flow conditions (intensity and direction), but as the operation of the CO_2 sensors imposed such a drain on the batteries, we decided to make only one measurement every 2nd hour, and to interpolate missing data later.This procedure was checked against hourly monitoring and found accurate enough.

Air flow was the most difficult parameter to monitor; air flow near the entrance of the cave is turbulent, and varies constantly. Even at station 3 , where the flow is practically laminar, its intensity often changes considerably on time-scales as small as several seconds; clearly one single measurement per hour would be a hit-or-miss exercice! Actually, as we were mostly intererested in wind-activity, we decided to make every hour eight measurements spaced one minute apart. For data analysis the mean of these 8 values was kept as representative value for the effective wind-activity. This strategy gave a very good recording of the overall wind pattern, and allowed to differentiate clearly between periods of low activity and periods of fast air movements. Besides these measurments a precise velocity pattern was being monitored separately from time to time.

A problem showed up when we first started the CO_2 measurements; the electrical pump and the quartz-clock of the sensors heavily disturbed the small voltage-signals of the anemometers, barometers and differential manometers. We solved this problem by never operating the CO_2 sensors when reading the other sensors. As the Mikromec dataloggers are able to run simultanously 9 independant monitoring programs, this was easy to implement.

The following table summarizes the overall recording strategy. As pointed out before, the electrical intensity to drive the loggers and all sensors was about 1.4A; this fell to 200mA if the CO_2 sensors were not working. The maximum daily consumption was 2.7 Ah, self-discharge of the batteries not included.

Table 2.3.1.

Instrument	***Switched on/off at hh:mm/hh:mm***	***Reading done at hh:mm***	***Comment***
Datalogger	xx:00 /xx:16		*8 programs simultaneously used; 9th program spare for fast measurements*
Thermometer	xx:00 /xx:16	xx:10	*readings stored by logger program #3*
Hygrometer	xx:00 /xx:16	xx:10	*readings stored by logger programs #1 to #7*
Barometer	xx:00 /xx:16	xx:10	*readings stored by logger programs #1 to #7*
Anemometer	xx:00 /xx:16	xx:10 to xx:16 *at 1 minute interval*	*readings stored by logger programs #1 to #7*
Differential Pressure	xx:00 /xx:16	xx:10 to xx:16 *at 1 minute interval*	*readings stored by logger programs 1 to 7*
CO2 Sensors	xx:00/xx:06	xx:03	*3 minutes time-lap to ensure warming up of sensor; 3 minutes after reading to assure that CO2 operation never coincides with anemometer readings. Readings are stored by logger program #8.*

The power requirements of the different sub-systems are given in table 2.3.2.

Table 2.3.2.

System	*sleeping*	*awake*	*Comment*
Timer/relay	4 mA	44 mA	
Cmos driver	0 mA	1 mA	
SSR	0 mA	5 mA	
Epson PX8	0 mA	80 mA	*own battery*
1 datalogger	0 mA	80 mA	*there are 2 dataloggers*
1 anemometer	0 mA	60 mA	*there are 2 anemometers with DC/DC converter. Intensity increases with wind velocity*
1 CO2 sensor	0 mA	600 mA	*sensor + pump 300 mA*
			DC/DC converter 300 mA
Total	**4 mA**	**max. 1.53 A**	

The typical discharge curves of the Dryfit A500 batteries (2 batteries in parallel) are given on the following figure; one can see that a discharge of 31.5 Ah produces a voltage drop of about 1.46 V. For the period given in the figure the daily energy consumption is 3.5 Ah; the excess of 0.8 Ah to the value given above is mainly caused by the self-discharge of the Dryfit batteries.

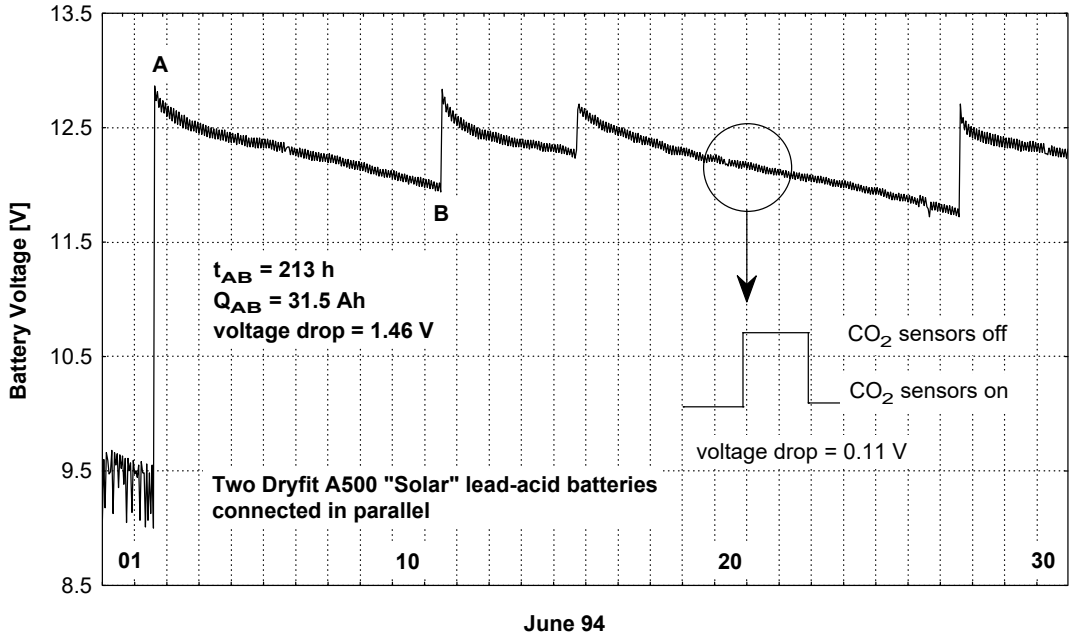

Fig.2.3.8. Discharge curves of the 2 Dryfit batteries connected in parallel. A discharge of 31.5 Ah causes a voltage drop of 1.46 V. Zoom shows that line-voltage drops 0.11V when the two CO2 sensors start operating. Low voltages on the left of the graph are due to exhausted batteries.

References

ANDRIEUX, C. - Contribution à l'Etude du Climat des Cavités Naturelles des Massifs Karstiques. Annales de Spéléologie, XXV, fasc.2, p.1 -239. 1970.

CRC Handbook of Chemistry and Physics - 67th edition. CRC Press. 1986-87.

CHOPPY, J. - Microclimats. Phénomènes Karstiques, Processus Climatiques, 4e partie, p.53-58. Spéléo-Club de Paris. 1990.

RECKNAGEL, Sprenger, Hönmann - Taschenbuch für Heizung und Klimatechnik 92/93, p. 104. OldenbourgVerlag. 1992.

2.4. Equipment Selection Guidelines and Environmental Specifications for Electronic Instrumentation in Caves

Guy Schintgen

2.4.1. Introduction

The guidelines for selecting a professional measuring system and the necessary environmental protection strategies should be based on experience in similar ambient conditions. However, the harsh climatic conditions in caves are not commonly found in industrial areas. Industry-grade materials like casings and cables may not necessarily work for long time spans in the damp and badly ventilated cave atmosphere.

The lack of a domestic voltage supply was an additional problem in the Moestroff Cave, which further restricted the choice of possible and available materials.

2.4.2. Instrumentation

Instrumentation, cabling and housings had to be compatible with the ambient conditions prevailing in the cave, i.e. a nearly constant temperature of about 10ºC and a relative humidity exceeding 95%. Equipment of protection level IP 65 (water-jet protection from all sides) appeared to be a good starting point. Connecting elements which penetrate the housings entail however a diminution of protection, especially connectors which do not possess a closing cap. Mounting all instruments into IP 65 grade enclosures would appear to be the ideal solution, but this is not the case in practice. If the enclosure has to be opened in the cave atmosphere in order to check the instrumentation, the humid cave air will invade the housing and will thus be locked up in it when it is closed again. Condensation, corrosion and other unwanted phenomena are to be expected without adequate counter-measures.

It was obvious that only rot-proof enclosures made of glass fibre-reinforced polyester could be used. In a research project which would last over 3 years, steel enclosures would not have been able to survive under prevailing conditions.

Industrial instruments work preferably with 230VAC or 24VDC; for the Phymoes project we had to use a supply of 12VDC provided by lead-acid batteries for several reasons. The available capacity of these batteries further restricted the choice of available instruments. The lack of 230VAC

voltage supply also precluded the usage of power-hungry heating resistors inside the enclosures, so we had to step down to more basic methods of dehumidification. A cloth bag with a generous amount (about 300g) of desiccant (Silicagel) proved to be very suitable in practice, as this product can be regenerated and used many times over.

In choosing the measuring instrumentation, we often had to decide whether it would be better to develop the instruments ourselves, or buy what was available on the market and adapt it to our requirements. In fact both possibilities had to be used.

Only some of the instruments could be connected directly to the available distribution voltage, while a voltage adaptation with DC/DC converters had to be built for other instruments. Special attention was paid to the possibility of cross-linking the instruments. The data-loggers had to be read-out from the cave entrance via a serial-type network laid inside the cave. This involved modifying the data-loggers in order to be able to switch them on and off remotely.

Fig. 2.4.1. shows part of the equipment installed at Salle Loubens, 6 m from the cave entrance.

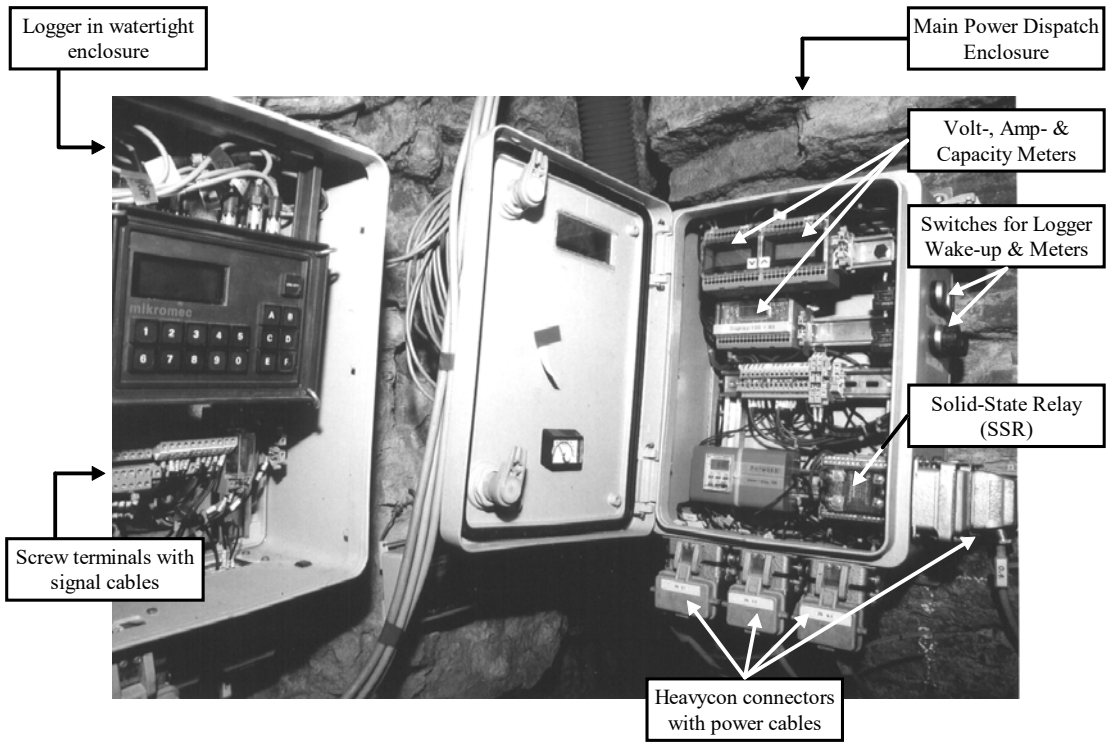

Fig. 2.4.1. Logger and main power switching equipment at Salle Loubens.

2.4.3. Connecting Techniques

A cave research project extending over many years makes great demands on the cables and the attached connecting elements. As the whole equipment was to stay in place to be used eventually in some future, we planned a plug and socket connection system.

Military plug and socket connectors seemed very suitable, as they are tough, compact and adequate for low voltages and currents, with gold-plated contacts and fool-proof interlocking systems. A great disadvantage is that they are not available in small quantities at a reasonable price. We preferred to use industrial connecting techniques based on PHOENIX CONTACT Heavycon connectors. These multi-pole connectors are made from tough compressed cast aluminium enclosures protecting the inside contacts against mechanical damage, dust, dirt and humidity as well as corrosive atmosphere.

The cable entrance is realised with preinstalled PG round cable glands with a neoprene sealing ring that can be cut out, as well as a pressure screw. These enclosures respond to protective standard IP 65 in accordance with IEC 529/DIN VDE 0470-1 when locked. All enclosures can be chosen with male or female connector elements. Through the asymmetric form of the insulating elements a wrong plugging of upper and lower elements is avoided (wrong polarity protection). As our enclosures include several sockets of the same polarity, a supplementary codification through a coding billet was necessary. The chosen contact blocks are made of glass fibre-reinforced polyamid, and the contact elements are made of silver-plated CuZn alloy. The electrical resistance of the contacts according to IEC 130-1/DIN 41630 is equal to 1.5 mΩ.

2.4.4. Cables

The cables to be used had to resist the tensile stress that occurs during installation and later cave visits. They also needed to be resistant to a corrosive environment (as leaking acid from batteries), and must be rot-proof and highly flexible. For these reasons heavy tough-rubber sheathed flexible cables were ruled out, and cables with a neoprene sheath were selected instead (ÖLFEX-110).

On both ends of each cable suitable identification labels were attached. In order to avoid problems with dissimilar end connections, the cables were always symmetrical. Thus, we did not have to pay too much attention during the installation, as each end fits. This system also involves a codification of the plug and socket connections on enclosures and cable ends.

The various characteristics like type, sex, pin layout of the connectors and cables was written down in a precise technical documentation; all references used were repeated systematically on the labels of the connector sleeves (fig.2.4.2).

Kabelbezeichnung : 2.1
Funktion : Daten-Steuerkabel vom Zentralgehäuse ZEN zum Mikromecgehäuse MIK1
Leitungstype : Ölflex-110 mit numerierten Adern
Aderzahl + Querschnitt : 10 x 0,5 qmm
Länge : 15 m
Konfektionierung Ende 1 : Heavycon Tüllengehäuse HC-B10-TFL/PG16G, mit Buchseneinsatz HC-B10-EBUS, Codierbolzen nach Bild 2
Anschlussbelegung Ende 1 :
1 : TxD
2 : RxD
3 : GND
4 : CTS
5 : RTS
6 :
7 :
8 :
9 : aktiv/passiv Umschaltung
10 : aktiv/passiv Umschaltung, grün-gelb

Konfektionierung Ende 2 : Heavycon Tüllengehäuse HC-B10-TFL/PG16G, mit Buchseneinsatz HC-B10-EBUS, Codierbolzen nach Bild 2
Anschlussbelegung Ende 2 :
1 : TxD
2 : RxD
3 : GND
4 : CTS
5 : RTS
6 :
7 :
8 :
9 : aktiv/passiv Umschaltung, -12 V
10 : aktiv/passiv Umschaltung, grün-gelb, Spule Relais
Bemerkungen: Grün-gelbe Ader wird auf Pos 10 benutzt

Fig.2.4.2. Extract of Technical Cabling Documentation

2.4.5. Conclusions

The care and effort taken in selecting the right equipment paid off: during the whole time-span of the Phymoes project, the only occurence of a problem related to cabling was a short circuit provoked by mice eating through one of the more fragile signal cables. The industry-grade enclosures, connectors and main cables behaved extremely well, and assured the continuous working of all instruments without any of the problems which often plague field measurements done without rigorous environmental protection measures.

2.5. Labour and Cost

Francis Massen

The work on project Phymoes started in 1990 with the first inquiries and procedures to lay the foundations for a proper research project. Some preliminary instruments were bought to make first spot measurements in order to get an idea of the magnitude of the parameters to be measured; a lot of time was spent to search for proper equipments, to construct the necessary hardware to make the access to the cave easier and to protect its entry. The period of continuous measuring started mid-July 1991 and ended September 1994 for most of the measurements.

The Phymoes team did not register every working hour done on the research project. Actually the cave-book which gives the time spent by the different members in the cave itself is the only written log. This time amounts to a total of approximately **800 man-hours**.

Besides this, the normal research work done in the lab or at home, the time taken in preparing papers, symposiums (as the International Symposium on Karst and Hydrology CIK), attending meetings and so on is several magnitudes higher. A serious check, based mainly on the work done by the project leader suggest that the in-cave time represents at most 5% of the total workload. This yields a time of about **16000 man-hours** or roughly **9 man-years**. As mentioned before, all this work was done free of charge.

The total credits allocated by the CRPCU to Phymoes amount to

LUF 2 300 000.- or US$ 74 000.-

Besides this sum, generous contributions were made by different sponsors, as listed below:

Subsidies of the R&D organisation of the Ministry of Education:	*227 000.-*
Subsidies of the Ministry of Education (software acquisition):	*125 000.-*
Sponsoring PHOENIX CONTACT:	*160 000.-*
Sponsoring Centre Universitaire (CIK, approx.):	*30 000.-*
Sponsoring Banque Générale (CIK, approx):	*25 000.-*
Sponsoring Commune de Diekirch (CIK, approx):	*38 000.-*
Service Géologique (water analysis, approx.):	*15 000.-*
Division de la Radioprotection (Radon dosimetry):	*200 000.-*
Labour done by Laboratoire de Physique, LCD (approx.)	*160 000.-*
Instruments bought by Laboratoire de Physique LCD:	*140 000.-*
Total:	***LUF 1 120 000.-***
	US$ 36 000.-

The total expenditure for the Phymoes project thus equals

LUF 3 420 000.- , or US$ 110 000.-

Even if this appears to be a significant amount, it would not have been possible to pay for the man-power involved. Using a very modest pay of LUF 500.- per man-hour yields a total of 8 million LUF, which would have pushed up the total project cost to a staggering LUF 11 million! The above amount does not include travelling costs, which have not been refunded to the team members.

The fact that all the funds available for this research project were used for buying equipment and covering running costs, and none for paying salaries and travel costs, remains probably an exceptional situation and should not be used as a guide line in planning future research projects. This was possible because all Phymoes members (except one) had a fully paid professional activity which covered their living expenses, and because they were willing to contribute their year-long efforts free of charge.

Part 3

Climatology

Part 3 Climatology

The study of underground climate requires the analysis and synthesis of large datasets involving many parameters, which are often not interrelated. Nevertheless, in a first step, let us analyze the most important parameters one per one; later on we will examine the possible relationships between these parameters.

3.1. Temperature

Francis Massen, Antoine Kies

3.1.1. Mean Temperatures over a 12 Month Time-Span

Regular recordings started on the first October 1991 and stopped on the 30th September 1994 which corresponds to a 3 year time-span; bad data (generally due to a faulty Rotronic sensor) have been interpolated where necessary. The contiguous good Rotronic data from station 4 are too sparse to give meaningful averages over a complete 12 month period. As the Hamster logger started recording on 5th May 1993, we nevertheless have a reliable picture for station 4 from that day on to September 1994.

The results of temperature measurements (in °C), rounded to the first decimal can be seen in table 3.1.1.

Several conclusions can be drawn from this table:

1. The mean deep-cave temperature is 9.4 °C; this is 1.6 °C higher than the temperature given by Choppy's law [Choppy, 1990], which expresses deep-cave temperature (including ice-caves!) as a function of latitude and altitude :

$$T = 54.3 - 0.9 * latitude - 0.006 * altitude$$
$$= 54.3 - 0.9 * 50 - 0.006 * 250$$
$$= 7.8\ ℃ \qquad \textit{[eq. 3.1.1]}$$

2. The differences between the yearly maximum and minimum temperatures at a given location decrease rapidly with increasing distance: an exponential fit on the maxima and minima of the 8760 hourly data from Jan.1993 to Dec.1993 gives the following result:

$$dT = 43.9 * e^{-0.099 * x} \qquad \textit{[eq. 3.1.2]}$$

where 0.099 represents the damping factor leading to a temperature relaxation length of 1/0.099=10 m for the cave air.

3. In 1993 there is a delay of about 45 days before the maximum outside temperature (06 Aug. 93) has reached station 4 (20 Sep. 93); the corresponding delay, before the following outside minimum (21 Feb. 94) can be first detected at station 4 (06 May. 94), is 74 days; no such clear-cut delays can be found for stations 2 and 3.

Table 3.1.1.

Station	*Sensor*	*Period*	*Mean +/- Std*	*Max. and Date*	*Min. and Date*
station1	***Rotronic***	*Oct91-->Sep92*	9.5 +/- 6.4	31.7	-6.3
(x=0m)				09 Aug 92	15 Dec 91
This is the outside reference		*Oct92-->Sep93*	9.7 +/- 6.5	36.1	-7.8
station				06 Aug 93	04 Jan 93
.		*Oct93-->Sep94*	10.3 +/- 7.4	39.8	-7.8
				03 Aug 94	21 Feb 94
		Oct91-->Sep94	9.9 +/- 6.8	39.8	-6.3
				03 Aug 94	15 Dec 91
station2	***Rotronic***	*Oct91-->Sep92*	10.7 +/- 2.3	18.5	5.1
(x=12m)				27 Jul 92	20 Dec 91
		Oct92-->Sep93	9.7 +/- 1.9	17.6	4.1
				16 Jul 93	06 Apr 93
		Oct93-->Sep94	10.4 +/- 3.0	18.8	2.9
				28 Jul 94	24 Dec 93
		Oct91-->Sep94	10.2 +/- 2.5	18.8	2.9
				28 Jul 94	24 Dec 93
station3	*Rotronic*	*Oct91-->Sep92*	9.8 +/- 0.6	10.9	8.8
(x=31m)					
no dates given, as max. and		*Oct92-->Sep93*	9.5 +/- 0.4	10.6	8.6
min. are so close					
		Oct93-->Sep94	9.0 +/- 0.2	9.4	8.2
		Oct91-->Sep94	9.4 +/- 0.5	10.9	8.2
station4	***Hamster***	*May93-->Sep93*	9.4 +/- 0.1	9.6	9.4
(x=50m)					
no dates given, as max. and		*Oct93-->Sep94*	9.4 +/- 0.1	9.6	9.3
min. are so close					

4. Curiously at the timescale of 1 hour, the maximum temperatures at station 2 (x=12 m) do occur prior to the outside maxima, the lead time being 13, 21 and 6 days for the years 1992, 1993 and 1994. During this summer period, the wind always blows into the cave, so one should expect that the cave maxima would follow the outside ones. This is indeed the case in 1993 and 1994 (but not in 1992) if the analysis is done on the daily mean temperatures, which are not so strongly influenced by the momentary outside wind pattern.

   If dry outside air enters the cave, it evaporates a greater quantity of water than does a more humid air. The latent heat needed for condensation is higher for dry air, so dry air induces near the entrance a stronger cooling effect than humid air.As a consequence, at periods of hot and dry weather, temperatures near the entrance may be lower than they are at periods of

rainfall. Alas, the mean outside humidities in July and August are very similar, so this hypothesis could not be confirmed by our data.

The convective heat transfer seems to be rather negligible for station 4, contrary to what happens for the other two stations at x=12 m and x=31 m. The main heat transfer mechanism into the deepest cave locations is pure conduction.

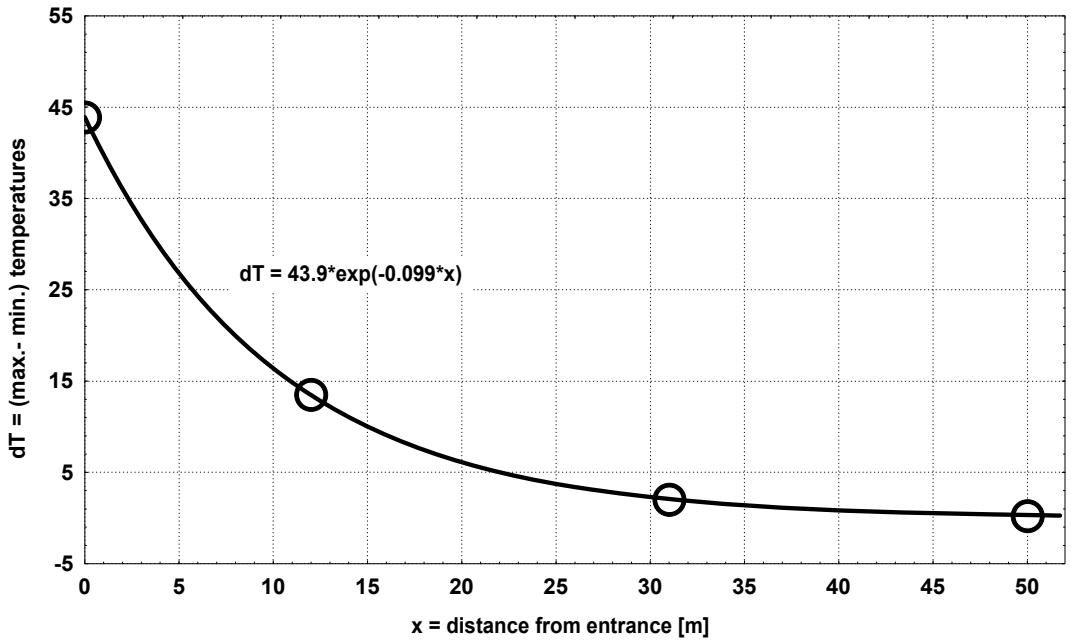

Fig.3.1.1. Difference of yearly maximum and minimum temperatures versus distance from entrance (year 1993)

3.1.2. Finding a Mathematical Model for T(t,x)

Cave air temperature is caused by heat flow into or out of the cave. The Moestroff Cave is a maze of very narrow galleries embedded into a relative great rock block, so the ratio of voids to solid matter is small. This means that in a first try one could compute T(t,x) by assuming that all heat reaches the cave by conduction trough the solid rock matter. To find T(t,x) we will use Fourier's law of heat conduction; a similar computation can be found in [Lebrun & Tercafs, 1972].

Fouriers equation of heat flow states:

$$\frac{\delta\theta}{\delta t} = \frac{\lambda}{\rho * c_p} * \frac{\delta^2\theta}{\delta x^2} \qquad \textit{[eq. 3.1.3]}$$

where:

θ = $T-T_0$ = rock temperature at instant t minus yearly mean rock temperature
t time t
λ thermal conductivity of rock
ρ density of rock
c_p heat capacity of rock
x distance to the rock surface

Let us start by using the mean monthly temperature values. Fourier's model assumes that the cave is embedded in a solid block of Muschelkalk; the cliff with the entrance represents the interface between the outside with its yearly cosine temperature pattern and the rock. Heat flows only from this cliff into the rock mass; in this simple one-dimensional model any heat flow from the rocks situated above or sideways is neglected. This assumption may be questionable, as the vertical heat flow from above into cave, located approximately 30 m deeper, is probably not negligible.

The solution of Fourier's differential equation for conductive heat-flow gives, using the boundary conditions formulated above:

$$T(x,t) = T_0 + A * e^{-k*x} * \cos(\omega * t - k * x + \varphi) \qquad \textit{[eq. 3.1.4]}$$

where:

x distance from entrance [m]
T_0 mean yearly outside temperature [°C]
t time [month]
A temperature amplitude = (yearly_maximum - yearly_minimum) [°C]
ω pulsation = $2\pi/12 = 0.5236$ [rad/month] = $2.02*10^{-7}$ [rad/s]
φ phase = π [rad] if origin of time (t=0) is January
k damping factor depending on pulsation ω, rock density ρ, heat capacity c_p and thermal conductivity λ

$$k = \sqrt{\frac{\omega * \rho * c_p}{2 * \lambda}} \qquad \textit{[eq. 3.1.5]}$$

The density and the heat capacity of the Muschelkalk have been measured very precisely on 11 rock samples taken from the cave; the thermal conductivity is a value that can be found for instance in Recknagel, the CRC handbook or Badino [Recknagel, 1992; CRC, 1986; Badino, 1995]:

- density of Moestroff Cave rock (Muschelkalk): $\rho = 2676 \pm 5$ [$kg*m^{-3}$]
- heat capacity of Muschelkalk: $c_p = 828 \pm 40$ [$J*kg^{-1}*K^{-1}$)]
- thermal conductivity of rock (Muschelkalk): $\lambda = 1.60$ [$W*m^{-1}*K^{-1}$]

The measured density of the Moestroff Muschelkalk is in good agreement with values published for dolomite or limestone:

- Limestone Pennsylvania : 2690 [kg*m^{-3}] [Handbook of Physical Constants]
- Dolomite: 2860 [kg*m^{-3}] [CRC Handbook,,1986]

The measured heat capacity differs by about 10% from the value of 929 given by the CRC Handbook for dolomite; Choppy gives c_p=420 for limestone, which seems far too low.

Using these values leads to a damping factor of **k = 0.37** [m^{-1}]

As we want to apply Fourier's equation on a time-step of a month, all relevant temperatures are computed from monthly averages, which were in 1993:

- mean yearly outside temperature = 9.5 [°C]
- maximum outside temperature =16.9 [°C]
- minimum outside temperature = 1.1 [°C]
- (yearly_max - yearly_min)/2 = amplitude = 7.9 [°C]
- period = 12 months

This gives the following result:

$$T(x,t) = 9.5 + 7.9 * e^{-0.37*x} * \cos(0.5236 * t - 0.37 * x + \pi)$$

[eq 3 1.6]

Using this equation, let us compare the measured and computed differences between the 1993 maximum and minimum values at the different stations (remember we consider here the monthly mean values!):

Table 3.1.2.

Station	*Measured Temperature [°C]*			*Computed Temperature [°C]*		
	maximum	*minimum*	*difference*	*maximum*	*minimum*	*difference*
1 (x=0)	16.9	1.1	15.8	17.4	1.6	15.8
2 (x=12m)	12	6.8	5.2	9.5	9.4	0.1
3 (x=31m)	9.8	9.0	0.8	9.5	9.5	0
4 (x=50m)	9.6	9.4	0.2	9.5	9.5	0

We clearly see that due to the high damping factor of 0.37 the differences between the maxima and minima computed with Fourier's law decrease much more rapidly than the measured data. Fourier's model does not take into account any convective heat transfer. As convection does certainly play a major role in the main gallery, we try to find a «Moestroff» damping factor k by fitting the measured data to equation

$$T(x,t) = 9.5 + 7.9 * e^{-k*x} * \cos(0.5236 * t - k * x + \pi)$$

[eq. 3.1.7]

Actually we can apply this computation to two different data sets:

1. The monthly mean air temperatures from the datalogger values: we have nearly 3 full years available (1994: January to November only), with 12 data-sets per year for each of the 4 stations. We have thus a good temporal resolution but a poor spatial one (only 4 values distributed from x=0 to x=50 m).

2. During 1992, 1993 and 1994, several manual temperature measurements were done using always the same 3 Testoterm sensors (precision 0.1°C) for air, surface and soil temperature; the measuring points were taken at x=0, 1, 2, 3, 4, 6, 12, 20 ,31, 38 and 50 m, and as a general rule temperature was measured at the bottom, at mid-height, at the ceiling and in the muddy soil covering the gallery.

   Five temperature profiles where made during 1992 (January, February, March, June and November) and six during 1993 (February, March, July, September, November, December): this gives us a rather fine spatial resolution, but a poorer temporal resolution than the monthly means.

   The ceiling air-temperatures were always, as expected, higher than the bottom air temperature and from point x=30 m onwards, the operator's presence increased the actual air temperatures considerably; as a consequence, Fourier's law might best be compared to the results given by the (undisturbed) soil temperature measurements.

   The table gives the results of the different computations; the parameter R expresses the coefficient of determination of the fit, and r the linear correlation between predicted and observed values; the best fit gives both R and a r close to 1. The non-linear fit to Fourier's equation was done using a combined Quasi-Newton-Simplex algorithm [Statistica version 4.5 software]. The table shows that the damping factors calculated from the two datasets differ by approx. 20%

   As the hourly 1993 data give a damping factor of k=0.099, the fitted values of the table are in good agreement. The differences between the theoretical (0.37) and experimental damping factors reflect the major influence of the convective heat transfer. Convection is a far more effective heat transport mechanism than conduction through the rock, which explains that the experimental damping factor is considerably lower than the theoretical one.

Table 3.1.3

Year	*Dataset*	*Number of Data*	*Mean (1)*	*Ampl. (2)*	*k (3)*	*R (4)*	*r (5)*
1992	*logger-data*	48	9.84	8.0	0.076	0.92	0.93
	manual-data	84	9.84	8.0	0.119	0.92	0.97
1993	*logger-data*	48	9.46	7.9	0.098	0.94	0.95
	manual-data	70	9.46	7.9	0.122	0.90	0.91
1994	*logger-data*	44	10.9	10.3	0.076	0.76	0.91
	manual-data	??	10.9	10.3	??	??	??

Note 1: mean yearly temperature computed from monthly means
Note 2: amplitude of cosine-wave
Note 3: damping-factor k found from fit
Note 4: coefficient of determination
Note 5: correlation between predicted and ob-served data

Fig. 3.1.2 shows the profiles of the soil temperature measured manually in five different months of 1993. The March 1993 curve shows the typical spring minimum near the entrance which is also given by the fitted Fourier profile; in this case the fitted damping factor is k=0.151.

As a conclusion one could say that the general form of Fourier's law gives a reasonably good model for computing T(t,x), if we divide the theoretically computed damping factor by approximately 4.

If we take k=0.1 as the mean damping factor, we should expect a phase-lag of 0.1*50 = 5 radians (i.e. 9.5 months) between the instants of the outside maximum and its occurrence at station 4; the amplitude of the thermal wave should be less than 0.1°C. Clearly our data cannot validate this: the precision of temperature measurements is too small, and the only possible time-lag found lies in the range between one and two months.

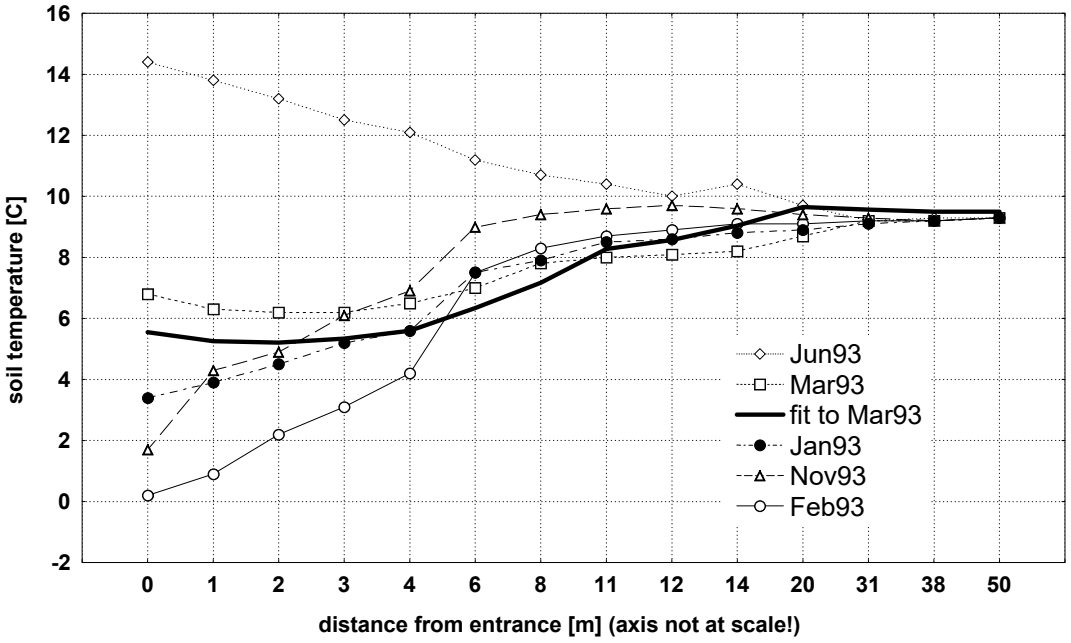

Fig.3.1.2. Profile of soil temperature for 1993 derived from manually measured data

3.1.3. Computing T(x) Using a Convective Model

Cigna develops in his paper [Cigna, 1961] a model for computing T(x) assuming a convective heat transfer from outside to inside. The following assumptions are made (fig. 3.1.3.):

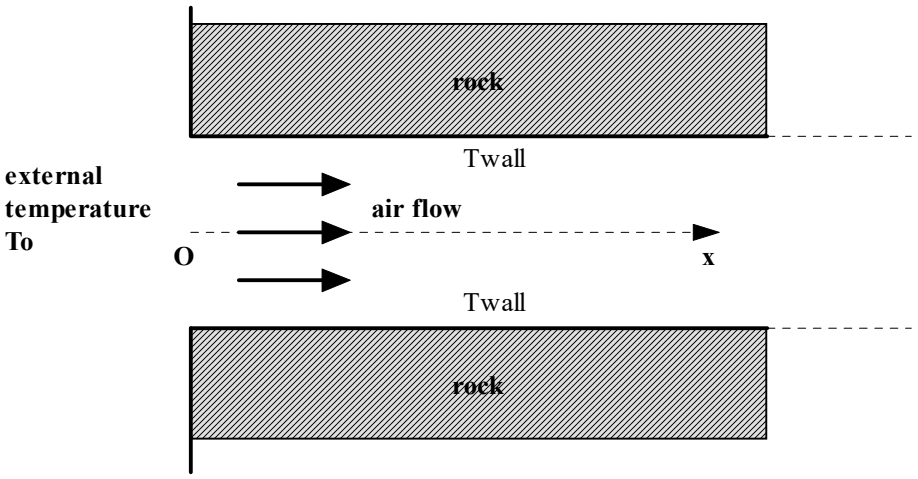

Fig.3.1.3. Cigna's model for computing T(x)

- the cave extends horizontally into the rock matrix
- the cave has a constant section, and its walls are at constant temperature
- the air flows with constant velocity v into the cave with negligible turbulence
- the outside temperature is constant

In that case, the temperature profile is given by the following expression:

$$T(x) = (\ T_0 - T_{wall}) * 0.692 * e^{-23.136 * \frac{D*x}{d^2*v}} + T_{wall} \qquad \textit{[eq. 3.1.8]}$$

where:

To	outside temperature [°C]
T_{wall}	wall temperature [°C]
D	diffusivity of air [m^2*s^{-1}]
d	hydraulic diameter of cave [m]
v	air velocity [$m*s^{-1}$]

Let us apply this formula to the situation on 20 June 1994, 07:00 UTC, and compare the results with manual measurements. We will restrict the computation to the first 20 meters and take as constant wall temperature the measured temperature at x= 11 m. The mean air velocity will be 60% of the value measured at station 2.

This gives the following situation:

- T_{wall} =	11.1 [°C].
- T_0 =	13.3 [°C]
- mean velocity ≈ 0.6*velocity at station 2 =	0.17 [$m*s^{-1}$];
- mean hydraulic diameter ≈	0.65 [m]
- measured air density ρ inside the cave =	1.2 [$kg*m^{-3}$]
- c_p of air =	1005 [$J*kg^{-1}*K^{-1}$]
- λ_{air} ≈	0.025 [$W*m^{-1}*K^{-1}$]
- diffusivity $D = \lambda/(\rho*c_p)$ ≈	$1.66*10^{-5}$ [m^2*s^{-1}]

The equation computes to

$$T(x) = 1.52 * e^{-0.0052*x} + 11.1 \qquad \textit{[eq. 3.1.9]}$$

Fig. 3.1.4 shows both the manual measurements and the computed values.

The correspondance between measured and computed values is not good: the damping factor in Cigna's formula is probably much too small. The relaxation length (inverse of the damping factor) is about 192 m; this has to be compared with the more realistic distance of about 10 m derived from the fitting of the Fourier equation to the measured data.

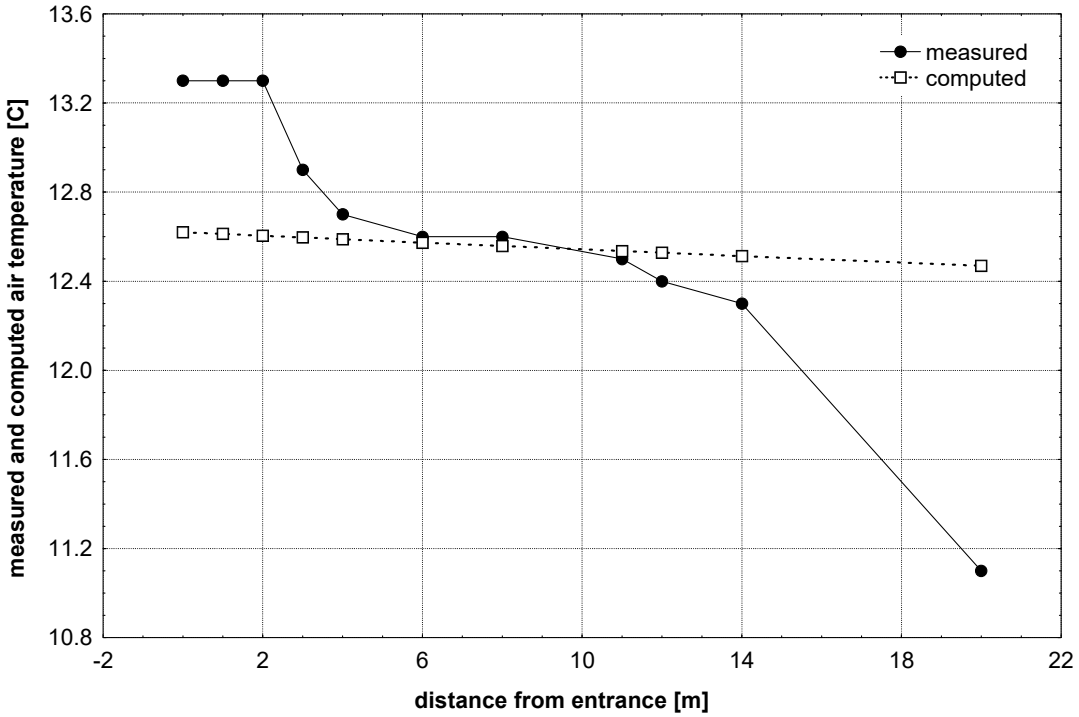

Fig.3.1.4. Computed and measured temperature profile near the entrance.

Wigley-Brown [Wigley, Brown, cit. in Choppy, 1986] give for the relaxation length (computed for a pipe flow) the expression $100*d^{1.2}*v^{0.2}$; this formula yields about 42 m under the above conditions, a value much closer to the observed one.

As a conclusion, one can say that the results of the theoretical model to compute T(x) does not agree well with the actual situation at Moestroff. This may be due to the many simplifying assumptions made, most of which are not met at Moestroff.

3.1.4. Instant Temperature Variations

It seems obvious that we cannot detect anymore the influence of rapid outside temperature variations at locations situated deep in the cave; let us look in this paragraph at what distance from the entrance the daily or hourly variations of the outside temperature can still be detected. Fig. 3.1.5 of the mean daily temperatures shows that the overall seasonal outside pattern can readily be observed at station 2 (one should note that during winter months, the temperature at station 2 often anti-correlates with the outside temperature; as will be seen later, this is due to a different air flow direction).

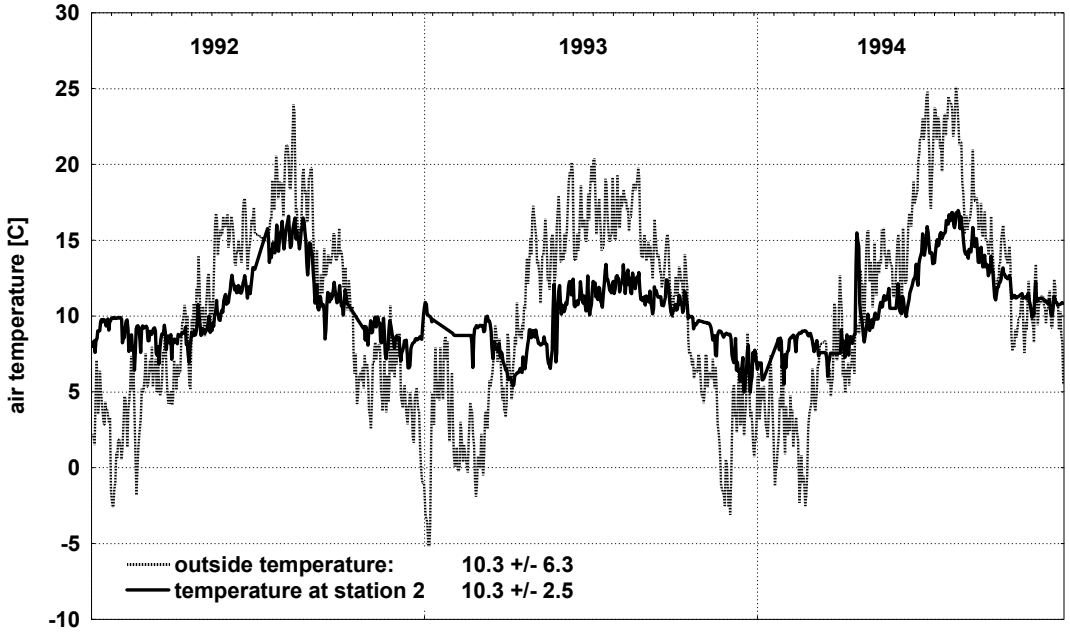

Fig. 3.1.5. Daily mean temperatures at station 1 and 2 from January 92 to November 94

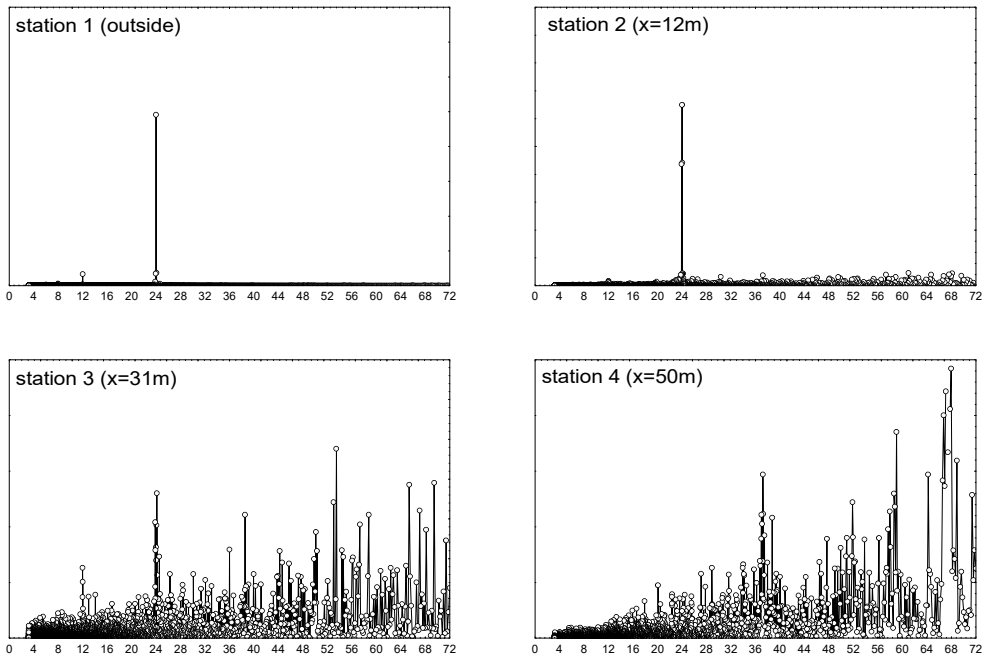

Fig. 3.1.6. Spectral analysis of temperature records from January 92 to November 92 (25 560 data)

The diurnal variations ca be detected up to station 3 (x = 31 m), but are lost at station 4 (x = 50 m): this can be shown by a spectral analysis on the same data set as above (fig.3.1.6, 25560 data points). There is a very clear cut 24h spectral peak at station 2, and a much smaller, but still detectable one at station 3. All diurnal patterns are lost at station 4.

In the successive plots, the different vertical axes have increasingly smaller scales.

References

BADINO, G. - Fisica Del Clima Soterraneo, p.44. Memorie dell'Istituto Italiano di Speleologia. Vol. 7, Serie II. Bologna. 1995.

CHOPPY, J. - La Température des Cavités. Spelunca, no.3, 1980. p.117-119. 1980.

CIGNA,, A. - Air Temperature Distribution near the Entrance of Caves. Symposium Internazionale di Speleologia. Memoria della Rassegna Speleologica Italiana, Como 1961.

CRC Handbook of Chemistry and Physics, 1986-87. - 67th edition. CRC Press

HANDBOOK of Physical Constants - The Geological Society of America Memoir 97. 1966.

LEBRUN, J. & TERCAFS, R. - Etude de la Convection Naturelle dans une Cavité Cylindrique Horizontale soumise à une Onde de Température Longitudinale. Collection des Publications de la Faculté des Sciences de l'Unoversité de Liège. No.34. p. 1-49. 1972.

RECKNAGEL, Sprenger, Hönmann - Taschenbuch für Heizung und Klimatechnik 92/93, p. 104. OldenbourgVerlag. 1992.

WIGLEY, T.M.L. & BROWN, M.C. - The Physics of Caves. In: Ford & Cullingford: The Science of Speleology, p.329-358. Academic Press. 1976.

3.2 Humidity in the Cave

Francis Massen, Antoine Kies

3.2.1. Instrumentation Problems

Of all climatic parameters, humidity surely was the one which was the most difficult to measure accurately and reliably. The problem with cave humidity is that normal levels are always extremely high, close to 100% relative humidity. As the Moestroff Cave has very slow air movements, electronic sensors become soaked with condensing water and cannot make useful measurement anymore.

The Phymoes datanet was based on electronic sensors, so we had to find electronic hygrometers working reliably up to 100% levels for long time spans; fan-driven psychrometers were out of question for reasons of cost and electrical power demand.

We tried several types of sensors:

1. TESTOTERM Hygrotest 600 hygrometer (capacitive sensor): this instrument rapidly went into saturation, even if exposed at station 2 where humidity variations and air flow are relatively important. After some hours of exposure, the readings became meaningless (exceeding 100% rel. humidity)
2. TESTOTERM stand-alone datalogger with integrated temperature and humidity sensor :
   This instrument was tested at the end of project Phymoes for the Luxembourg Testoterm dealer. The temperature sensor worked fine, but the humidity sensor (a special ceramic sensor) went into saturation after several hours of exposure, contrary to the manufacturers specifications which say that this type of sensor should be unaffected by extremely high humidity levels or even condensing water.
3. ISEDD capacitve EE-HC500 sensor : same behaviour as the Testotherm sensor
4. ROTRONIC SA-100 combined thermometer/hygrometer :
   The hygrometer, specified for working up to 100%, became unservicable after several weeks, and never returned to correct operation
5. ROTRONIC YA-100 combined thermometer/hygrometer :
   This sensor is a special version of the preceding one, to be used in difficult weather conditions. It worked much better than the SA-100, but nevertheless we had many breakdowns: some due to bad solder joints, some to amplifier failures, some to failures of the sensing element and some to unspecified breakdowns. The YA-100 used outside the cave mostly worked as specified by the manufacturer; but the constant high humidity levels together with low or even non existent air movements in deep cave locations were much too harsh conditions for this type of sensor.

6. PH. SCHENK Hamster (dual T/H waterproof sealed logger) :
   The hygrometer part of this instrument was almost useless in the cave.

   The humidity levels at station 3 were practically always 100%, as this station has walls constantly covered by a thin water film (water is seeping down through the ceiling fissure), we did remove the hygrometer after several months.

   Station 2 showed quite important variations in humidity; at station 4, small humidity changes could still be measured frequently, so we decided to keep working hygrometers at stations 1 (outside), 2 and 4. In all computations, the relative humidity at station 3 is taken as 100%.

   As the electronic devices behaved in such a pitiful manner, we went back to the basics of humidity measurements by looking for affordable low-power dew-point sensors. We bought two sensors from Kroneis (Austria), and installed them at stations 2 and 4. The results were much better than with the previous instruments; the Kroneis sensors were able to measure very small humidity changes, and worked well for long periods of time. We nevertheless had several breakdowns, one due to a bad NTC sensor, and one caused by water entering the sensor-head.

   These dew-point sensors operate by cooling a small mirror (glued to a Peltier element) down to the point where condensation occurs. This point is detected by comparing the light beams reflected from the cooled and from a reference mirror held at ambient temperature. An NTC sensor attached to the cooled mirror measures the dew-point temperature, and a second NTC sensor the ambient air temperature.

   The relative humidity can be computed from the signals given by these NTC sensors in the following manner:

1. Temperature of NTC-sensor :

$$T = \frac{V - 0.407 * Vref}{0.00559149 * Vref} \qquad \textit{[eq 3.2.1]}$$

   where:

   V voltage output of the sensor
   V_{ref} reference voltage equal to 2.512V (usually read by datalogger)

2. Saturated water-vapour pressure corresponding to a temperature T:

$$p_{sat} = 6.1078 * e^{\frac{17.08085*T}{234.175+T}} \qquad \textit{[eq 3.2.2]}$$

   where:

   p_{sat} saturated water-pressure [mbar, HPa]
   T air temperature [°C]

   This formula from the Smithsonian Meteorological Tables [cit. in Kroneis, W., 1991] is valid for the temperature range of 0..100 °C.

3. Relative humidity =
   p_{sat}(dew point temperature)/p_{sat}(ambient_temperature)*100

3.2.2. Why Measure Humidity in Caves?

There are two main reasons why the knowledge of relative humidity is important :

1. The difference of air densities between outside and the cave air is the most important parameter which commands air movements in a cave like Moestroff.
2. An energy balance can be computed only if one knows the relative humidities of the air entering the cave and the air in the cave itself.

The density of air is a function of temperature, pressure and water content or vapour pressure; several authors like Andrieux, CRC, Recknagel, Choppy give expressions relating the air density to these parameters. In our case, we had to calculate the water vapour pressure from the measured relative humidity and the air temperature. The cave air temperature does not vary widely, so we could use a simple second-order polynomial to compute the saturated water-pressure. The polynomial given by Choppy [Choppy, 1990] has been rechecked and was found adequate. It yields the following expression for the air density:

$$\rho = \frac{0.34855}{273.16 + T} * \left[p - \frac{0.406 * H}{3600} * \left((T + 6)^2 + 180 \right) \right]$$

[eq 3.2.3]

where:

ρ density of moist air [kg/m^3]
T temperature of moist air [°C]
p air pressure [mbar, Hpa]
H relative humidity [%]

3.2.3. Humidity Pattern Outside and In Cave

One consequence of the many breakdowns of the hygrometers is a lack of continuous data of a comparable quality as those given by the thermometers; as a general rule, missing data are interpolated for evaluation. During 1994, a complete misbehaviour of the outside Rotronic sensor at station 1 made its data useless. We used instead the data recorded by a DAVIS weatherstation working continuously at the author's (F. Massen) house, situated about 2 km airline distance from the cave entrance.

The following table resumes the mean values and standard deviations (all values correspond to relative humidity expressed in %) computed from the hourly data (the humidity at station 3 is always 100 %).:

Table 3.2.1.

Location	*1992 (whole year)*	*1993 (whole year)*	*1994 (Jan->Nov)*	*Jan92->Nov94*
Station 1 (x= 0m)	81.6 ± 10.8	78.3 ± 13.3	78 ± 14.1	79.3 ± 12.8
Station 2 (x=12m)	84.2 ± 23.4	93.8 ± 6.3	96.4 ± 2.2	86.0 ± 18.7
Station 4 (x=50m)	97.0 ± 1.2	98.3 ± 0.8	98.6 ± 2.2	98.0 ± 1.7

For 1993 and 1994 the data are of the best quality; the high standard error at station 2 in 1992 is due to the many misbehaviours of the sensor.

Unlike the temperature data, no seasonal pattern is clearly visible for neither station; a spectral analysis done on the complete data-set from Jan.92 to Nov.94 (25560 data points) shows that the 24h peak of the outside (station 1) humidity values can still be detected in the data-series of station 2, but not anymore at station 4 (fig. 3.2.1).

Even if the spectral analysis shows a 24h peak in the station 2 data, the daily changes usually are quite different from those from outside: outside humidity has a distinct 24 hour pattern, but values at station 2 often show rapid oscillations superposed on the periodic background. They reflect the influence of oscillating air movements in the gallery (fig.3.2.2).

During the summer months (a period of inflowing air) the humidity at station 2 oscillates far less than at the outside, whereas the amplitudes can be of similar or even higher magnitude during the colder months. Table 3.2.2. shows the situation for the first seven days of December 92 and August 93.

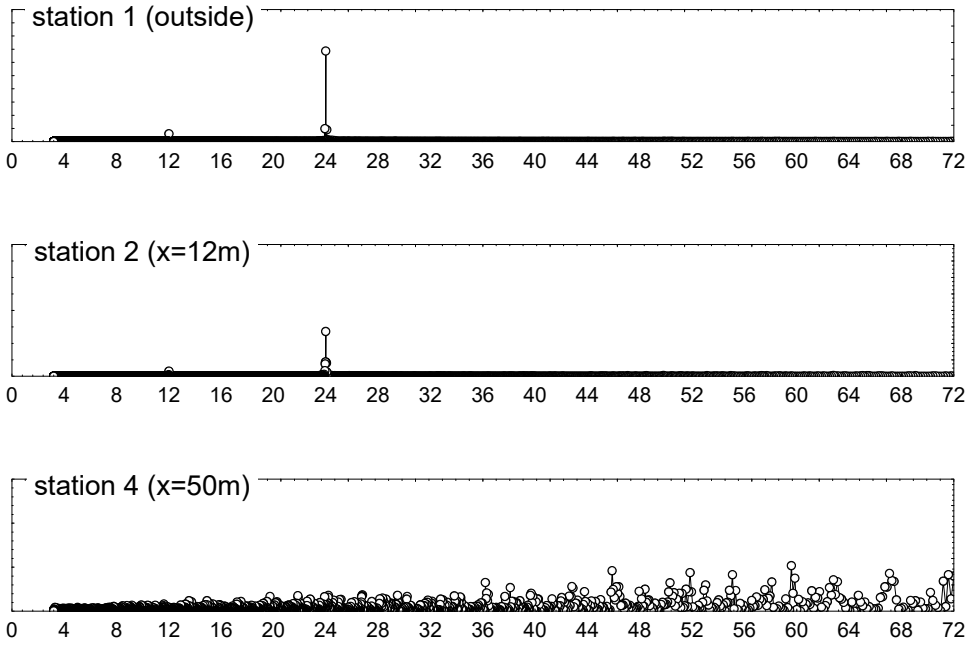

Fig. 3.2.1. Power spectrum of humidity data at station 1, 2 and 4 (Jan.92 to Nov.94)

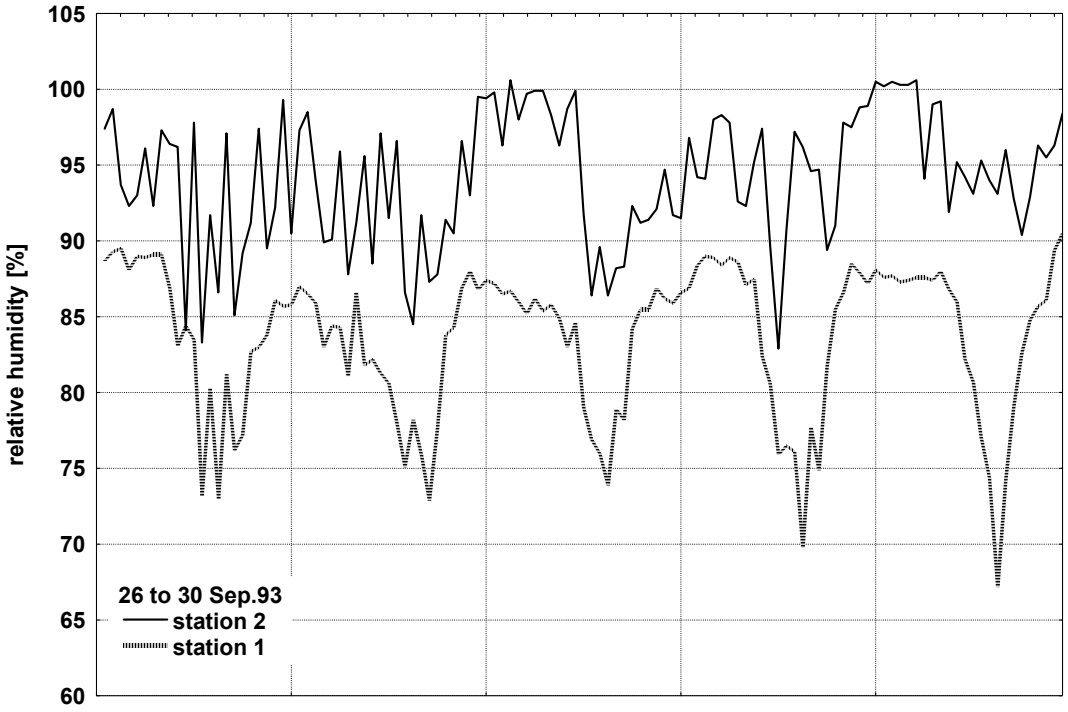

Fig. 3.2.2. Compared daily humidity values at station 1 and 2

Table 3.2.2.

Period	*Mean Outside Temperature [Celsius]*	*Mean Humidity Amplitude (1) A*	*Mean Humidity Amplitude (2) B*	*Quotient of A/B*
1 to 7 Dec.92 (168 measures)	5.9	9.1	14.2	1.56
1 to 7 Aug.93 (168 measures)	17.5	45.9	18.5	0.40

Note 1: difference between daily minimum and maximum relative humidity at station 1
Note 2: difference between daily minimum and maximum relative humidity at station 2

We will see in the chapter on air movements that the difference of the summer and winter air flow can explain this situation.

References

CHOPPY, J. - Microclimats. Phénomènes Karstiques, Processus Climatiques, 4e partie, p.53-58. Spéléo-Club de Paris. 1990.

KRONEIS, W. - Erläuterungen zur Berechnung der Feuchtigkeitsgrössen und zur Anwendung der Tafeln. (instruction notices for the Kroneis NTC dewpoint sensor). 1991.

3.3. Results of the Water Analyses in the Moestroff Cave

Claude Boes, Massen Francis

3.3.1. General Observations and Water Availability

The water analysis in the Moestroff Cave was hampered by several difficulties; the most significant were:

1. The access to the cave and the moving around in the cave caused the same problems than for the monitoring of the other physical values, and the installation of an automatic water analysis station was not possible.
2. The overall amount of water infiltrating into the cave was generally very small during the preparation- and the monitoring-period of the project.
3. The locations where water was infiltrating rather regularly were very scarce in the neighbourhood of the electronic measuring stations.

With the exception of the stalactite/stalagmite site near the "Salle Claude" (M-R6), where after long rain periods, the usual water dripping could change into a constant flow, no other site with large infiltration was accessible in a reasonable time. Even this location could not be regularly monitored, due to the difficult access (gallery with a very flat constriction).

The results of one "water expedition" going into the deeper realms of the cave are incorporated in the tables. The aim was to check locations which were characterized as "water points" during the topography expeditions in the Sixties. This was physically very exhausting (only crawling progression possible with some very flat parts), since all the analysis instrumentation had to be pulled along. The total time, including the water and CO_2-analyses made on the tour, was about four hours, of which three hours of crawling progression. Since there was always a lot of maintenance to be done on the four electronic stations, it was not possible to repeat such expeditions on a regular basis, moreover because the amounts of water found were very small.

The usual amounts of water being so reduced, we had to collect it in polyethylene bottles which we put under "confirmed" infiltration points. To obtain a general appreciation of the amounts of water infiltrating into the cave, an aluminium gutter of 50 cm length was installed on a wall near station 3, which was found to be constantly wet during the preparation period and the first part of the project. Thus it was possible to check not only the amounts of water on a regular basis, but if enough water was present, it could be brought to the laboratory of the *Administration de l'Environnement, Division des Eaux* (courtesy of the *Service Géologique*

du Luxembourg) for a complete analysis. The spacing in time of the samples was therefore dependant on the amounts infiltrating. The chemical analysis results are in consequence always to be considered as medium values over rather long collecting periods (up to 5 weeks). The exact number of days per sample can be found in table 3.3.1. Due to the low variations found, the chemical analysis of the collected water was abandoned in the later stages of the project.

Table 3.3.1.

Start	End	Mid-Period	Days	Vol. [ml]	Vol. per day	Rain Findel [mm]	Rain Findel per day	Rain Bettendorf [mm]	Rain Bettendorf per day
10-Jan-93	20-Feb-93	30-Jan-93	41	158	3.85	91	2.21	no data	no data
20-Feb-93	13-Mar-93	2-Mar-93	21	143	6.81	9	0.42	no data	no data
13-Mar-93	27-Mar-93	20-Mar-93	14	65	4.64	4	0.29	no data	no data
27-Mar-93	17-Apr-93	6-Apr-93	21	122	5.81	24.	1.16	20	.95
17-Apr-93	8-May-93	27-Apr-93	21	90	4.29	43.	2.03	5	.24
8-May-93	12-Jun-93	25-May-93	35	234	6.69	92.	2.63	52	1.49
12-Jun-93	3-Jul-93	22-Jun-93	21	185	8.81	25.	1.19	12	.57
3-Jul-93	15-Aug-93	24-Jul-93	43	250	5.81	93.	2.15	49	1.14
15-Aug-93	11-Sep-93	28-Aug-93	27	250	9.26	55	2.04	30	1.11
11-Sep-93	5-Oct-93	23-Sep-93	24	219	9.13	107	4.46	98	4.08
5-Oct-93	25-Nov-93	30-Oct-93	51	244	4.78	106	2.08	94	1.84
25-Nov-93	6-Jan-94	16-Dec-93	42	74	1.76	258	6.14	296	7.05
6-Jan-94	21-Feb-94	29-Jan-94	46	197	4.28	144	3.13	76	1.65
21-Feb-94	19-Mar-94	6-Mar-94	26	61	2.35	48.	1.85	52	2.00
19-Mar-94	25-Apr-94	6-Apr-94	37	130	3.51	82.	2.22	84	2.27
25-Apr-94	16-May-94	5-May-94	21	140	6.67	45.	2.16	31	1.48
16-May-94	20-Jun-94	2-Jun-94	35	225	6.43	57.	1.62	63	1.80
20-Jun-94	13-Jul-94	1-Jul-94	23	115	5.00	23.	0.99	2	0.09
13-Jul-94	13-Sep-94	13-Aug-94	62	500	8.07	106	1.71	no data	no data
13-Sep-94	5-Oct-94	24-Sep-94	22	258	11.7	55	2.50	49	2.23
5-Oct-94	16-Nov-94	26-Oct-94	42	264	6.29	76	1.81	112	2.67
16-Nov-94	14-Dec-94	30-Nov-94	28	143	5.11	61	2.18	54	1.93
14-Dec-94	8-Feb-95	11-Jan-95	56	242	4.32	282	5.04	271	4.84
8-Feb-95	6-Mar-95	21-Feb-95	26	212	8.15	93	3.58	98	3.77
6-Mar-95	3-Apr-95	20-Mar-95	28	215	7.68	93	3.32	64	2.29
3-Apr-95	29-Apr-95	16-Apr-95	26	163	6.27	55	2.12	55	2.12

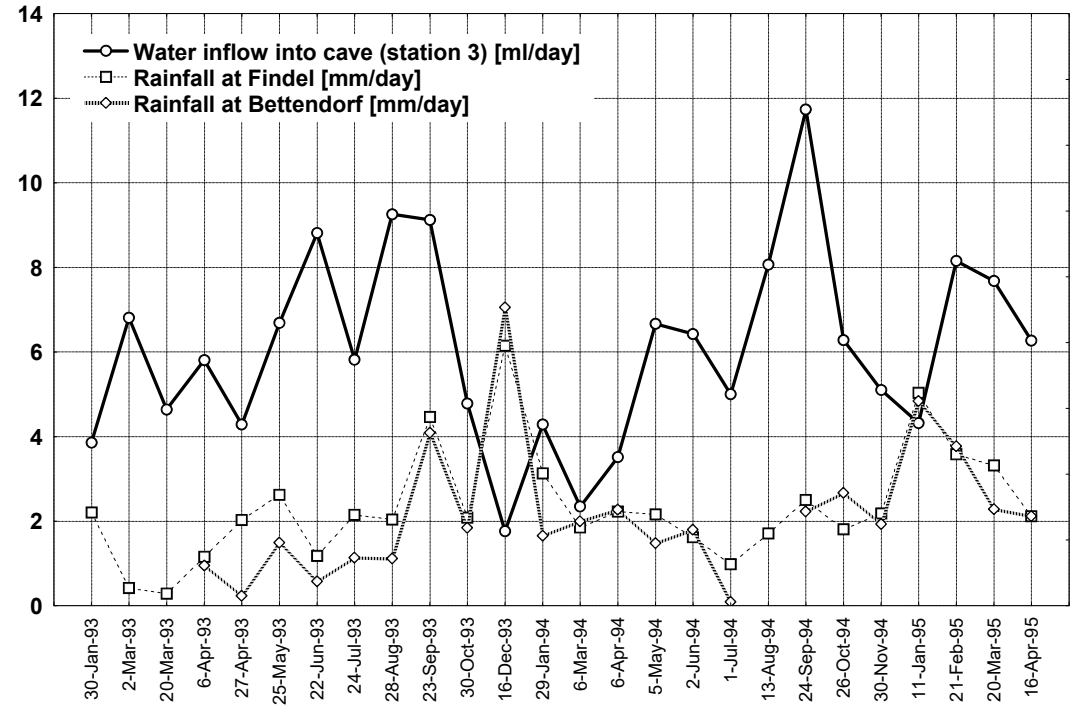

Fig. 3.3.1. Overview of rain and infiltration water amounts in aluminium gutter at station 3

The amounts of water collected inside the cave seem to follow the rain fall with a certain time lag (fig. 3.3.1). Actually, the crosscorrelation computed on the data has its peak for a time-lag of two periods, but the computed correlation between inflowing water and outside rainfall is a negative one, clearly an impossible situation. Since the sampling intervals are not of the same duration, one can not reasonably calculate an accurate time lag; besides, the rather long delays between the samples do not allow to find a possible shorter time lag. That the inseeping waters appear in the cave with a certain delay on the rainfall should be obvious. But that delay could be different at various locations in the cave, and could well be of much shorter duration than that of the sampling periods. The CO_2 data might even suggest a time lag of only a few days (see chapter 3.3.5).

An automatic water-monitoring station was planned, but the project was abandoned due to the practical problems concerning the long-time stability of pH-sensors (electrolyt-bleeding, risk of sensor drying) under the difficult maintenance conditions. A station at the stalactite site near the *Salle Claude* would also have required yet another data-logger. The combined additional costs and practical problems made it impossible to carry through this part of the project.

3.3.2. Interpretation of the Concentrations of the Different Ions Monitored.

The chemical values obtained from the different water samples collected are compiled in tables 3.3.2a (results of the water analysis done by the Laboratoire des Ponts et Chaussées) and 3.3.2b (spot sampling done by Claude Boes). The graphical representations and the relationships between the different ions are to be found in the corresponding subdivisions.

Even though the collection periods could be rather long, the chemical values for nitrates were found to be in the same range than the on-site analyses made using indicator sticks.

Since nitrate was the only stable ion measured both on site and in the laboratory, we can be confident that the values measured using the indicator sticks are in the correct range. The only difference lies in the fact that the unavoidably long collection periods may have leveled out peaks of higher concentrations for the ion concentrations.

Table 3.3.2a. (Laboratoire Ponts et Chaussées)

Sampling date	Location	Conduc.	pH	Cl-	SO4-	NO3-	NO2-	NH4+	Na+	K+	T.H.	C.H	CaH	MgH	NonCH
02-Sep92	JR3	450	8.0	0.73	0.39	0.50	0.00	0.01	0.30	0.01	2.4	1.50	0.68	1.72	0.90
30-Sep92	MIK2	286	7.2	0.17	0.05	0.33	0.00		0.21	0.13	1.8	1.72	0.56	1.24	0.08
01-Oct to 25-Oct92	MIK2	300	7.3	0.21	0.06	0.47	0.00		0.12	0.08		0.00			
10-Nov to 24-Nov92	MIK2	300	7.3	0.28	0.09	0.37	0.00	0.02	0.11	0.06	1.6	1.65			-0.03
	MIK2	288	7.6	0.21	0.08	0.35	0.00	0.01	0.10	0.06		0.00			
20-Feb93	MIK2	295	7.8	0.20	0.10	0.40	0.00	0.01	0.12	0.07	1.6	1.34	0.60	0.96	0.22
10-Oct92 to 20-Feb93	Stat.3	440	7.9	0.51	0.32	0.52	0.00	0.01	0.14	0.07	2.3	1.66			0.64
13-Mar93	MIK2	305	8	0.14	0.14	0.34	0.00	0.01	0.10	0.06	1.7	1.34			0.32
13-Mar93	Stat.3	415	8	0.48	0.32	0.44	0.00	0.01	0.13	0.07	2.3	1.60			0.66
17-Apr93	MIK2	269	8	0.15	0.10	0.42	0.00	0.01	0.11	0.06	1.6	0.68	0.56	1.04	0.92
12-Jun93	MIK2	276	7.5	0.20	0.14	0.34	0.00	0.01	0.10	0.06	1.6	1.56	0.60	1	0.04
12-Jun93	Stat.3	372	7.7	0.59	0.48	0.45	0.00	0.01	0.12	0.06	2.1	1.50	0.55	1.53	0.58

Notes:

Conduc. = conductivity [µS/cm]
TH = total hardness [mmol/l]
CH = carbonated hardness [mmol/l]
CaH = Ca hardness [mmol/l
MgH = Mg hardness [mmol/l]
NonCH = non carbonate hardness [mmol/l]
1 [°f] = 4.008 mg/l; all hardnesses as Ca hardness
all ionic concentrations in [mmol/l]

Table 3.3.2b. (Claude Boes)

Sampling date	Location	pH (1)	pH (2)	Cl- mg/l	SO4- mg/l	NO3- mg/l	NO2- mg/l	NH4+ mg/l
02-Feb-91	J00					<10		
05-Mar-91	JR3 / bottom	7.6-7.8				10		
05-Mar-91	JR3 / ceiling	7.6				<10		
27-Mar-91	JR3	7.2-7.4				10		
19-May-91	JR3 / bottle	7.6-7.4				10		
19-May-91	N0 / ceiling	7.2-7.0				25		
19-May-91	N0 / poodle	7.2-7.0				25		
19-May-91	O0 / ceiling	7.0-6.8				50		
19-May-91	O0 / podle	7.0-6.8				50		
19-May-91	OL2	6.5				>250		
11-Aug-91	JR3 / bottle	7.2-7.4				10-25		
08-Oct-91	JR3 / bottle	7.2-7.4	7.5			10		
08-Oct-91	KR0 / ceiling	7.4	7.5			10-25		
08-Oct-91	M00 / ceiling	7.0	6.5-7.0			25		
08-Oct-91	O0		6.5-7.0			25-50		
08-Oct-91	QL14 poodle	7.0				10		
08-Oct-91	QL14 ceiling	7.0				10		
09-Nov-91	O0 dir O0R ceiling 1	7.0-7.5	7.7-7.2			25-50		
09-Nov-91	O0 dir O0R ceiling 2	7.5	7.0-7.2			25		
09-Nov-91	QL14 ceiling	7.5	7.4			10		
09-Nov-91	QL14 poodle	7.5	7.4			10		
09-Nov-91	UL19 (4.r.) poodle	7	7			25-50		
09-Nov-91	Z resp B'	7	7			25		
09-Nov-91	RL14 ceiling	7				25		
18-Apr-92	JR3 bottle	7				100		
18-Apr-92	O0 corner KL	7	7.0-7.2			25		
18-Apr-92	ML00 / ML01 point 1	7				25-50		
18-Apr-92	ML00 / ML01 point 2	7				25		
18-Apr-92	QL02 ceiling	6.5	6.5			100-250		
18-Apr-92	MR04	7	6.5			50		
18-Apr-92	ceiling	7.0-7.5	7.2-7.4			50		
18-Apr-92	ceiling / stalagtite	7.5	7.2-7.4			25		
18-Apr-92	stalagtite	7.5	7.4			25-50		
18-Apr-92	NR07 (salle Claude) ceiling	6.5	6.5			25		
16-May-94	MIK2	7.0		<25	200	25	0.25-0.50	<0.2

Note: (1) two-color vesrion of indicator strip
(2) three color version of indicator strip
The readings of the colors in the near neutral region were always difficult to read, even with halogen headlights .

3.3.2.1 Conductivity

The conductivities measured lie in the range between 270 - 450 [$\mu S*cm^{-1}$] (see table 3.3.2a), which characterises the Moestroff infiltration waters as being a "weakly mineralized" type. The conductivity appears to be a good parameter against which to check the concentrations of other ions. The corresponding graphs will be shown below.

3.3.2.2. Ion Balance

The ion balance for cations and anions has been calculated according to the following formula:

$$\sum [Cl^-; 2*SO_4^-; NO_3^-; NO_2^-; 2x\ HCO_3^-]$$

$$\sum [NH_4^+; Na^+; K^+; 2*[Ca^{2+} + Mg^{2+}]$$

As can be seen in figure 3.3.2., the ion balance shows an excess of cations. This is mainly due to the unusually high amount of Mg^{2+} ions in relation to the Ca^{2+} ions.

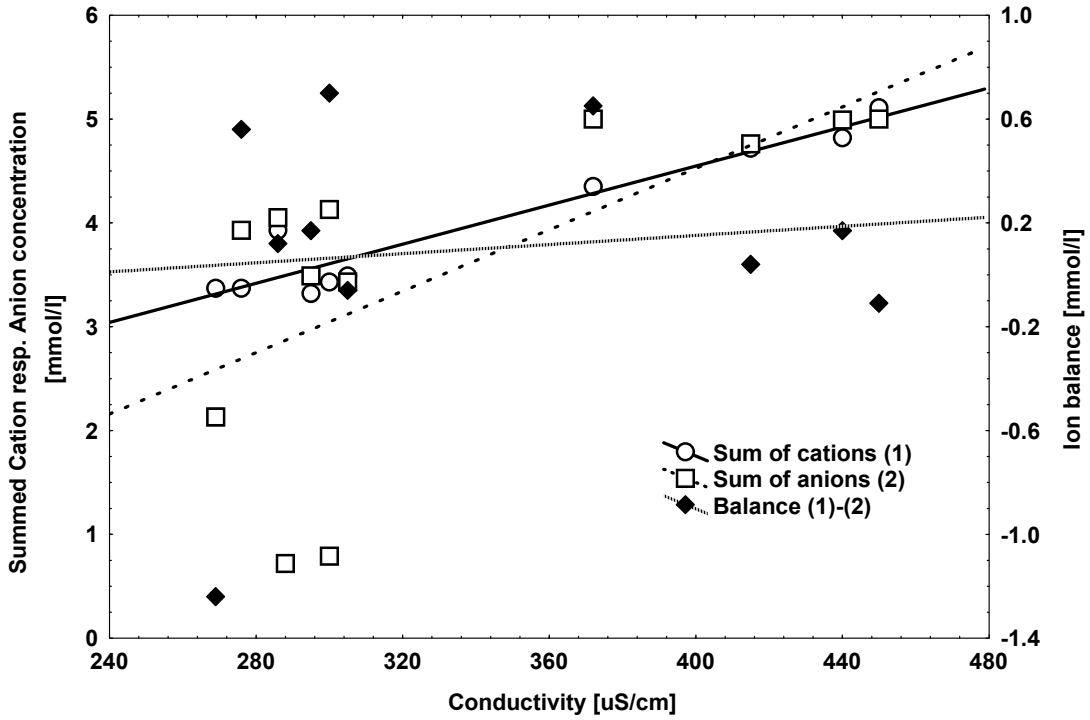

Fig. 3.3.2. Cation and anion concentrations in function of conductivity (in µS/cm) with regression lines.

The rise in conductivity is related on the contrary to the contribution of the anions. Among the anions, the chloride ions are mostly responsible for the increase in conductivity (see figure 3.3.3).

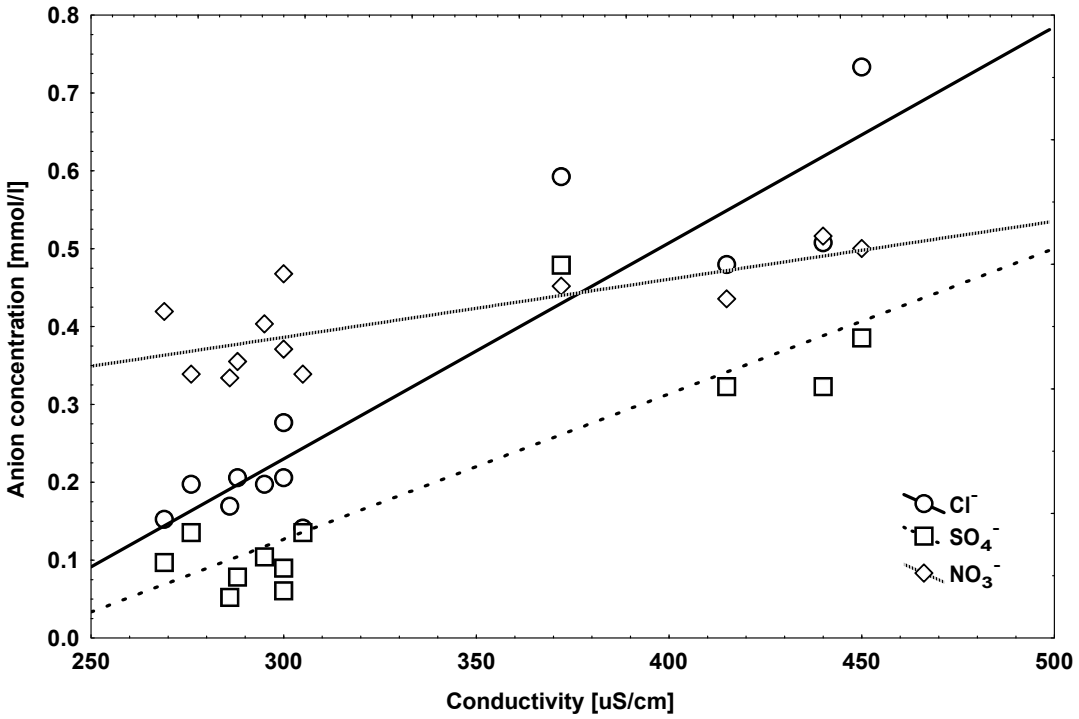

Fig. 3.3.3. Chloride-, Sulfate- and Nitrate-ion concentrations in function of conductivity (in µS/cm) with regression lines

3.3.2.3. The Ca/Mg Ratio

The ratio for Ca/Mg concentration lies around 0.5 for all the analyses available. In clean water it should be at a value around 5.0. This is a first possible indication that the infiltrating water does not have drinking water quality.

3.3.2.4. Hardness

The **total hardness** of the Moestroff infiltration water lies between 9 - 23 °f (≅ 5 - 13 °d), which ranges the water into the category of smooth waters, hardness-degree 2 on the german scale. The total hardness grows linearly with the conductivity, the increase being mostly due to the rising Mg^{2+}-concentration, the Ca^{2+}-concentration staying more or less stable. This is a very unusual observation (see figure 3.3.4).

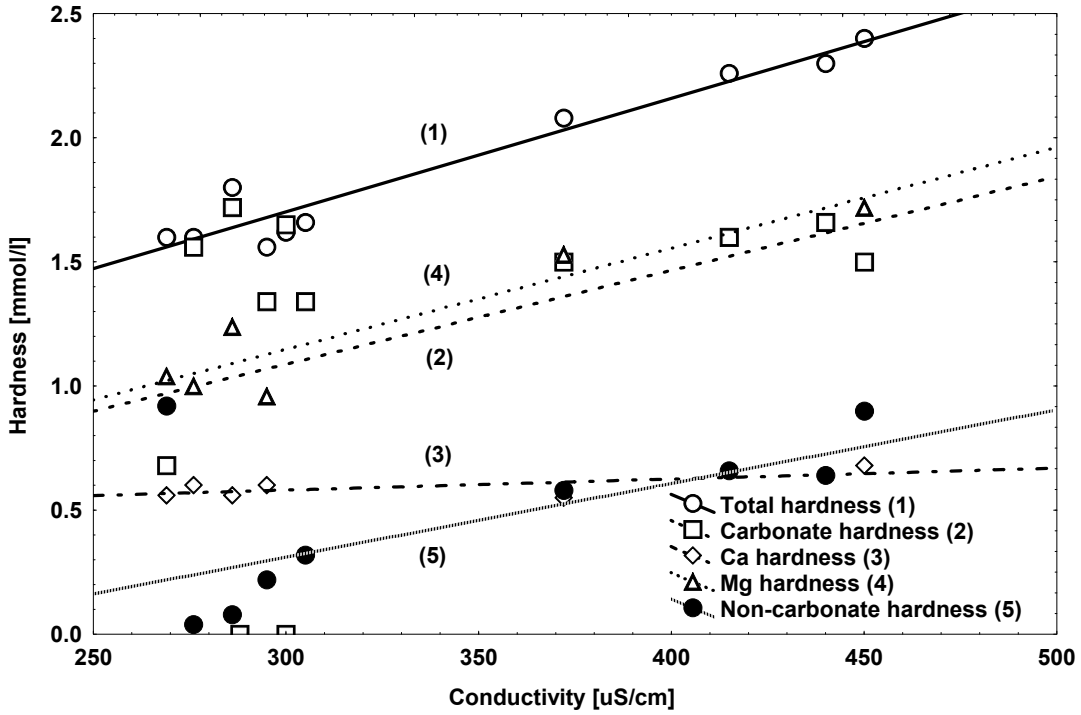

Fig. 3.3.4. Hardness in function of conductivity

It is also interesting to look at the linear correlation between anions and the total hardness. Here it is the regression-line of the non-carbonate hardness which has, together with the chlorides, the steepest slope.

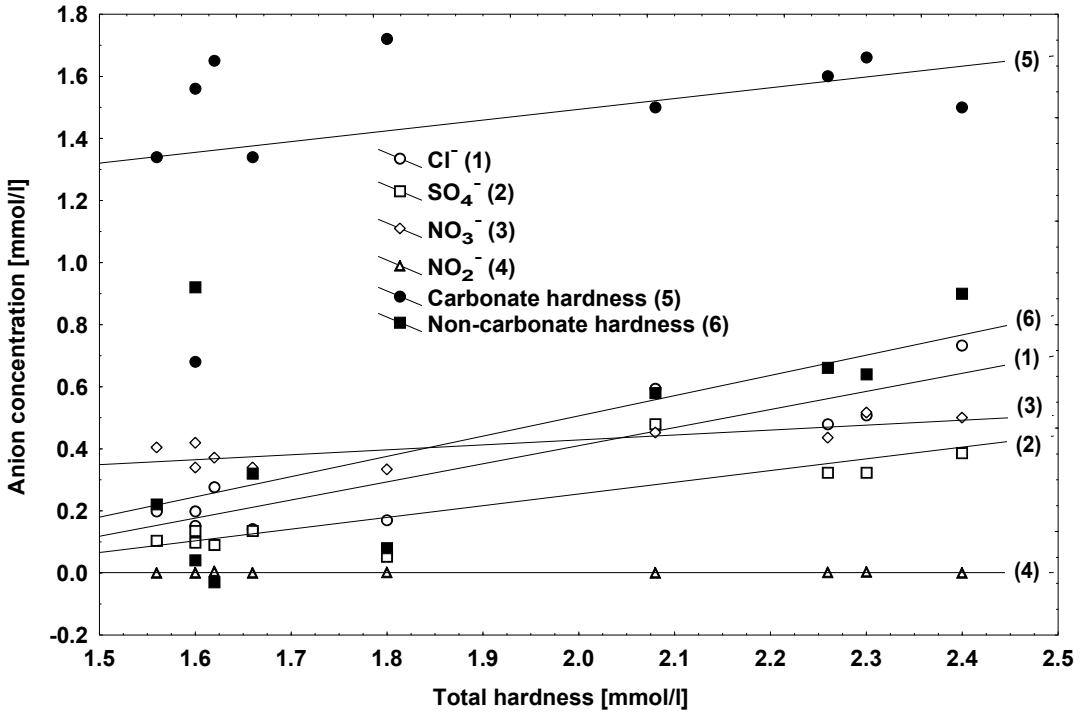

Fig. 3.3.5. Anion concentrations in function of hardness

The difference TH - CH (see table 3.3.2a) represents the **Non-Carbonate Hardness**. It is equivalent to the Ca^{2+} and the Mg^{2+} amounts, which do not stem from the dissolution of substances like $X^{2+}CO_3^{2-}$. (with X^{2+}: Ca^{2+} or Mg^{2+}) .

The minerals from which they could originate are of the form:

XSO_4^{2-}

$X^{2+}(Cl_2)^-$

$X^{2+}(NO_3)_2^-$ or similar.

The Mg^{2+} concentrations being higher than those of the Ca^{2+} ions, there must be another source for the additional magnesium found. This will be discussed below.

3.3.2.5. Sulfate/Calcium Ratio

Normally the Ca^{2+} concentrations are higher than the SO_4^{2-} concentrations, which is also the case for the Moestroff water. This means that we do not have a sulfate excess. Concerning the high amount of Mg^{2+} ions present, we have to find an other counter-ion. Additionally, we have no indication for an exchange of Ca^{2+} or Mg^{2+} ions against alkali ions. Neither do sulfate-fertilizers seem to be present in noticable amounts.

3.3.2.6. Chloride Ions

The concentration of chlorine ions lies between 6 - 26 mg/l (0.14 - 0.73 mmol/l), with a majority of the values being situated below 10 mg/l. So the possible impact of fertilizers like KCl or NH_4Cl seems to be rather reduced. For the highest conductivities, the chlorines contribute mostly among the non-carbonate ions (see figure 3.3.3).

3.3.2.7. Nitrates Ions

Nitrate ions can originate from either fertilizers, high NO/NO_2 concentrations in the air, or bacteria. The monitoring was two-fold: on site using indicator sticks, and in the lab usiing agreed methods for monitoring of drinking water. The values found in the Moestroff cave vary from 0 - 250 mg/l, with many values lying between 20 and 50 mg/l. The very high values of 100 resp. 250 mg/l could only be found on two days: (19 May 1991 and 18 April 1992). These very high values may have been caused by natural fertilizer having been brought out on the fields above the cave area in the week(s) before. In any case, they speak clearly for a short-time pollution.

If we look only at those water samples where full analyses are available, we find that, with respect to waters of high conductivity, the nitrate-ions show the least additional contribution (see fig. 3.3.3).

3.3.3. General Appreciation

The most unusual result of the infiltration waters of the Moestroff cave is the low Ca/Mg ratio, combined with an anion deficit in the ion-balance. None of the anions monitored can counter-balance the cation excess. Therefore the monitoring for other anions, like silicates and phosphates (which seem the most probable), would be a first step which might help to understand this phenomenon.

More probable however is the following: if we consider the solubility products of $CaCO_3$ and $MgCO_3$, we find:

$CaCO_3$: $4.82 * 10^{-10}$ mol/kg
$MgCO_3$: $1 * 10^{-5}$ mol/kg

This means that $CaCO_3$ will precipitate first, increasing the relative Mg^{2+} concentration. This would involve that $CaCO_3$ is deposited. This assumption is supported by the relatively thin, (therefore probably very young) calcite layer covering the walls in many places of the cave.

3.3.4. Material Loss Through Water Dissolution

When considering the amount of material in the water infiltrating the entire cave, it could be interesting to estimate the quantity of rock dissolved in an area equivalent to that of the cave. The estimation will be based on the volumes of water (and their composition) which were collected in the 0.5 meter long gutter installed on the wall at station 3.

During two full years (21^{th} March 1993 - 20^{th} March 1995), the amount of water collected was 4435 ml, equivalent to 2217 ml per year. Let us assume that the water percolating down through the ceiling fissure separates evenly on both sides of the gallery. Remembering that the length of the gutter is 0.5 m, this gives a total volume of:

$$2*2*2217 = 8868 \text{ ml}/(\text{m}^{-1}* \text{year}^{-1}) = 8.868 \text{ l}/(\text{m}^{-1}* \text{year}^{-1}).$$

The average total hardness in the cave (different sampling points !) is 18.9 °f; since 1°f ≡ 10 mg $CaCO_3$/l, the mass of dissolved rock is 189 mg $CaCO_3$ per liter.

The amount of dissolved rock per year and per meter of cave is:

$8.868*189 = 1676$ mg = 1.676 g. Assuming a total gallery length of approximately 4000 m, the total amount of rock dissolved all over the cave in one year is $4000 * 1.676 = 6.704*10^3$ g = 6.704 kg.

As the density of $CaCO_3$ (Muschelkalk) has been found to be 2676 kg/m^3 the volume of rock dissolved per year amounts to:

6.704/2.676 ≅ 2.5 dm^3 per year

This is a very crude estimation of the amount of rock dissolved in the strata above, and over an area like that covered by the Moestroff Cave. It is up to the reader to take these values as a basis for estimations in geological time-scales...

References:

HÖLTING, B. - Hydrogeologie, Einführung in die Allgemeine und Angewandte Hydrogeologie, 4. Aufl. 1992, F. Enke Verlag, Stuttgart, ISBN 3-432-90794-X

HÜTTER, L. A. - Wasser und Wasseruntersuchung, 6. Aufl. 1994, Salle & Sauerländer , Frankfurt am Main ISBN 3-7935-5075-3 (Salle), ISBN 3-7941-3270-X (Sauerländer)

MAQUIL, R., MASSEN, F., (Eds.) - Comptes Rendus du Colloque International de Karstologie à Luxembourg 25-26 Août 1992. Service Géologique du Luxembourg 1994

SCHROEDER, D., BLUM, W.E.H. - Bodenkunde in Stichworten, 5. rev. Aufl. 1992 , Ferdinand HIRT Reihe. ISBN 3-443-03103-X Gebrüder Borntraeger, Berlin 1992

VOIGT, H-J. - Hydrogeochemie, Eine Einführung in die Beschaffenheit des Grundwassers, VEB 1990, Leipzig. ISBN 3-540-51805-3 Springer-Verlag Berlin, ISBN 0-387-51805-3 Springer-Verlag, New York

3.4. AIR MOVEMENTS

Francis Massen, Antoine Kies

3.4.1. Introduction

Air movements are the original cause of the variations of most underground parameters as temperature, humidity and gas concentrations.

To study cave air movements, a good knowledge of the direction and velocity of air movements is needed. Air velocities in the Moestroff Cave are usually low, well below 100 cm/s: this means that mechanical anemometers (which generally have a lower detection limit of 10 to 20 cm/s and a precision worse than 10 cm/s) cannot be used. This leaves hot-wire anemometers as the only alternative. As these instruments measure the absolute value of air speed, a supplementary device must be used to detect the direction of airflow.

There is quite some disagreement between scientists concerning the cause of air movements in a cave. The air flow into or out of a balloon-type cave is usually thought to be caused by atmospheric pressure variations [Mangin, personal communication 1995]. If the cave has several openings to the outside, and if these openings are situated at different altitudes, the differences of internal and external air densities are the primary cause of cave wind [Andrieux, 1970]. Halbert and Michie [Halbert & Michie, 1982] even state that *"the most important factor in a cave's climate is the presence of single or multiple entrances. This distinction is so basic that it is possible by knowing this fact alone to predict in general terms the characteristics of the climate of the cave."*

Actually, we also have to take into account the fact that the wind blowing outside may completely change the characteristics of the air flow driven by a density gradient; this means that measuring the external wind conditions at the cave entrance is essential, and that the study of air movements must be able to separate the times with no external wind from those when outside wind blows. Many studies of cave climate do not meet this condition.

When we started the Phymoes project, nothing was known about wind in the Moestroff Cave, except the fact that a visitor leaving the cave could experience air movements when he approached the entrance.

In the first year, we used two Airflow TA-2 hotwire anemometers installed at stations 2 and 3 for continuous measurements, and incense sticks for spot measurements; the hotwire sensors were always mounted in the center of the gallery cross-section. Even if this first monitoring could only measure the absolute values of cave wind, they allowed to draw several preliminary conclusions:

1. The incense sticks showed that air moves always in a same direction over a gallery section; we did not find convective Rayleigh cells, often described in balloon-like caves.
2. Air velocity varies quickly on a small time-scale (order of magnitude of minutes), even when the direction of air flow remains the same; the Reynolds numbers are usually high (> 10000) at station 2 and low (<1000) at station 3: this means that air flow is practically always turbulent at station 2 and often laminar at station 3.
3. This laminar and turbulent nature could be verified by visual inspection of the smoke given by burning incense sticks.
4. Despite the rapid air velocity variations, the seven single measurements done at the beginning of each hour are sufficient to distinguish periods of high from those of low wind activity. The averages of these measurements are stored in the dataloggers and are used to compute velocities and air flow. Whenever rapid sampling (sampling time of 1 second or even less) was needed, it was usually done separately from the routine monitoring, using a spare programming facility of the dataloggers.

Figure 3.4.1. shows the situation in Octobre 1994; the first plot gives the result of the hourly measurements for the whole month (744 data points, each one being the average of the 7 measurements which are taken at every full hour, separated by a one minute interval). One sees that at the beginning and at the end of the month wind activity was significantly higher than during the mid-month period.

The second plot zooms on the day of the 5th October (24 points; the external Davis weatherstation reported **no external wind during that day!**), and the last one gives the result of a rapid measurement campaign starting the same day at 09:21:57 and ending at 09:50 (1683 data points, sampling interval 1 second). Even if the 2nd plot suggests a period of constant low wind, the fast samples indicate some wind velocity peaks of small duration which are clearly visible .

3.4.2. The Cause of Air Movements in the Moestroff Cave

The radon monitoring which started in February 1992 gave the first indication on the seasonal airflow direction in the main gallery: after one year of measurements, we saw that the mean radon concentrations (integrated over a three weeks period) were low in summer and considerably higher during the cold months; this suggested that air was flowing into the cave during the warm period and out of it during the colder period.

As shown in chapter 1, the cliff which holds the main cave entrance has many other secondary openings, which are situated below the main entry.

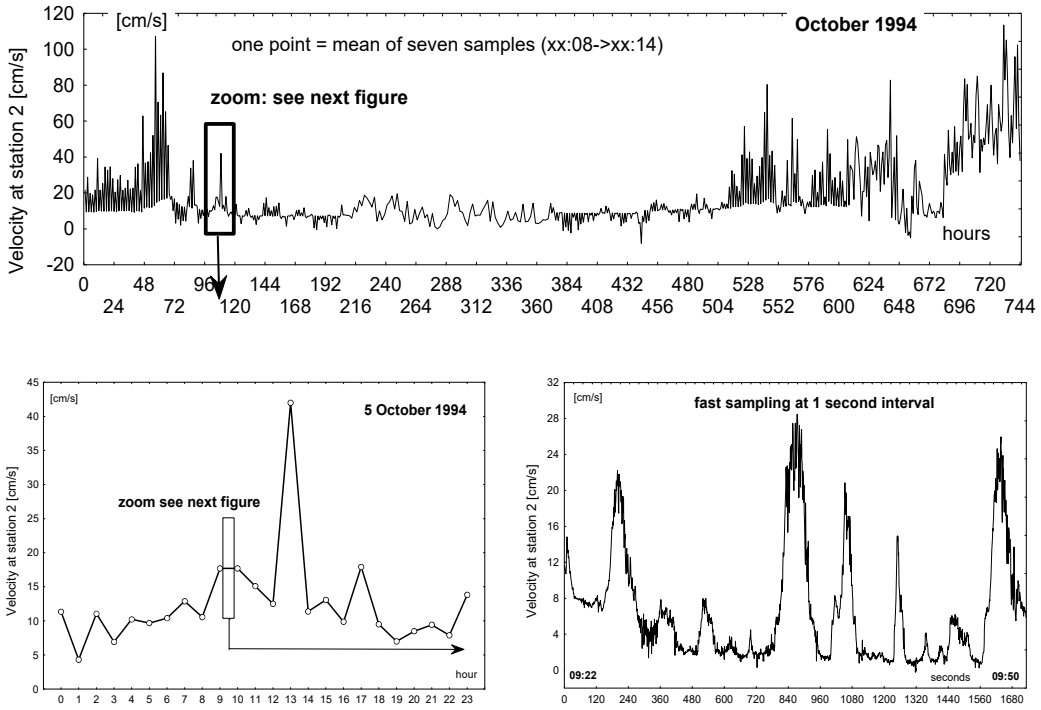

Fig. 3.4.1. Coarse and fine velocity pattern

There is the possibility of a multi-storey maze, the accessible system being the top stage; the lower stage(s) may be too narrow to be accessible to an explorer, but would allow the circulation of air (fig. 3.4.2). A simple chimney-effect model predicts in that case that air should flow into the cave during the period where the external air density is lower than the internal one (the « hot » period) and out of the cave during the colder period.

To understand the mechanism of this chimney effect, let us imagine two air cylinders A and B extending from the lower to the upper storey; A is situated outside the cave, B inside. (fig. 3.4.3). In summer cylinder A contains warmer and less dense air than cylinder B; this means that the pressure at its bottom is lower than that at the bottom of air cylinder B containing the colder and denser cave air. This pressure difference pushes the air out of the cave through the bottom storey, and this air will be replaced by fresh air sucked into the cave through the main entrance of the upper storey. During the colder months the opposite happens and the circulation reverses.

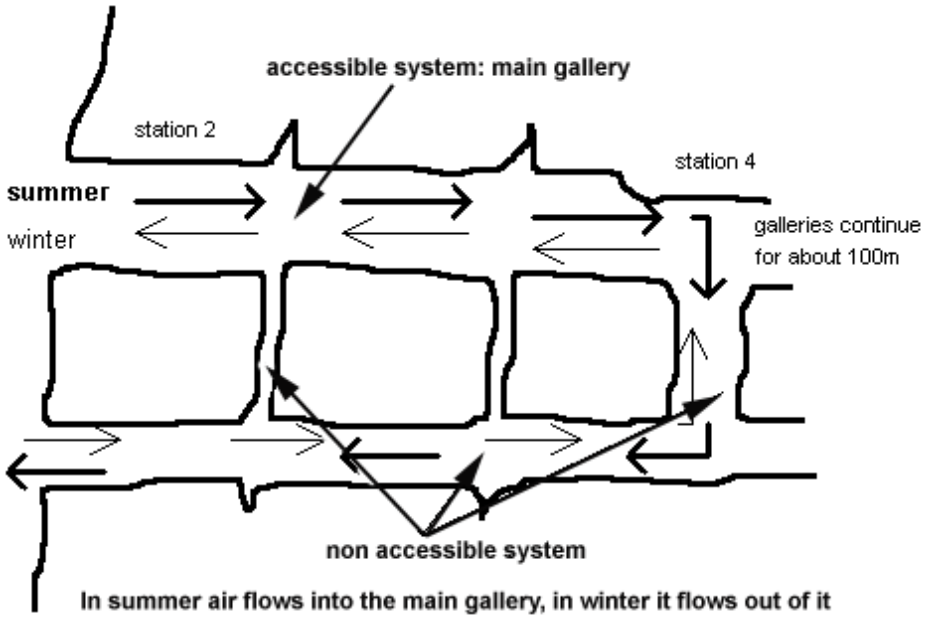

Fig. 3.4.2. Air movements can be explained by chimney effect between two storeys

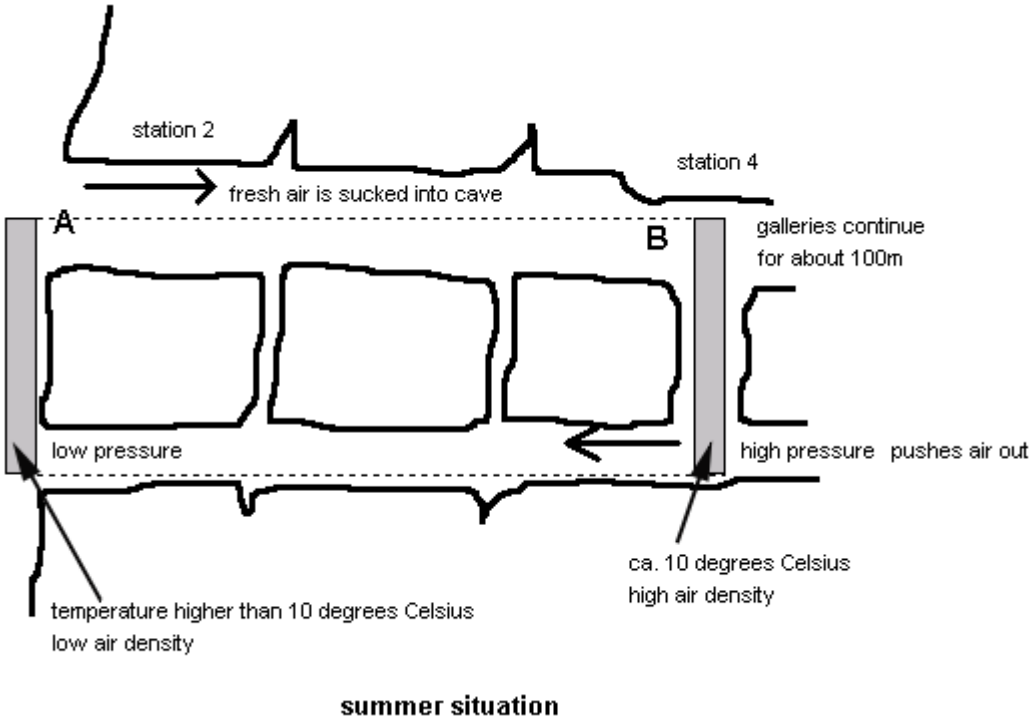

Fig. 3.4.3. Chimney effect explained for summer situation

As mentioned above, there exist globally 2 possible causes for airflow in caves: barometric pressure changes (which are active in balloon-like caves) and differences of inside and outside air densities (which are characteristic for dynamic caves); both causes may coexist, but one may dominate the other. The seasonal variations of radon gas in the Moestroff Cave suggest a predominantly dynamic cave mode; we will use our con-

tinuous measurements to establish quantitatively that the air movements in the Moestroff Cave are caused by differences of inside - outside air densities most of the time.

Since April 1993 the differential air pressure between the inside and outside was measured by a very precise SETRA manometer: this pressure gave a clear information of the direction of air flow. *A positive differential pressure (dP>0) means that pressure at the entrance of the cave is higher than that at station 4 and air flows into the cave; a negative differential pressure (dP<0) corresponds to a lower pressure at the entrance than at station 4, and air is flowing out of the cave*.

In all our investigations, we had to neglect air movements in the lateral galleries of the maze. Observations by incense sticks showed that these lateral movements do exist; in the case of dP>0, they seem to be outflows from the main gallery flow, rather than feeders of this flow.

In the analysis of air movements, it was often important to retain only the data corresponding to a windless outside situation. No external wind means that the outside-mounted weatherstation registered no wind gusts. Usually outside wind activity increases the differential pressure dP measured between the entrance and station 4: the positive linear correlation between gust and dP is small (r=+0.21 for 5088 cases in 1994), but nevertheless statistically significant even at the 0.01 level. Fig. 3.4.4 shows the linear fit computed for these data: a gust of 5 m/s will rise dP by about 0.5 Pa, increasing inflow or reducing outflow.

The hypothesis of an airflow caused by the difference of outside-inside air densities dρ means that the two parameters dP and dρ should have opposite signs (the differential pressure is positive for inflow which happens when the difference dρ between outside and inside air density is negative), so we should expect a clear majority of cases corresponding to that situation.

Let us analyse the data corresponding to the periods extending from 05 Oct.93 to 31 Mar.94 and 01 Aug.94 to 30 Nov.94; as dP and dρ can be positive or negative, we have the 4 possible situations given in table 3.4.1.

Table 3.4.1.

	dP>0 *air flows into the cave*	*dP<0* *air flows out of the cave*
dρ>0 («winter»)	658 cases = 15.7%	2147 cases = 51.2 %
dρ<0 («summer»)	1222 cases = 26.8 %	157 cases = 3.8 %

From the 4184 cases, 3369 cases (=80.5%) correspond to dP and dρ having opposite signs; this means they do support the assumption of an air

movement caused by a difference of outside and inside air densities. The 19.5% other cases may correspond to measurement errors like sensor drift, or to barometric pressure changes which could not be measured.

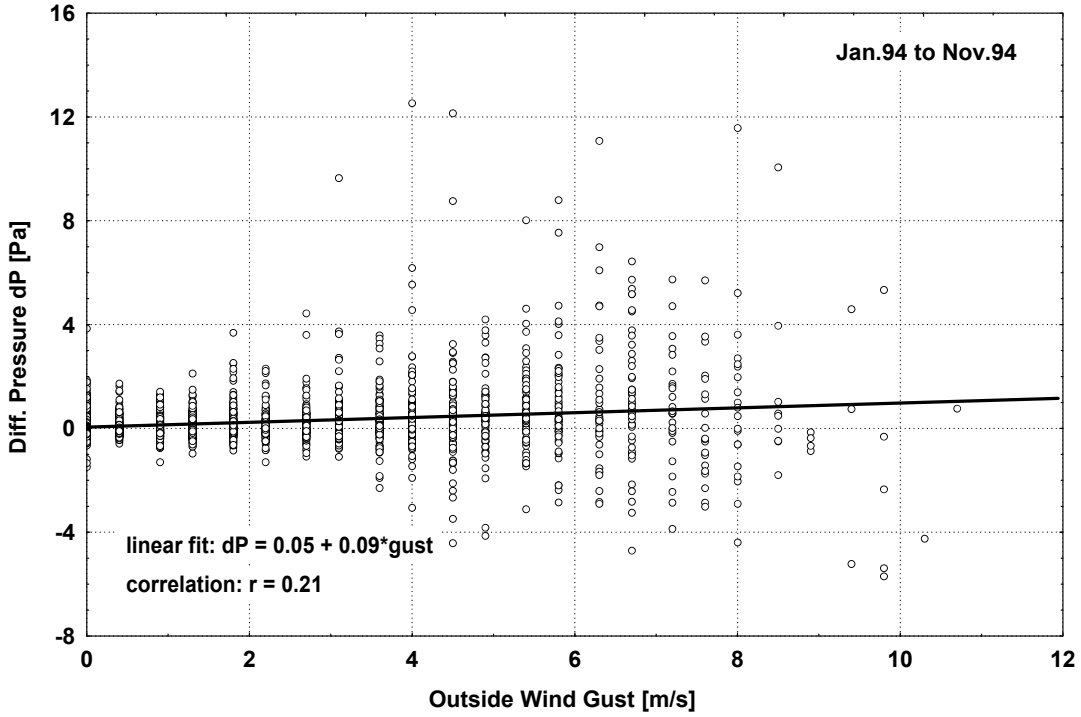

Fig. 3.4.4. Differential pressure increases with outside wind gust (5088.data points from 1994)

3.4.3. Pressure Drop in the Cave and Difference of Air Densities

In this chapter we will try to find a relationship between the measured pressure drop dP and the differences of outside and inside air densities.

We will take the data set of the months January 1994 to March 1994 and August 1994 to November 1994, and use only the points corresponding to no external wind gust; this subset of 5088 points corresponds to a period of well working outside anemometer, differential pressure and velocity sensors, and extending over both winter and summer seasons. The measurement period will again be divided into the data points corresponding to $d\rho<0$ ("inflow", summer) and $d\rho>0$ ("outflow", winter); $d\rho$ is the difference between the outside air density and that computed from station 4. We assume that no external wind blows when the Davis weatherstation registers zero gust. If we plot dP as a function of $d\rho$, retaining only the hours where the external wind was zero, we should get a straight line with a zero offset; actually the linear regressions to the winter and summer data give:

- Jan.94 --> Mar.94 (717 data): $dP = -12.5*d\rho + 0.4$ *[eq. 3.4. 1]*

- Aug.94 --> Nov.94 (2045 data): $dP = -5.1*d\rho + 0.2$ *[eq. 3.4. 2]*

The zero offset should be considered as the sign of inevitable errors of the differential manometer. This analogue sensor was prone to a zero drift which could not be avoided completely, but which was minimised by frequent checks and adjustments made in the cave itself. For the following analysis we subtract the zero offsets of the linear regressions from the the raw dP data for both periods.

The linear correlation between dP and dρ is r= -0.74, significant at the 0.01 level. The best linear fit to the whole data-set is (fig. 3.4.5):

$$dP = -7.2*d\rho \qquad \textit{[eq. 3.4.3]}$$

which means that a commonly found difference of air densities of 0.02 $kg*m^{-3}$ creates a pressure drop of 0.14 Pa between station 4 and Salle Loubens near the entrance of the cave. This very small difference of air pressure nevertheless is high enough to create air movements of a mean velocity close to 0.2 $m*s^{-1}$ and a mean flow-rate of 300 m^3*h^{-1}.

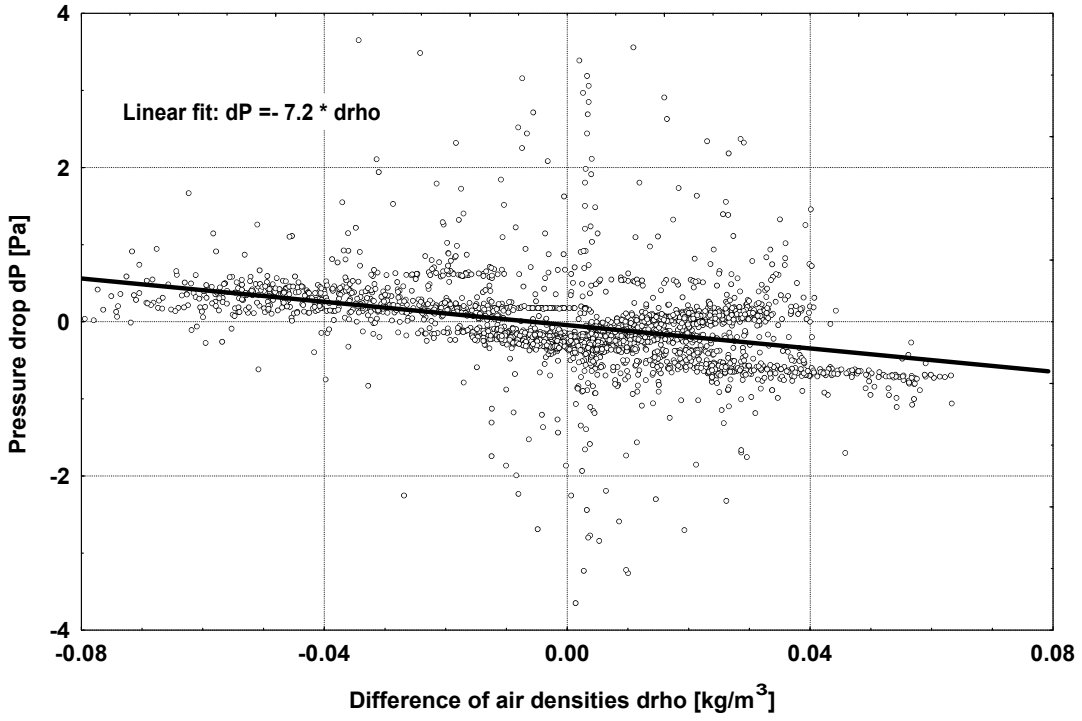

Fig. 3.4.5. Relation-ship between the pressure drop dP along the main gallery and the difference dρ of the air densities outside and in deep cave (station 4).

3.4.4 Effects of Changes of the Atmospheric Pressure

If changes in atmospheric pressure influence the airflow in the cave in a measurable manner , we should find at least some occurrence of this event among our numerous data. As outside gusts might completely mask the influence of the atmospheric pressure changes, we concentrate exclusively on no-gust data and look for periods where p_{at} experiences fast variations. For the whole period from Oct. 93 to Nov. 94 we find only two such events, as shown on fig. 3.4.6. At first glance one would conclude from the plot that a rapid drop of p_{at} followed by a fast rise provokes a high positive differential pressure pulse (which means a pulse of inflowing air).

Let us first examine the situation given in the upper graph of fig. 3.4.6, which corresponds to a period of 6 days from 21 to 26 August 1994, during which no external wind was blowing. During the day preceding the atmospheric pressure low, the mean outside temperature was T = 17 °C and mean dρ = -0.0303 [kg*m^{-3}]; the following day, we had T=17.8°C and dρ = -0.0346 [kg*m^{-3}] (dρ = air density difference between outside and station 2). This means that except for the changing atmospheric pressure, we were in a period of rather constant meteorological conditions.The sudden **drop** of the atmospheric pressure seems to induce two **inflow pulses** of a few hours duration. Fig. 3.4.7. shows that the difference of air densities between the outside and station 2 drops sharply during the second dP pulse, which is an indirect proof of a rather large inflowing air quantity.

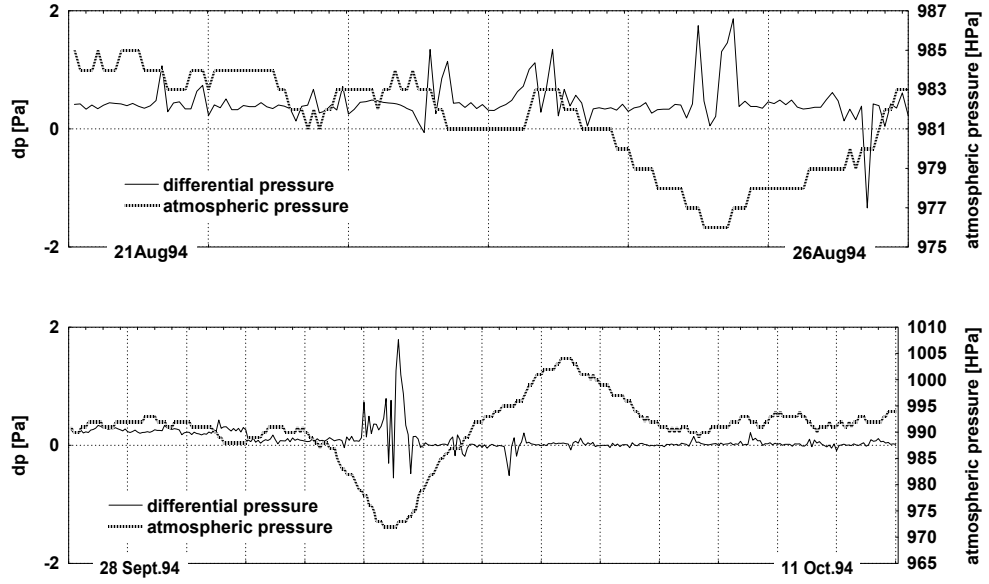

Fig. 3.4.6. Changes in barometric pressure and differential pressure dP (scale on time axis is 1 day)

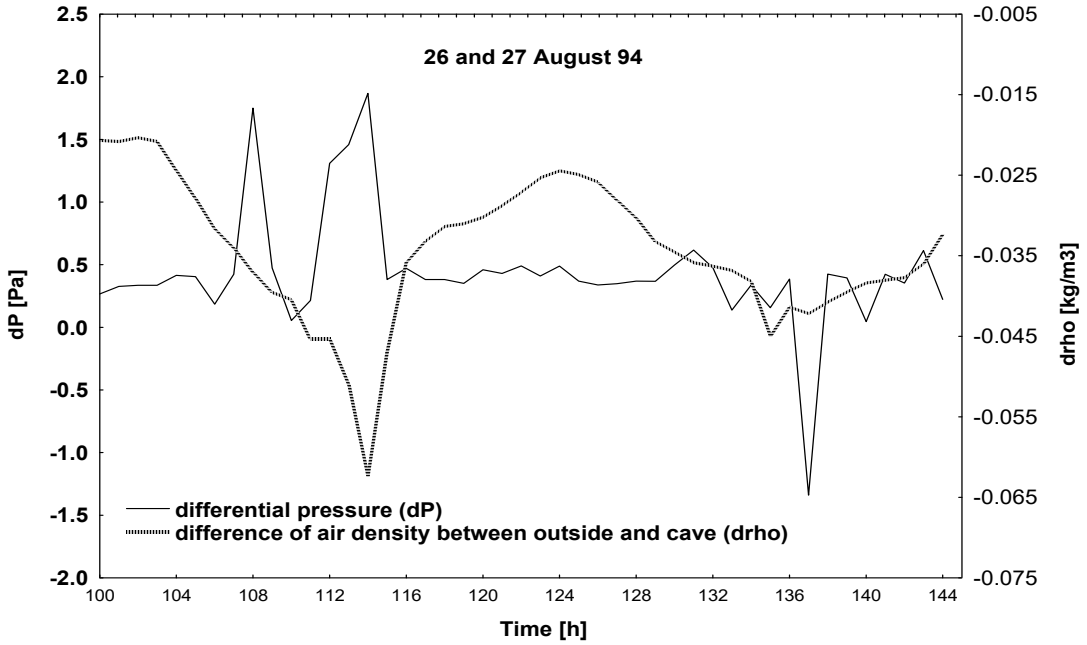

Fig. 3.4.7. Rise of differential pressure dP (possibly caused by sharp drop of atmospheric pressure) coincides with drop in the difference of air densities between outside and station 2: both pulses are a sign of a strong air inflow.

A second, somehow similar situation is given in the bottom graph of fig. 3.4.6. which corresponds to a windless period of 14 days from 28 Sep.94 to 11 Oct.94. Here the sudden drop of atmospheric pressure (duration: 80 hours) separates a warm period from a cold period: the mean values for the outside temperature and dρ are 14°C and -0.0185 [kg*m^{-3}] during the 5 preceding days, 8.9°C and +0.0054 [kg*m^{-3}] during the 5 following days, which shows that this is the crossover-period for the mean cave air temperature.

The period of high dP values (there are 3 peaks) lasts 14 hours; the rise from normal to peak is 1.6 Pa; during the same 7 hours where this happens, dρ **increases** by 0.0032 [kg*m^{-3}], contrary to the usual situation where an inflow triggered by a positive dP brings fresh air into the cave, and as a consequence decreases the difference between the outside density and that near the entrance. It seems that falling outside temperatures with the transition of dρ from negative to positive values put the cave in a unstable situation, provoking some heavy oscillations of the cave air (see fig. 3.4.8.); the situation comes back to "normal", where dP and dρ vary again in opposite manner, about 24 hours after dP has passed its peak.

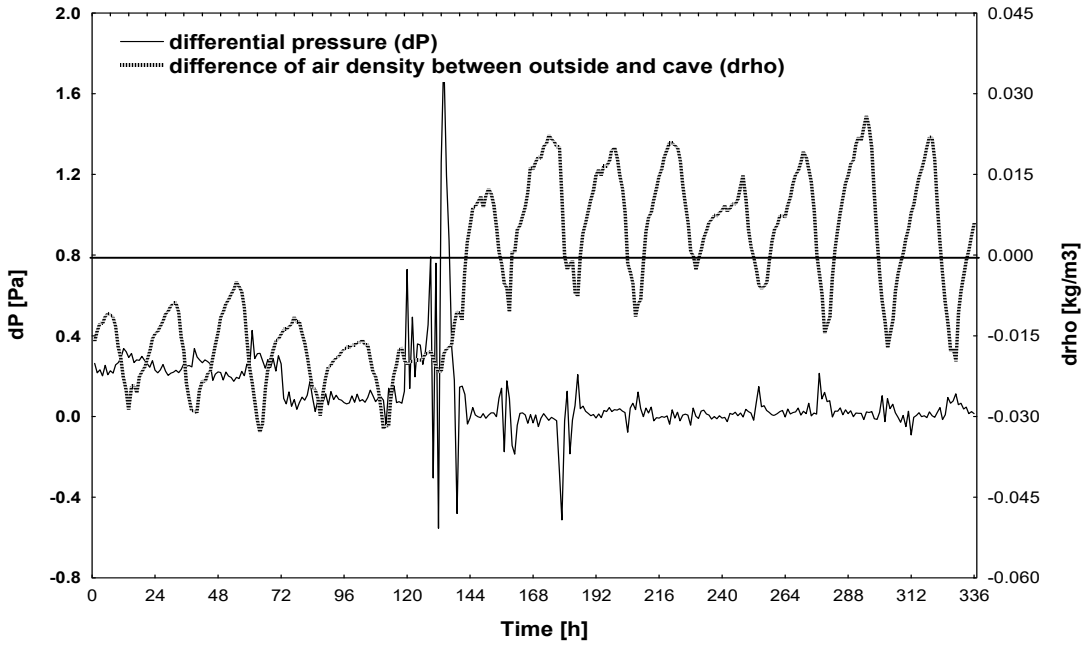

Fig. 3.4.8. Oscillations of dP when dρ rises from negative to positive values and is close to zero level

Detecting the response of air movements or differential pressure to changes of the atmospheric pressure is extremely difficult, as these responses, if they exist, are masked by other parameters (as temperature variations, outside wind...). The two situations given in fig. 3.4.6. seem to suggest that a rapid fall and subsequent rise of p_{at} may induce pulses of inflow. The Moestroff Cave is **not** a balloon-type cave, which exhales when p_{at} falls. If one reverts to figure 3.4.3 explaining the chimney effect, an inflow pulse in response to a p_{at} drop seems possible: if the atmospheric pressure decreases, outside air density does the same, and the air pressure at the basis of the depicted cylinder at the outside falls also, which, assuming constant conditions deep in the cave, increases the pressure difference between the basis of the inside and outside cylinders. The result would be a sharp outflow pulse through the lower storeys, and as a consequence an inflow pulse into the main gallery. The duration would be the time necessary to return to "normal" differences of air densities, which are caused either by the mixing of inflowing and cave air, by a p_{at} rising again or by both phenomena. We must confess that we do not have enough good experimental data to validate this hypothesis.

Situations like that shown in figure 3.4.6. remain exceptional events; the seasonal variations of the radon concentration and the number of cases verifying the dynamic model are good arguments to conclude that the Moestroff Cave has a predominantly dynamic behaviour. If the cave reacts to rapid changes in atmospheric pressure, this response is usually not detectable, being swamped by the air movements induced by thermal gradients or outside wind.

3.4.5 Synchronism Between v, dρ and dP.

The time-synchronism between air velocity, dP and its cause dρ is difficult to detect visually during periods of rapid hourly changes of the outside temperature; to get a clear picture, one has to pick up periods of very regular diurnal temperature oscillations and low outside wind activity. Let us take as an example two one-week periods, the first from 16 to 22 February 1994, and the second from 2 to 8 August 1994.

3.4.5.1. Period of Monitoring February 1994

During this cold winter period of 168 hours, the mean and extremal values of outside temperature, difference of air density, differential pressure and velocity at station 2 are given in table 3.4.2; the velocity data for station 3 were not available due to a sensor malfunction. The next figure 3.4.9. shows these four parameters after applying a 5 point moving average to filter the fast oscillations.

There is a good synchronism between air speed v, difference of air densities dρ and differential pressure dP: high dP and dρ values correspond to high velocities. As dρ is greatest when the external temperature is lowest, we have an opposite variation of external temperature and air velocity in the cave. The hourly measurements cannot detect any time lag between air velocity and the other parameters. The outside wind gusts mainly seem to dampen the diurnal variations of the density differences dρ and increase the pressure difference dP between inside and outside, pushing more fresh air into the cave as expected.

Table 3.4.2.

parameter	*mean*	*minimum*	*maximum*
outside temperature	-1 °C	-6.1 °C	+12.1 °C during 3 hours higher than 10°C
dρ (outside-stat.2)	+0.0483 kg*m^{-3}	-0.0100 kg*m^{-3} during 3 hours lower than 0 kg*m^{-3}	+0.0724 kg*m^{-3}
dP (always negative: outflow!)	-0.29 Pa	-0.58 Pa	-0.06 Pa
v at station 2	9.5 cm*s^{-1}	0	18.1 cm*s^{-1}

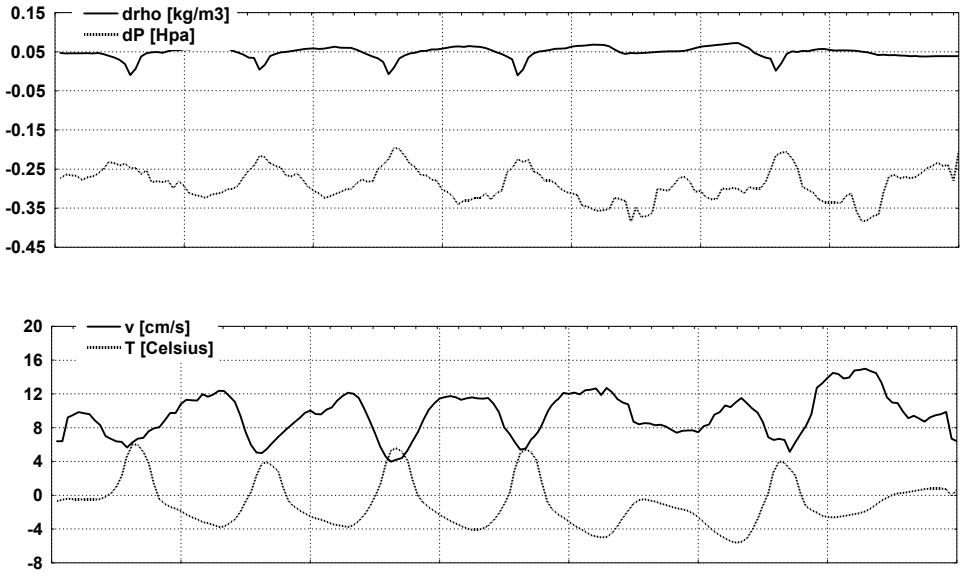

Fig. 3.4.9. Differential pressure dP, air velocity v at station 2, difference of air densities dρ and external temperature T (16 to 22 Feb. 1994, scale in days)

Wigley [Wigley, 1967] explains that air movements in caves, especially cave breathing, is mainly caused by atmospheric pressure changes which induce the air flowing through the porous medium in which the cave is embedded. In that case there must exist a time-lag between the maxima of air velocity and those of maximal atmospheric pressure changes (which can be found by computing dp_{at}/dt). Fig. 3.4.10. shows these two parameters for the same period as above, with a 5 point moving average applied .

A synchronous pattern as that given by Wigley cannot be observed: the whole period corresponds to constant outflow, whereas Wigley's theory demands a change of flow direction according to positive or negative values of dp_{at}/dt. There might be 2 days out of 6 where maximal atmospheric pressure changes (corresponding to $dp_{at}/dt=0$) seem to precede by some hours the maximum outflow velocity; again this behaviour cannot be observed in a consistent manner.

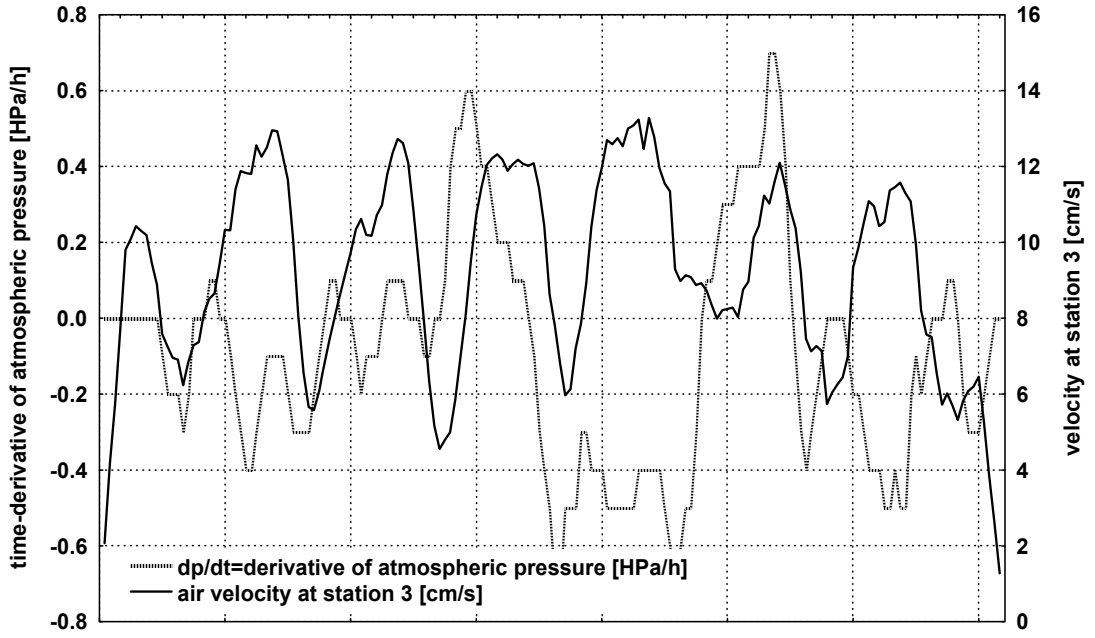

Fig. 3.4.10. Air velocity and rate of change of atmospheric pressure (scale in days)

3.4.5.2. Period of Monitoring August 1994

The 7 days period from 2 to 8 August 1994 corresponds to a typical hot summer period. For the 168 hours, using the velocity data of station 2, we find the mean values given in table 3.4.3. Fig. 3.4.11 gives plot the time series of the 4 parameters, after applying a 5 hour moving average.

These two examples of the cold February and warm August periods show that the time synchronism between air velocity and its causal factors dP and dρ are visible when the external temperature varies smoothly. During both winter and summer periods, v and dρ change synchronously. As temperature and dρ have opposite phase, there is a lag of about 12 hours between the moments of maximum cave wind velocity and those of maximum external temperature.

Table 3.4.3.

parameter	*mean*	*minimum*	*maximum*
outside temperature	23.4°C	17.7°C	never below 10°
dρ (outside-stat.2)	-0.0294 kg*m^{-3}	-0.0982 kg*m^{-3} never higher than 0	-0.0113 kg*m^{-3}
dP (always positive except 2 for 2 hours): inflow!	0.55 Pa	-0.10 Pa	1.11 Pa
v at station 2	26.9 cm*s^{-1}	0	46 cm*s^{-1}

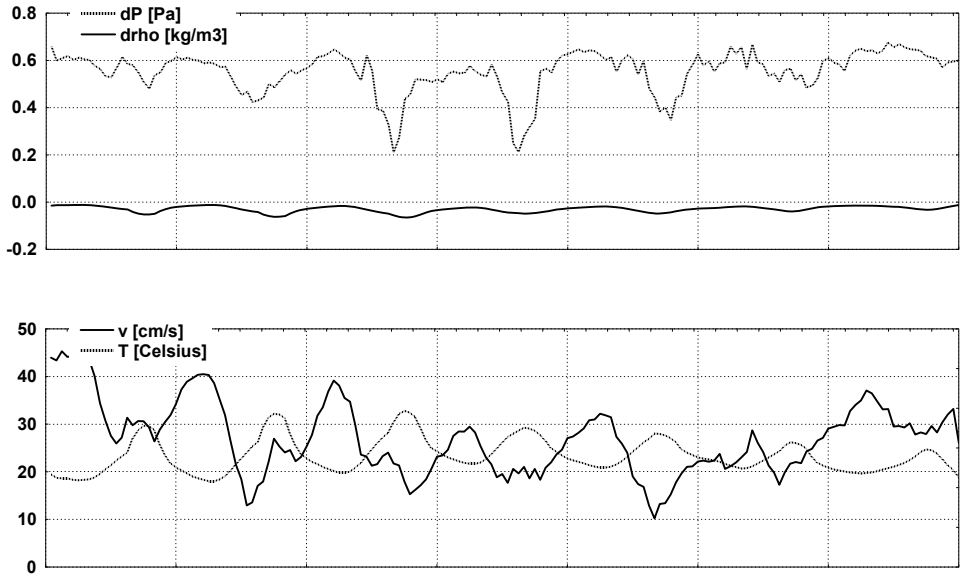

Fig. 3.4.11. Differential pressure dP, air velocity v, difference of air densities dρ, and external temperature T (2 to 8 Aug. 1994, scale in days)

3.3.5.3. Fourier Analysis Over Long Periods.

The preceding analysis extended over a week in spring- and in summertime. Let us check if we can find some long-time common periodicity by computing the Fourier spectrum over the whole period (5088 hours) for which we have good gust and dP values (Jan. 1994 to Mar. 1994 and Aug. 1994 to Nov. 1994). Figure 3.4.12 shows that we find a common 24h period among all parameters, except atmospheric pressure.

This means that the cave natural ventilation system responds globally to the 24 hour external temperature cycle, as should be expected from the fact that we can detect the 24h peak in the temperature patterns up to station 3 (chapter 3.1.4.).

3.4.6. Turbulent and Laminar Flow

Many tests done with incense sticks showed that the flow of air is turbulent most of the time at station 2 and sometimes also at station 3. At the deepest station 4 air movements are not measurable anymore, but the smoke from incense sticks always shows a laminar flow pattern. A big question was the possible existence of convective Rayleigh cells, with for instance inflowing air at the bottom and outflowing air at the ceiling of the gallery. This is frequently observable in larger caves, but could not be detected in Moestroff: many observations showed that in- or outstreaming air flows were always in the same direction over the whole section of the

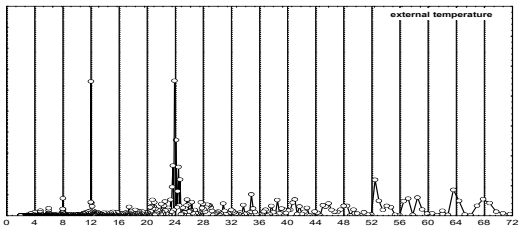

external temperature

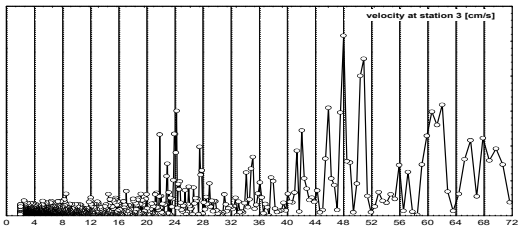

air velocity at station 3

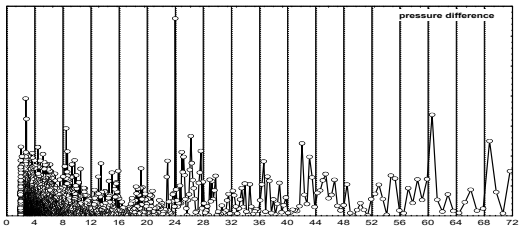

pressure difference

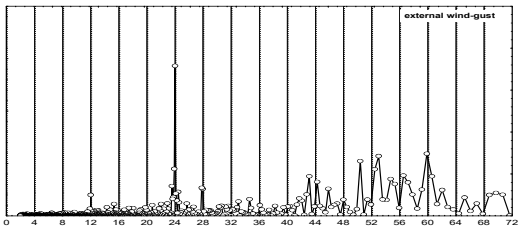

external wind gust

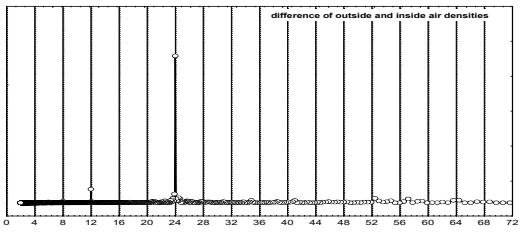

difference of outside and inside air densities

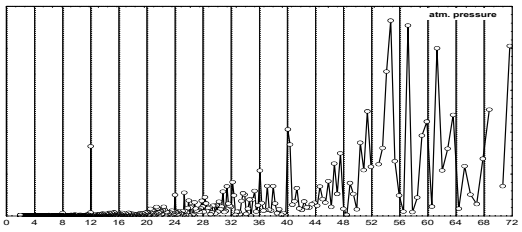

atmospheric pressure

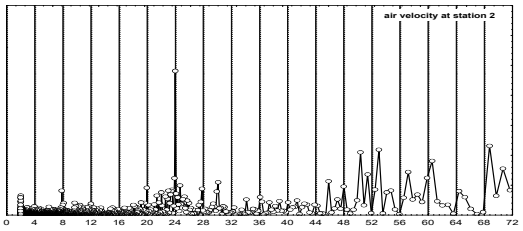

air velocity at station 2

Spectral analysis over the periods from Jan.94 to March 94 and Aug.94 to November 94

Fig. 3.4.12. All data except atmospheric pressure show 24h peak

gallery. Thus the mean velocity at stations 2 and 3 could be measured with a single hot-wire anemometer, whose sensor was mounted at the centre of the gallery. In computing Reynolds numbers, flow and other parameters, we usually use the hydraulic diameter defined as the ratio of four times the gallery section divided by its perimeter.

Several fluid-dynamics parameters may be used to test for turbulence, the best known being the Reynolds and Richardson numbers.

3.4.6.1. The Reynolds Number

Let us use the following definition of the Reynolds number [Netz, 1983; Lebrun & Tercafs, 1972]:

$$\mathrm{Re} = \frac{v * d_h}{\nu} \qquad \textit{[eq. 3.4.4]}$$

where

v mean velocity over the section of the gallery [m*s^{-1}]

d_h hydraulic diameter (= 4*section/perimeter) [m]

ν cinematic air viscosity of the air [m^2*s^{-1}]

The cinematic air viscosity can be computed using the expression given by Netz [Netz, 1983]:

$$\nu = \frac{1}{p} * \frac{4.87 * T^{1.5}}{1 + \frac{172.6}{T}} * 10^{-6} \qquad \textit{[eq. 3.4.5]}$$

where

p local atmospheric pressure [hPa]

T air temperature [K]

As a first quick check let us compute the critical velocities for the stations 2 and 3, i.e. the velocities above which flow becomes turbulent:

The cinematic viscosity ν of air at 10°C and 1000 HPa is 1.44*10^{-5} m^2*s^{-1}; the critical velocity v_c = Re*ν/d_h= 2300*1.4410^{-5}/d_h, which gives 4.5 cm*s^{-1} for station 2 and 5.7 cm*s^{-1} for station 3.

As the measured velocities at station 2 are most of the time larger than 4.5 cm*s^{-1}, we should expect turbulent flow at this location; at station 3 the velocities often oscillate around mean values close to 4 to 5 cm/s, so both turbulent and laminar flows occur there.

To compute the Reynolds numbers, we use the data from Jan.92 to Nov.94; due to a sensor malfunction, we have missing data at station 2 for the 3 months from Oct. 1992 to Dec. 1992.

Table 3.4.7. gives, in multiples of 1000, the mean values and standard variations of the Reynolds numbers for the 3 years (the standard deviations are always huge, mostly close to the mean values).

Figure 3.4.13. shows the monthly mean values for station 2 and station 3. At first glance there seems no apparent seasonal trend, except lower values during April, May and October; during these periods we have the lowest mean temperature differences between the inside and outside and, as a consequence, the smallest air movements.

The distinction between inflow and outflow in table 3.4.4. is done using the difference (external temperature - local temperature) : a positive diffe-

rence means inflow. Outflow and inflow turbulence does not differ in a spectacular manner, contrary to what one could intuitively expect (assuming outflow to be less turbulent than inflow).

Table 3.4.4. Reynolds numbers (mean ± standard deviation, in multiples of 10^3)

	station 2			*station 3*		
year	*whole year*	*inflow*	*outflow*	*whole year*	*inflow*	*outflow*
1992	11±8 (Jan->Sep)	11±9 (Jan->Sep)	11±7 (Jan>Sep)	1±2	1±2	2±2
1993	10±7	10±7	9±7	2±2	2±3	2±2
1994 (Jan-Nov)	12±8	14±8	9±7	1±1	1±1	2±2

The Reynolds numbers at station 2 are always well in excess of 2300, a value usually assumed as marking the boundary between laminar and turbulent flow in smooth pipes; the air movements are certainly turbulent at the entrance of the cave. The mean monthly values at station 3 are much smaller than those at station 2, but the hourly pattern show that we certainly have both turbulent and laminar regimes at this station.

There remains a question: does the external wind have a great influence on the Reynolds numbers? Let us again take the subset of 5088 data-points from the 1994 data (Jan. 1994 to Mar.1994 and Aug. 1994 to Nov. 1994) which gives the Reynolds numbers shown in table 3.4.5. (in multiples of 1000, mean ±std):

Table 3.4.5.

station	*all values*	*no outside gust*	*inflow and no outside gust*	*outflow and no outside gust*
station 2	11±8	11±8	12±8	11±8
station 3	1±1	1±1	1±1	1±1

One can readily see that neither the existence of an outside gust nor the direction of the airflow cause significant changes to the mean Reynolds numbers. The correlation between the Reynolds numbers for station 2 and 3 are highly significant (at the alpha=0.01 level). As a crude rule of thumb one can state that usually the Reynolds numbers at station 3 are about ten times smaller than those at station 2.

Table 3.4.6.

correlation between Reynolds numbers at station 2 and station 3		*linear fit forced through origin:*
all values:	0.51	Rey_3=0.096*Rey_2
no outside gust:	0.49	Rey_3=0.090*Rey_2

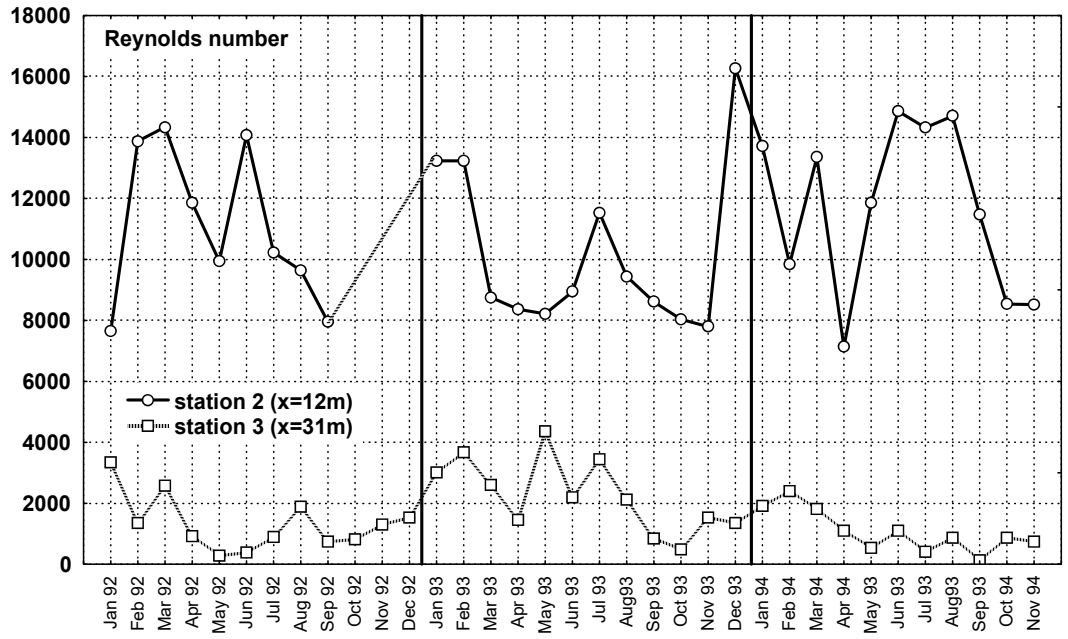

Fig. 3.4.13. Mean monthly Reynolds numbers

3.4.6.2. The Richardson number Ri

The Richardson number is related to the vertical temperature and velocity gradients across the section of a pipe [Lebrun & Tercafs, 1972; Parker, 1988]

$$Ri = 9.81 * \frac{1}{273} * \frac{\frac{dT}{dy}}{\left[\frac{dv}{dy}\right]^2} \qquad \textit{[eq. 3.4.6]}$$

where

T temperature [°C or K]

y vertical height [m]

v air velocity [m*s^{-1}]

At station 2 the height of the gallery is approximately 1.3 m; let us take the data of the manual measurement series done on 18 Nov. 1993 at 08:00 UTC: temperature was 10.2°C at the bottom of the gallery and 10.4°C at the top, so dT/dy ≈ 0.15 [K*m^{-1}]. As the velocity of the air must be 0 both at the bottom and at the top, and as v has been measured approximately at the centre of the gallery, dv/dy may be taken as v/(height/2) = v/0.66.

The measured velocity was v=0.27 [m*s^{-1}], so dv/dy ≈0.27/0.66 = 0.41 and R_i computes to:

$$R_i \cong \frac{9.81}{273} * \frac{0.15}{0.41^2} \cong 0.03 \qquad \textit{[eq. 3.4.7]}$$

The critical R_i number which separates turbulent from laminar flow is 0.25, with turbulence corresponding to $R_i < 0.25$; the R_i number found above shows that air flow must be turbulent at station 2. The Reynolds number computed at the same time is R_e=13700.

3.4.7. Computing an Apparent Friction Factor.

The relationship between pressure-drop and velocity of an turbulent air flow in a pipe is given by the classical formula of Darcy-Weisbach [Recknagel, 1992; Atkinson, Smart & Wigley, 1983]:

$$dp = \frac{f * L * v^2 * \rho}{4 * R} \qquad \textit{[eq. 3.4.8]}$$

where:

f friction factor

L pipe length [m]

v air velocity [m*s^{-1}]

ρ air density in the cave [kg*m^{-3}]

R hydraulic radius [m]

Let us take this formula to estimate the unknown friction factor using once again the 5088 point data-subset of 1994 (see chapter 3.3.3). The air velocity is lower than the measuring limit of the hot-wire anemometer after station 3 (x = distance from entrance = 31 m); the openings of the differential pressure sensor are situated at x = 6 m and x = 50 m. So let us assume a total gallery-length of 31-6 = 25 m and reduce proportionally the measured pressure drop by multiplying dP by 25/(50-6). The hydraulic diameters at station 2 and 3 are 0.73 m and 0.58 m, which gives a mean hydraulic radius of (0.73+0.58)/4 = 0.33 m. All other means are computed from the corresponding values measured at station 2 and station 3.

The following table 3.4.7 summarizes the results:

Table 3.4.7.

	inflow	*outflow*
mean air velocity	0.144 $m*s^{-1}$	0.104 $m*s^{-1}$
mean air density	1.2031 $kg*m^{-3}$	1.2127 $kg*m^{-3}$
mean measured pressure drop	0.26 Pa	-0.13 Pa
computed pressure drop	f*0.47 Pa	-f*0.25 Pa
apparent friction factor f	0.55	0.52

According to Atkinson the **apparent** friction factor f should be quite large for a heavily constricted cave: its magnitude may even approach or be in excess of 1. As this factor is independent of flow direction, we should find approximately the same value for inflow and outflow: our data show that this is indeed the case, with **f ≈ 0.5**.

The friction factor f computed in the above way is often called "**apparent** friction factor", because the various constrictions, crawlways, turns or other changes in an underground gallery give much higher values for f than those corresponding to the wall-roughness alone. Let us verify what a classical calculation of wall roughness would yield if the true friction factor were 0.5.

We use the formula given by Recknagel [Recknagel, 1992] corresponding to turbulent air flow in a rough tube:

$$\frac{1}{\sqrt{f}} = 2\log\left[\frac{\frac{\varepsilon}{D}}{3.71}\right] \qquad \textit{[eq. 3.4.9]}$$

where:

f friction factor

D (hydraulic) diameter of gallery [m]

ε roughness of wall [m]

Taking f=0.5 and D = 0.66 m we get **ε=12.5 m**, clearly an impossible high value! The apparent friction factor should be considered as a global, useful **empirical** parameter for a given cave gallery; its knowledge allows to compute the mean velocity from the measured pressure difference, or vice-versa.

3.4.8. Convection and Conduction

Heat enters and leaves the cave, depending the changing (seasonal) air flow conditions. We showed in chapter 2 that the Fourier equation corresponding to a situation of pure heat conduction through the rock gives temperature profiles deviating markedly from the measured profiles. The difference is certainly caused by convective heat transfer.

To estimate the relative importance of convective versus conductive heat transfer **through the cave air**, one often uses the Nusselt number which is defined as [Lebrun & Tercafs; 1972]:

$$Nu = \frac{convective\_heatflow}{conductive\_heatflow} = \frac{Q * \rho * c_p * dT}{\frac{\lambda}{L} * dT * S} \qquad \textit{[eq. 3.4.10]}$$

$$Nu = \frac{\mathrm{v} * S * \rho * c_p * dT}{\frac{\lambda}{L} * dT * S} = \frac{L * \mathrm{v} * \rho * c_p}{\lambda} \qquad \textit{[eq. 3.4.11]}$$

where:

Q volume air flow over gallery section [m^3*s^{-1}]

ρ density of air [$kg*m^{-3}$]

c_p specific heat of air [$J*kg^{-1}*K^{-1}$] = 1007 for dry air

dT temperature difference [°C or K]

L length of gallery [m]

λ thermal conductivity of air [$W*m^{-1}*K^{-1}$] = 0.024 for dry air

As c_p for moist air is difficult to evaluate, let us calculate the Nusselt number for dry air, which is certainly smaller than the real N_u number for moist air. We will apply our calculations to the portion of gallery situated between stations 2 and 3; thus L = 19 m, and v and ρ are the means of the corresponding values at these 2 stations.

We find:

$$Nu = \frac{L * \mathrm{v} * \rho * 1007}{0.024} \qquad \textit{[eq. 3.4.12]}$$

which gives the results shown in table 3.4.8 for typical winter and summer months. The extremely high Nusselt numbers show that the heat transfer occurs practically only through convection; conduction by cave air plays a negligible role.

Table 3.4.8.

month	*mean ext. temperature*	*mean temperature difference (1)*	*mean velocity (1)*	*mean air density (1)*	*Nusselt number for dry air (*10^3*)*
January 1994	3.6	-1.9	0.16	1.22	156
August 1994	19.1	+6.2	0.16	1.20	153

(1) between station 2 and 3

3.4.9. Energy Balance

In this paragraph we will compute the yearly thermal energy flows into and out of the cave and try to find the net balance. Let us again stress that we assume that the cave has only one single entrance in the main storey: this means that in summer all the air will enter the cave through the main entrance, and in winter all outflow will be through this same opening. The air entering the cave brings a certain enthalpy and kinetic energy to the underground system. As the air velocities are low, we can readily neglect the kinetic energy in comparison to the enthalpy.

We first will compute an expression of the enthalpy of 1 m^3 moist air entering the cave, following a reasoning given by Badino [Badino, 1995].

Let us start by a mass of moist air consisting of 1 kg dry air and d kg water vapour (so the total mass is m = 1+d). The enthalpy of this mixture consists of 3 parts:

- H1 = enthalpy of 1 kg dry air at T °C = c_p*1*T = 1007* T [J]

  *1007 [J*kg^{-1}*K^{-1}] = specific heat of dry air*

- H2 = evaporation energy corresponding to d kg water vapour, which will be restored when condensation occurs

  = 2501*10^3*d [J]

  *2501000 [J*kg^{-1}] = latent heat of water vapour*

- H3 = enthalpy of d kg water vapour at T °C = 1930*d*T [J]

  *1930 [J*kg^{-1}*K^{-1}] = specific heat of water vapour*

The total enthalpy in Joule of m = 1+d kg moist air is :

$$H_m = H_1 + H_2 + H_3$$
$$H_m = 1007 * T + d * \left[2.501 * 10^6 + 1930 * T\right] \qquad \textit{[eq. 3.4.13]}$$

It can be shown [Recknagel, 1992; Badino, 1995] that

$$d = 6.22*10^{-4} * p_V \qquad \textit{[eq. 3.4.14]}$$

where p_V is the water vapour pressure in [hPa]; p_V is equal to (H%/100)*p_{sat} where H% is the relative humidity in percent and p_{sat} the saturated water vapour pressure in [hPa]. For the temperature range valid in the caves, we may use the following good approximation to p_{sat} [Choppy, 1992], as seen in chapter 2:

$$p_{sat} \cong \left(\frac{T}{6}+1\right)^2 + 5 \qquad \textit{[eq. 3.4.15]}$$

which finally allows to express d as a function of T and H%:

$$d \cong 1.728*10^{-7} * H\% * \left[(T+6)^2 + 180\right] \qquad \textit{[eq. 3.4.16]}$$

H_m represents the enthalpy of m = (1+d) **kg** of moist air; the enthalpy H_v of 1 $\mathbf{m^3}$ of moist air is equal to H_m divided by the density of moist air.

Using the expression of this density found in chapter 2, we can express the enthalpy H_v as a function of the **measurable** parameters air temperature T, relative humidity H% and air pressure p:

$$H_v = \frac{1007*T + 1.728*10^{-7} * H\% * \left[(T+6)^2 + 180\right] * (2.501*10^6 + 1930*T)}{\frac{0.34855}{273.16+T} * \left[p - \frac{0.406}{3600} * H\% * \left((T+6)^2 + 180\right)\right]}$$

[eq. 3.4.17]

where

T air temperature [°C]

H% relative humidity [percent]

p air pressure in [hPa]

H_v enthalpy of 1 m^3 of moist air [J]

The dominant factor influencing H_v is temperature; actually the curves of H_v and T vary almost identically, as shown by the next figure 3.4.14. which plots H_v (upper graph) and T (lower graph) at station 2 in Dec.93.

If the air enters the cave with a velocity v [$m*s^{-1}$] through a gallery-section of S m^2, we can compute the total energy entering the cave during one hour by:

*Energy = Hv*v*0.74*S*3600/3600000 = Hv*v*0.74*S/1000 [kWh]*

[eq. 3.4.18]

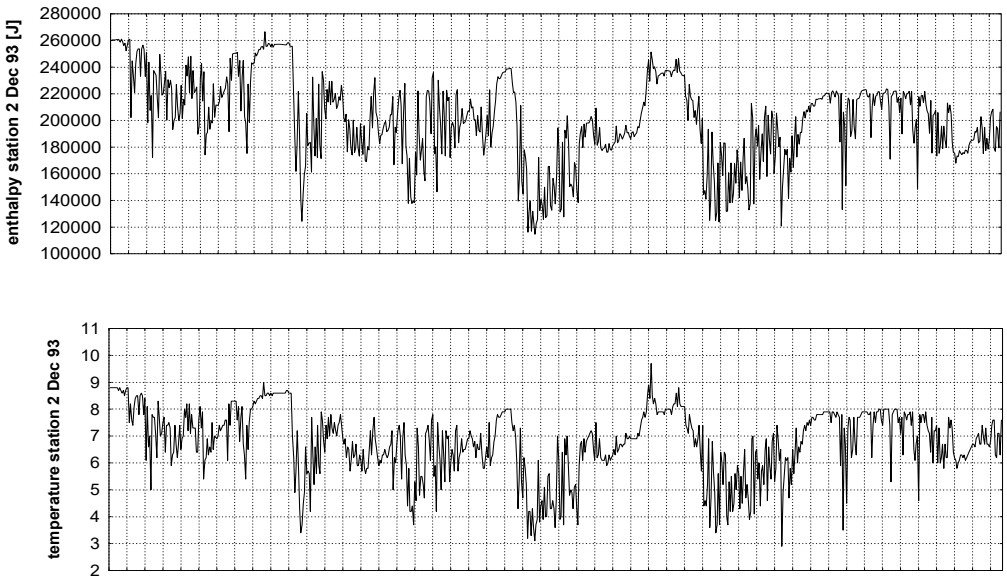

Fig. 3.4.14. Variations of enthalpy and external temperature in Dec.93(subset;ticks mark hours)

The multiplier 0.74 is used to compute an approximate mean velocity over the whole section from the centre velocity v (factor valid for very rough pipes) [Parker, 1988].

The balance over a whole month can be computed as follows: Independently of the flow direction, air enters the cave during all the time, either through the single entrance of the main gallery or from the lower situated galleries. The corresponding energy E_{in} is computed by using the external temperature, relative humidity and air pressure, and the velocity v at station 2 (multiplied by 0.74): $E_{in} = H_v(T_{ext},H_{ext}\%,p,v)$. All the air which enters the cave must leave it again; we will assume that during its journey in the cave this air has taken the mean cave temperature of 9.4°C and will become saturated at 100% relative humidity, its pressure being the same as the outside atmospheric pressure; let E_{out} denote the energy leaving the cave: $E_{out} = H_v(9.4°C,100\%,v,p)$.

The net energy balance is:

$$\Delta E = E_{in} - E_{out} = H_v(T_{ext},H_{ext}\%,v,p_{ext}) - H_v(9.4,100,v,p)$$

[eq. 3.4.19]

Table 3.4.9 shows the results for a whole year, starting in December 1993 and ending November 1994.

Table 3.4.9

month	*Ein [Kwh]*	*Eout [Kwh]*	*ΔE [KWh]*
Dec93	18457	30256	-11799
Jan94	13596	25684	-12088
Feb94	5945	16851	-10906
Mar94	18986	25094	-6108
Apr94	11011	13123	-2112
May94	24901	22735	+2166
Jun94	35868	27877	+7991
Jul94	49294	29079	+20215
Aug94	46653	29079	+17574
Sep94	27668	21615	+6053
Oct94	16853	16467	+386
Nov94	16323	15852	+471
Totals	285557	272980	+12577

The net balance over 12 month is:

- Dec91--->Nov92: -22050 (estimated) [KWh]

- Dec92--->Nov93: -24722 [KWh]

The negative balance means that the cave actually lost energy to the outside during these two years, whereas it gained 12577 [KWh] during the period from Dec. 1993 to Nov. 1994.

The autumn months are those of minimal energy transfer (and corresponding minimal perturbation of the underground system), and the two summer months of July and August do usually inject into the cave more or less the same amount of thermal energy than it looses during the following two cold winter months of December and January:

- 1992: inflow Jul.92 + Aug.92 = 61332 [KWh]

outflow Dec.92 + Jan.93 = 57935 [KWh]

- 1993: inflow Jul.93 + Aug.93 = 56265 [KWh]

outflow Dec.93 + Jan.94= 55940 [KWh]

The correlation between the monthly energy balance ΔE and the mean monthly outside temperature T_m is very high: r=0.97!

The following two figures (fig. 3.4.15 & 3.4.16) show the seasonal variations of these two parameters and the linear fit of ΔE to T_m . Actually the linear fit gives a good model to estimate the monthly energy balance from the mean external temperature, without resorting to the complicated calculations involving H%, v and p. According to the model, the reversal temperature that gives a zero energy balance is 10.7°C, about 1.3°C above the measured mean cave temperature of 9.4°C.

If we force the linear fit through (T_{ext} = 9.4°C; dE = 0) we get the following equation:

$dE \cong 1442*T - 1644$ with dE in [KWh] and T in [°C] *[eq. 3.4.20]*

Let us insist again on the various simplifying assumptions made in this chapter; we have for instance completely neglected that oscillating air movements may not extend throughout the whole cave. The computed values of E_{in} and E_{out} should be seen as rough and probably too high estimates.

The contribution of the geothermal heat flux to the energy balance of the cave is negligible; if we assume a mean geothermal flux of 0.0418 $W*m^{-2}$ [Badino, 1995], a total gallery length of 3500 m with a mean width of 0.5m, we will get for the whole cave a geothermal flux of 73 W, which corresponds to a monthly energy of 53 KWh, about 2 to 3 order of magnitudes smaller than the energy E_{in} or E_{out} computed above.

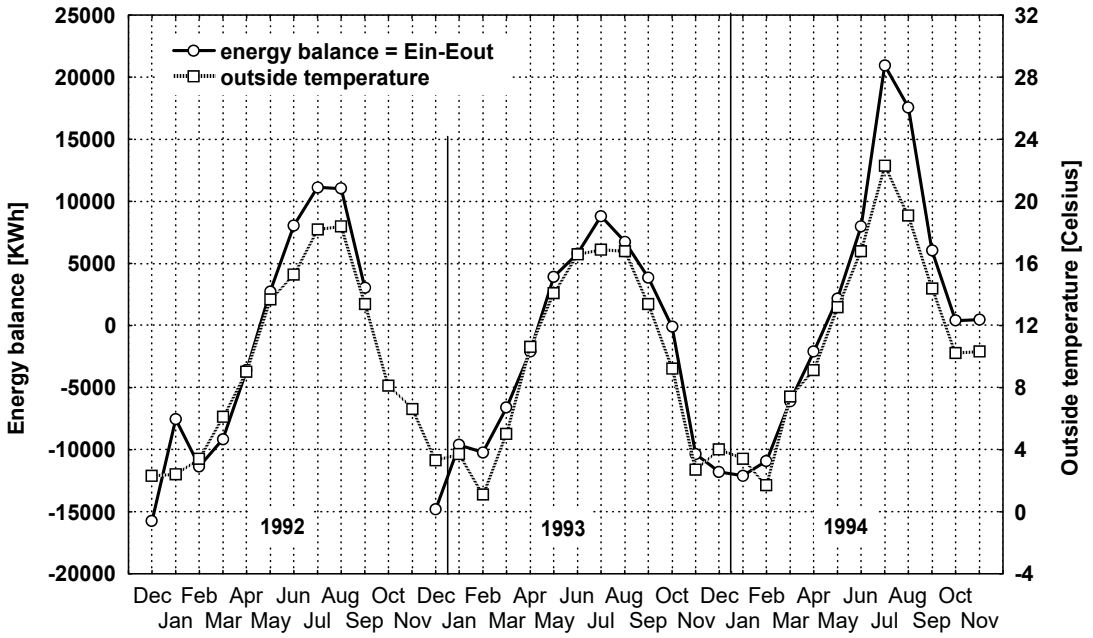

Fig. 3.4.15. Seasonal pattern of energy balance and outside temperature

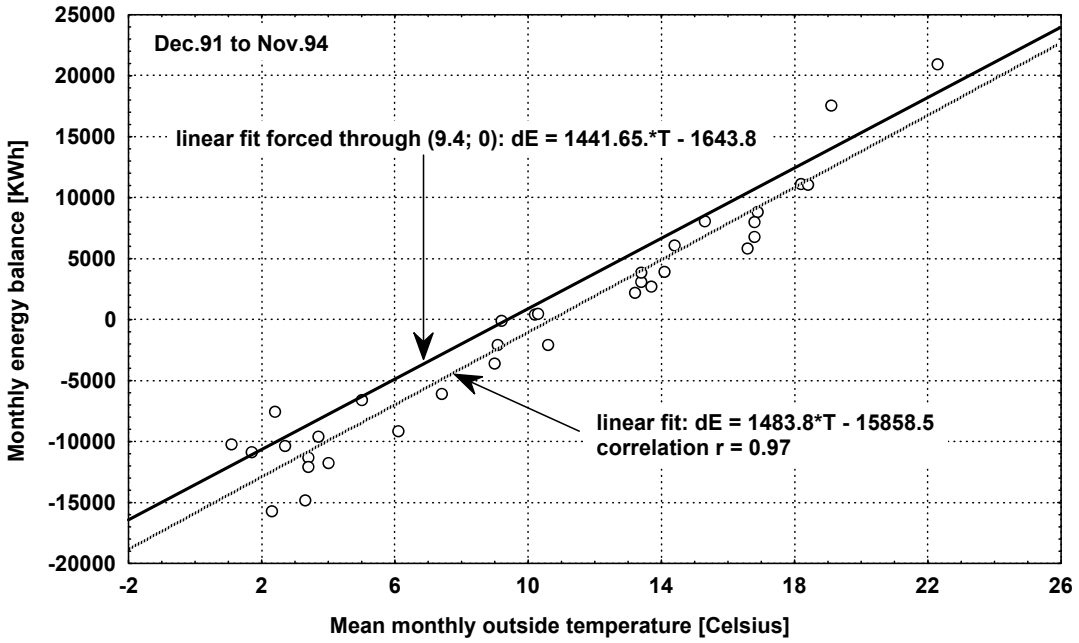

Fig. 3.4.16. Linear relationship between monthly energy balance and mean monthly outside temperature

3.4.10. Air Flow Oscillations

3.4.10.1. Existence of Oscillating Air Movements

Many attempts were made during cave visits to detect eventual periodic reversals of airflow direction or periodic changes of the magnitude of wind velocity. Analyses with smoke using incense sticks often showed that the direction of airflow reversed within one or two minutes; the readings of the anemometers also varied often periodically at the same rythm. To get a clearer picture of this phenomen, we did several fast measurement campaigns by using sampling intervals much shorter than the usual one hour interval.

The first of these campaigns was done in 1992, when neither the differential pressure sensor nor the external weatherstation were installed. As no direct measurement of air flow directions or external gusts are available, the needed information has to be inferred in an indirect manner.

If external wind blows into the cave, the difference $\Delta\rho_{12}$ between the outside air density and that at station 2 (situated only 12 m from the entrance) becomes very small; as the fresh air inflow does not extend up to station 4, the corresponding difference $\Delta\rho_{14}$ is not affected and does not change accordingly in an appreciable manner.This means that $\Delta\rho_{12}$ and $\Delta\rho_{14}$ differ much when there exists an outside gust; conversely, when $\Delta\rho_{12}$ is

close to $\Delta\rho_{14}$, no external wind blows into the cave, and the only air movements are those driven by differences of air densities.

Flow direction can be detected by looking for the algebraic sign of $\Delta\rho_{14}$: a positive sign means outside air entering the cave (winter) and vice-versa. If no external gust exists, another clue is given by the variations of air temperature at station 2: if air blows out of the cave, this temperature is nearly constant, which is not the case if fresh air enters the cave.

The check for possible periodicities is done mainly by calculating its power spectral density (PSD) or the autocorrelation function: they are among the best tools available for analysing frequency spectra or common periodicities. The original FFT algorithm demands that the series length be equal to a power of two. Even if the DADiSP software used can compute the FFT for series of arbitrary length, tests have shown that in theses cases a small but noticeable spectral smearing may occur. To avoid all problems resulting from the padding of series, we always use for our analysis subsets whose lengths are a power of two. As wind velocity and pressure differences vary very quickly, we systematically apply a digital lowpass FIR (finite impulse response) filter to block out the too fast variations. A 100 point FIR with a 3dB passband ripple and a 40dB stopband attenuation is computed using the digital filter package of the DADiSP software (version 3.01b). The cutoff frequency will usually be 0.05 Hz, which means that periods shorter than 20 seconds will be discarded. Before computing the PSD, or autocorrelation, the mean is substracted and a Hamming window is routinely applied (in the case of the PSD) to the low-pass FIR-filtered signal. The following figures show this FIR filter, the magnitude of its frequency response and the result of applying the filter to a velocity sampled at 0.25 Hz.

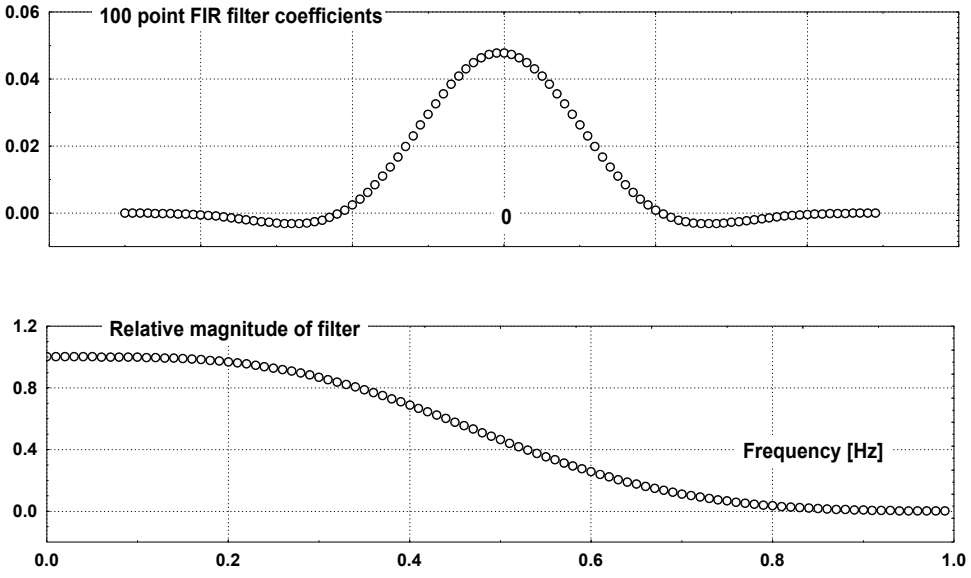

Fig. 3.4.17. FIR digital filter: coefficients and relative magnitude

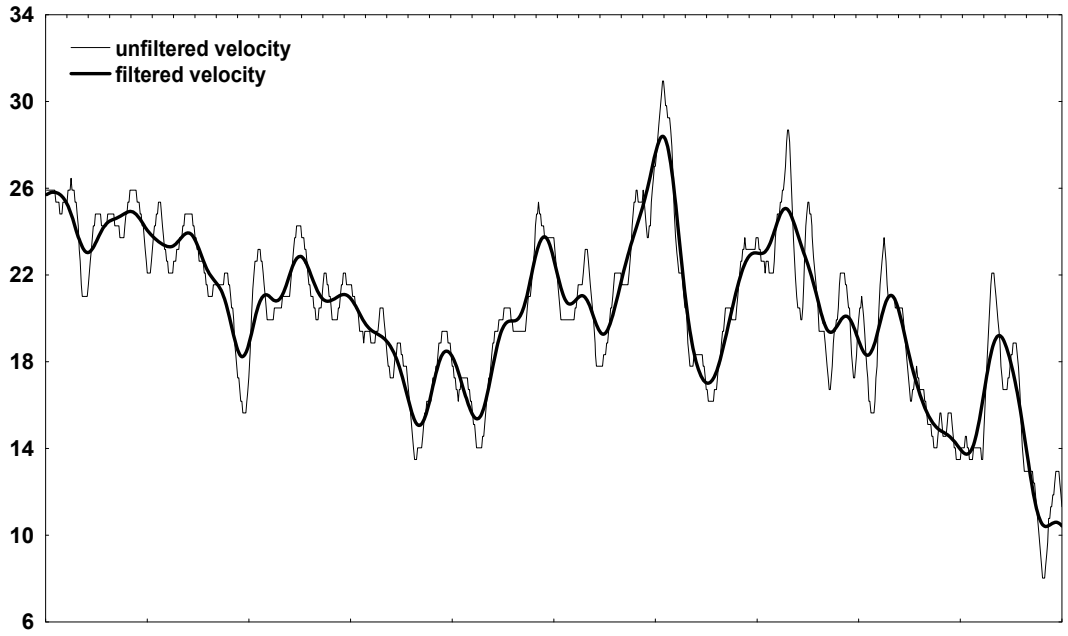

Fig. 3.4.18. Result of digital filtering on velocity data(sampling frequency 0.15 Hz)

3.4.10.2. Results of the Eight Fast Measurement Campaigns

We will now look in more detail at the 8 different fast measurement campaigns, and try to detect features common to all.

campaign #1	
date:	28 to 29 February 1992 (start: 14:30 UTC)
sampling rate:	15 Hz
number of samples:	13500; 8192 used for FFT
duration:	900 s
signal sampled:	v_2 velocity at station 2
mean outside temperature:	13.1°C
mean temp. at station 2:	9.1°C probably inflow
mean $\Delta\rho_{12}$ -0.01650 kg/m^3	negative means **inflow**
mean $\Delta\rho_{14}$: -0.01248 kg/m^3	small difference between $\Delta\rho_{12}$ and $\Delta\rho_{14}$ suggests no external gust

Visual inspection of $v_2(t)$ suggests a possible periodicity; the power spectrum has two very distinct peaks at about 90 s and 48 s.

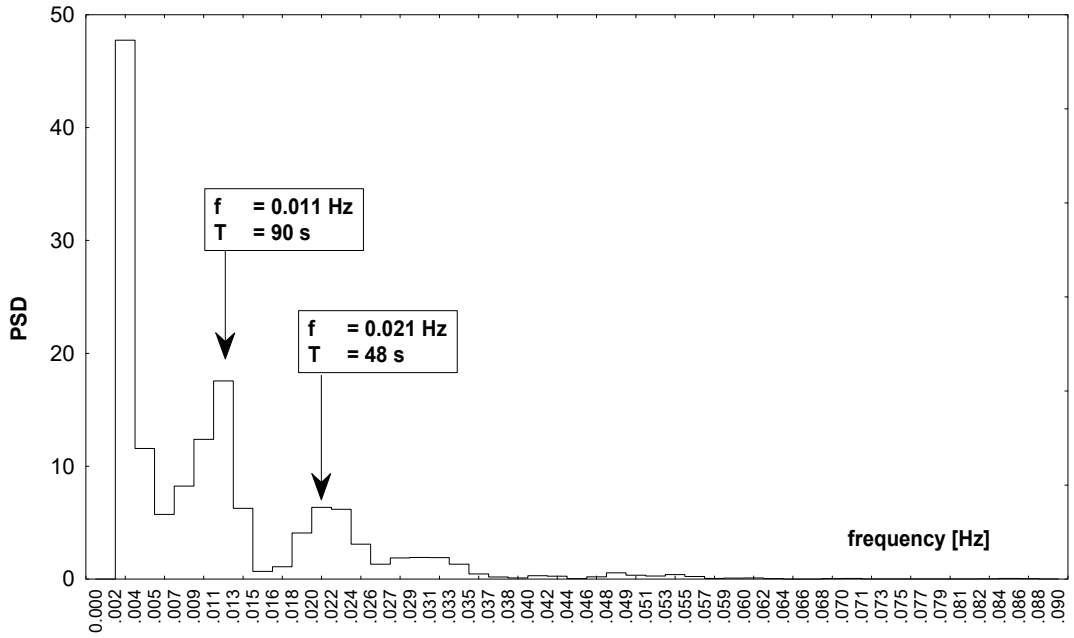

Fig. 3.4.19. Power spectral density of velocity at station 2 shows peak at 90 s

campaign #2	
date:	28 Feb. to 7 March 1992 (start: 16:30 UTC)
sampling rate:	0.5 min^{-1} = one sample every 2 minutes
number of samples:	5691; first 4096 used for FFT
duration:	≈190 hours
signal sampled:	v2, v3, velocities at station 2 and station 3 and all other usual parameters
mean outside temperature:	6.1°C
mean temp. at station 2:	8.9°C probably outflow
mean $\Delta\rho_{12}$: +0.01429 kg/m^3	positive sign means **outflow**
mean $\Delta\rho_{14}$: +0.01924 kg/m^3	small difference between $\Delta\rho_{12}$ and $\Delta\rho$14 suggests no external gust

The next figure shows how flow direction can be deduced from the variations of the air temperature outside and at station 2: the first 3 days show that the latter is nearly constant for most of the day, and changes only if the outside temperature exceeds aproximately 9°C. This means that we usually have a normal thermally induced outflow of cave air, and during five days out of nine no appreciable outside gust.

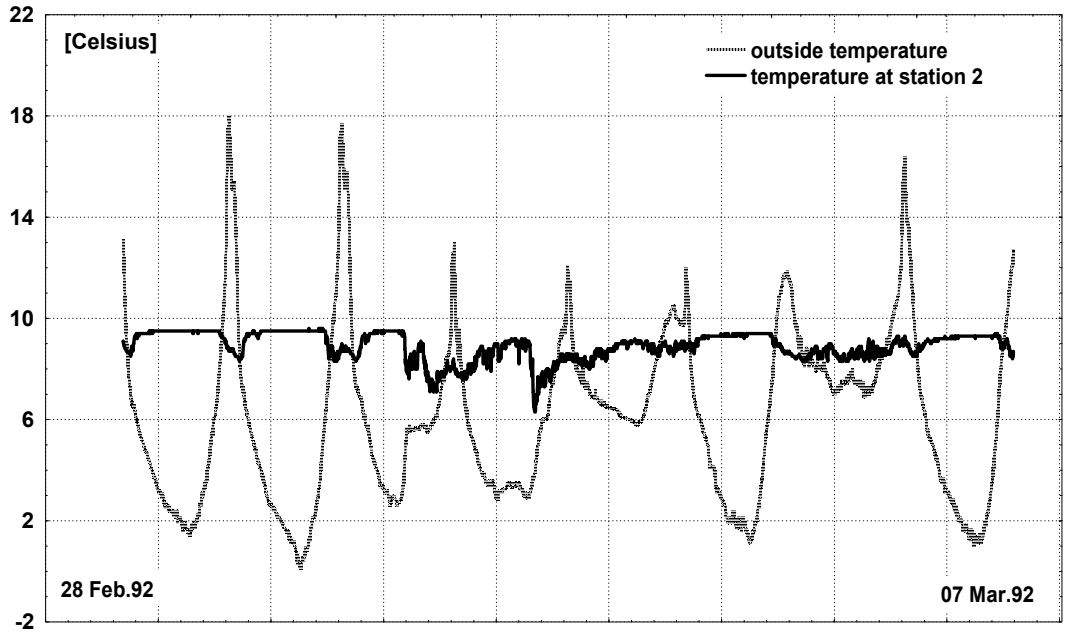

Fig. 3.4.20. Variations of temperature outside and at station 2 point to thermal induced inflow

Both measured velocities vary synchronously, as shown by fig. 3.4.21. which allows an easy check of the daily 24 hour period.

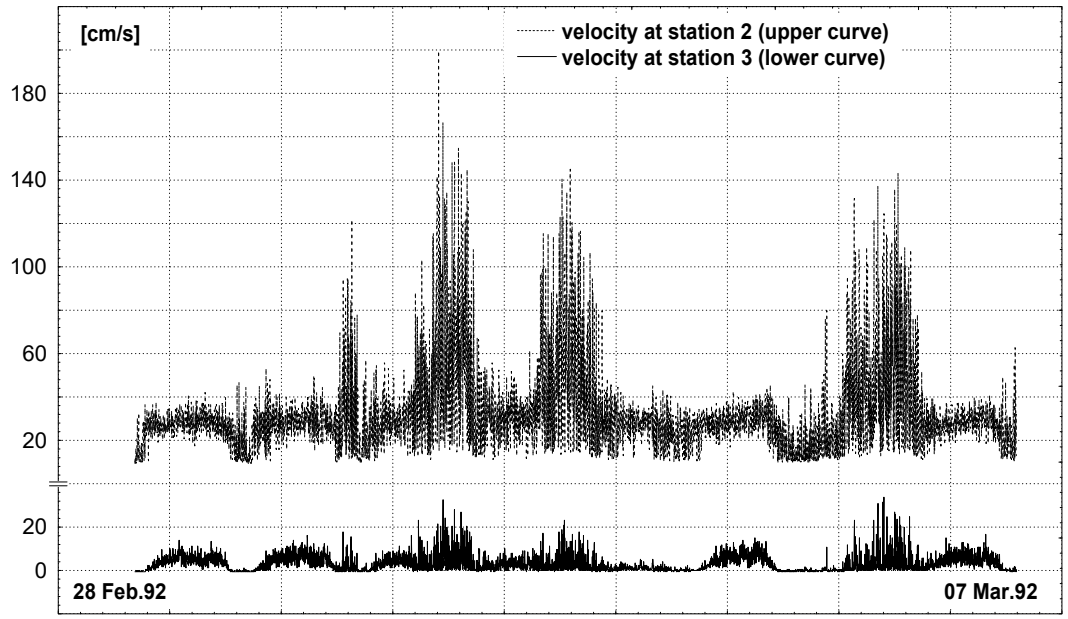

Fig. 3.4.21. Velocities at station 2 and 3 vary synchronously

The rather low sampling interval of 2 minutes does not allow to detect short periods in the 100 s range; the data may be used nevertheless to look for periods of longer duration. Actually, there are none: the sole periods given by the autocorrelation for velocities is the 24 hour period, as shown

by figure 3.4.22. (the autocorrelation values of the velocities are scaled for representation)

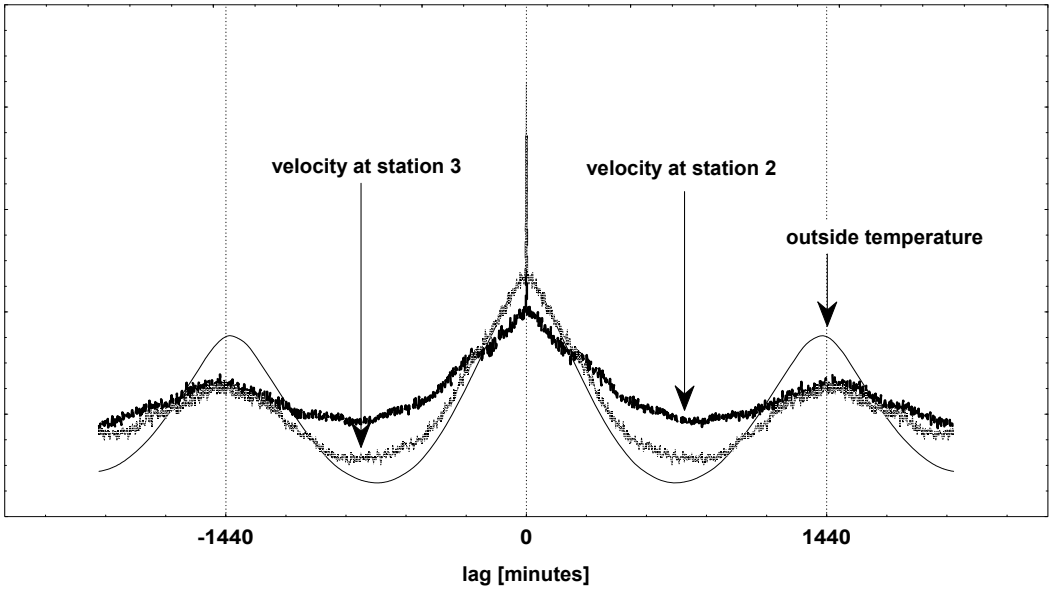

Fig. 3.4.22. Autocorrelation of outside temperature and air velocities and stations 2 and 3 show a common peak at a lag of 1440 minutes: the three signals have a 24h period..

campaign #3	
date:	2 May 1992 (start: 13:20 UTC)
sampling rate:	15 Hz
number of samples:	39999; first 32768 used for FFT
duration:	≈ 2667s
signal sampled:	v_2 velocity at station 2
mean outside temperature:	12.1°C
mean temp. at station 2:	9.0°C possible small inflow
mean $\Delta\rho_{12}$: -0.01330 kg/m^3	negative sign means **inflow**
mean $\Delta\rho_{14}$: -0.01010 kg/m^3	small difference between $\Delta\rho_{12}$ and $\Delta\rho_{14}$ suggests no external gust

This series corresponds to a moment where outside and deep cave temperatures are close; reversals of air flow direction are not impossible. The main peaks of the power spectrum are located at 231 s, 98 s and 54 s.

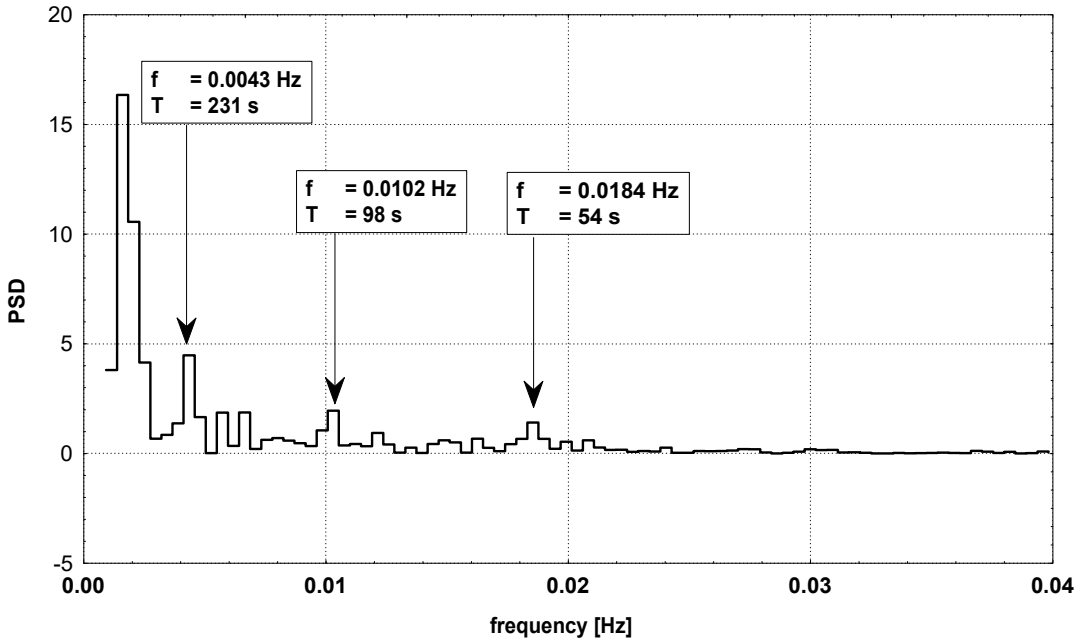

Fig. 3.4.23. Power spectral density function of velocity at station 2 shows 3 possible periods

campaign #4	
date:	29 Sep 1992 (start: 11:00 UTC)
sampling rate:	1 min^{-1}
number of samples:	5762; first 4096 used for FFT
duration:	≈ 4 days
signal sampled:	v_2 velocity at station 2
mean outside temperature:	13.2°C
mean temp. at station 2:	10.4°C probably constant inflow
mean $\Delta\rho_{12}$: -0.01276 kg/m^3	negative sign means **inflow**
mean $\Delta\rho_{14}$: -0.01671 kg/m^3	small difference between $\Delta\rho_{12}$ and $\Delta\rho_{14}$ suggests no external gust

This slow sampling campaign resembles #2 but corresponds to a period of inflow whereas campaign #2 was one of outflow. The graph of $v_2(t)$ (Fig. 3.4.24) clearly shows the influence of the external temperature on inflow: the velocity at station 2 increases with the difference of outside and inside temperature and air density. As in campaign #2, the sole period detectable is the daily 24h period.

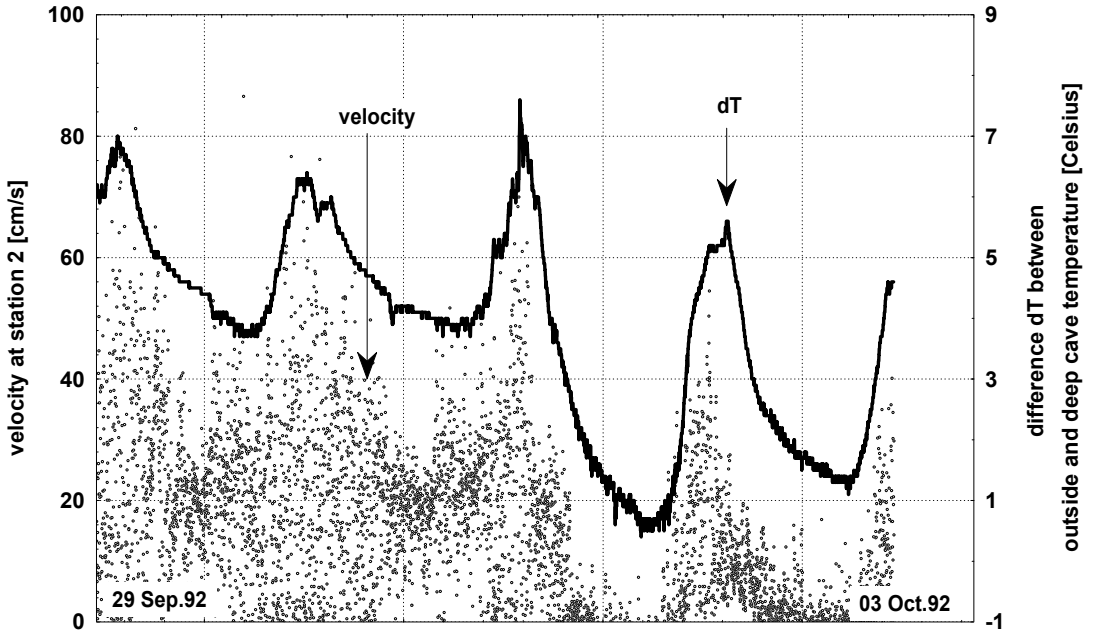

Fig. 3.4.24. Air velocity at station 2 varies according to the temperature difference between cave and outside

The last 4 campaigns were all pereformed in 1994; outside gusts are monitored by a weatherstation and pressure drop between entrance and deep cave is measured by a differential manometer.

campaign #5	
date:	29 Jan 1994 (start: 16:00 UTC)
sampling rate:	0.1Hz for velocity v2 at station 2 1 min^{-1} for velocity v_3 at station 3 and differential pressure dP between Salle Loubens (x=6m) and station 4 (x=51 m)
number of samples:	17292 and 2880
duration:	≈ 48 hours
signal sampled:	v_2,v_3, dP
mean outside temperature:	3.3°C
mean temp. at station 2:	6.7°C probably constant outflow
mean $\Delta\rho_{12}$: +0.01811 kg/m^3	positive sign means **outflow**
mean $\Delta\rho_{14}$: +0.02846 kg/m^3	great difference between $\Delta\rho_{12}$ and $\Delta\rho_{14}$ suggests existence of external gust
mean measured external gust:	2.6 m/s

This campaign represents an interesting situation as the external gusts cannot be ignored anymore. They strongly interfere with the normal ther-

mally induced outflow by forcing fresh air into the cave. This influence can be shown by computing the autocorrelation function over 2 subsets of the velocity, where one contains a period of gusts and the other none. Fig.3.4.25 shows a 3600 point (10 hours) subset of v_2 and dP, where the first 5 hours correspond to a practically gust-free situation. The auto-correlations computed over the first 5 hours and over the 5 last hours do both have a peak close to 100 - 110 s; this means that the external gusts do not completely override the resonant behaviour of the cave!

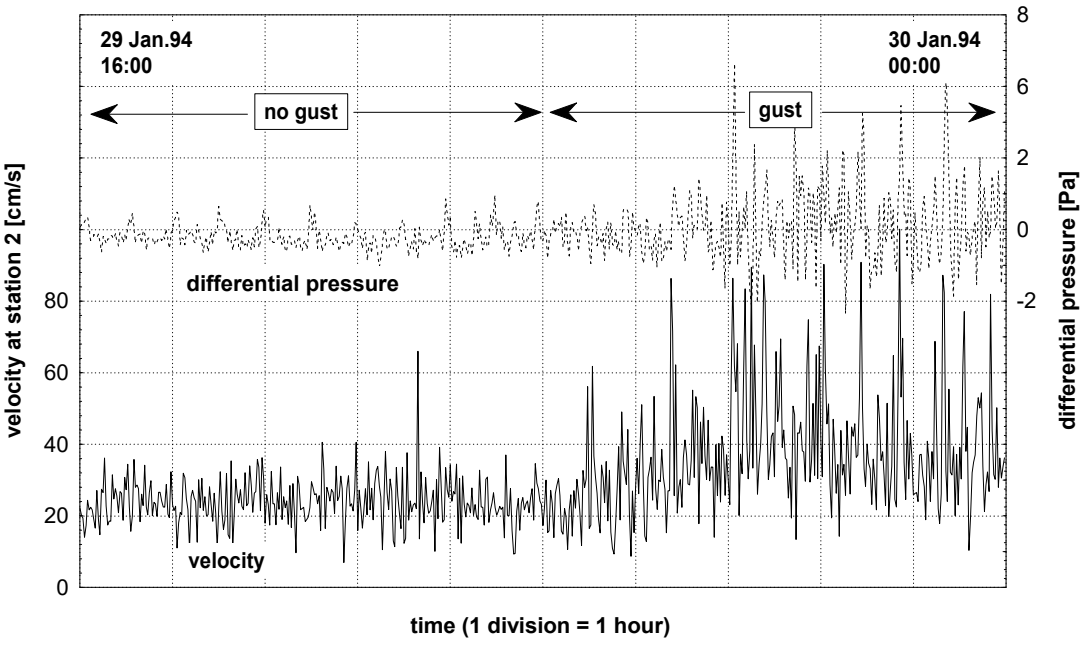

Fig. 3.4.25. Air velocity and pressure drop during a no-gust and a gust period.

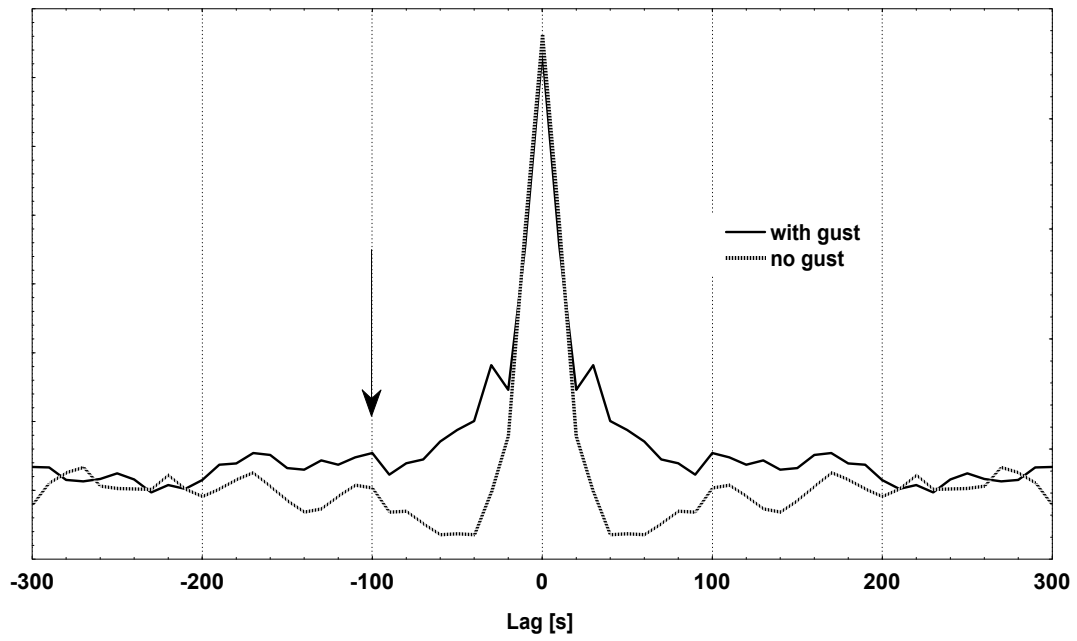

Fig. 3.4.26. Autocorrelation of velocity shows approx. same period for the no-gust and gust situation.

To economize electrical power, the CO_2 sensors could not be kept running continuously during this campaign: they were switched on every half hour for about 5 minutes. The operation of the CO_2 sensors has a clear influence on the voltages of the other signal lines; for that reason, readings were routinely done when CO_2 sensors were powered off. During this fast campaign, this was not possible as all instruments had to be kept running continuously. Even if the perturbations caused by the CO_2 sensors cannot be detected visually in the data series, the autocorrelations show a very distinct 30 minutes period (Fig.3.4.25. is based on the first 600 data from dP series). This is truly a fake period, akin to that of 20 s caused by the digital filtering; one must be very careful in the interpretation of autocorrelation peaks and spectral lines not to retain these artefacts!

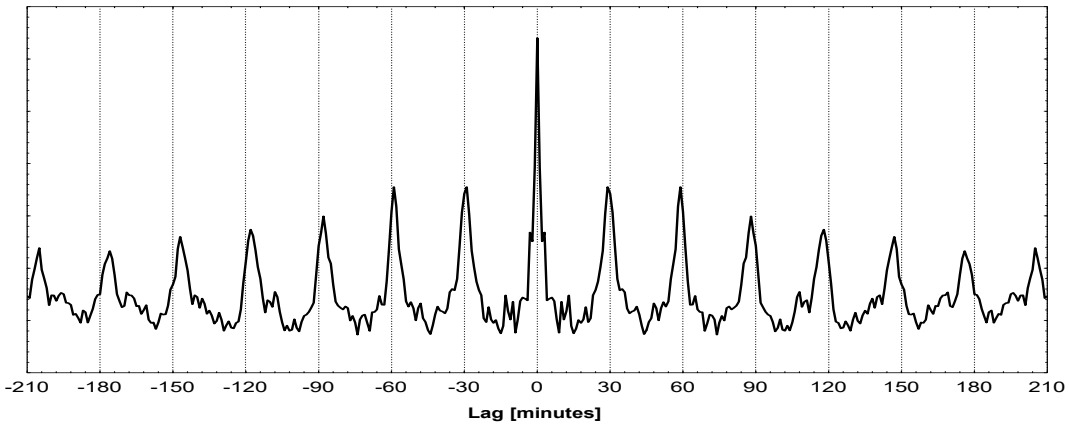

Fig. 3.4.27. Autocorrelation shows that CO2 sensor causes fake period of 30 minutes in dP signal

The last 3 campaigns all have been made in October 1994; the first two correspond to a no-gust and outflow situation, the last one to a moment where outside and inside temperatures are very close but with outside wind activity.

campaign #6	
date:	5 Oct 1994 (start: 09:23 UTC)
sampling rate:	1Hz
number of samples:	1680; 1024 used for FFT
duration:	≈ 28 minutes
signal sampled:	v_2, v_3, dP
mean outside temperature:	5.6°C
mean temp. at station 2:	11°C probably constant outflow
mean $\Delta\rho_{12}$: +0.02630 kg/m^3	positive sign means **outflow**
mean $\Delta\rho_{14}$: +0.02846 kg/m^3	small difference between $\Delta\rho_{12}$ and $\Delta\rho_{14}$ suggests no external gust
mean measured external gust:	0 m/s

Visual inspection of $v_2(t)$ points to a possible period of approx.170 s, the PSD (see Fig.3.4.28) gives a common period of T ≅ 172 s for both v_2 and v_3, and a value of same magnitude (≅ 205 s) for dP.

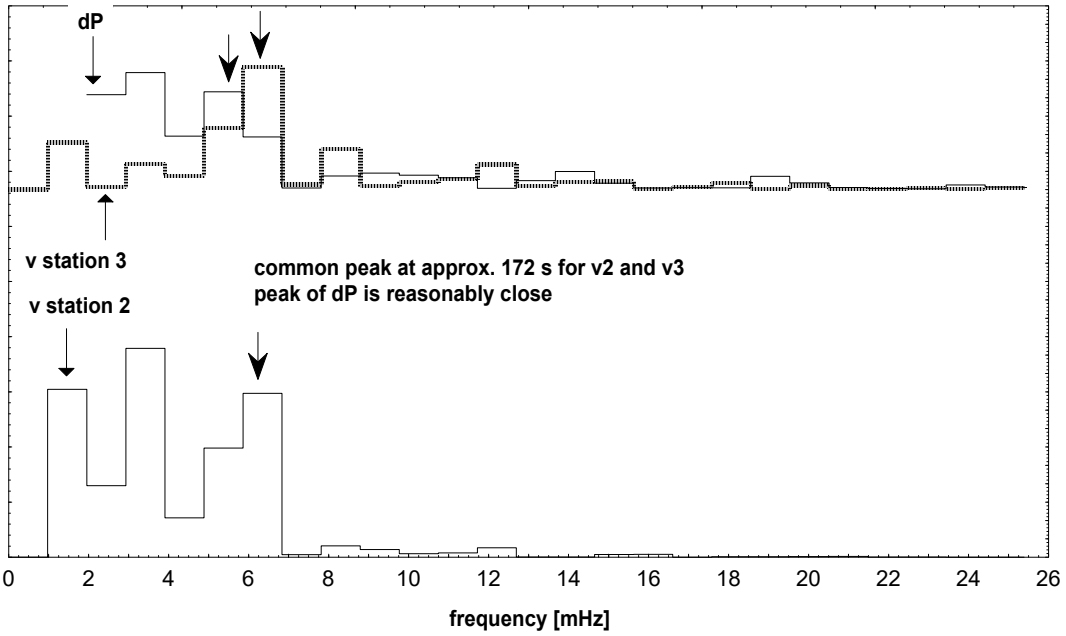

Fig. 3.4.28. PSD of v2 and v3 shows common period of approx. 172 s; periodicity of dP is of same magnitude.(v3 and dP data are scaled and shifted on the plot)

campaign #7	
date:	19 Oct 1994 (start: 09:46 UTC)
sampling rate:	1Hz
number of samples:	1860; 1024 used for FFT
duration:	≈ 0.5 hour
signal sampled:	v_2, v_3, dP
mean outside temperature:	7.5°C
mean temp. at station 2:	11.2°C probably constant outflow
mean $\Delta\rho_{12}$: +0.01905 kg/m^3	positive sign means **outflow**
mean $\Delta\rho_{14}$: +0.01217 kg/m^3	small difference between $\Delta\rho_{12}$ and $\Delta\rho_{14}$ suggests no external gust
mean measured external gust:	0 m/s

This series corresponds to a time where the outside air temperature is rather close to that of the cave; we have here the well-known interseasonal situation which may lead to unstable air-flows [Andrieux, cited in Choppy, 1986] with many possible short-time inversions of the flow direction. The dP(t) series shows small pressure drops which often oscillate between positive and negative values. A possible periodical reversal of flow direction should be found by looking at the autocorrelation function: as the

measured velocities are absolute values, their period should be half that of the pressure drop dP which causes the air movement. Fig. 3.4.29 shows the autocorrelations of v_2 and dP: we can clearly detect a peak at about 218 s for dP and one of about 111 s for v_2, which confirms the precedent assumption. The autocorrelation of velocity at station 3 (not shown here) suggests a period of about 103 s, close to that of velocity at station 2.

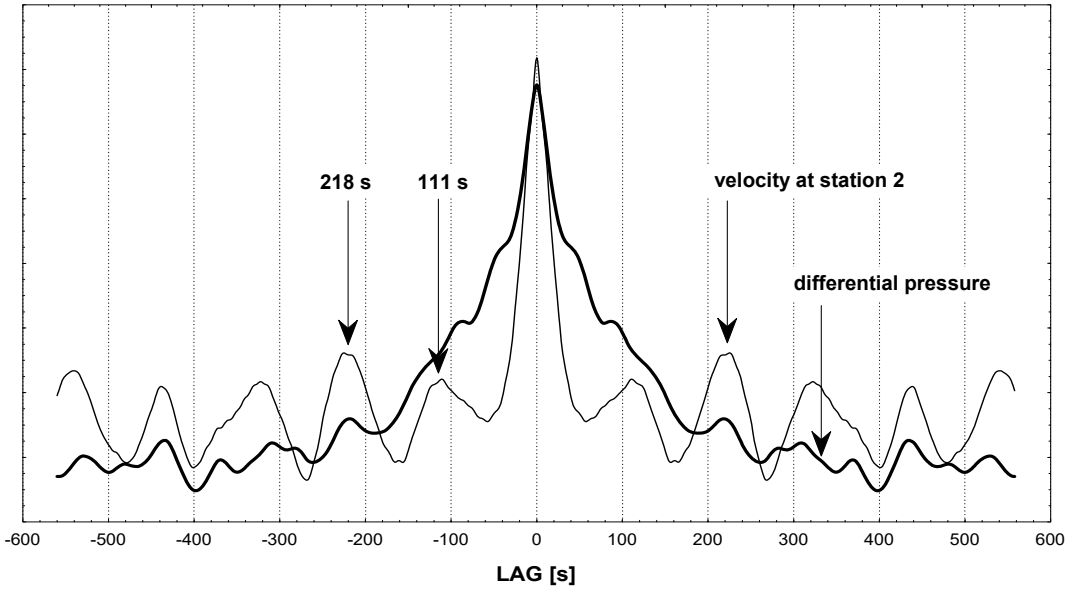

Fig. 3.4.29. Autocorrelation of v and dP shows that the period of v is half that of dP.

campaign #8	
date:	26 Oct 1994 (start: 10:06 UTC)
sampling rate:	1Hz
number of samples:	1260 for v_2, 1860 for dP and v_3
duration:	≈ 0.5 hour
signal sampled:	v_2, v_3, dP
mean outside temperature:	10.2°C same outside and inside
mean temp. at station 2:	10.2°C temperatures suggest either no flow or forced inflow
mean $\Delta\rho_{12}$: +0.0010 kg/m^3	near zero could mean forced inflow
mean $\Delta\rho_{14}$: -0.0014 kg/m^3	great difference between $\Delta\rho_{12}$ and $\Delta\rho_{14}$ suggests external gusts
mean measured external gust:	2.2 m/s

We have here again a situation where the outside temperature is close to the deep cave temperature of 9.4°C. As the outside gusts are not negligible (similar to that of campaign 5), a possible oscillation of the thermally induced airflow may or may not be modified. The autocorrelations show the following peaks:

v_2	53 s
v_3	85 s
dP	41 s

In campaign #5 we saw that the outside gusts did not completely mask the resonant period of about 110 s; could it be that this time it would accelerate the air movement by halving the resonant period at the station closest to the entry, leaving it undisturbed in deep cave?

3.4.10.3. Summary of the Fast measurement Campaigns and Discussion

Out of the 8 campaigns, 6 correspond to sampling rates smaller than or equal to 10 seconds; only these series can show the potential oscillations in the 50 to 200 s range we are trying to detect. If we separate the results according to gust/no gust and inflow/outflow, we get the following picture:

Table 3.4.10.

gust	*outflow*	*inflow*
no	subset of #5: Tv_2 110 s v_3 and dP not available	#1: Tv_2=90 s v_3 and dP not available
	#6: Tv_2=Tv_3 172 s Tv_3 not detectable T_{dP}=198 s	#3: possible oscillation Tv_2=45 s v_3 and dP not available
	#7: Tv_2=111 s Tv_3=103 s T_{dP}=218 s possible oscillation	
yes	subset of #5: Tv_2 ≅110s v_3 and dP not available	#8: possible oscillation Tv_2=48 s Tv_3=90 s T_{dP}=45 s

These results show that a periodic variation of air flow velocity at station 2 with a period in the 90 s - 110 s range can be found in **all** cases when there are **no external gusts**. In one of the two cases for which data are available, the period of the velocity at station 3 is the same.

When external wind blows, we find the same situation in one of the two cases. Finally, we have one case of no external wind where external and internal temperatures are close: this corresponds to an unstable situation with possible periodic reversals of the air flow direction. In such a case, the period of v_2 (remember that v_2 is the absolute value of flow velocity!)

should be half of that of the differential pressure; the data of campaign #7 do indeed confirm this.

Oscillating air movements in caves have frequently been measured; these investigations generally found more or less periodic reversals of flow direction at a time scale from several tens of seconds to a few minutes. Sometimes these oscillations are reported to be caused by small variations of the atmospheric pressure [Wigley & Brown, cit. in Choppy, 1986] which usually last for several hours, much too long to be appliable in Moestroff. Polli reports oscillations which happen at intervals of about 25 s to 75 s in the Grotte Gigante, and which agree with microbarometric changes registered outside the cave. Dublyanski [Dublyanski & Sockova, cit. in Choppy, 1986] report oscillating air movements of periods of several tens of seconds in Ukrainian gypsum mines which, like Moestroff, have a labyrinth structure. The Breathing Cave of Faust, which is also an anastomosic cave, shows a complex resonant behaviour, with multiple periods extending from 100 s to 1000 s.

The same complexity which exists at the Moestroff Cave makes the detection of hidden periods difficult and somewhat risky. The main reason why we used the autocorrelation function of air velocity rather than its power spectrum is that the results of the former are usually much easier to interpret.

One of the models most often found to explain oscillations in balloon-type caves is that of an Helmholtz resonator. It can readily be shown that a spherical cave of volume V, connected through a cylindrical gallery of section S and length N to the outside, may resonate with a fundamental frequency [Cigna, 1967] of:

$$N_0 = 54 * \sqrt{\frac{S}{V * L}} \qquad \textit{[eq.21]}$$

where:

S section of the gallery leading to the balloon [m^2]

L length of the gallery [m]

V volume of the balloon-cave

N_0 fundamental frequency [Hz] if air temperature = 10°C

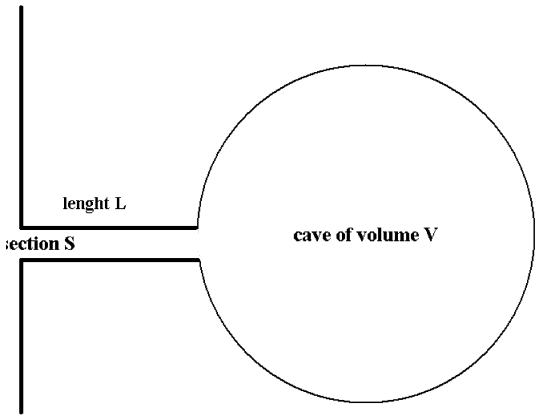

Fig. 3.4.30. Model of theHelmholtz resonator

We have seen that most of the time the pressure drop dP in the main gallery does not reverse its sign periodically, but that its magnitude varies around a certain offset; the same applies to the air flow which results from these pressure differences. Choppy gives an example of a similar situation reported by Moore and Sullivan in the Breathing Cave [Moore & Sullivan, cit. in Choppy, 1986], where an oscillationg air movement in a gallery causes variations of the flow amplitude in an adjacent section.

A possible model for the situation found in the Moestroff Cave could be the following:

Let us suppose that the cave is composed of two parts: a chimney-like structure resulting from the two superposed maze-storeys for approximatively the first 50 m, and a second part connected to this structure which, even if being a maze, globally behaves either like a balloon cave (model 1) or an organ tube (model 2). The chimney-structure creates the main seasonable thermal induced flow (either in or out), whereas the second part would modulate this flow by its resonant behaviour.

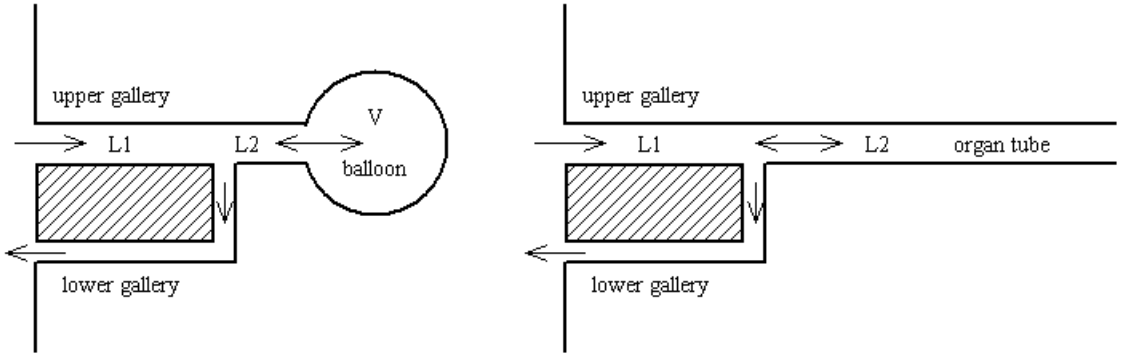

Fig. 3.4.31. Two possible models for Moestroff Cave

We have 3 series (#3, #7, #8) which correspond to unstable situations with possible periodic changes of airflow direction; each time we find a period for v_2 of approx. 50 s, about half of 110 s which is the period of the stable situations (i.e. unstable frequency = double of stable frequency). This doubling of frequency could be explained if the product V*L in the equation above would decrease in the case of same outside and inside temperatures, that is in the absence of thermally induced air flow.

Could this mean that when an important thermal air flow exists, the total length (L_1 or $2*L_1$) of the first part of the gallerie(s) should be added to L_2, and that in the unstable situation with negligible thermal air flow, the oscillator parameter L would be restricted to L_2 + V ?

Let us make a quick computation of the V*L product of the Helmholtz formula, assuming a main section S of about 1 m^2 and a resonant period of 110 s. One would find for $V*L \cong 35*10^6$ m^4; with a possible L of 100 m, this would give a deep-cave volume $V \cong 35000$ m^3. The total known length of 3500 m corresponds to a cave volume of $2*3500 = 7000$ m^3 at most (taking into account a possible 2 storey structure with a mean section of 1 m^2), five times less than that given by the model.

The second organ-tube model gives a gallery length corresponding to $\lambda/4$, where λ is the wave-length corresponding to the fundamental frequency N_0.

As N_0= 0.01 Hz, $\lambda/4$ = length of gallery = 8500 m, assuming the velocity of sound being 340 m/s. Using the double frequency of the unstable situation yields a tube length of 4250 m, quite close to the actual known cave development!

As a conclusion one may say that of the 2 models the organ-tube formula gives a reasonably good result if applied to the unstable interseasonal oscillation pattern. As the actual cave geometry with its complicated maze structure is very different from the simple tube, one should nertheless not be too confident in the validity of this model.

References

ANDRIEUX, C. - Etude des Circulations d'Air dans la Grotte de Niaux. Conséquences. Karstologia no.1, 1er semestre 1983, p.19-24, 1983.

ANDRIEUX, C. - Contribution à l'Etude du Climat des Cavités Naturelles des Massifs Karstiques. Chap. 5: Climatologie Souterraine, p.230-234. Annales de Spéléogie, tome 25, fasc.2, 1970.

ATKINSON, T.C., SMART, P.L., WIGLEY, T.M.L. - Climate and Natural Radon Levels in Castleguard Cave, Columbia Icefields, Alberta, Canada. In: Arctic and Alpine Research, vol.15, no.14, 1983, p.487-502, 1983.

BADINO, G. - Fisica Del Clima Soterraneo, p.44. Memorie dell'Istituto Italiano di Speleologia. Vol. 7, Serie II. Bologna, 1995.

CHOPPY, J. - Dynamique de l'Air. Phénomènes Karstiques, série 1.1.: Processus Climatiques. Spéléo Club de Paris, 1986.

CIGNA, A. - An Analytical Study of Air Circulation in Caves. International Journal of Speleology, vol. III, p. 41-54. 1967.

DUBLYANSKI, V.N., SOCKOVA, L.M. - Microclimate of Karts Cavities of the Mountain Crimea. Proceedings of the 7th Intern. Congress of Speleology, Sheffield. p.158-160, 1977.

HALBERT, E.J., MICHIE, N. - The Climate above and below Ground. IN: Wombeyan Caves, Occasional Paper no. 8, p.137-154. Editors: Dyson, H.R., Ellis, R. Julia, J. Sydney Speleological Society. P., 1982.

CRC Handbook of Chemistry and Physics - 67th edition. CRC Press, 1986-87.

LEBRUN, J.; TERCAFS, R. - Etude de la Convection Naturelle dans une Cavité Cylindrique Horizontale soumise à une Onde de Température Longitudinale. Collection des Publications de la Faculté des Sciences de l'Université de Liège. No.34. p. 1-49, 1972.

MOORE, G.W., SULLIVAN N.G.- - Speleology, 2nd edition. Zephyrus Press Inc. Teaneck., 1978.

NETZ, H. - Formeln der Technik. Hanser Verlag München, Wien, 1983.

PARKER, S.P., editor - Fluid Mechanics Source Book. McGraw-Hill Book Co., 1988.

POLLI, S. - La Grotta Gigante del Carso di Trieste quale Cavita Barometrica. Atti VI Congr. Naz. di Speleologia, Trieste 1954. Le Grotte d'Italia (3a) I, p.1955-1956, 1956.

RECKNAGEL, Sprenger, Hönmann - Taschenbuch für Heizung und Klimatechnik 92/93, p. 104. OldenbourgVerlag, 1992.

WIGLEY, T.M.L. -Non-Steady Flow through a Porous Medium and Cave Breathing. Journal of Geophysical Research. Vol.72, no.12, June 15, 1967. p.3199-3205, 1967.

3.5. Carbon Dioxide

Francis Massen, Camille Ek, Antoine Kies

3.5.1. General Remarks

Carbon Dioxide concentrations in cave air have been measured for quite some time by many authors; sometimes only to differentiate cave air conditions from those of the outside, but very often also to check for dangerous concentrations of that gas in *"foul air caves"*.

James [James, 1977] gives a list of six possible CO_2 sources in caves:

1. Diffusion of gaseous CO_2 through soil and rock into the cave
2. Evolution of CO_2 from cave waters
3. Production of CO_2 by micro-organisms
4. Respiration of plants and animals
5. Burning of hydrocarbons
6. Volcanic gases.

Clearly points 5 and 6 do not apply to Moestroff; point 2 relates mostly to the outgasing of water-borne CO_2 during the formation of speleothems, or when CO_2 - loaded water seeps into the cave from the top soil layer. As the Moestroff Cave is rather poorly covered by calcite layers, the outgasing is probably negligible. The inseeping water volumes are rather small; but as the soil cover through which this water percolates is quite close to the galleries, this water-film could in theory be an important CO_2 source. The importance of diffuse transport mechanisms is also probably moderate, but James' list forgets two mechanisms which, as will be seen later, play a major role in Moestroff: inflow of outside air and air movements from one part of the cave to another.

Probably the second most important factor is biological activity: many authors like Ek [Ek & Gewelt, 1985] agree that most of the cave CO_2 has a biogenic origin: CO_2 comes from microbial activity in the cave soil or in the soil covering the cave, and from plant and animal respiration (like the respiration of tree roots). This biogenic activity is most noticeable in caves located near the surface, especially when the layers covering the cave system are heavily fissured and fractured, as is the case for the Moestroff Cave. CO_2 produced in the topsoil percolates down through these pathways to the cave galleries, where concentrations vary with outside temperature and cave air movements (the latter being often caused by inside-outside temperature differences).

The following figures summarizes the various contributing factors.

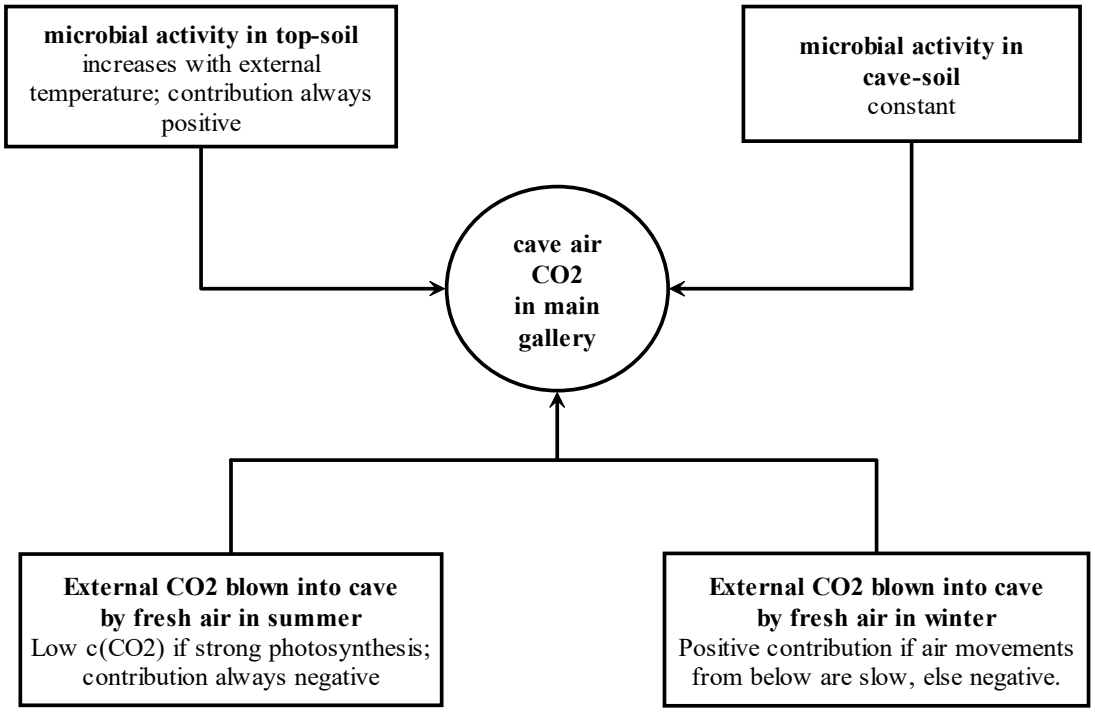

Fig. 3.5.1. The various contributing factors to cave air CO_2

Measuring CO_2 in confined galleries is fraught with problems, the most severe being that the outbreathing of the operator (concentration in expired air may reach 40000 ppm typically) completely changes the actual situation. Ek [Ek & Gewehlt, 1985] have used a respiration apparatus with a CO_2 - absorbing device passing the air through soda lime. This cumbersome and strainful method can clearly be used only for a few spot measurements, but not for long-time continuous campaigns.

We did some preliminary measurements with a Gastec detector, which is similar to the well known Dräger, to get a first check on ambient conditions. These measurements were done without any breathing apparatus; but care was taken to make fast measurements without expiring. If more than one caver was involved, the first to penetrate the cave did the measurements.

These first checks showed a possible CO_2 concentration of about 600 to 1000 ppm (ppm = parts per million; 10^4 ppm = 1 vol.%) in the main gallery and at least the double in the ceiling fissures. These findings were later on rechecked with a portable NDIR sensor. The higher CO_2 values in the ceiling fissures do well agree with the assumption of a biogenic origin in top-soil.

We never found dangerous levels of "natural" CO_2 in the cave; the practically horizontal structure makes the presence of foul air sumps unlikely, so does the continuous temperature - driven ventilation. When one or more cavers stayed at the same place, CO_2 concentrations very

quickly exceeded 3000 ppm, which is the upper limit of detection of the sensors. There exists no known report of CO_2 caused health problems like severe headache or accelerated pulse rate from visits to the Moestroff Cave during the last 36 years; so we might assume that CO_2 levels always remain well below 30000 to 40000 ppm [James, Pavey & Rogers, 1975] even if several cavers gather at the same place.

In the next chapters we will first analyze the diurnal variations of CO_2 in cave air; next we will study the seasonal variations and look for a possible year-long trend; finally we will investigate if there exists a relationship between CO_2 levels and external wind or rainfall.

The CO_2 concentrations will always be expressed in ppm (volume parts per million) reduced to standard laboratory conditions (T=25°C, p=1013.25 hPa); actually the Gascard sensor readings correspond to these conditions, so that no conversion formula is needed.

Station 3, at 31 m from entrance, was the deepest located measuring station for CO_2; this location is near the vertical of the border line between the forest canopy and free field. General conclusions are , in a strict sense, valid only for the first part of the gallery.

3.5.2. Diurnal Variations of c(CO_2)

During the last two years of project Phymoes, a Valtronics NDIR CO_2 sensor which works by pure diffusion (see Part 2, chapter 3) was functioning at a location situated in the cliff, about 1 m above the main entrance of the cave. This position was chosen to avoid outflowing air reaching the sensor. Frequent breakdowns were due to the sensitivity of the instruments to high humidity levels; a heavy or continuous rain-fall nearly always drove the sensor into saturation, which gave impossible high readings. The time-span to reach again a good working condition was often many days. Thus we have only relatively short periods which are usable to study the outside CO_2 variations and to look for a synchronism with inside c(CO_2) changes.

The period from 1 to 10 May 1994 is a good example demonstrating the synchronism between outside and inside diurnal CO_2 concentrations: for that time span the outside temperature was practically always higher than 10°C, resulting in inflow of fresh air into the cave. The synchronism between the c(CO_2) at all stations can be seen in the plot of the 3 data series; a spectral analysis very clearly shows a common 24 hour peak.

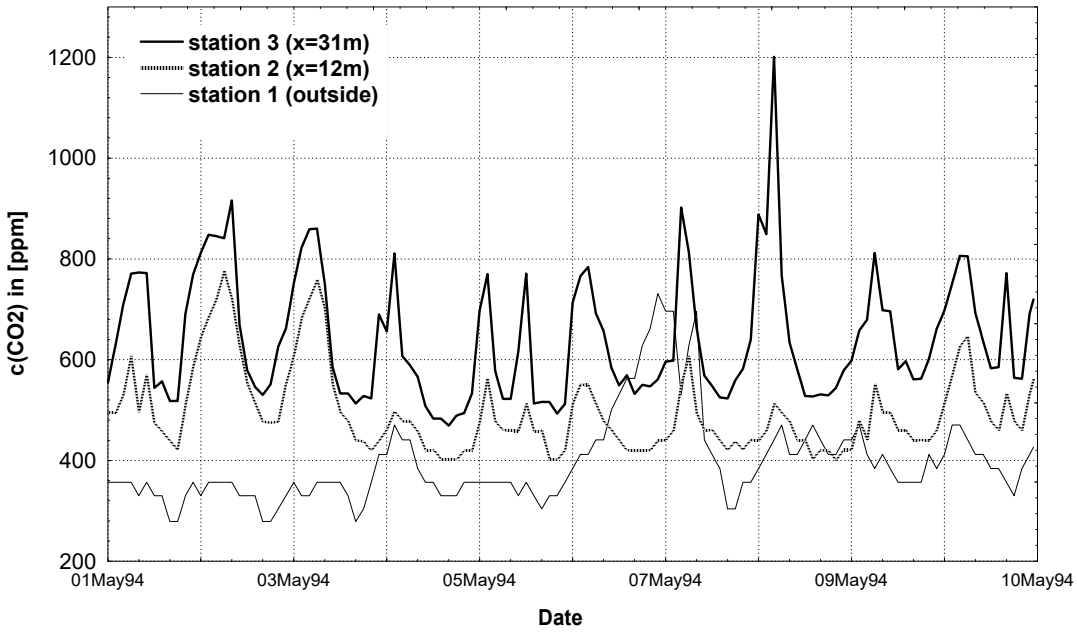

Fig. 3.5.2. Variations of CO_2 at the outside, station 2 and station 3

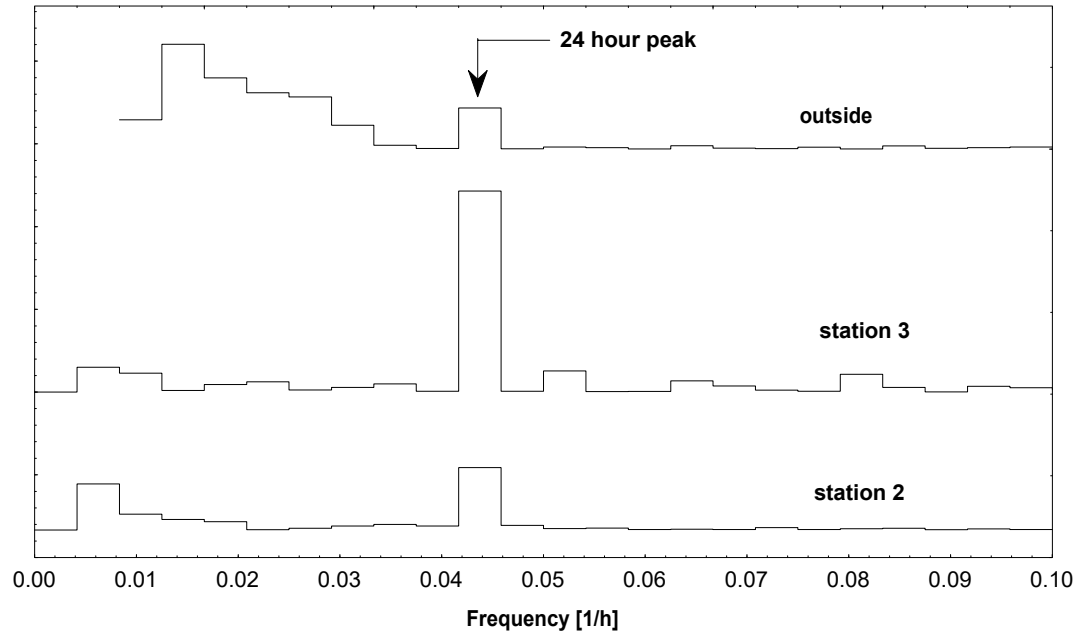

Fig. 3.5.3. The power spectral density plot shows a common 24 hour peak for the CO_2 concentrations at all stations (spectra are shifted vertically for display)

The high peak on the 7th May of outside c(CO_2) is the typical footprint of an instrument failure, due to a 36 hour long period of continuous high humidity levels (>94%).

Let us take the first 5 days of May 94, where all data are good, to calculate the overall means and standard deviations:

Table 3.5.1.

01..05 May 94 location	*mean concentration and standard deviation (STP) [ppm]*	*typical daily amplitude swing (max-min) [ppm]*
outside	346 ± 35	78
station 2 (x=12m)	515 ± 99	283
station 3 (x=31m)	632 ± 122	386

This example shows the usual situation where both the mean concentration and the daily amplitude increase with the distance from the cave entrance, the lowest values being the outside ones.

The same analysis can be repeated for a period of very low outside temperature and no external gust. From the 1st to 4th January 1993 outside temperature varies between-6 and +2°C, with a mean value of -4.4°C; the difference $\Delta\rho_{14}$ of air densities between inside and deep cave (station 4) is +0.03105 kg/m^3, and $\Delta\rho_{12}$ is very close to that value: applying the same criteria as in the chapter on air flow oscillations, this means constant outflow and no external gust.

Visual inspection allows to detect a 24h period in the signal of outside c(CO_2), but not in that of the variations of c(CO_2) at station 3; the PSD function confirms this impression. There are no values for station 2 available, as the sensor was not yet installed.

The following table 3.5.2. summarizes the data:

Table 3.5.2.

01..04 Jan 93 location	*mean concentration and standard deviation (STP)]*	*typical daily amplitude swing (max-min)*
outside	463 ± 26	98
station 2 (x=12m)	not available	n.a.
station 3 (X=31m)	792 ± 24	not detectable

Note: concentrations in [ppm]

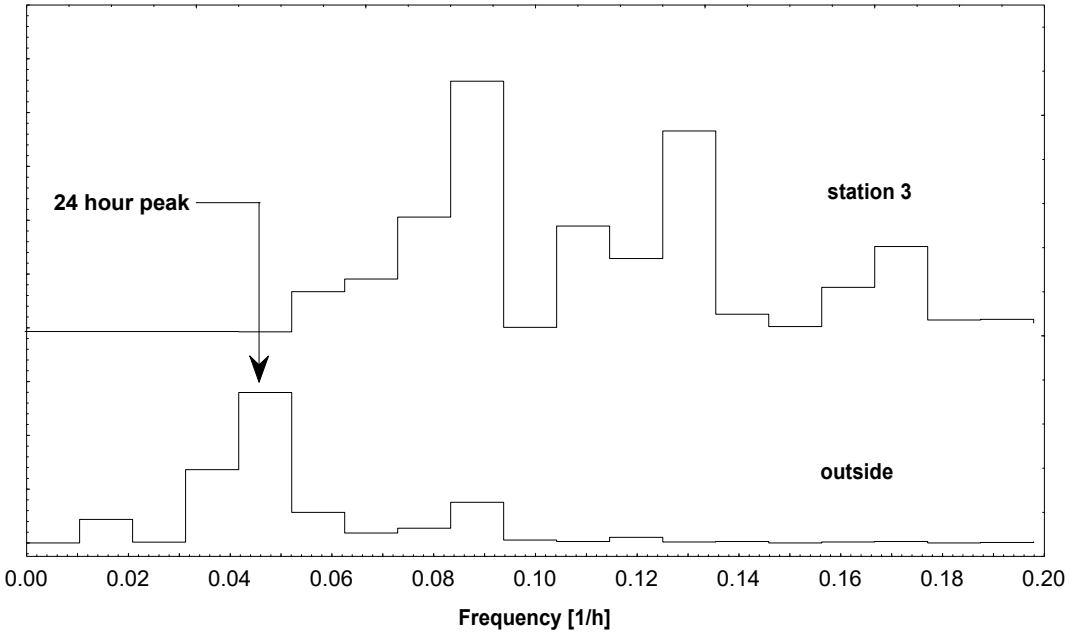

Fig. 3.5.4. When air is flowing out, a 24 hour period shows up in the outside CO_2 pattern, but not in that of station 3.

Comparing the 2 tables leads to some interesting conclusions:

1. The outside c(CO_2) is higher in January than in May; this is a consequence of reduced photosynthesis due to lower solar irradiance.
2. In May the standard deviation (std) of outside c(CO_2) is higher than that of inside c(CO_2); in January the std's are about the same. This could be the consequence of the reduced microbial activity in the top soil covering the cave: during the cold days, this activity and its contribution to cave CO_2 is constantly low; during the warmer May days, it varies in an important manner during the day, which shows up by higher daily amplitude swings.
3. No hasty conclusion should be drawn on the rather small difference of the mean inside c(CO_2) in January 93 and May 94, as minor undetectable air movements could have an influence besides that of temperature. The only conclusion allowed for the moment would be that the winter CO_2 concentrations in the cave do not seem to swing as much as do the summer ones (in winter standard deviations are much smaller than in summer). This would mean that the contribution of the microbial activity happening in the cave gallery itself is probably almost constant throughout the year.

As a general rule, CO_2 concentrations are highest at night, at around 05:00 UTC time, and lowest after 12:00, as shown on figure 3.5.5 which gives

the data for the 3 days from 6 to 8 April 1992 (one measurement every two hours); the high night concentration coincides with a time where photo-synthesis is zero and where thermal induced wind movements are usually low.

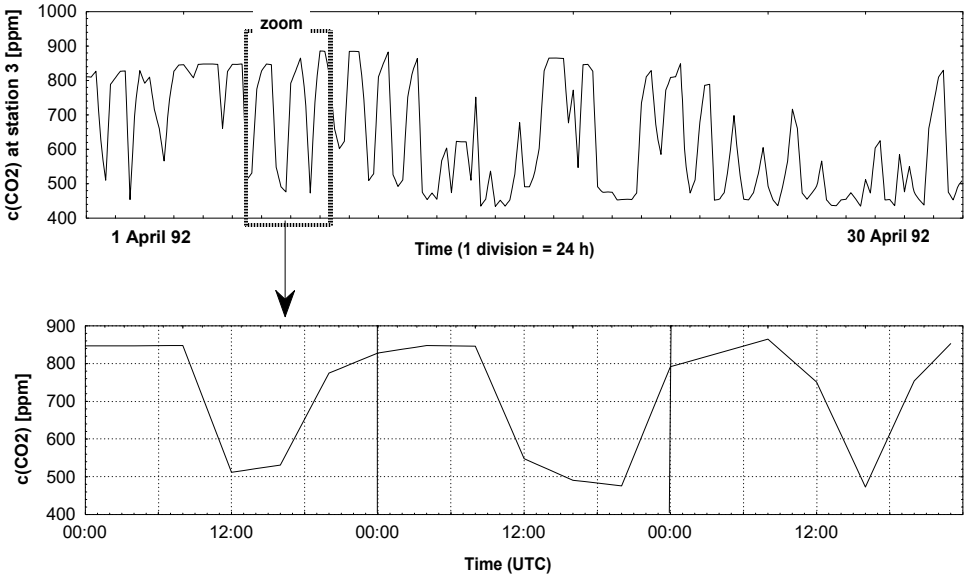

Fig. 3.5.5. Daily CO_2 pattern at station 3: April 92 values and zoom on 6th to 8th April

3.5.3. Seasonal Variations of CO_2

To study year-long CO_2 patterns we will use the concentrations measured at station 3 (31 m from the entrance) starting in April 1992 and ending in November 1994. Missing values due to sensor or logger malfunctions have been replaced by linear interpolation.

We have some outside reference data from an air quality measuring station operated by the Luxembourg Ministry of Environment. This station is located at Vianden, 12 km North from Moestroff, at an altitude of 360 m asl. Unfortunately the data from Vianden are rather uncomplete, as the CO_2 sensor was operating correctly for about 31% of the time during 1993 and 1994. Let us first look at the trimestrial means (± standard deviations) for the 3 years 1992 to 1994 (table 3.5.3):

Table 3.5.3.

	1992	*1993*	*1994*
trimester 1	not available	584 ± 191	684 ± 124
trimester 2	561 ± 154	627 ± 203	692 ± 156
trimester 3	540 ± 216	683 ± 224	854 ± 271
trimester 4	644 ± 217	827 ± 251	892 ± 269
whole year cave	585 ±	681 ± 237	771 ± 229
whole year Vianden	not available	322 ± 24	334 ± 15

Obviously the CO_2 concentration is highest during the 4th trimester of the year.

If we compute a linear regression from the hourly values for each year, we always get positive slopes, as expected from the trimestrial data. One should note that the 1992 data are restricted to the last 9 months, and the 1994 data to the 11 first months; the missing Dec.94 may at least partially explain the highest slope for this year. Such situations with highest CO_2 concentrations in autumn have been reported for instance in the Altamira Cave [Villar et al., 1985☸, Choppy ☯Choppy, 1988☸ and James ☯James & Dyson , 1981☸.

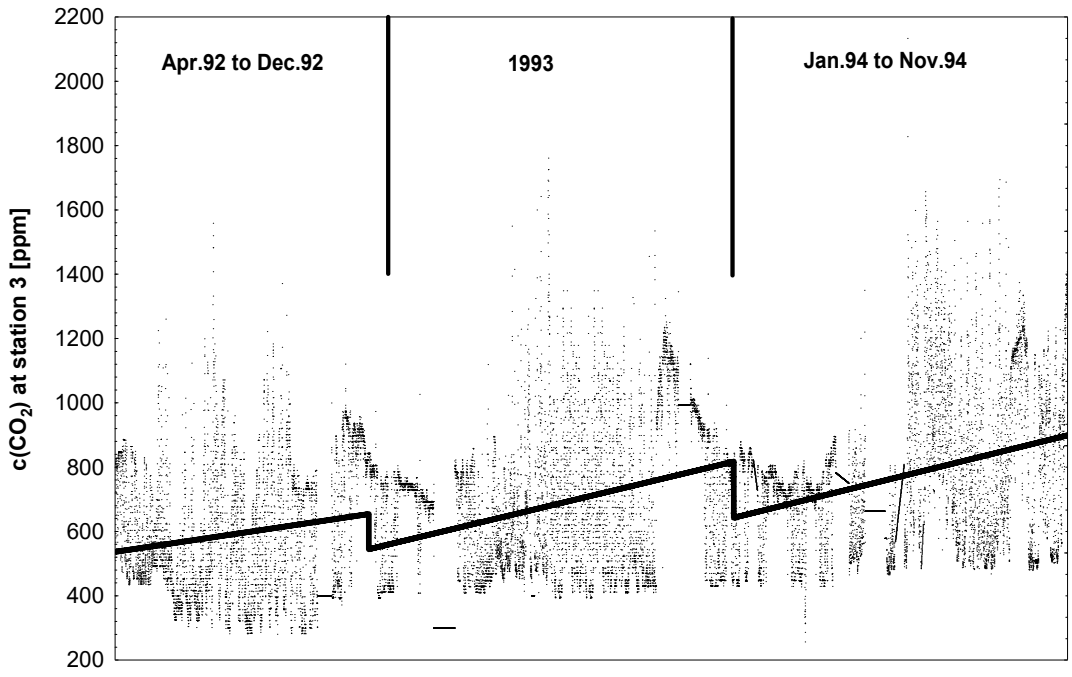

Fig. 3.5.6. Seasonal CO_2 pattern shows a rising trend from January to December

It is easy to explain these increased concentrations in autumn:

- The falldown of the leaves in the forest covering part of the cave creates a rich nutrient source for the microbes in the topsoil, increasing their activity and as a consequence the CO_2 percolating down to the cave [James & Dyson, 1981]
- Mean outside temperatures are close to that of the deep cave; this means that thermally induced inflow will vanish, which reduces the diluting effect of CO_2 - poor fresh air mixing with cave air.

If we compare the measurements from station 2 and 3 for the January 1994 to November 1994 period, we see that the variations of $c(CO_2)$ are reasonably well synchronized; the statistical correlation is r=0.47, significant at the $\alpha = 0.05$ level. The CO_2 concentrations at station 3 are always higher than those at station 2, and can be expressed as:

$$c(CO_2\ stat3) = 0.81*c(CO_2\ stat2) + 311 \qquad [eq.3.5.1]$$

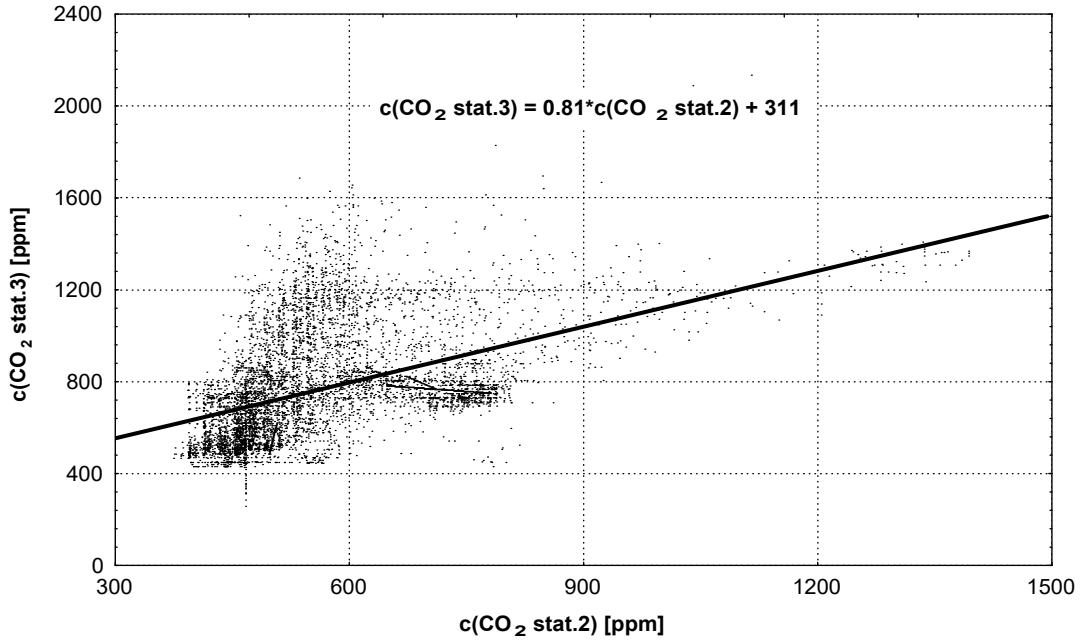

Fig. 3.5.7. Linear correlation between CO_2 at station 2 and 3

As said above, the seasonal $c(CO_2)$ variations are caused by two factors which are **not** independent: the external temperature and the intensity and direction of air flow. High external temperatures increase top-soil microbial activity, and as a consequence should increase cave-air $c(CO_2)$. But high external temperatures also increase fresh air inflow, which reduces or

may annihilate the positive effect related to microbial activity. To get an idea of the net balance, we will look in the next chapter at the relation-ship between $c(CO_2)$ and temperature, distinguishing inflow and outflow periods.

3.5.4. $c(CO_2)$ and External Temperature

Let us recall that outside air flows into the main cave gallery when the external temperature is higher than the mean cave temperature of 9.4°C, and flows out of the cave (reaching the main gallery by inflowing through the deeper located storeys) if outside temperature is lower than 9.4°C. Let us use a safety margin of 1°C and speak of inflow when outside temperatures ≥10°C and outflow when outside temperatures ≤ 9°C.

If we divide the whole data-series from April 1992 to November 1994 according to these criteria, we get the following results for the $c(CO_2)$ at station 3 ($c(CO_2)$ in ppm ,T in °C):

Table 3.5.4.

Outflow (T≤9 ℃)	***Inflow (T≥10 ℃):***
9344 cases	*13207 cases*
mean ± std: 726 ± 222 [ppm]	*mean ± std: 655 ± 242 [ppm]*
*$c(CO_2)$ = -10.1*T + 769*	*$c(CO_2)$ = +17.2*T + 387*

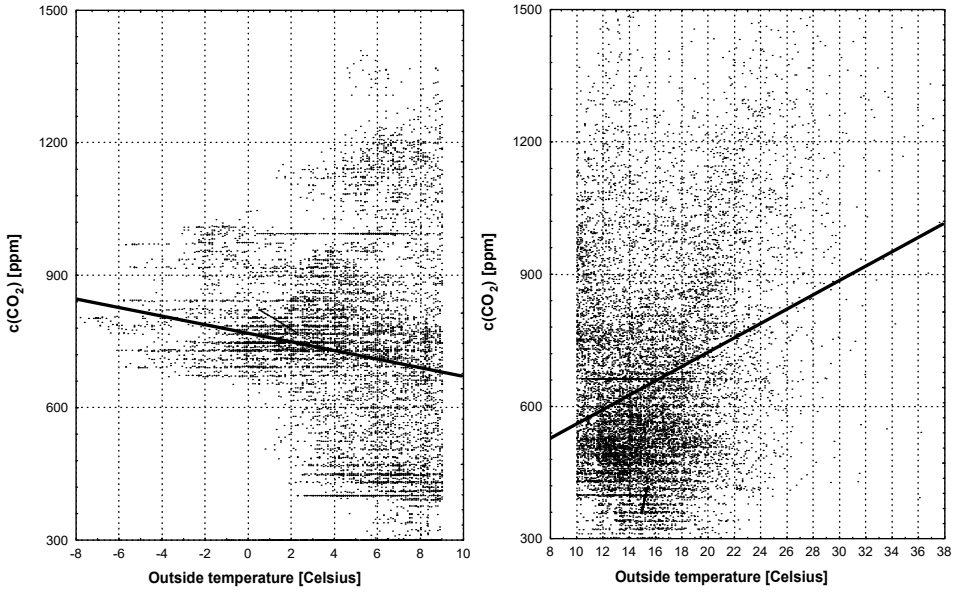

Fig.3.5.8. CO_2 and external temperature for outflow and inflow periods (data from station 3)

The negative slope of the regression line of the outflow-data can be explained as follows: when air flows into the cave through the bottom storeys, it carries into the main gallery the CO_2 generated both in these galleries and in the cracks and fissures lying inbetween. The measured CO_2 mostly comes from a microbial breakdown occurring in the cave itself, and not from the biological CO_2 - generating activity in the top soil, as this source decreases with lower temperatures. Very low outside temperatures increase the air flow from the lower to the upper storey, and hence increase the CO_2 concentration at station 3, at least up to a certain point.

When outside temperatures are higher than 10°C, the positive slope of the regression-line shows that the increased biogenic activity with its resulting CO_2 percolating down into the cave from the topsoil overrides the diluting effect due to higher thermally induced inflow of fresh, CO_2 - poor outside air.

The slopes of the two regression lines suggest a possible parabolic relationship between $c(CO_2)$ and outside temperature; a quadratic fit on all data from Apr.92 to Nov.94 gives a parabola with a positive concavity, having its lowest value at T=11.9°C (fig. 3.5.9).

$$c(CO_2) = 1.17 * T^2 - 27.8 * T + 798 \qquad \textit{[eq.3.5.2]}$$

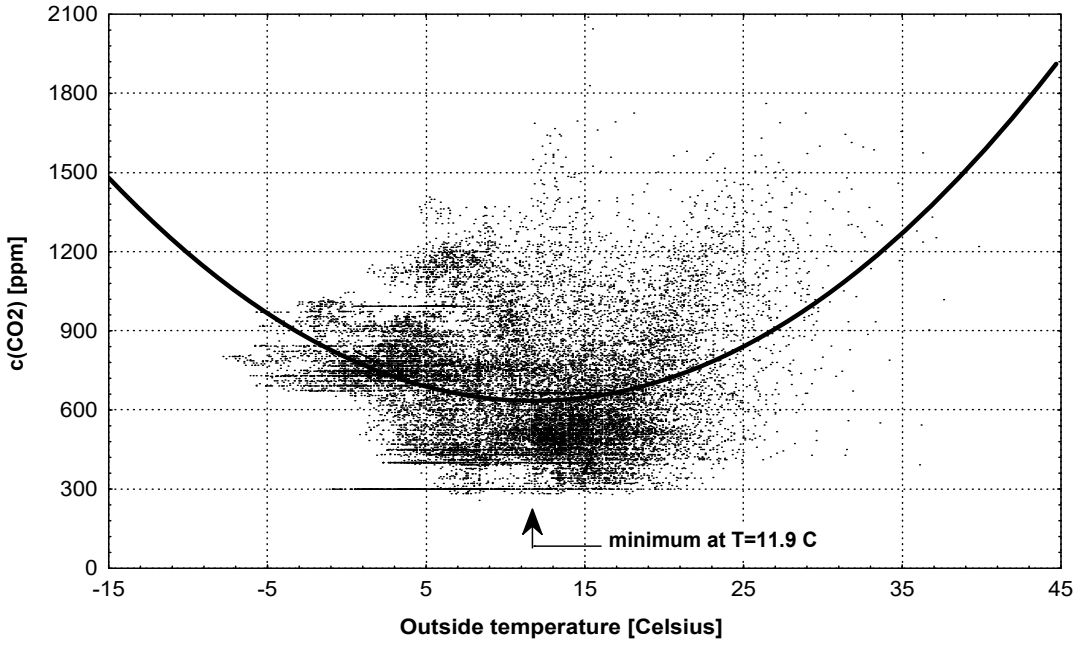

Fig. 3.5.9. Parabolic fit to CO_2 concentration versus outside temperature (23376 cases)

We will comment on the position of the minimum later on. For the moment let us just note that in the case of the Radon concentrations, we also find a parabolic relationship between c(Rn) and outside temperature; this parabola has a negative concavity, and the explanation is different.

The preceding analysis was done without any attention given to the outside wind situation: we have seen for instance in the study of in- and outside air densities that external gusts blowing into the cave may completely change the "normal" no-wind situation. The period from July 1994 to November 1994, for which good outside gust data are available, will be used to redo the above computations, to check if outside gusts have a noticeable influence on CO_2 concentrations. Table 3.5.5. summarises the situation.

The conclusions from these data are easy to draw.:

1. As a general rule, CO_2 concentrations at station 3 are higher when air enters the cave from the lower storeys (= outflow) than when fresh air flows straight into the main gallery. The concentrations are not only higher, but they vary much less, as shown by the smaller standard deviations.
2. External gusts have practically no influence on mean concentrations (computed over long periods) when air flows out, and only a modest one when air flows normally into the cave.
3. We find for this subset of 1994 the same situation as in the general case of the 1992 to 1994 period: the linear regression between CO_2 and temperature has a negative slope for outflow and a positive one for inflow.

Table 3.5.5.

wind situation	***outflow (T≤9 ℃)***	***inflow (≥10 ℃)***
all data Jul.94 to Nov.94		
3672 cases	410 cases	2212 cases
mean ± std: 726 ± 222	mean ± std: 1132 ± 154	mean ± std: 831 ± 264
	$c(CO_2)$ = -45.9*T + 1477	$c(CO_2)$ = +20.5*T + 538
no gust		
2609 cases	318 cases	2212 cases
mean ± std: 952 ± 242	mean ± std: 1121 ± 169	mean ± std: 880 ± 258
	$c(CO_2)$ = -51.6*T + 1514	$c(CO_2)$ = +20.5*T + 538
always gust		

1063 cases	101 cases	846 cases
mean ± std: 665 ± 224	mean ± std: 1168 ± 87	mean ± std: 703 ± 235
	$c(CO_2)$ = -25.5 *T + 1350	$c(CO_2)$ = +18.9*T + 386

The negative slopes of the linear regression lines valid for the outflow situation tell us that the concentrations rise with falling temperatures (at least up to a certain point), and fall when temperatures increase and approach the limit of 9°C. When the air movement reverses and air flows into the cave during the warmer days, the CO_2 concentrations increase with outside temperature despite the fact that these higher temperatures push more fresh air into the cave!

If we use only the hours where outside gusts happen (947 cases), we find again the same sign of the linear regression slope as above. This means that the outside wind blowing into the cave does not reverse the no-gust temperature - dependant trend at station 3, but it certainly does influence $c(CO_2)$! (more on this at the end of this sub-chapter).

We now can refine somehow the conclusions that may be drawn from the parabolic fit which we first tried on the complete April 1992 to November 1994 series. When we compute the same parabolic fit using exclusively the nogust and inflow data from the Apr.94 to Nov.94 series, we find a curve very similar to the first one, having again its minimum at T=11.9°C:

$$c(CO_2) = 1.54 * T^2 - 36.5 * T + 1025 \qquad \textit{[eq.3.5.3]}$$

This means that when the outside temperature rises from 10 to about 12°C, the increase of the thermally induced inflow of CO_2 - poor air swamps the increase in the biogenic CO_2 produced in the top soil which percolates down into the cave. If the outside temperature is higher than 12°C, the microbially generated CO_2 reaches such levels that the balance between inflowing CO_2 - poor fresh air and biogenic CO_2 tips in favour of the latter: CO_2 levels increase with rising outside temperature in the cave at station 3.

If we take all data, including those which correspond to outside gusts, or if we restrict our analysis to no gust situations, we always have a minimum of the parabolic fit at 11.9°C. This confirms the conclusion given above, namely that outside gusts have no visible influence on the mean CO_2 concentrations measured over a longer period. In the next chapter, we will see that this conclusion is not valid for the instantaneous CO_2 concentrations.

All comments and computations are applicable to the situation at station 3. We will analyse now the CO_2 data at **station 2** (x=12 m), which is much

more exposed to outside climatic conditions. The available data extend from January 1994 to November 1994.

Similar to what we found for station 3 in the analysis of the Apr.92 to Nov.94 data, the mean concentrations at station 2 are higher when air flows out than when it flows into the cave (638 ppm versus 523 ppm).

Other results are noticeably different. The plot of $c(CO_2)$ versus outside temperature (fig.3.5.10) shows that the highest CO_2 values occur when the outside temperature lies between 5 and 10°C: clearly outflowing air brings CO_2 from the deep cave to the entrance, but this transport seems optimum only for the given temperature range. Above 10°C, CO_2 values rapidly level off, before increasing slightly when outside temperature is close to 20°C. The figure shows that a parabolic fit over the whole data series is clearly inadequate.

If we restrict our data to the period between July.94 and Nov.94 and keep only data of inflow and no gusts (2212 cases), the computation of the loss function shows that a parabolic fit is distinctly better than a linear one. The result of the fit is:

$$c(CO_2) = 1.012 * T^2 - 43.74 * T + 945 \qquad \textit{[eq.3.5.4]}$$

The concavity of the parabola is the same as for station 3; the minimum lies at T=21.3°C, much higher than the correspondent minimum at station 3 for the same period.

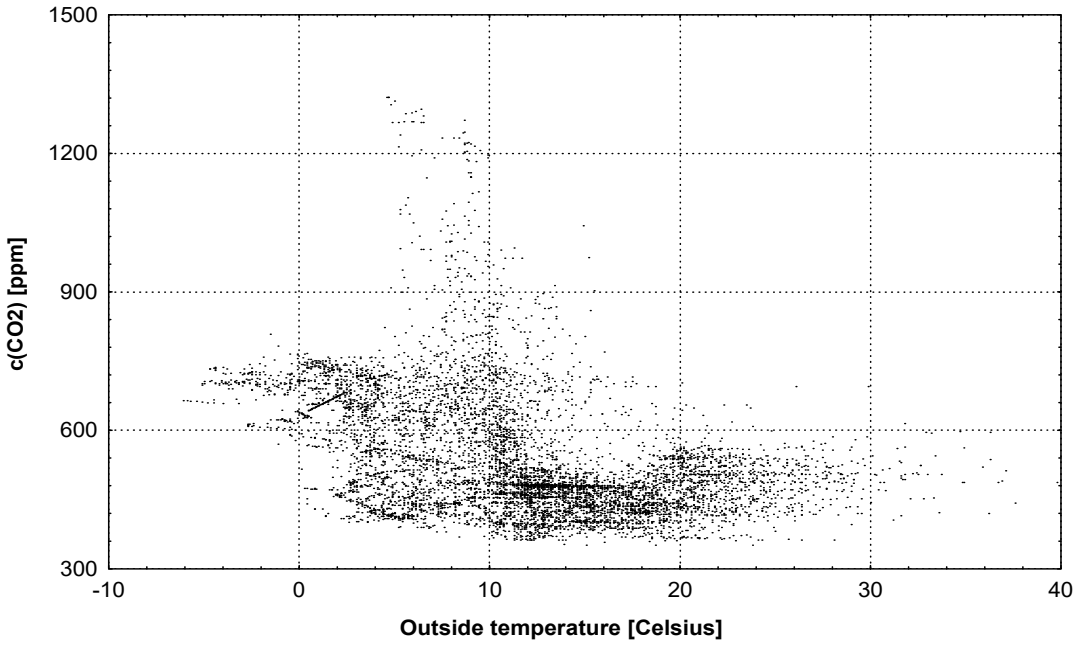

Fig. 3.5.10. CO_2 versus external temperature at station 2 (inflow, outflow and gust situations)

The explanation is that CO_2 levels fall sharply with increasing temperature when fresh air starts flowing into the cave (as should be expected). A rise happens only when the outside temperature is higher than approx. 21°C, which is the break-even point between the negative contribution of inflowing CO_2 - poor air and the positive one of top-soil CO_2 generation; this top-soil CO_2 reaches the station near the entrance not in the same magnitude as it does at station 3. In the deep cave, the top-soil CO_2 can flow to station 3 from all surrounding parts. At station 2, close to the cliff, approximately half of the surrounding environment lies outside. As a consequence we can expect to find there at most 50% of the corresponding amount of top-soil generated CO_2 which we have at station 3.

As a conclusion one can say that the CO_2 situations at station 2 and 3 differ in two important points:

1. At station 2, near the cave entrance, c(CO_2) is highest when air flow is minimal (T in the 5 - 10°C range), at station 3 situated deeper in the cave, no such sharply cut temperature range for the highest CO_2 values can be found.
2. At station 2, the equilibrium point between the lowering (inflow) and augmenting mechanism (top-soil CO_2 generation) happens at a far higher temperature than at station 3.

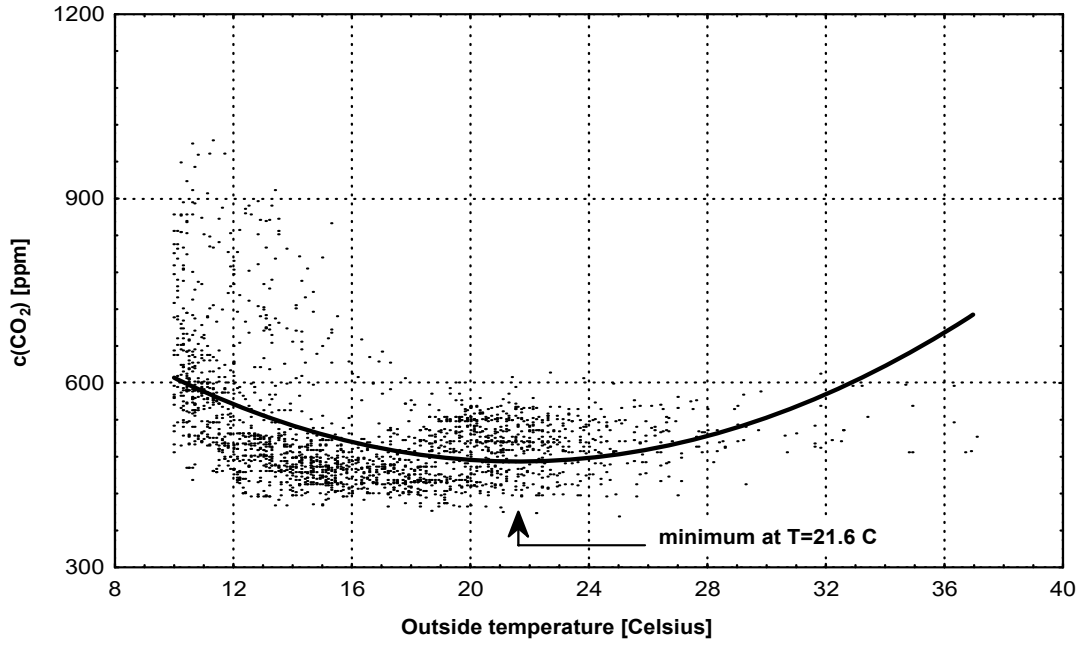

Fig. 3.5.11. Parabolic fit of c(CO_2) at station 2 to outside temperature; inflow, no gust.

3.5.5. c(CO_2) and Cave Air Wind

The thermally induced air movements into or out of the cave are caused by the temperature difference between the outside and inside of the cave; as the deep cave temperature is practically constant, cave wind is a function of the sole outside air temperature when no external wind blows! We found in the preceding chapter that outside wind gust does not change noticeably the mean CO_2 concentrations measured over long periods. This cannot be the case if we analyze short time series, which should show the influence of air movements caused by outside wind. To study the impact of outside gusts, we will take the special case where $T_{outside} \approx T_{cave}$, which means that there should be practically no thermally induced flow. This situation happens over a longer time range in autumn; we will use the data from October 1994 and retain only those 106 values where the absolute value of the difference between outside and deep cave temperature is less than 0.5°C:

$$\left|T_{outside} - T_{station3}\right| < 0.5\ ℃$$

Any air movements that exist will be caused by outside wind (gust is measured with a resolution of 0.5 m/s). Figure 3.5.12 shows the corresponding c(CO_2), local air velocities and outside gusts. Two observations are obvious:

- At the end of the month, CO_2 concentrations drop sharply
- This drop coincides with an increase of the outside gusts and the local air velocities caused by the external wind, which blows fresh air into the cave.

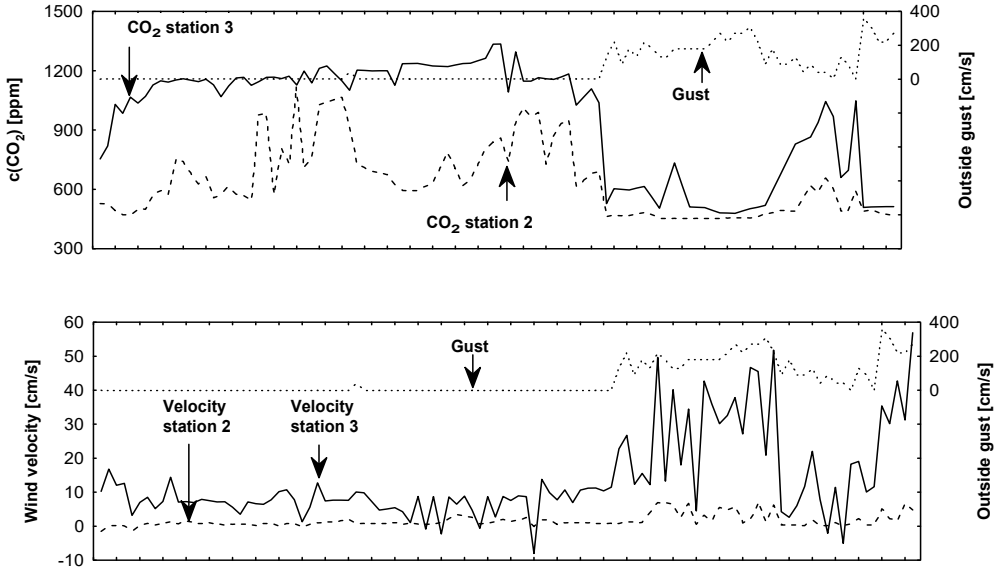

Fig. 3.5.12. CO_2 levels, local wind velocities and outside gusts (Oct.94, $T_{outside} \approx T_{cave}$)

If we plot CO_2 concentrations against the inflowing quantity of fresh air at station 2, we see that CO_2 levels at the entrance fall abruptly in a step-wise manner when inflow exceeds 200 m^3/h. The decrease at station 3 is more gradual and smooth: less of the air entering the cave reaches that station, as a major part escapes from the main gallery into the other pathways, and as a consequence ambiant cave air is less diluted at station 3 than at station 2. (fig. 3.5.13).

To predict the influence of outside gusts on c(CO_2), we need a good empirical fit; computations show that the best one is exponential. The results given by applying a Newton-Simplex algorithm are found in table 3.5.6.

The damping factors in both expressions are reasonably close, that of station 2 being higher, as the influence of outside wind is stronger near the entrance. A theoretical infinite high gust would push the CO_2 levels at both stations down to similar asymptotic values (420 and 475), which should correspond to the outside concentration (see fig. 3.5.14).

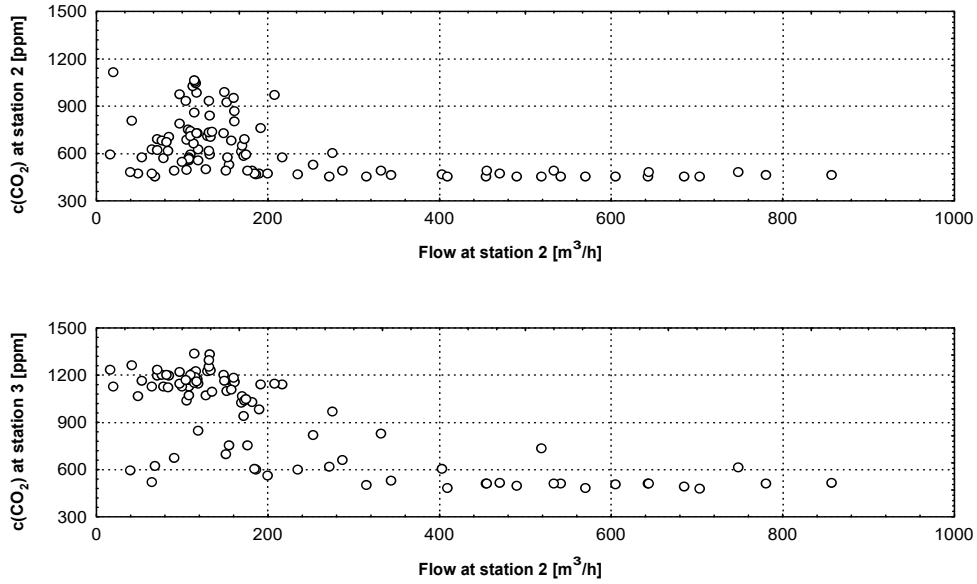

Fig. 3.5.13. CO_2 levels versus forced inflowing air quantity (Oct.94, $T_{outside} \approx T_{cave}$)

Table 3.5.6.

station	*fit of c(CO2) in [ppm] to gust in [m/s]*	
station 2	$c(CO_2) = 446 + 273 * e^{-1.334 * gust}$	r=0.63
station 3	$c(CO_2) = 470 + 680 * e^{-1.094 * gust}$	r=0.92

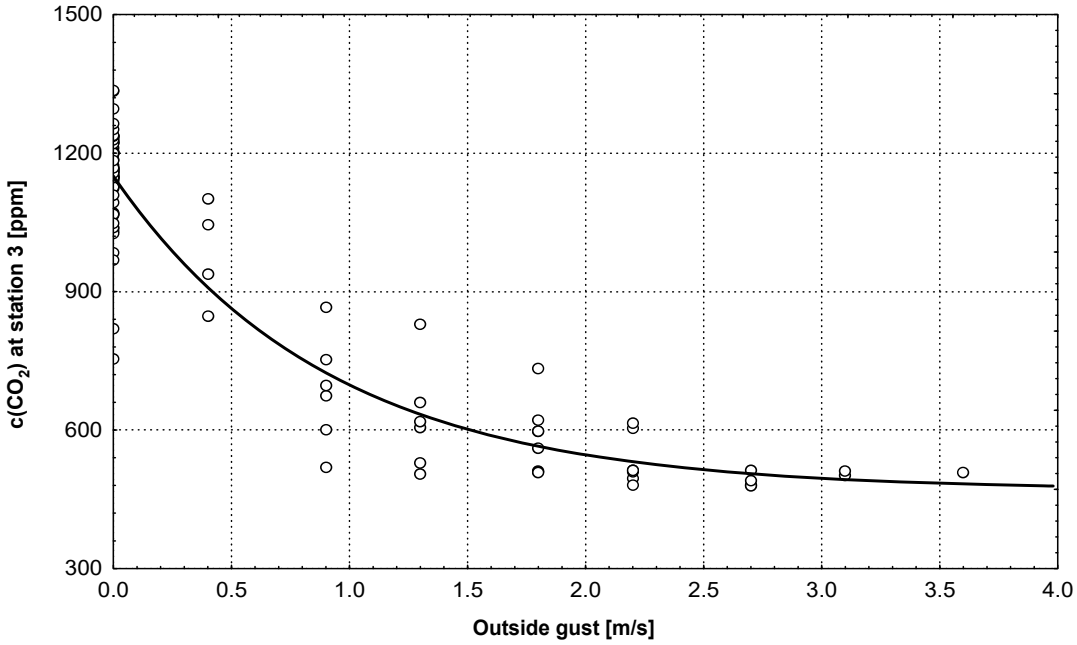

Fig. 3.5.14. CO_2 concentrations (here values at station 3) can be fitted to outside gust by an exponential curve

3.4.6. c(CO_2) and Rainfall

Up to now, we have seen that c(CO_2) is influenced by 2 independent parameters: outside temperature, which is the dominant factor, and outside wind the influence of which is detectable only under special conditions. A third parameter could be external rainfall.

There are several plausible arguments in favour of a positive influence of rainfall on cave air c(CO_2).

1. Rainwater with many dissolved bicarbonates contains much more CO_2 than would be expected from water in equilibrium with a gaseous concentration of 350 ppm [Caro, 1965; Hoffmann, E.+G., 1962, cit. in Choppy, 1988]; this fixed CO_2 will be partially released when this water enters he cave.

2. When external rain falls on the top soil cover, the CO_2 produced by microbial activity cannot escape as easily upwards to free air, as the **moist** soil constitutes a barrier which reduces this way. On top of that, soil-humidity enhances CO_2 production, and more CO_2 will percolate down into the cave. It is assumed that usually only 5 to 10% of the biogenic CO_2 produced in the topsoil does not escape into the atmosphere; a reduction of the outgassing into free atmosphere should produce rising CO_2 levels in the cave.

   The influence of rainfall on c(CO_2) has at least partially been analyzed by Renault [Renault, 1980], without any clear conclusion being given in that report.

As the different percolating mechanisms do probably take some time, we must be prepared that a possible CO_2 rise can be observed only after some delay on the rainfall. To tackle this problem, we will use the following procedure in our investigations:

1. All computations of $c(CO_2)$ and rainfall will be done using the daily means, as a possible influence will certainly not be detectable on the very short hourly time span.
2. The crosscorrelation function of these means will be computed. If this function shows no detectable peak, we will conclude that no relationship does exist.
3. If the crosscorrelation function has a detectable peak, we will use this peak to find the time-lag between rainfall and the consecutive rise of $c(CO_2)$.
4. The $c(CO_2)$ data series will be shifted according to the found time-lag .
5. An xy-graph of $c(CO_2)$ versus rainfall will be drawn and the linear-regression computed. If the slope is positive, we conclude that rainfall may produce an increase in $c(CO_2)$ after a certain time-lag. If the slope is negative, the data do not support the validity of our starting hypothesis.

   To use this strategy, we will use two periods for which we have good CO_2 data for both measuring stations and good rain-fall values.

Series February 1994 to May 1994 (2880 data, 120 daily means):

Visual inspection of $c(CO_2)$ series of station 2 shows a possible time-lag of 2 days (fig. 3.5.15); this is confirmed by the crosscorrelation function. The linear regression has a positive slope. The same time-lag and positive regression-line slope can be found for the $c(CO_2)$ at station 3.

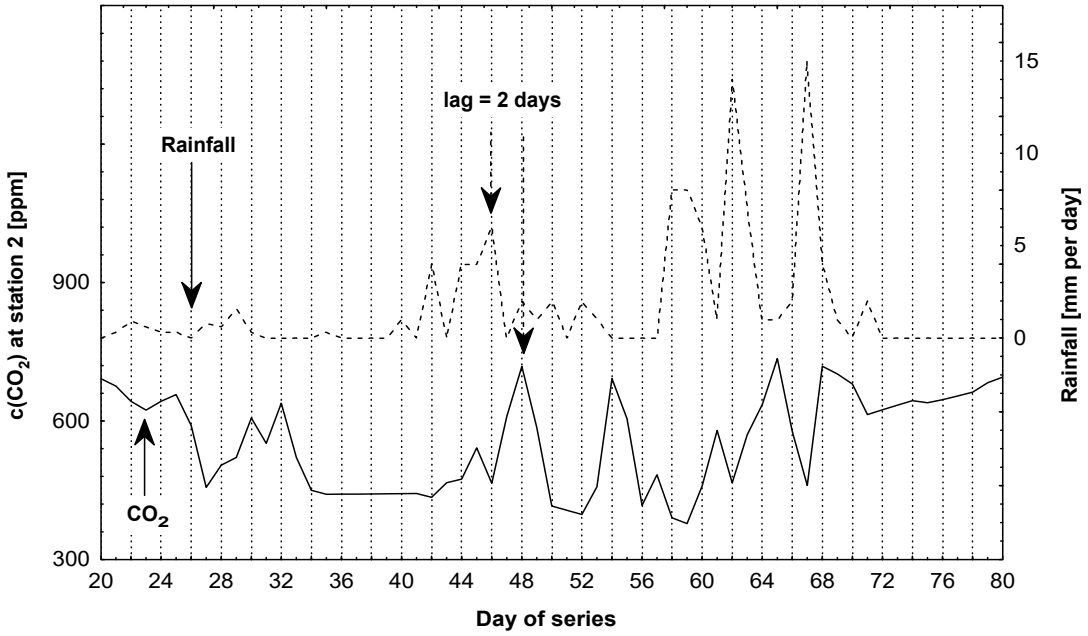

fg_340j: Two days possible time-lag between c(CO_2) at station 2 and rainfall.

Series December 1993 (744 data, 31 daily means):

This time, visual inspection does not give any clue for a time-lag, but the crosscorrelation function shows a peak displaced at t= 5 days (fig. 3.5.16). Applying this 5 days shift and doing the same computations as above yields again regression lines with positive slopes for both stations.

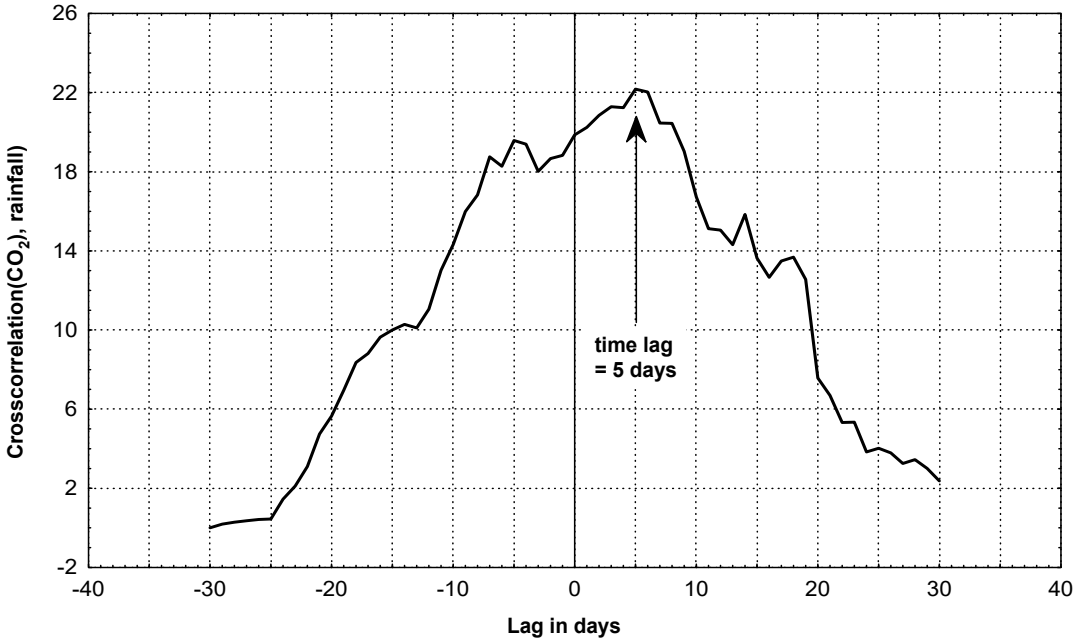

Fig. 3.5.16. Crosscorrelation between CO_2 and rainfall points to 5 day time-lag

So both series seem to validate the hypothesis that rainfall will increase, after a delay of 2 to 5 days, the CO_2 concentrations in the cave at both measuring stations.

3.4.7. Conclusion

Let us summarize the 3 most important results of our study on cave CO_2 in the Moestroff Cave:

1. The high CO_2 levels in the ceiling fissures and the increase of c(CO_2) with outside temperature are two strong indirect hints that biological CO_2 generation in the top soil is an important source of cave CO_2.
2. Air flow patterns in the cave have a significant impact on c(CO_2), as well on a seasonal as on a daily or even hourly time-scale. Both the intensity and the direction of airflow in the cave change local c(CO_2).
3. Three independent climatic parameters do influence c(CO_2): outside temperature, outside wind and probably rainfall. Outside temperature plays the dominant role throughout the seasons. The influence of outside wind can be detected unambiguously only in the interseasonal periods, when outside and cave temperatures are very close. Rainfall seems to increase c(CO_2) after a time-lag of several days.

REFERENCES

CIGNA, A. - Air Temperature Distributions near the Entrance of Caves. Symposium Internazionale di Speleologia. In: Memoria della Rassegna Speleologica Italiana, Como 1961.

CHOPPY, J. - Microclimats. In: Phénomènes Karstiques. Spéléo-Club de Paris. 1986.

EK, C., GEWELT M. - Carbon Dioxide in Cave Atmospheres. New Results in Belgium and Comparison with some other Countries. In: Earth Surface Processes and Landforms, vol. 10, p.173-187. 1985.

JAMES, J. - Carbon Dioxide in Cave Atmosphere. Trans. British Cave Ass. Vol 4, No. 4, p.417-429. 1977.

JAMES J., PAVEY, ROGERS - Foul Air and the Resulting Hazard to Cavers. 1975.

JAMES, J., DYSON, J. - CO_2 in Caves. Caving International Magazine, no. 13, October 1981.

RENAULT, Ph. - Le CO_2 dans l'atmosphère de quelques cavernes du Quercy. Spéléo-dordogne, no.75, p. 1-116, 1980.

VILLAR, E., FERNANDEZ, P.L., QUINDOS, L.S., SOTO, J. - Natural temporal evolutions of CO_2 contents in the air of the "Paintings Chamber" at Altamira Cave. NSS Bulletin, October 1985, p. 12-16. 1985.

3.6. Radon Generation and Transport in Rocks and Soils

Kies Antoine, Francis Massen

3.6.1. Introduction

All common rock types and soils derived from them contain a significant amount of radioactive elements occurring naturally, such as uranium, thorium and potassium. Whereas potassium undergoes a simple form of radioactive decay, the decay of uranium and thorium is complex and proceeds sequentially along a chain of radioactive elements.

Natural **uranium** consists principally of two isotopes, ^{238}U and ^{235}U, of which the first is the most abundant (99,73%) and is the only one of concern for the present work. In the complex decay chain of ^{238}U fourteen steps are passed before reaching the stable end product ^{206}Pb.

Uranium is present in varying concentrations (mean = 2 ppm) in the soils and rocks; it decays through elements with long half lives to radium 226, which itself has a half life of 1620 years. Due to differences in chemical and physical properties and to the mineralogy of the host rock, uranium and the long-lived decay products may be partly removed by chemical and physical processes and movement of water, thus giving rise to radioactive disequilibrium (radioactive equilibrium: the number of atoms of each decay product being produced is equal to the number of atoms of that product being lost by radioactive decay; radioactive equilibrium excludes migration of members of the decay chain). In the oxidized zone of the terrestrial near-surface environment, uranium and thorium may both be mobilized, but in different ways [Curie et al., 1904]. Thorium is largely transported in insoluble resistate minerals or is adsorbed on the surface of clay minerals. By contrast, uranium may either move in solution as a complex ion, or like thorium , in a sorbed or detrital phase.

Radium 226 (^{226}Ra) decays to the isotope 222 of the noble gas radon with a half live of 3.82 days. After production, the radon atom gets unbound and is relatively free to move, provided it reaches the host material's pore space. Once in the pore space, macroscopic transport of radon is possible, by diffusion or by fluid flow in theses spaces. Due to its long life-time, part of the produced radon can enter the air or water phase; here it is transported by diffusion or convective flow of the medium in which it is dissolved. The concentration and mobility of radon 222 in rock and soil interstices control the potential of the rocks and soil to supply radon to fissures and cracks and finally to a cave.

As ^{238}U, Thorium 232 (^{232}Th) experiences a complex decay process before reaching stable ^{208}Pb. One of the members of the decay chain is radon 220 (also called thoron), but due to its short live time of 55 seconds, its

concentration is often negligible. Besides, the radon monitors used in this work measure only radon 222 or its decay products, therefore whenever we mention *radon*, it is only the isotope ^{222}Rn which is referred to.

In general, the concentration and mobility of radon in soil are dependent on several factors, the most important of which are:

- radium content of rocks and soils and their distribution in the soil grains
- porosity
- permeability to gas movement
- moisture content.

These characteristics are determined by the rock's and soil's parent-material composition, their age of maturity, their geological history and by external factors like pressure, humidity, temperature...

Not all radium contained in soil grains and grain coatings will result in mobile radon when the radium decays. Depending on where the radium is distributed in the soil, many of the radon atoms may remain imbedded in the bulk containing the parent radium atom, or become imbedded in adjacent grains. The portion of radium that releases radon into the pores and fractures of rocks and soils is called the **emanation fraction**. When a radium atom decays to radon, the energy generated is strong enough to send the radon atom a distance of about 40 nanometers (1 nm = 10^{-9} meters), this is known as alpha recoil. Moisture in the rocks and soils lessens the chance of a recoiling radon atom to become imbedded in an adjacent grain [Tanner, 1980]. Because water is more dense than air, a radon atom will travel a shorter distance in a water-filled pore than in an air-filled pore, thus increasing the likelihood that the radon atom will remain in the pore space. Intermediate moisture levels enhance radon emanation but do not significantly affect permeability. However, high moisture levels can significantly decrease the gas permeability of the rock and soil and impede the displacement of radon. The emanation of radon from rock and soil minerals and migration of radon in the ground have been reviewed by Tanner [Tanner, 1980], more specific work on the ground as a source of indoor radon has been done by the same and several other authors [Tanner, 1986; Nazaroff, 1988; Nero, 1988].

Relatively soon after the discovery of radon in 1900 the so called emanation of Thorium (thoron or ^{220}Rn) by E. Rutherford, emanation of Radium (^{222}Rn) by F. Dorn), the harmfulnes of this radioactive gas was proven by P. Curie [Curie et al., 1904] on mice; in 1907 Rutherford pointed out the possible physiological effects on humans. High radon concentrations were expected and measured especially in uranium mines and the harmfulnes of radon for underground workers was recognized. The main measuring devices were based on the ionising effect of alpha-particles and on the scintillation of different substances. The increasing interest on the health effect of radiation and the discovery that indoor

radon concentrations can be comparable to those in mines lead to the 'radon boom' of the last decennials. Existing measuring devices were improved, older ones rediscovered, new devices were introduced (A. George [George, 1996], H. Surbeck for radon in water [Surbeck, 1995]). Today's instruments can be used to monitor radon in underground locations more easily and definitely in a more accurate way than in the past. Part of the knowledge gathered in the study of indoor radon availability can be used for the study of the dynamics of underground radon concentrations. Collecting data of the continuously varying underground radon levels is not only useful for radioprotection purposes, but increasingly radon is used as an omnipresent natural tracer gas in geology, [Kemski, 1996], in hydrogeology [Hunyadi et al, 1991], in karstology [Haql et al, 1996] and in geophysics.

Radon is easily detectable even in small quantities: in air at a 'concentration' of 10 Bq/m^3 which is a typical resolution of normal radon monitors, only 5 million radon atoms are in one cubic meter, or one radon atom for $5*10^{18}$ molecules of air. Unfortunately, radon sources exist everywhere and, a priori, their location is not known. This complicates the interpretation of radon measurements and needs an interdisciplinary expertise of physicists, radiochemists, hydrogeologists, geologists, geophysicists, etc. The observations of subsurface fluid motions traced by natural radon lead to new research fields such as basic transport phenomena, mapping of active faults, investigations of volcanic and seismic activities, earthquake prediction, rock gliding in mines, investigations of climate in a cave, etc.

3.6.2.Radon Measuring Devices

Several types of devices were used in the cave to measure mainly ^{222}Rn gas concentrations.

Mean radon concentrations, 2 to 3 weeks integrating measurements

- **Solid state nuclear track detectors** or **etched track detectors** of the Karlsruhe type; they rely on the use of Makrofoil, a plastic material, to record the tracks caused by the α particles emitted during the decay of radon and its decay products (decay products: short-lived elements before reaching ^{210}Pb, see fig. 3.6.1). This damage can be revealed later by etching the plastic in a caustic solution. This last operation was performed at the laboratory of the Division de la Radioprotection, Luxembourg.
- To a lesser extent the **electret ion chamber**: a Teflon sheet having a permanent surface charge is placed at the bottom of a conducting plastic chamber; radon diffuses into the chamber volume and the electrets lose

their charge because of the air ionisation produced by radon and its decay products.

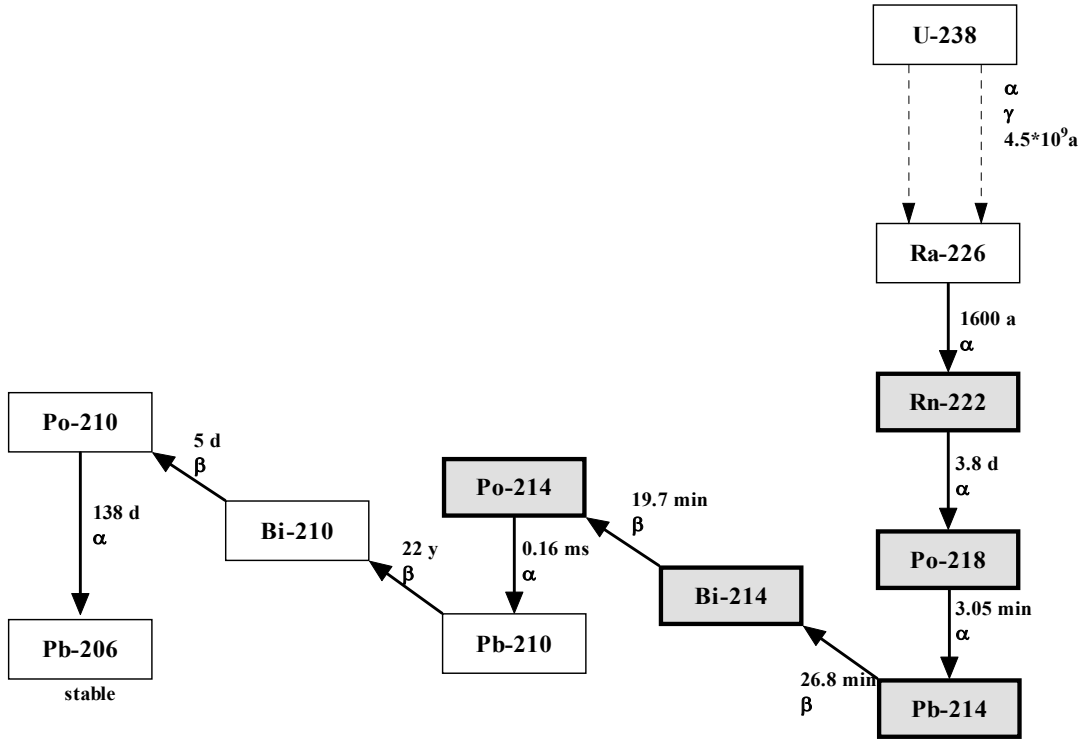

Fig. 3.6.1. Decay products of ^{238}U and radon daughters

Continuous monitoring of radon

- **Alphaguard** electronic sensor from Genitron Instruments, integrating over a period of 1 hour, sometimes of 10 minutes. In an ionisation chamber an electrical field is established between two electrodes. Filtered air is allowed to diffuse into the chamber, the pulses generated by the ionizing of individual alpha particles are counted.
- Silicon diode based **Alphanuclear** detector, measuring interval 1 hour

Point measurements

- Thomson and Nielsen **radon sniffer**, the only active device for the measurement of the radon progeny concentration. A pump draws ambient air to a filter paper which traps the decay products of radon on a filter paper where they are measured using a solid state detector. The measuring time was 1 or 2 hours.
- **Scintillation cells** or **Lucas cells** for cave air and for soil gas measurements: The cell is a cylinder with one end closed by a transparent window and whose internal surface is covered by a scintillator, usually ZnS:Ag. After inlet of air, the light pulses resulting from the interaction of alpha particles released by the decays and the scintillation are recorded by a photomultiplier.

  The scintillation cells are used also to measure radon concentrations in the pores of the sediment at the bottom of the cave, at a depth up to 1 m, by the gas extraction method. Rods of 8 mm inner diameter were hammered into the soil, after driving down the lost end dip some more 5 cm in order to create a free space, soil gas was sucked out of the sediment and introduced in a scintillation cell to be measured in the laboratory 3 hours later, when radon is in equilibrium with its short-lived progeny.

  At different time intervals all the mentioned radon monitoring devices were tested and compared.

In the Moestroff cave the bottom of the galleries is covered by a thick layer of sediment. In the pores of the sediment the radon concentration was 50 ± 5 kBq/$m^{3;}$ this was confirmed by repeated measurements. The radium content of the sediment and the rock was measured with a highly pure germanium detector using radon-tight boxes. With 105 ± 5 Bq/kg the radium concentration in the sediment is much higher than in the limestone the activity of which is 37 ± 3 Bq/kg. As the sediments prove to be rather permeable, the radon availability of the sediments is high and their contribution to the radon concentration is not negligible, especially for the interior locations where the layer of sediments is much more important than near the entrance.

The extreme humidity conditions caused some problems for the different measuring devices. Monitoring radon and other climatological parameters in the air of a mine or a cave with air humidity of nearly 100% is not easy, as the high humidity often plays havoc with the monitors. During the last years we gathered some extremely valuable lessons concerning the influence of humidity on radon instrumentation.

The **nuclear track** detectors proved to be well working even at 100% humidity in the cave. We did some intensive research using unprotected and protected detectors; the protection against water-vapour was achieved

by enclosing the detectors into radon-permeable polyethylene bags. Detectors exposed repeatedly side by side did not show significant differences. We could not validate the warnings given by Medici and Rybach [Medici et al., 1992] who report huge differences for these detectors used in dry and humid air; the good behaviour of nuclear track detectors of the same type in very humid mines was confirmed recently by Muth [Muth, 1995].

The **electrets**, electrostatic charged mylar foils which lose their charges if exposed, proved not to be of use at the very high humidity level of the cave. High air humidity leads to excessive discharges and as a consequence the measured concentrations were often too high. This is a pity, as these devices can be read out easily with an electrostatic voltmeter and do not need the complicated etching process of the nuclear track foils. The electrets performed much better in the gypsum mine and gave most of the time valuable results. One great advantage of the electrets is the possibility of intermediate measurements, one big disadvantage is the imperative knowledge of the gamma background for correcting the data.

We had no problems with the **Lucas cells**: at our experience they performed best of all the devices under the extreme humidity conditions. An advantage of the scintillation cells is that the background noise of this simple device is low and a set-up can be achieved at a reasonable cost.

To our knowledge, we were the first research group using the **Alphaguard** device for long time continuous measurements in a cave. The Alphaguard has an integrated datalogger and sensors for temperature, pressure and humidity. The first P30 Alphaguard model, despite the manufacturer's specifications, gave nonsense readings after a couple of days in the cave and finally stopped functioning. After drying, the instrument functioned correctly again for some time. After the manufacturer made some modifications, the newer models behaved much better; we could maintain a maximal continuous working performance for 55 days in the cave. To achieve this, one has to use the internal heater of the device by powering it with an external battery, or use the electrical domestic power supply if it is available. A drawback is that the heating interferes with the internal temperature and humidity sensors which give wrong readings in this case. Nevertheless, exposed to extreme humidity conditions, the new model still gives sometimes meaningless concentrations, usually high easily detectable spikes (fig. 3.6.2); a single high value is normally followed by a low one, after which the detector recovers and reverts to correct operation. The possibility proposed by the manufacturer to use a water-tight bag extends the duration of correct operating conditions, but thus most information on rapidly changing radon concentrations is lost.

The **Aphanuclear** showed no problems but this device is not sensitive enough for concentrations below 2 kBq/m^3. If the readings are smoothed

or filtered, this device with its low power requirements can be very useful for the study of long time evolution.

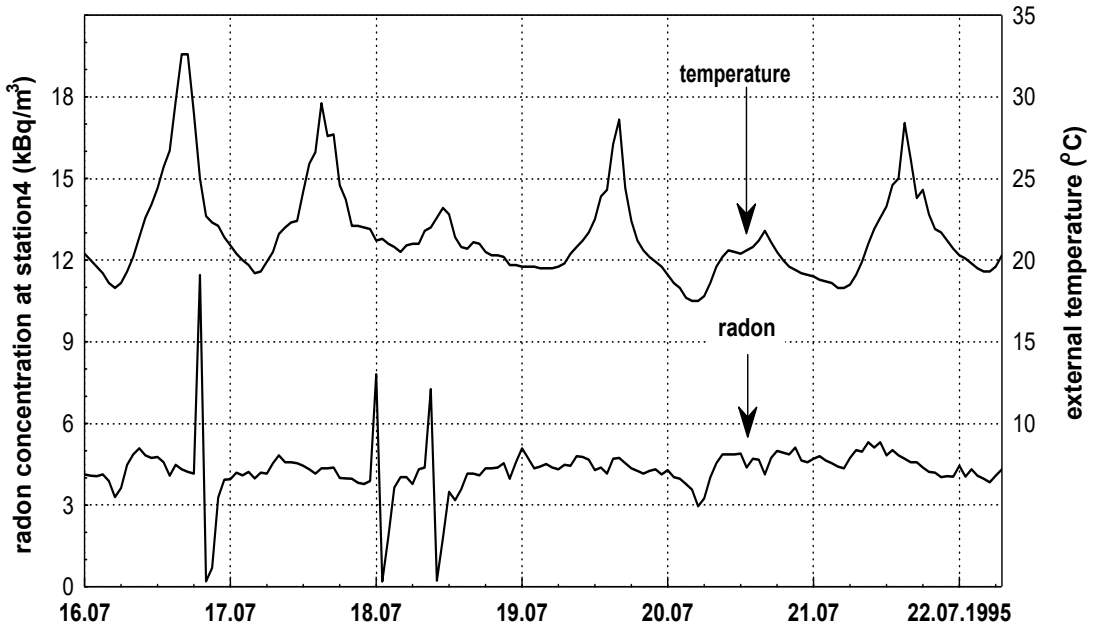

Fig. 3.6.2. In a period of low radon dynamics, spikes in the radon measurements of the Alphaguard, due to high air humidity, are easily detectable and can be eliminated.

3.6.3. Radon Measurements

Caves are commonly considered as a static environment where, in complete darkness, parameters as temperature and humidity are stable. But other parameters may experience very high variations due to many exchanges between the cave air, the fracture system, the outside, the sediments and the water in the cave. Air radon concentration is one of these parameters which undergoes high dynamics in response to changes of other factors of the environment.

In a long-term study of radon concentrations in mines or caves, it is important to analyze the interactions of meteorological, climatic and pedologic factors which affect radon concentrations on minutely, hourly, daily, and seasonal time scales. A simultaneous measurement of other gases is often of great interest. The installation of an external weatherstation is mandatory as radon levels are always correlated to some extent with outside air temperature, atmospheric pressure, wind speed, humidity and rainfall. Depending on the time-scale of the study, daily or seasonal, not all the parameters mentioned are needed.

3.6.3.1.Seasonal Radon Pattern

Fig. 3.6.3 shows the result of monitoring radon over three years, based on nuclear etched track integrating measurements exposed in the three interior stations. The seasonal pattern is mainly the result of air movements due to differences of external and internal air densities caused by varying external temperatures, the internal temperature can be considered as constant. This is a classical temperature-induced air movement (chimney effect) in underground locations which have openings to the exterior situated at two different levels at least. The observed radon pattern, with maximum values in those periods, autumn and spring, when inside-outside temperature differences are minimal, can be interpreted if one admits the existence of one or more systems of galleries under the explored cave, some of which communicate to the outside via small openings and fissures in the cliff (see chapter 1.1.).

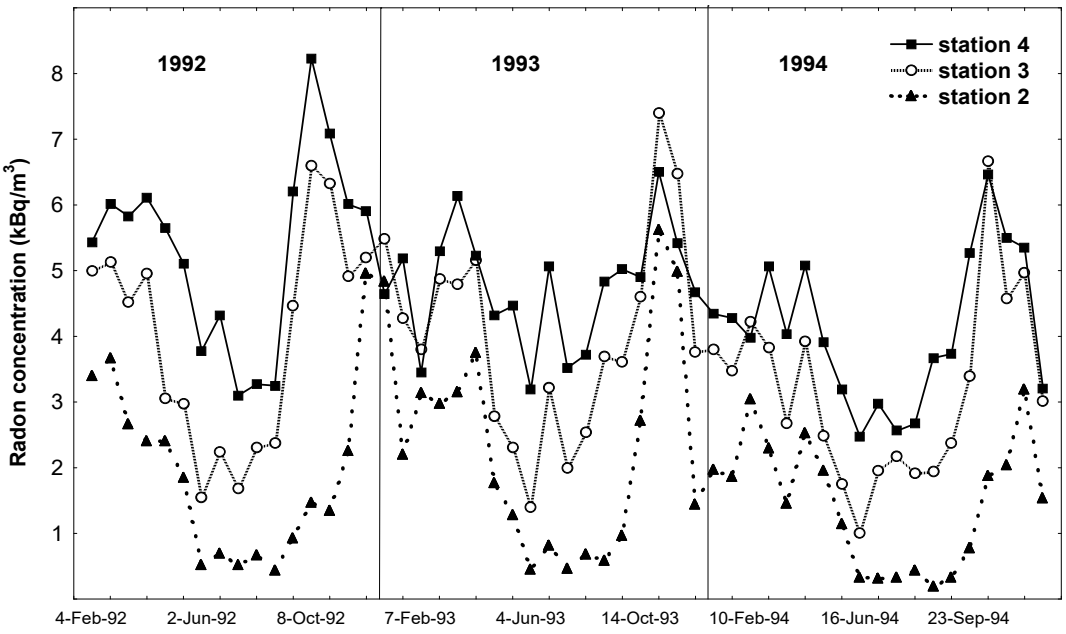

Fig. 3.6.3. Time evolution of mean radon concentrations over three years in three different locations in the main gallery, at 12 m (st. 2), 31 m (st. 3) and 50 meters (st. 4) from the entrance.

In the *cold period*, the lighter radon-enriched air of the system rises, and pushes cave air out through the exit. During this movement, the air gets enriched in radon from the fracture system and from the sediments. The radon levels in the cave are highest when these air movements are very low, this happens at temperatures slightly below the cave temperature of 9.5°C as seen on fig. 3.6.4. Higher temperature differences move a greater air volume, thus the speed of air flowing through the fracture system is increased, and as a consequence the radon concentrations of the air entering the cave galleries from below decrease.

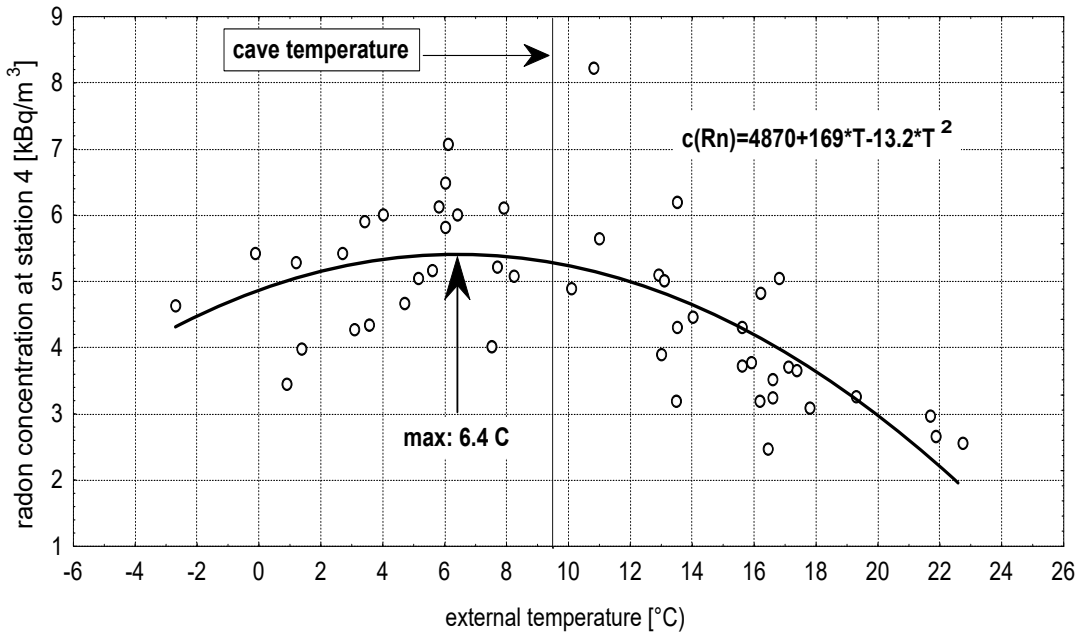

Fig. 3.6.4. Radon concentration at station 4 in the Moestroff cave, 50 meters from the entrance, against temperature can be fitted by a parabola.

In *summer*, the process reverses, the direct inflow of outside air into the cave leads to the lowest radon concentrations. This effect is most effective for locations near the entrance.

There is a slight asymmetry in the way the radon changes between summer and winter. In springtime, radon levels in the cave vary gradually whereas in the fall they experience a rapid increase.

The radon transport processes depend essentially on the configuration and the connection of the underground cavities, passages and other communications to the exterior, such as fissures and fractures. Due to the particular location of the Moestroff multi-storey cave, with an upper main gallery and with openings on a cliff, the seasonal radon pattern is quite different from those reported elsewhere for caves [Hingmann et al., 1995; Hunyadi et al., 1990]. For horizontal caves and for caves with most passages above the entrance elevation, a typical pattern of temporal radon changes are summer maxima and winter minima [Kies et al., 1995]; in caves where most passages are below the entrance, but with no communication to the exterior, the wintertime air stagnation in the cave results in high radon concentrations during the cold season. [Kies et al., 1993; Haql et al., 1996].

We explain the air movements and the seasonal radon behaviour, essentially governed by the chimney effect, by the existence of not accessible

galleries below the actual cave with multiple small openings in the cliff. In the cold season, radon-enriched air entering the cave from below leads to higher radon concentrations than in the summer when fresh air entering the cave through the main entrance is loaded gradually with radon during its movement through the cave. In summer with the main inflow of air through the entrance, radon concentrations (in kBq/m^3) experience a linear increase.

$$c(x) = 0.018 + 0.083 * x \qquad \textit{[eq. 3.6.1]}$$

with the distance x to the entrance; in winter when the cave exhales, a higher exponential increase

$$c(x) = 5.4 * (1 - e^{-0.065 * x}) \qquad \textit{[eq. 3.6.2]}$$

is observed (fig. 3.6.5).

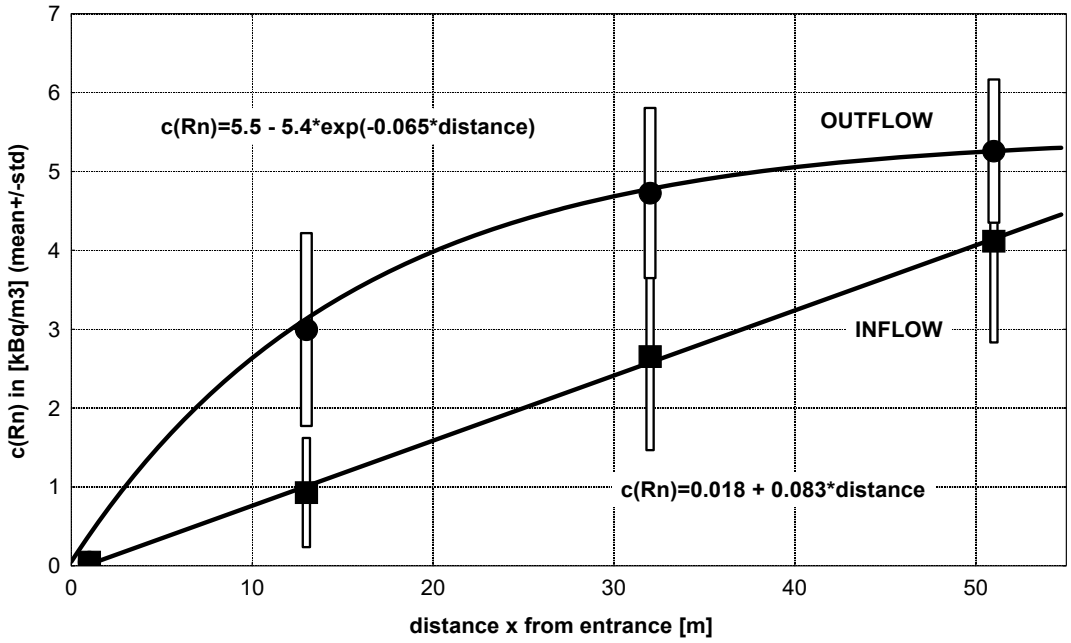

Fig. 3.6.5. Radon versus distance from entrance

Equation 3.6.2 is a steady state solution of the one dimensional transport equation due to radon production, decay and molecular diffusion and to fluid flow in a cylindrical void embedded in a rock matrix [Clements et al.,1974; Bates, 1980; Nazaroff, 1992]:

$$\frac{dC}{dt} = D\Delta C - \nabla(\bar{v}C) - \lambda C + \Phi \qquad \textit{[eq. 3.6.3]}$$

where

C radon concentration in pore space [m^{-3}]

D diffusion coefficient of radon [m^2*s^{-1}]

v velocity of air carrying radon [$m*s^{-1}$]

λ decay constant of radon [s^{-1}]

Φ radon source term [m^3*s^{-1}].

A particular steady state solution of this equation, assuming a constant velocity v and the boundary conditions:

$$C(0,t) = C_0 \approx 0, C(\infty,t) = C_\infty = \frac{\Phi}{\lambda} \qquad \textit{[eq.3.6.4]}$$

is $$C(z) = C_\infty(1 - e^{-\frac{z}{l}}) \qquad \textit{[eq. 3.6.5]}$$

where l is the characteristic transport length. For the Moestroff cave this characteristic length is is approximately 15 m, very close to the relaxation distance found for the temperature profile (see chapter 3.1).

The variation of mean radon concentration with external temperature is quite different at the three stations. If no distinction is made between inflow and outflow periods, the best overall fits are linear for stations2 and 3, and parabolic for station 4 (fig. 3.6.6).

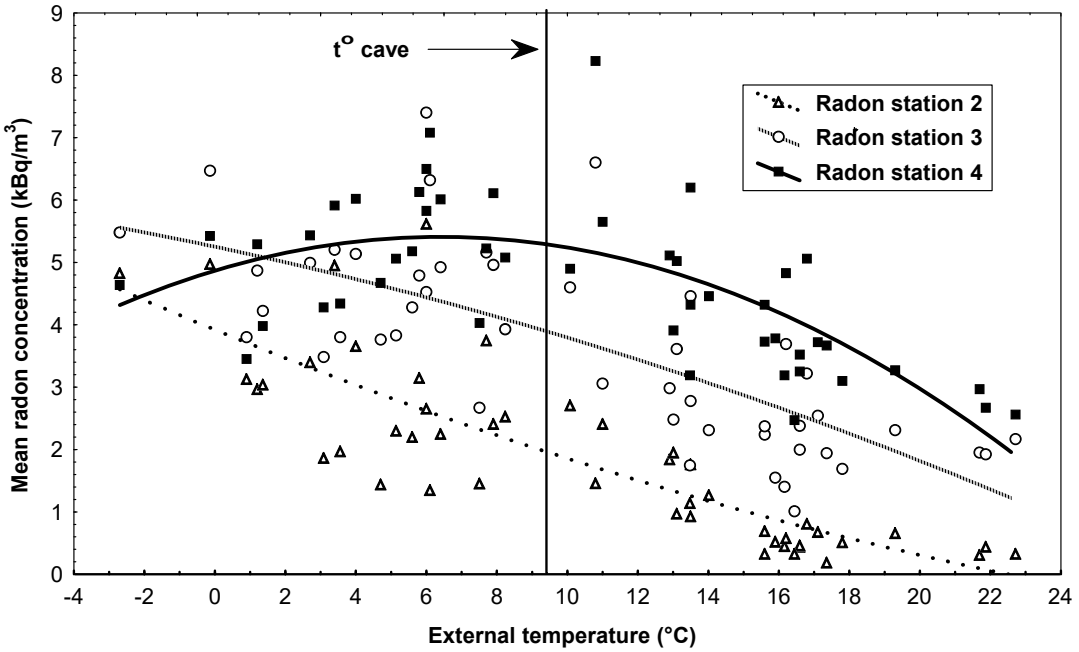

Fig.3.6.6. Variation of c(Rn) with outside temperature

Near the entrance at **station 2**, radon concentrations continuously decline with increasing outside temperature; under very cold weather conditions

the exhaling radon-enriched air has a concentration of 5 kBq/m^3, which is the steady state radon concentration of the interior of the galleries. Increasing outside temperatures lower the exhalation which gradually changes to inhalation of fresh air. At the deepest located **station 4**, the changes in mean outside temperature have the smallest effects on radon concentrations, but even this location experiences the diluting effect of the important thermally induced air movements especially in summer. The interposed **station 3** has an intermediate behaviour in the cold season when stations 2 and 4 experience an opposite evolution, which leads to a near constant mean value of 5 kBq/m^3.

If one wants to study the influence of air movements on radon concentration, the periods where air flows into the cave have to be separated from those where it flows out of it. As should be expected, air movements usually decrease the local radon levels at all stations, as shown in fig. 3.6.7.

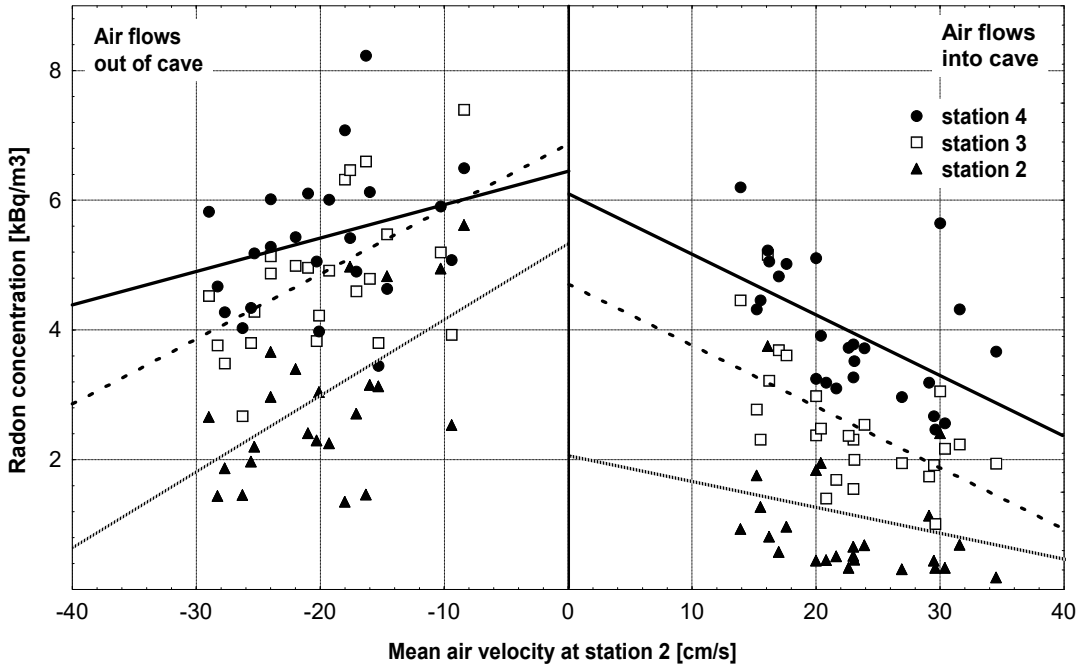

Fig. 3.6.7. Local c(Rn) versus air velocity measured at the entrance of the cave (station 2)

A good correlation between Radon and CO_2 concentrations in soil air is often reported [Kemski, 1996]. In the Moestroff Cave, there is no correlation between Rn and CO_2 levels when air moves into the cave, and a very good one (correlation of 0.59 at the significance level $\alpha = 0.01$) when air flows out (fig.3.6.8). Only in the last case that part of carbon dioxide which comes from the microbial breakdown activity happening in the

lower storeys and fissures is detectable in the cave air monitored at station 3.

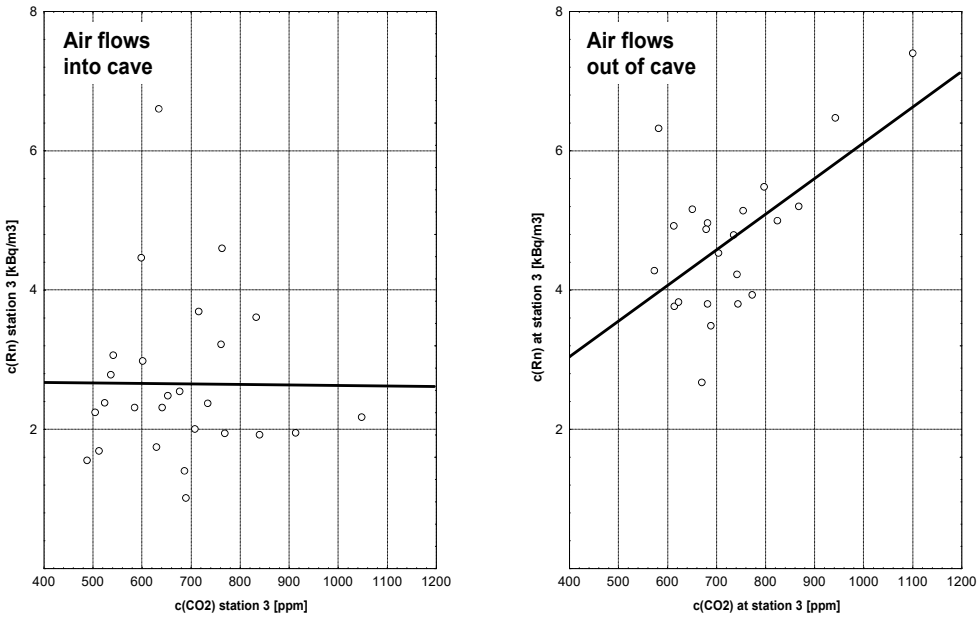

Fig. 3.6.8. Radon versus CO_2 at station 3 (inflow and outflow)

3.6.3.2. Short-Term Radon Observations

While air temperature in the caves and mines is nearly constant, depending on the geometry and morphology of the cave, radon concentrations often experience huge changes, not only seasonally, but above all on very short time scales [Hunyadi, 1991; Hyland, 1993; Hingmann, 1996]. Many of these short time variations can be explained by the thermally induced air movements (chimney-effect); the variations in intensity and direction of these air movements have been studied in chapter 3.5. Besides these thermally induced air movements, the effect of changing atmospheric pressure and of external wind gusts [Massen, 1995] proved to be important.

When air is moving, there is a gradual drop in pressure along the galleries. The pressure drop dP can be equated using the Darcy-Weinbach equation for flow pipes [Atkinson, 1983].

$$dP = \frac{f \cdot L \cdot v^2 \cdot \rho}{8 \cdot R} \qquad \textit{[eq. 3.6.5]}$$

where:

dP pressure drop [Pa]

f friction parameter

L cave length [m]

v average wind speed [$m*s^{-1}$]

R hydraulic radius [m] (R=area/perimeter)

ρ air density [$kg*m^{-3}$]

As dP is proportional to the square of the wind speed, this differential manometer is more sensitive to detect air movements than are anemometers. Normally the air speeds are very low and one has to rely on hot-wire devices which give no information about the direction of air movement. A precise differential SETRA manometer [Massen, 1995], with 50 meters plastic tubing extending from the entrance to station 4, was installed (see also chapter 3.4.2). The recorded pressure differences were never higher than 10 Pa, the sensitivity of the instrument allowed to detect variations as low as 10 mPa. This instrument measured the wind direction in an indirect way: air is flowing from high pressure to low pressure regions, a higher pressure at the entrance is coupled with inflowing air and a lower entrance pressure with outflowing air. Many manual checks with incense sticks verified the good reliability of that sensor, which helps to give a clear picture of both short term and seasonal wind patterns.

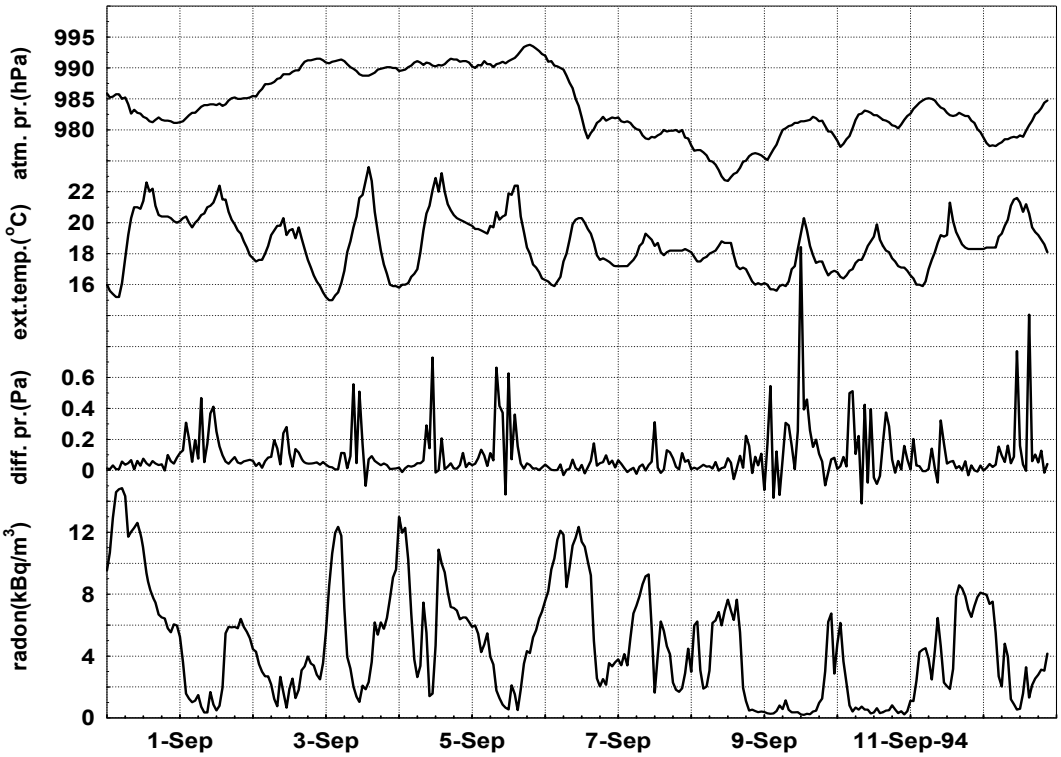

Fig. 3.6.9. *The radon levels at station 4 are compared to the time series of differential pressure between outside and station 4, external temperature and atmospheric pressure*

The plots of short term measurements of fig 3.6.9 illustrate the complex interplay of the various parameters, typical for underground locations with openings at different levels and having an important fracture system where radon can concentrate before being pushed into the galleries [Bates, 1980]. At periods of low wind activity and low dP oscillations, the radon levels are highest. The effect of changing atmospheric pressure is apparent only during these periods.

For the discussion of the observed changing radon levels and the causes of air movements in the Moestroff cave, one has to consider the location of the main entrance up in the cliff exposed to the South, with the lower presumed openings situated near the vegetation canopy of the forest. Beside the classical chimney effect discussed so far, two other effects should be retained:

- First, a gradient of air temperature along the cliff, resulting in a pressure gradient which may enhance or impede the steady state air movements.

  Secondly, wind velocities are higher at the exposed upper location of the entrance than down the cliff. A Bernoulli effect pressure reduction near the main entrance ($dP = 1/2*\rho*v^2$) induces supplementary variable outflow conditions.

  Fig.3.6.9 gives an example of the short time variations of the radon concentrations typical for a cave with a well developed fracture system. Oscillating air movements and gusts of cave air are able to move radon enriched air to a certain location, but also to remove it from there. Convection caused by variations in outside temperature is most of the time responsible for the dynamics of radon cave concentrations as shown by the anticorrelation of the temperature difference and the radon concentration.

  We may distinguish two important processes contributing to the exchange of radon between the rocks and the galleries environment [Schery, 1982].

- The first is the conventional transport with a combined diffusional and convective flow in the galleries.
- The second process is diffusion and flow out of cul-de-sac chambers such as closed-ended cracks and smaller pore spaces. In these cracks the ratio of surface area to volume is so large that they normally contain radon at a high concentration. Variations in the absolute pressure and local pressure gradients due to nearby flow conditions induce the outflow of radon enriched air, and as a consequence yield substantial contributions to the radon concentration in the cave air [Bates, 1980; Clements et Wilkening, 1974].

The first of these processes governs mean radon concentrations or concentrations in underground locations without cracks and openings. The

second is responsible for the important short-time spikes in the radon levels.

In the rare periods when there are negligible air movements or low differential pressure variations in the Moestroff Cave, the radon concentrations experience the influence of atmospheric pressure changes as documented in part of Fig. 3.6.9 and in Fig. 3.6.11. Normally this enhancement of radon flux due to pressure variations is masked in the conditions of radon depletion due to movements of air. Physically the convective processes along the galleries and tight air path ways are in competition with the diffusive processes perpendicular to the walls of the galleries. A critical speed of air flowing in the gallery can be defined when one equals the transport distances of radon by diffusion and by flow during the mean life-time τ = period/ln2 of radon:

$$v_c \tau = x_d = \sqrt{2D\tau}$$

$$v_c = \sqrt{\frac{2D}{\tau}} \qquad \textit{[eq. 3.6.6]}$$

where:

D diffusion coefficient of radon in air ($D \cong 1\ cm^2*s^{-1}$)

x_d characteristic transport length ($x_d \cong 11$ m)

v_C critical speed ($v_C \cong 0{,}05\ mm*s^{-1}$)

In the fracture system and in fissures, diffusion is the dominant migration cause of radon. An air velocity substantially higher than the critical velocity will be able to wash out radon from the fractures. Otherwise, due to diffusion, radon accumulates in the fracture system or near the walls. Oscillating small air-movements carry, with some time-delay, radon out of the fissures and fractures into the cave, which explains the very high dynamics of a cave with a well developed fracture system.

An atmospheric pressure drop increases the exhalation of radon out of the rocks and sediments into the fracture system, thus producing a local increase of the radon concentrations. Decreasing atmospheric pressure drains air from the cave; increasing pressure pushes air into the cave through the entrance. The volume of air passing through the entrance, due to a pressure variation of Δp_{at} is

$$\Delta V \approx -\frac{V_{cave}}{p_{at}} \Delta p_{at} \,. \qquad \textit{[eq. 3.6.7]}$$

where:

V_{cave} volume of the cave [m^3]

p_{at}, Δp_{at} atmospheric pressure and pressure change [Pa].

If we assume 4 km of galleries having a section of 1 m^2, the volume is 4000 m^3; for a pressure drop of 10 HPa, ΔV = 40 m^3. If the pressure drop happens in 6 hours, the velocity through a single gallery of a section of 1 m^2 would be some 2 mm/s. These pressure drop induced air movements are able to free part of the radon from the fissures and assure a mixing of radon in the cave. An increasing atmospheric pressure lowers the radon flux out of the rocks and sediments: less radon accumulates in the fracture system.

In the next part **some typical radon patterns** obtained at Moestroff are analyzed. The parameter rainfall, which often influences radon concentrations in caves, proved to have no significant impact in the Moestroff cave. All attempts for correlation, with or without time delays, failed. The small amount of percolating water may explain this, thus this often quoted radon source can be neglected. The observed radon levels are the result of the complex interplay of external factors as temperature, wind velocity, temperature gradients along the cliff, atmospheric pressure variations and cave specific factors as morphology of the maze cave, radium content in the sediments and in the rocks.

The first example covers a typical bright weather period in July 1994 (see fig. 3.6.2 at chapter 3.6.2). The outside temperature varies between 18 and 30 ^{O}C. During this period with low wind activity, the inflow of air into the galleries has a limited diluting effect at station 4 where radon concentrations are rather high. Bright weather periods with temperatures not decreasing below some 16^{o}C show similar radon patterns.

Whenever the temperature variations induce lows approaching or going below the cave temperature, oscillating air movements in the cave induce higher dynamics in the radon concentrations. Fig. 3.6.10 shows huge variations in the radon levels at station 3.

In the early morning, when outside-inside temperature difference is lowest and close to the cave temperature, radon concentrations are highest. When the external temperature approached the cave temperature in the night of the 12th June 1994 every air movement in the cave stopped, thus permitting an accumulation of radon in the fissures and fractures. Growing outside temperatures induce air movements and the washout of the accumulated radon; a radon high is observed at station 3. Once this radon evacuated, the inflow of fresh air leads to a rapid decrease of the radon level. In this example the anticorrelation of external temperature and radon concentrations is perfectly documented.

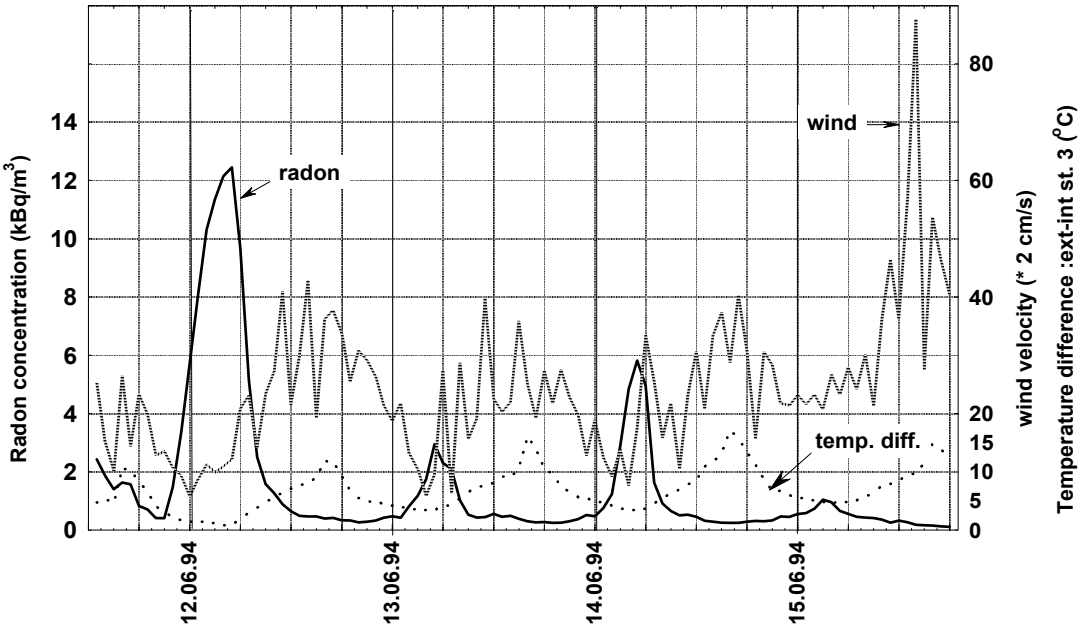

***Fig. 3.6.10**. Due to periods of minimal outside-inside temperature differences and air flows, radon concentrations may reach very high levels even in a 'radon-low' season.*

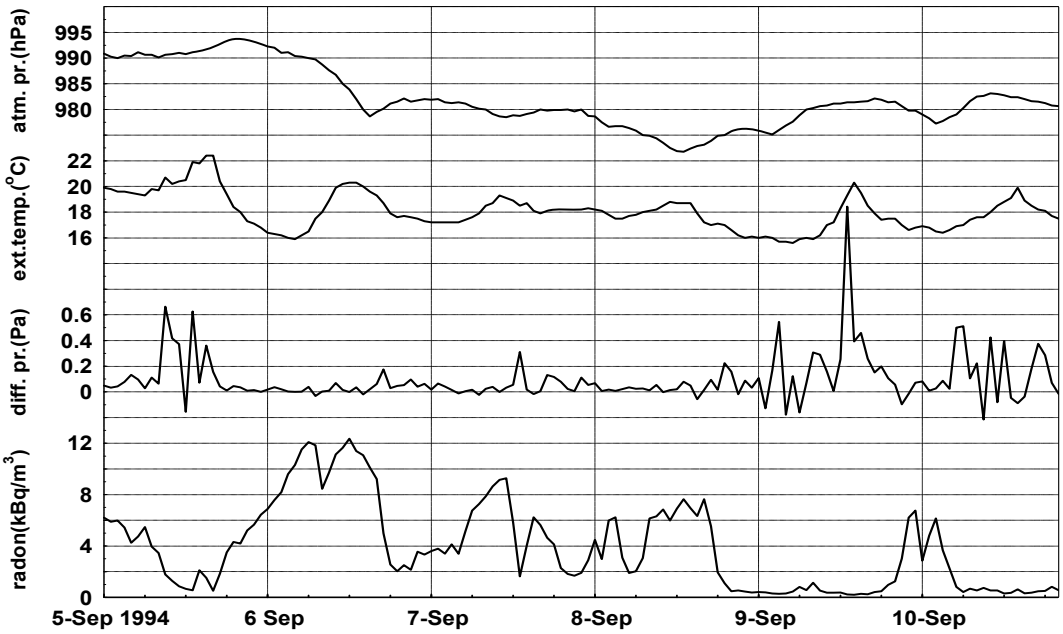

***Fig. 3.6.11.** Detail of figure 3.6.9 showing among other the influence of changing atmospheric pressure on radon levels at station 4.*

Fig. 3.6.11 is a close zoom on a part of figure 3.6.9. In the period from the 6th to the 9th September 1994 the recorded differential pressures are low, documenting a low wind activity at station 4. During this period mean radon concentrations are high at station 4; the increase during the night

from 5th to 6th of September is due to the atmospheric pressure decrease, freeing radon as explained earlier. Variations in temperature and external wind gusts induce spikes in the differential pressure The coupled air movements lower radon concentrations dramatically, the radon levels recover gradually between the different periods of fresh air input. In periods of high frequency of differential pressure spikes, i.e. of oscillating air movements, radon concentrations cannot build up and the concentrations are very low. Fig. 3.6.12 shows, at a different scale, for nearly the same period of September 1994, the radon levels and the outside temperatures. This figure proves that outside temperatures can explain, as discussed before, a lot of the observed radon features especially before September 5th. But the knowledge of other parameters is needed for further interpretations.

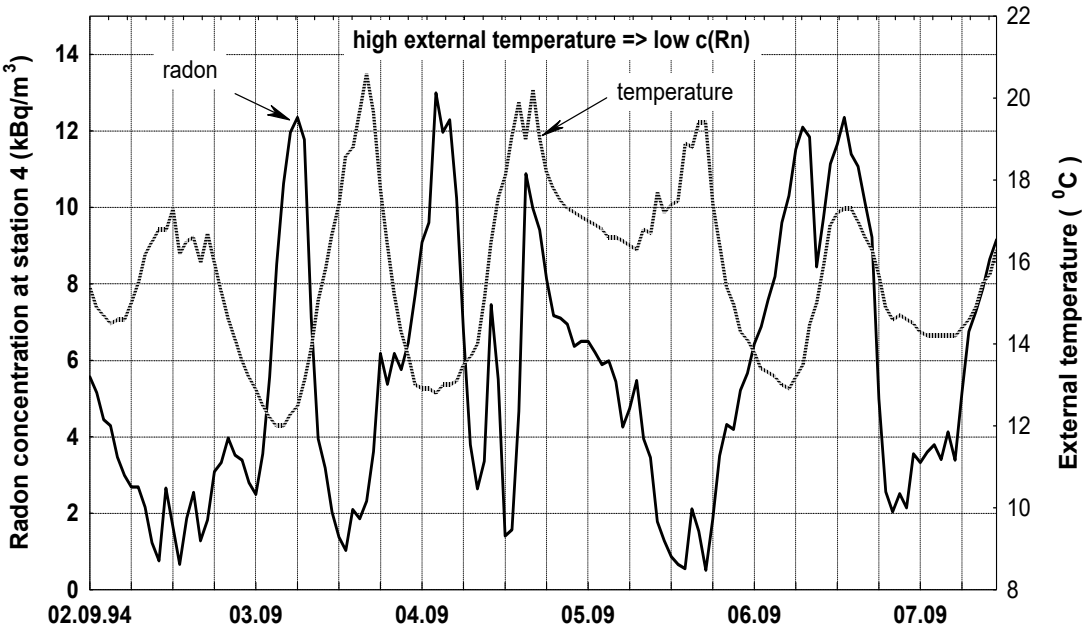

Fig. 3.6.12. Radon levels and outside temperature from 6 Sep.96 to 9 Sept.96

3.6.3.3. Continuous Short Term Radon Measurements in October 1996

Long-term radon monitoring was done at the three locations in the cave without interruption for 3 years. This was not possible for continuous monitoring, the necessary equipment being too expensive and demanding in electrical power. However, in October 1996, three identical Alphaguards were available and were installed for 10 days at the 3 stations. The period of exposure proved to be well chosen, as it covered both rather stable late autumn weather and a typical disturbed windy period. As the weatherstation near the entrance had already been removed, the climate data were taken from the weatherstation installed at the Lycée Classique Diekirch situated at a distance of less than 10 km from the cave.

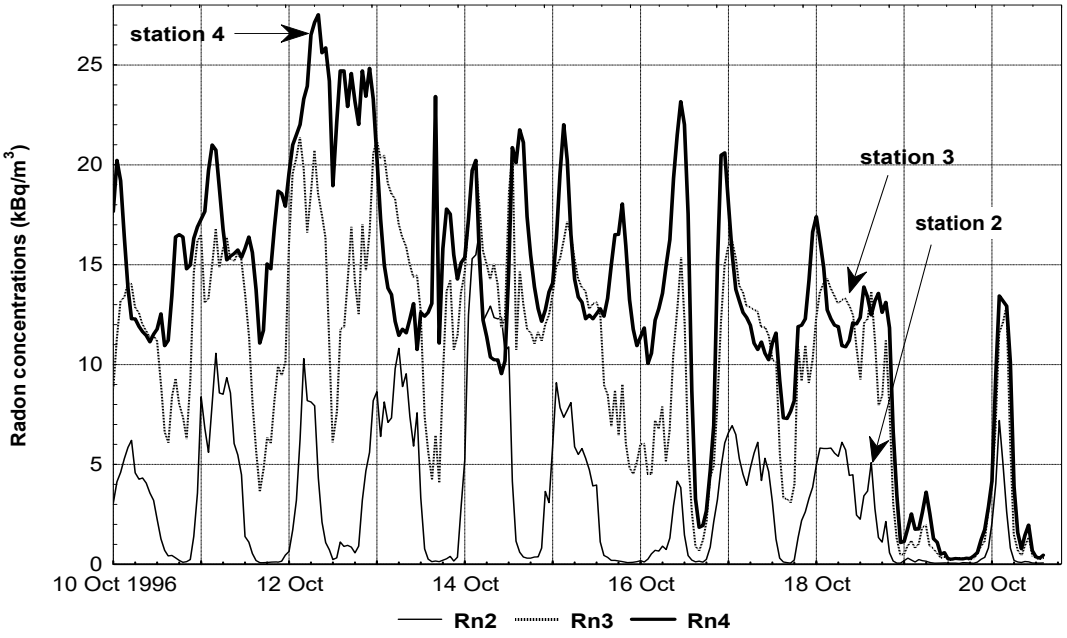

***Fig. 3.6.13**. Simultaneous record of radon concentrations at the three stations inside the cave in October 96*

Fig. 3.6.13 shows a detail of the evolution of the radon concentrations c2, c3 and c4 at the 3 stations 2, 3 and 4. In accordance with the long-time study of chapter 3.6.2.1, October is the month where mean radon levels are highest. For the studied period they were unusually high: mean concentrations were 3.5 kBq/m^3 at station 2; 10.3 kBq/m^3 at station 3 and 13.1 kBq/m^3 at station 4. Wind activity was moderate with an exception of the last days (fig. 3.6.14) where high velocities reduced radon levels dramatically at the three stations.

As expected, the station near the entrance was more affected by moderate winds than locations deeper in the cave. A plot of radon concentrations against wind velocities (fig. 3.6.15) shows that wind velocities higher than 3 m/s depressed radon at station 4; wind velocities beyond 2 m/s did the same for station 2. It is interesting to notice the similar influence of wind activity and threshold wind velocities on CO_2 concentrations as documented in chapter 3.5.5. Whereas the depletion of radon due to outside winds is easily understandable for locations near the entrance, it is difficult to explain the rapid shutdown of radon levels at station 4. Due to its deeper location and protected by the maze of tight galleries, this station seemed to be better protected against exterior influences. Once more the very sensitive behaviour of radon as a tracer gas is documented. The drop of radon concentrations shows that high mean wind velocities, paired with strong wind gusts, are able to move fresh outside air to deeper parts in the cave in a more effective way than temperature differences do.

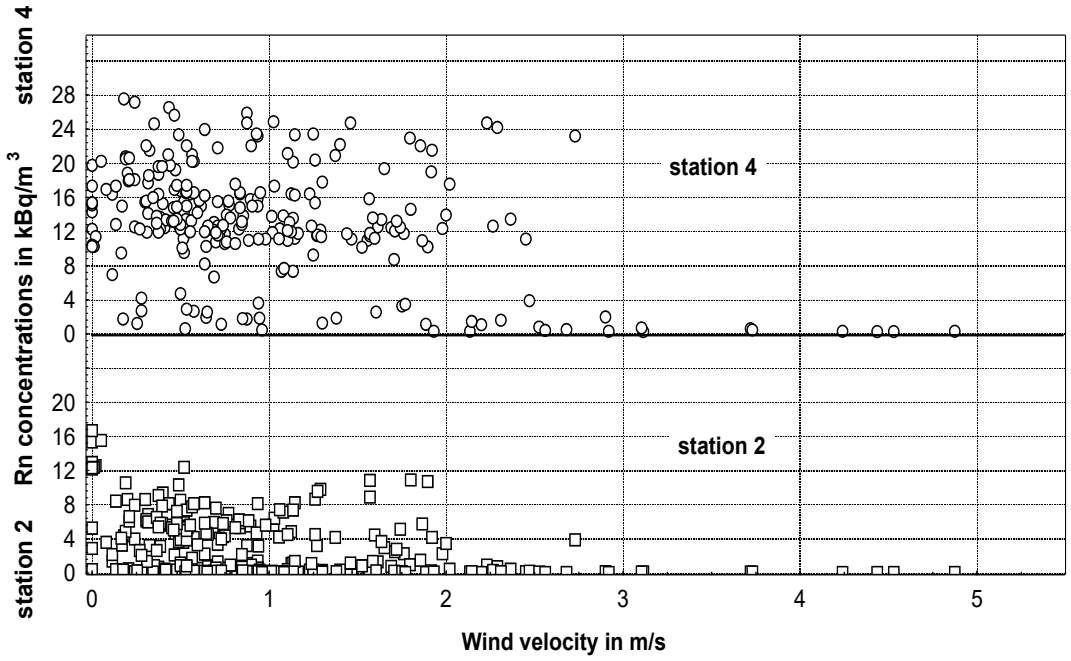

***Fig. 3.6.14**. Radon levels in stations 3 and 4 versus wind velocity measured in Diekirch.*

The cause of the observed rapid drop is the Bernoulli effect. Due to the depression caused by a wind gust near the entrance, radon-rich air is moved to the entrance; but this will not lower c3 and c4. When the wind gust stops, air pressure recovers and fresh air enters the cave. In order to depress radon concentrations at station 4 in the observed way, the air flowrate must be very high. This explanation makes sense only if the volume of the cave situated deeper than station 4 is very large. Another interpretation is given by the multi-storey structure of the cave: different velocities at the different heights along the vertical cliff induce vertical air-pressure gradients which induce air movements in the multi-storey cave system. But in order to affect in such a way c4, the flow rate must be high and the hydraulic resistance of the galleries leading to station 4 low, suggesting the existence of well developed lower galleries. There may be other explanations due to still unknown features of the Moestroff Cave.

In figure 3.6.15 the influence of external temperature is documented, it shows that for moderate wind activities it is the outside-inside temperature differences, or the differences in air densities, which most influence radon concentrations as they induce or not air movements in the cave.

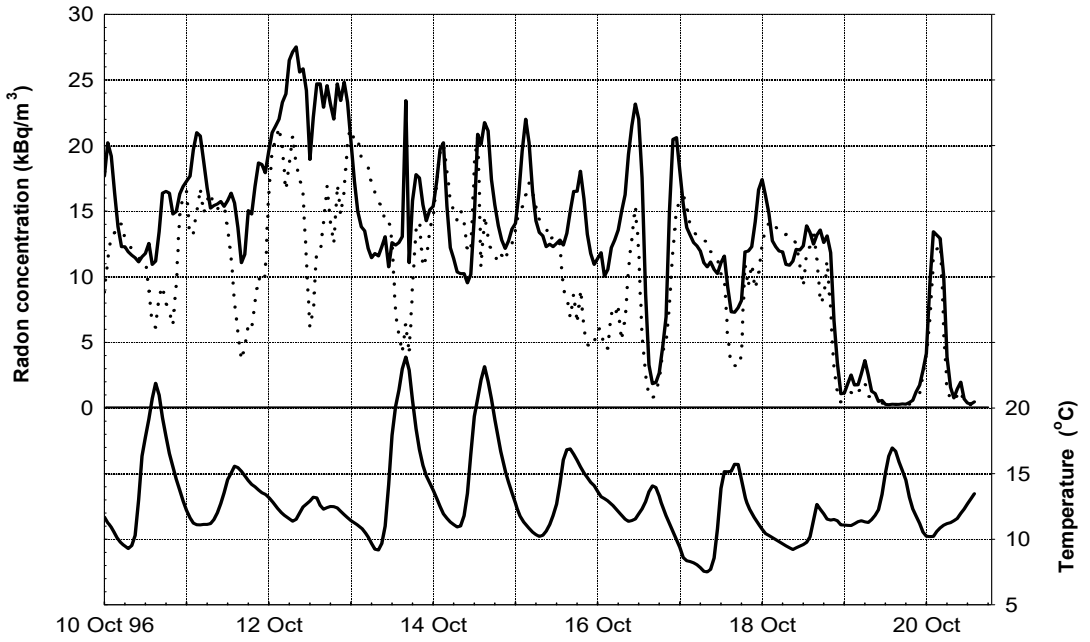

Fig 3.6.15*. Plot of the exterior temperature and the radon levels measured at the two most remote stations 3 and 4.*

The long-term study (fig. 3.6.3) showed mean radon levels at station 3 intermediate between those at station 2 and 4, except in late autumn where mean c3 is very close to or even higher than mean c4. The continuous monitoring confirmed and explained this observation. During the daily changing temperature pattern, when outside temperature was more than 5 degrees above cave temperature, c3 had intermediate values; this changed whenever outside temperature approached the cave temperature. At night below 12°C, c3 was often higher than c4 as shown by the plot of c4-c3 against outside temperature in fig. 3.6.16. In the night from 13th to 14th of October, the temperature low was paired with nil wind activity, for this period even radon levels near the entrance were higher than those at station 4.

At night, air temperature at the base of the cliff is normally lower than near the entrance, leading to an inflow into the lower storeys and an outflow through the main gallery. This explains the maxima in the radon signal at temperatures higher than the cave temperature: Radon rich air accumulated in the lower fracture system is carried from below upwards to station 3 and 2, and these rather low air movements do not affect station 4. When the outside temperatures are decreasing significantly, they induce higher ventilation rates which change the above mentioned situation.

During the 12th of October outside temperature was low; station 4 and the interior of the cave were nearly isolated from outside influences. The constant high radon levels measured suggest a steady state radon concentration of 24 kBq/m3 in the deeper parts of the cave in the absence of

outside influences. The high radon concentrations at station 4 were abruptly depressed to half of their value when outside temperature declined in such a way that air exchange increased and fresh air reached station 4. It is interesting to notice that c3 and c2 are less affected by this temperature decline. The increased flow rate moves air with a lower radon percentage from deeper locations to the entrance, temporarily c4 is more affected by this diluting effect than c3 and even c2.

During the first half of the period, atmospheric pressure decreased regularly and increased to the end of the period, No influence on radon concentration of these changing atmospheric pressures could be detected.

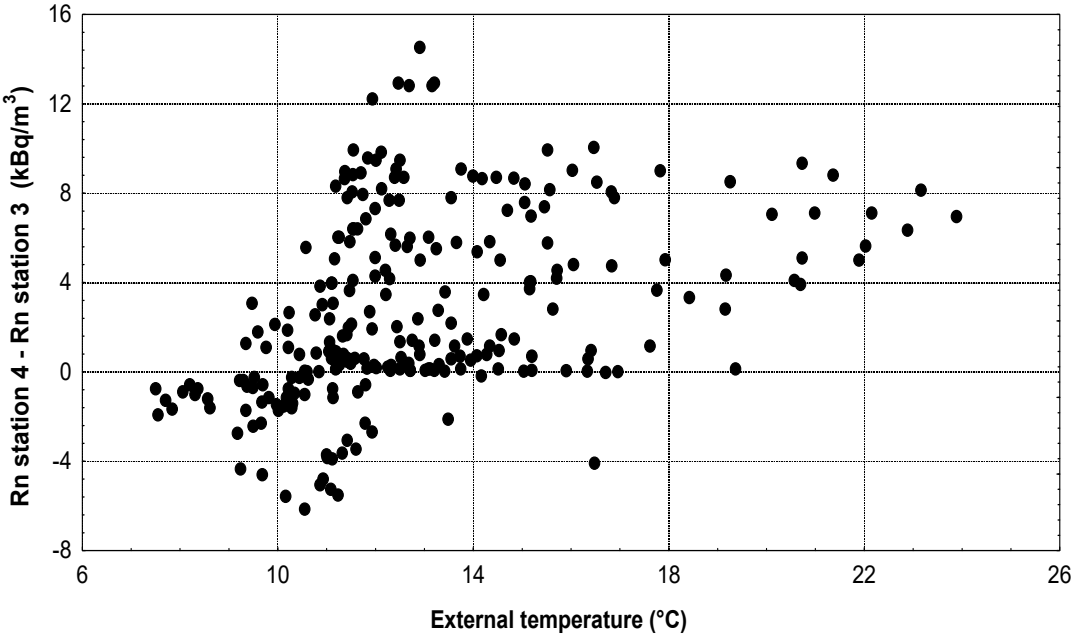

***Fig. 3.6.16**. The difference of radon concentrations measured at station 4 and station 3 is plotted against outside temperature.*

3.6.3. Conclusion

The study of the spatial and temporal distribution of radon concentration in mine or cave environments is of interest not only for health purposes, but radon is a suitable natural tracer gas to study subsurface transport processes. This tracer role of radon is well documented in the present Moestroff study. From all measured parameters, radon concentrations experienced the highest variations and reacted significantly to small outside influences. Outside-inside temperature differences, creating air movements in the cave, showed to be the dominant factor influencing radon.

References

ATKINSON, T.C., SMART PL. & WIGLEY T.M.L. - Climate and Natural Levels in Castleguard Cave, Columbia Icefields, Alberta, Canada, Artic and Alpine Research, Vol.15, No. 4, pp. 487-502, 1983.

BATES, R.C. & EDWARDS, J.C. - Mathematical Modelling of Time Dependent Radon Flux Problems; Second International Mine Ventilation congress, 412-419, New York; 1980.

CLEMENTS, W.E. & WILKENING, M.H. - Atmospheric Pressure Effects on 222Rn Transport Across the Earth-Air Interface, Journal of Geophysical Research 79, 5025-5029, 1974.

CURIE, P., BOUCHARD, Ch. & BALTAZARD, V. - Action Physiologique de l'Emanation du Radium, Comptes Rendus de l'Académie des Sciences, t. CXXXVIII, p. 1385, Paris, 1904.

GEORGE, A.C. - State-of-the-art Instruments for Measuring Radon/Thoron and their Progeny in Dwellings - a Review.Health Physics, Vol. 70, no.4, p.451-463, 1966.

HAKL, J., HUNYADI, I. & VÁRHEGYI, A. - Monitoring in Caves in Radon Measurements by Etched Track Detectors, Llíc R. and Durrani S. A. editors, Applications in Earth Sciences, Word Scientific, in press, 1996.

HINGMANN, H. & ALLINGER, Th. - Messungen der Radonkonzentration in hessischen Bergwerken, 9. Radonstatusgespräch, Berlin, 15/16. Oktober, 1996.

HUNYADI, I., HAKL, J. et al. - Regular Subsurface Radon Measurements in Hungrian Karstic Regions, Nucl. Tracks Radiat. Meas., Vol. 19, 321-326, 1991.

HYLAND, R. & GUNN, J. - Natural Radon Concentrations in the Wild Caves of England and Wales: Implications for Cave Users. Report commissioned by the Health and Safety Executive, Limestone research Group, Hudderfield University, Queensgate, GB, 1993.

IVANOVICH, M. & HARMON, S. - Uranium-Series Disequilibrium, Oxford Science Publications, Clarendon Press, Oxford, 909 pgs, 1992.

KEMSKI, J., KLINGEL, R. & SIEHL, A. - Das geogene Radonpotential in Umwelt-radioaktivität. Agemar Siehl (Herausgeber), Ernst & Sohn, Germany, 1996.

KIES, A. & MASSEN, F. - Radon and Underground Climate in Moestroff Cave; presented at the 2nd CIGG, July 1993, Besançon (France).In: DUBOIS C. (editor): Gas Geochemistry. Science Reviews, p.63-70, 1995

KIES, A., MASSEN, F. & FEIDER, M. - Measuring Radon in Underground Locations, Third International Conference, Rare Gas Geochemistry, Guru Nanak Dev Univ., Amritsar, India, Dec. 10-14, 1995.

MASSEN, F., KIES, A. & SCHINTGEN, G. - Problems and Results of Long-time Climatological Measurements in a Confined Maze Cave (Moestroff Cave, Luxembourg).

Paper presented at the International Symposium on Show Caves and Environmental Monitoring, Fabrosa-Soprana, Italy, 24-26 March 1995. Preprint ed. CIGNA, A.

MEDICI, F. & RYBACH, L. - Radon und Geologie/Wasser, Radonprogramm Schweitz, Bericht ueber die Ergebnisse der Jahre 1987 bis 1992, Bundesamt f. Gesundheitswesen, Bern, 1992.

MUTH, A. - Einsatz von Passivdosimetern zur Bestimmung der Radon- und Radonfolgeproduktkonzentration in verschiedenen Bergwerken, Diplomarbeit, Fachhochschule Giessen (Germany), Ref. H. Hingmann, 1995.

NAZAROFF, W. W. - Radon Transport from Soil to Air, Reviews of Geophysics 30, 137-160, 1992.

NAZAROFF, W. W., MOED, B. A. & SEXTRO, R. G. - in: Radon and its Decay Products in Indoor Air, John Wiley & Sons, p. 57-112, 1988.

NERO, A. V. - in: Radon and its Decay Products in Indoor Air, John Wiley & Sons, p. 1-55, 1988.

SCHERY, S.D., GAEDDERT, D.H. & WILKENING, M.H. - Transport of Radon From Fractured Rock, Journal of Geophysical Research 87, 2969-2976, 1982.

SURBECK, H. - Radon as a Tool in Hydrogeology; Obstacles and Prospects, Third International Conference, Rare Gas Geochemistry, Guru Nanak Dev Univ., Amritsar, India, Dec. 10-14 1995, to be published, 1995.

TANNER, A. B. - Radon Migration in the Ground: A supplementary review, in Gesell T. F. and Lowder W.M., eds., Natural radiation environment III: Springfield, Va., National Information Service, U.S. Department of energy report CONF-780422, v.1 p. 5-56, 1980.

TANNER, A. B. - Geological Factors that Influence Radon Availability, in Indoor radon, APCA International Speciality conference, Philadelphia, Pa. Feb. 1986, Proceedings: Pittsburgh, Pa., Air Pollution Control Association Special Publication SP-54, p. 1-12, 1986.

Part 4

Appendices

A : Publications & Symposia

B : Scientific Equipment

C : References

D : List of Figures

E. Addresses, Photographers

Appendix A - Symposia and Publications

From 1991 to the end of 1996, Phymoes members organized or attended the following meetings, and presented or published the papers quted hereafter:

25-26 August 1992:

Colloque International de Karstologie (CIK), International Symposium on Karstology, Diekirch and Luxembourg

Symposium organised by Phymoes and the Geological Service of Luxembourg.Two Field Guide books published.

Paper presented at the symposium: "First Results from Climatic Measurements in the Moestroff Cave". (Authors: F.Massen, C.Boes, C.Ek, S.Faber, P. Kayser, A.Kies, G.Schintgen, G. Waringo).

Proceedings published in 1995: "Comptes Rendus du Colloque International de Karstologie à Luxembourg", vol. XXVII des Publications du Service Géologique du Luxembourg. (Editors: R. Maquil, F.Massen).

5-10 July 1993

2nd CIGG, Deuxième Colloque International sur la Géochimie des Gaz,

2nd International Colloquium on Gas Geochemistry

Université de Franche-Comté, Besançon, France

A. Kies and F.Massen attended this meeting and presented the paper "Radon and Underground Climate in the Moestroff Cave" (Authors: A. Kies, F. Massen). The proceedings of this meeting, published in 1995 by Science Reviews, Northwood (Editor: C. Dubois), include the Phymoes paper.

21 avril 1994

Conference presented by F. Massen at the Centre Universitaire de Luxembourg: "Le climat souterrain de la grotte de Moestroff"

24-26 March 1995

International Symposium on Show Caves and Environmental Monitoring, Fabrosa Soprana, Italy.

G. Schintgen and F. Massen attended this meeting, and presented the paper "Problems and Results of long-time Climatological Measurements in a Confined Maze Cave (Moestroff Cave, Luxembourg)" (Authors: F. Massen, A. Kies, G. Schintgen). This paper has been published in the “Proceedings of the International Symposium Show Caves and Environmental Monitoring” (Editor A.A. Cigna), Fabrosa Soprana (Cuneo, Italy), 1966.

22 May 1995

DADiSP meeting, London.

Meeting of selected European dealers of the DSP Development Corporation, Cambridge, MA, USA. F. Massen presents, as an invited key-note speaker, an expose on the usage of the DADiSP software in the Phymoes project.

10-14 December 1995

3rd ICRIGG

3rd International Colloquium on Rare Gas Geochemistry, Guru Nanak Dev University, Amritsar, India.

A. Kies attends to this symposium and presents the paper "Measuring Radon in Underground Locations" (Authors: A.Kies, F.Massen, M. Feider)

20 October 1996

11te Internationale Schulungs- und Diskussionswoche des Verbandes der deutschen Höhlen- und Karstforscher e.V. und des Verbandes der Oesterreichischen Höhlenforscher, Bollendorf, Germany.

Phymoes organizes the first day of this meeting; five exposés are given:

Die Geologie der Höhle von Moestroff (S. Faber)

Die Erforschung der Höhle durch den Luxemburger Höhlenverein (E. Sinner)

Das Forschungsprojekt Phymoes (F. Massen)

Die Problematik der Langzeit-Messungen in unterirdischen Feuchträumen (G. Schintgen)

Temperatur, Feuchte, Luftströmung, CO_2 und Radon (F. Massen; coauthor A. Kies)

In the afternoon a guided tour through selected parts of the Moestroff Cave was made.

Appendix B

List of Scientific Equipment and Manufacturers

TYPE	MODEL	SPECIFICATIONS	MANUFACTURER
Datalogger	Mikromec	- 8 channels, 14 bit A/D - inputs: voltage (mV to 10V) current (0-20mA) frequency - fully programmable - 64k RAM - 12VDC lead acid battery - water resistant case IP65	TECHNETICS Langemarckstr. 112 D-7800 Freiburg i. Br. Fax: (49) 761 40 80 18
	Hamster	- special purpose logger with built-in temperature sensor - no external sensors - completely sealed case - 5 year autonomy (lithium cell)	Ph. SCHENK Gmbh & Co.Kg Jedleseerstr. 59 A-1210 WIEN Fax: (43) 222 38 12 28 12
Temperature & relative humidity	YA-100CT	- sensor driven by logger Mikromec - resolution 0.1°Celsius, 1% rel. hum. (range 0-100%) - power: 12VDC - power consumption ca. 10mA - signal : 0-1 V	ROTRONIC Messgeräte Gmbh Postf. 63 01 08 D-6000 Frankfurt-Main Fax: (49) 069 42 51 18
Dewpoint (rel. humidity)	Taupunktsensor 620	- dewpoint and ambiant air tempe-rature measured by NTC sensors - resolution better than 0.1° Celsius - power 12 VDC - power consumption: 80 mA - signal: depends on reference voltage	KRONEIS Iglaseegasse 30-32 A-1191 WIEN Fax:(43) 222 32 66 04
Air pressure	SCX15AN	- sensor driven by logger Mikromec - 0-1200mbar - resolution 1 mbar - power: 12V - signal : resistance (bridge)	SENSORTECHNICS Gmbh Aubinger Weg 27 D-8039 PUCHHEIM Fax:(49) 089 800 83 33

Air velocity	TA2-2	- hot wire anemometer - 0-2m/s - resolution 1 cm/s - battery driven (6V) - power consumption ca. 80 mA - signal : 0-2V	AIRFLOW Lufttechnik GmbH Postf. 1208 D-5308 RHEINBACH Fax: (49) 2226 72 72
CO2 concentration	Gascard 3000	- OEM board - NDIR with pump - Range 0-3000 ppm - resolution: only limited by logger - power 24VDC - power consumption: 250-300mA - output 4-20mA	EDINBURGH SENSORS Ltd Riccarton GB- EDINBURGH EH14 4AP Fax: (44) 31 449 5848
Differential air pressure	Setra 264	- high-precision differential pressure sensor : 0.01Pa precision: only limited by logger - 0 - 2.54mm Water Column - power: 12-24VDC - power consumption: 10mA - signal: 0-2.5 V	GEC Composants GEC France S.A 2 rue Henri Bergson F-92665 ASNIERES CEDEX Fax:(33) 1 47 33 11 31
RADON (activity)	Karlsruher Modell	- Makrofoil Nuclear Etched Track device - precision ca. 6% - passive device - measures true Radon concentration (non EEC)	
RADON (activity)	Alphaguard P30	- portable, battery driven (12 VDC) - no pump, ionisation chamber - built-in datalogger - built-in thermometer, hygrometer, barometer, relocation sensor - autonomy 10 days / 3000 data points - sampling interval 10 min. or 1 hour	GENITRON INSTRUMENTS GmbH Heerstr. 149 D-6000 FRANKFURT/M -90 Fax: (49) (0) 69 97 65 14 0
RADON (activity)	LUK 3	- portable Radon measurement system based on Lucas cells (air and soil gas)	SMM Ing. Jiri Plch S.K. Neumanna 2008 182 00 PRAHA 8
RADON (Working level)	Radon-Sniffer	- portable, battery driven (6-12VDC) - pump sucks air through filter - alpha count displayed on LCD - programmable working time - ca. 20% precision	THOMSON & NIELSEN ELECTRONICS LTD. 4019 Carling Ave KANATA Ontario K2K 2A3 Canada

WEATHER (exterior)	Weathermonitor II	- automatic working small weatherstation with datalogger - battery driven, 12VDC; 11mA - cup anemometer, wind direction, termperature, humidity, rainfall - sampling interval 1 hour - storage capacity = 2 month	ICS Electronics Ltd Unit V Rudford Industrial Estate Ford Arundel, West Sussex GB BN 18 0BD Fax (42) 0903 731 105

Appendix C - List of References

ANDRIEUX, C. - Sur la Mesure Précise des Charactéristiques Météoclimatiques Souterraines. Annales de Spéléologie, XX, fasc.3, p. 319-340. 1965.

ANDRIEUX, C. - Contribution à l'Etude du Climat des Cavités Naturelles des Massifs Karstiques. Chap. 5: Climatologie Souterraine, p.230-234. Annales de Spéléogie, tome 25, fasc.2, 1970.

ANDRIEUX, C. - Etude des Circulations d'Air dans la Grotte de Niaux. Conséquences. Karstologia no.1, 1er semestre 1983, p.19-24, 1983.

ATKINSON, T.C., SMART, P.L. & WIGLEY, T.M.L. - Climate and Natural Radon Levels in Castleguard Cave, Columbia Icefields, Alberta, Canada. In: Arctic and Alpine Research, vol.15, no.14, 1983, p.487-502, 1983.

AHORNER, L. - Present-day stress field and seismotectonic block movements along major fault zones in Central Europe, Tectonophysics 29, 233-249, 1975.

BADINO, G. - Fisica Del Clima Soterraneo, p.44. Memorie dell'Istituto Italiano di Speleologia. Vol. 7, Serie II. Bologna, 1995.

BATES R.C. & EDWARDS, J.C. - Mathematical Modelling of Time Dependent Radon Flux Problems; Second International Mine Ventilation congress, 412-419, New York; 1980.

BERG, D. - Die Klüfte im Paläozoikum und Mesozoikum von Luxemburg und der westlichen Eifel. Ihre Beziehungen zur allgemeinen Tektonik und ihr Einfluß auf das Gewässernetz, Service Géologique du Luxembourg publications, Vol. XVI, 1965.

CHOPPY, J. - La Température des Cavités. Spelunca, no.3, 1980. p.117-119. 1980.

CHOPPY, J. - Dynamique de l'Air. Phénomènes Karstiques, série 1.1.: Processus Climatiques. Spéléo Club de Paris, 1986.

CHOPPY, J. - Microclimats. Phénomènes Karstiques, Processus Climatiques, 4e partie, p.53-58. Spéléo-Club de Paris. 1990.

CIGNA, A. - An Analytical Study of Air Circulation in Caves. International Journal of Speleology, vol. III, p. 41-54. 1967.

CIGNA, A. - Air Temperature Distributions near the Entrance of Caves. Symposium Internazionale di Speleologia. In: Memoria della Rassegna Speleologica Italiana, Como 1961.

CLEMENTS, W.E. & WILKENING, M.H. - Atmospheric Pressure Effects on 222Rn Transport Across the Earth-Air Interface, Journal of Geophysical Research 79, 5025-5029, 1974.

COÛTEAUX, M. - Letter to J. Bintz dated 1. 3. 1965.

CRC Handbook of Chemistry and Physics - 67th edition. CRC Press, 1986-87.

CURIE, P., BOUCHARD, CH. & BALTAZARD, V. - Action Physiologique de l'Emanation du Radium, Comptes Rendus de l'Académie des Sciences, t. CXXXVIII, p. 1385, Paris, 1904.

DITTRICH, D. - Beckenanalyse der Oberen Trias der Trier-Luxemburger Bucht. Revision der stratigraphischen Gliederung und Rekonstruktion der Paläogeographie, Service Géologique du Luxembourg publications, Vol. XXVI, 1989.

DUBLYANSKI, V.N. & SOCKOVA, L.M. - Microclimate of Karts Cavities of the Mountain Crimea. Proceedings of the 7th Intern. Congress of Speleology, Sheffield. p.158-160, 1977.

EK, C. & GEWELT, M. - Carbon Dioxide in Cave Atmospheres. New Results in Belgium and Comparison with some other Countries. In: Earth Surface Processes and Landforms, vol. 10, p.173-187. 1985.

FRANCE-JOURNAL - 3. Expedition der luxemburgischen Höhlenforschergruppe. France-Journal, 7. 8. 1964.

FRANCE-JOURNAL - " Groupe Spéléologique Luxembourgeois " feierte fünfjähriges Bestehen. France-Journal, 19. 8. 1964.

GSL (Groupe Spéléologique Luxembourgeois) - Rapport du IIe camp spéléologique à Moestroff (22. -26. 7. 1961). La Vie Souterraine, 2, Luxembourg, Sept. 1961, p. 4-6.

GSL (Groupe Spéléologique Luxembourgeois) , - Rapport d'activités. La Vie Souterraine, 7, Luxembourg, Oct. 1963, p.12-14.

GSL (Groupe Spéléologique Luxembourgeois) - Rapport d'activités. La Vie Souterraine, 8, Luxembourg, Aug. 1964, p. 11-13

GSL (Groupe Spéléologique Luxembourgeois) - Rapport sur la IVe expédition d'été du GSL à Moestroff, du 8 au 22 juillet 1964. La Vie Souterraine, 9, Luxembourg, Sept. 1966, p. 27-35.

HAKL, J., HUNYADI, I. & VÁRHEGYI, A. - Monitoring in Caves in Radon Measurements by Etched Track Detectors, Llíc R. and Durrani S. A. editors, Applications in Earth Sciences, Word Scientific, in press, 1996.

HALBERT, E.J. & MICHIE, N. - The Climate above and below Ground. IN: Wombeyan Caves, Occasional Paper no. 8, p.137-154. Editors: Dyson, H.R., Ellis, R. Julia, J. Sydney Speleological Society. P., 1982.

HANDBOOK of Physical Constants - The Geological Society of America Memoir 97. 1966.

HEMMER, C. - Notizblock. Letzebuerger Land, 35, 28. 8. 1964.

HINGMANN H. & ALLINGER, TH. - Messungen der Radonkonzentration in hessischen Bergwerken, 9. Radonstatusgespräch, Berlin, 15/16. Oktober, 1996.

HÖLTING, B. - Hydrogeologie, Einführung in die Allgemeine und Angewandte Hydrogeologie, 4. Aufl. 1992, F. Enke Verlag, Stuttgart, ISBN 3-432-90794-X

HUNYADI, I., HAKL, J. et al. - Regular Subsurface Radon Measurements in Hungrian Karstic Regions, Nucl. Tracks Radiat. Meas., Vol. 19, 321-326, 1991.

HÜTTER, L. A., - Wasser und Wasseruntersuchung, 6. Aufl. 1994, Salle & Sauerländer, Frankfurt am Main ISBN 3-7935-5075-3 (Salle), ISBN 3-7941-3270-X (Sauerländer)

HYLAND, R. & GUNN, J. - Natural Radon Concentrations in the Wild Caves of England and Wales: Implications for Cave Users. Report commissioned by the Health and Safety Executive, Limestone research Group, Hudderfield University, Queensgate, GB, 1993.

IVANOVICH, M. & HARMON, S. - Uranium-Series Disequilibrium, Oxford Science Publications, Clarendon Press, Oxford, 909 pgs, 1992.

JAMES, J. - Carbon Dioxide in Cave Atmosphere. Trans. British Cave Ass. Vol 4, No. 4, p.417-429. 1977.

JAMES J., PAVEY, ROGERS - Foul Air and the Resulting Hazard to Cavers. 1975.

JAMES, J. & DYSON, J. - CO_2 in Caves. Caving International Magazine, no. 13, October 1981.

KIES, A. & MASSEN, F. - Radon and Underground Climate in Moestroff Cave; presented at the 2nd CIGG, July 1993, Besançon (France).In: DUBOIS, C. (ed.): Gas Geochemistry. Science Reviews, p.63-70, 1995

KIES, A., MASSEN, F. & FEIDER, M. - Measuring Radon in Underground Locations, Third International Conference, Rare Gas Geochemistry, Guru Nanak Dev Univ., Amritsar, India, Dec. 10-14, 1995.

KRIEPS, R. - Die Höhlenforscher von Moestroff. Letzebuerger Land, 34, 21. 8. 1964

KRONEIS, W. - Erläuterungen zur Berechnung der Feuchtigkeitsgrössen und zur Anwendung der Tafeln. (instruction notices for the Kroneis NTC dewpoint sensor). 1991.

LEBRUN, J. & TERCAFS, R. - Etude de la Convection Naturelle dans une Cavité Cylindrique Horizontale soumise à une Onde de Température Longitudinale. Collection des Publications de la Faculté des Sciences de l'Université de Liège. No.34. p. 1-49, 1972.

LIU, H.S. - Satellite-determined stresses in the crust of Europe, in Seismic activity in Western Europe, P. Melchior (ed.), NATO ASI Series C, Vol. 144, 1985.

LUXEMBURGER WORT - Höhlenforschung in Moestroff. Luxemburger Wort, 14. 8. 1964

MASSEN F., KIES A. & SCHINTGEN G. - Problems and Results of Long-time Climatological Measurements in a Confined Maze Cave (Moestroff Cave, Luxembourg). In Cigna, A.(ed.): Proceedings of the International Symposium Show Caves and Environmental Monitoring, Fabrosa-Soprana (Cuneo, Italy), 24-26 March 1995. Stazione Scientifica di Bossea, 1996.

MAQUIL, R. & MASSEN, F. (eds.) - Comptes Rendus du Colloque International de Karstologie ä Luxembourg 25-26 Août 1992. Publications du Service Géologique du Luxembourg, Vol. XXVII, 1994.

MAQUIL, R., EK, C. & FABER, A. - Le Muschelkalk Supérieur: Stratigraphie et Hydrogéologie de la région de Diekirch-Moestroff, in Comptes Rendus du Colloque International de Karstologie à Luxembourg, R. Maquil and F. Massen (eds.), Publications du Service Géologique du Luxembourg, Vol. XXVII, 29-43, 1994.

MEDICI F. & RYBACH L. - Radon und Geologie/Wasser, Radonprogramm Schweitz, Bericht ueber die Ergebnisse der Jahre 1987 bis 1992, Bundesamt f. Gesundheitswesen, Bern, 1992.

MEY, T. - Junge Speläologen und Geschichtsforscher " op Kâpendall" und auf dem Uresbierg". Letzebuerger Journal, 169, Luxemburg, 26. Juli 1962, p.4.

MOORE, G.W. & SULLIVAN, N.G.- - Speleology, 2nd edition. Zephyrus Press Inc. Teaneck., 1978.

MÜLLER, B., ZOBACK, M.L., FUCHS, K., MASTIN, L., GREGERSEN, S., PAVONI, N., STEPHANSSON, O. and LJUNGGREN, Ch. - Regional pattern of tectonic stress in Europe, SFB 108 Berichtsband 1990-1992, 725-767, Universität Karlsruhe, 1992.

MUTH, A. - Einsatz von Passivdosimetern zur Bestimmung der Radon- und Radonfolgeproduktkonzentration in verschiedenen Bergwerken, Diplomarbeit, Fachhochschule Giessen (Germany), Ref. H. Hingmann, 1995.

NAZAROFF, W. W. - Radon Transport from Soil to Air, Reviews of Geophysics 30, 137-160, 1992.

NAZAROFF, W. W., MOED, B. A. & SEXTRO, R. G. - in: Radon and its Decay Products in Indoor Air, John Wiley & Sons, p. 57-112, 1988.

NERO, A. V. - in: Radon and its Decay Products in Indoor Air, John Wiley & Sons, p. 1-55, 1988.

NETZ, H. - Formeln der Technik. Hanser Verlag München, Wien, 1983.

NEUMANN-REDLIN, Ch. - Hydrogeologische und hydrochemische Untersuchungen im Oberen Muschelkalk und Keuper Luxemburgs, Service Géologique duLuxembourg publications, Vol. XXII, 1971.

NILLES, L.N. & KRIER, T. - Villa Rustica " op dem Haischen ". Revue Letzebuerger Illustre'ert, 32, Luxembourg 11. Aug. 1962, p. 10-18.

NILLES, L.N. & KRIER, T. - Höhlenforschung op Kâpendall. Revue Letzebuerger Illustre'ert, 33, Luxembourg 18. Aug. 1962, p. 28-29.

PARKER, S.P., editor - Fluid Mechanics Source Book. McGraw-Hill Book Co., 1988.

POLLI, S. - La Grotta Gigante del Carso di Trieste quale Cavita Barometrica. Atti VI Congr. Naz. di Speleologia, Trieste 1954. Le Grotte d'Italia (3a) I, p.1955-1956, 1956.

RECKNAGEL, Sprenger, Hönmann - Taschenbuch für Heizung und Klimatechnik 92/93, p. 104. OldenbourgVerlag. 1992.

RÉPUBLICAIN LORRAIN - La plus grande caverne du Grand-Duché livre ses secrets. Le Républicain Lorrain, Luxembourg, 27 Juillet 1962.

RÉPUBLICAIN LORRAIN - 3e expédition du groupe spéléologique qui poursuivra l'exploration de la caverne. Républicain Lorrain, 6. 8. 1964.

RÉPUBLICAIN LORRAIN - 3e expédition à la caverne de Moestroff: les spéléologues veulent porter la longueur du couloir exploré à 4000 mètres. Républicain Lorrain, 13. 8. 1964.

RÉPUBLICAIN LORRAIN - Joyeux anniversaire pour les spéléologues qui fêtaient la cinquième année d'existence de leur groupe. Républicain Lorrain, 18. 8. 1964.

RENAULT, Ph. - Le CO_2 dans l'atmosphère de quelques cavernes du Quercy. Spéléo-dordogne, no.75, p. 1-116, 1980.

SCHERY, S.D., GAEDDERT, D.H. & WILKENING, M.H. - Transport of Radon From Fractured Rock, Journal of Geophysical Research 87, 2969-2976, 1982. India, Dec. 10-14 1995, to be published, 1995.

SCHINTGEN, G. & SINNER, E. -Rapport sur le IIIe camp d'été du GSL à Moestroff du 20 au 31 juillet 1962 (1ère partie). La Vie Souterraine, 6, Luxembourg, Fév. 1963, p. 8-13.

SCHINTGEN, G. & SINNER, E. -Rapport sur le IIIe camp d'été du GSL à Moestroff du 20 au 31 juillet 1962 (2e partie). La Vie Souterraine, 7, Luxembourg, Oct. 1963, p 4-8.

SCHNEIDER, P. - Scout (Bulletin de la FNEL), 1957.

SCHROEDER, D.; BLUM, W.E.H., - Bodenkunde in Stichworten, 5. rev. Aufl. 1992 , Ferdinand HIRT Reihe. ISBN 3-443-03103-X Gebrüder Borntraeger, Berlin 1992

SURBECK, H. - Radon as a Tool in Hydrogeology; Obstacles and Prospects, Third International Conference, Rare Gas Geochemistry, Guru Nanak Dev Univ., Amritsar,

TANNER, A. B. - Radon Migration in the Ground: A supplementary review, in Gesell T. F. and Lowder W.M., eds., Natural radiation environment III: Springfield, Va., National Information Service, U.S. Department of energy report CONF-780422, v.1 p. 5-56, 1980.

TANNER, A. B. - Geological Factors that Influence Radon Availability, in Indoor radon, APCA International Speciality conference, Philadelphia, Pa. Feb. 1986, Proceedings: Pittsburgh, Pa., Air Pollution Control Association Special Publication SP-54, p. 1-12, 1986.

VILLAR, E., FERNANDEZ, P.L., QUINDOS, L.S. & SOTO, J. - Natural temporal evolutions of CO_2 contents in the air of the "Paintings Chamber" at Altamira Cave. NSS Bulletin, October 1985, p. 12-16. 1985.

VOIGT, H.J., - Hydrogeochemie, Eine Einführung in die Beschaffenheit des Grundwassers, VEB 1990, Leipzig.ISBN 3-540-51805-3 Springer-Verlag Berlin, ISBN 0-387-51805-3 Springer-Verlag, New York

WIGLEY, T.M.L. -Non-Steady Flow through a Porous Medium and Cave Breathing. Journal of Geophysical Research. Vol.72, no.12, June 15, 1967. p.3199-3205, 1967.

WIGLEY, T.M.L.; BROWN, M:C. - The Physics of Caves. In: Ford & Cullingford: The Science of Speleology, p.329-358. Academic Press. 1976.

ZEYEN, C. - La découverte du réseau Adrienne. La Vie Souterraine, 9, Luxembourg, Sept. 1966, p. 6-7.

Appendix D - Email Addresses, Fax Numbers and Authors of the Photographs

Email Addresses and/or Fax Numbers:

BOES Claude	claude.boes@goodyear.e-mail.com
EK Camille	Fax: (+32) (0)4 366 57 22
FABER Sonja	Fax: (+352) 78 88 97
KIES Antoine	kies@cu.lu
MASSEN Francis	francis.massen@ci.educ.lu
SCHINTGEN Guy	guyschin@pt.lu
SINNER Ed	Fax: (+352) 83 50 15
WARINGO Guy	guy.waringo@ci.educ.lu

The photographs were taken by:

Sonja Faber:	D
Jerôme Kohnen	C, F
Antoine KiesL	
Francis Massen	E, G, H, I, N (upper right)
Guy Schintgen	B, J, K, M
Rose Strahm	N (group photo)
Kayser Pit	N (upper left)

B Plateau "Auf dem Knaupert" covering the Moestroff Cave.

C Ladder leading to the cave; entrance is to the right of the person on top.

D Cliff with main entrance and secondary openings of the lower storey.

E Typical key-hole cross-section of main gallery near 1st Relay.

F Usual gallery profile, with silt layer covering the floor.

G Heavy drilling work for installation of the access ladder.

H Welding the entrance door

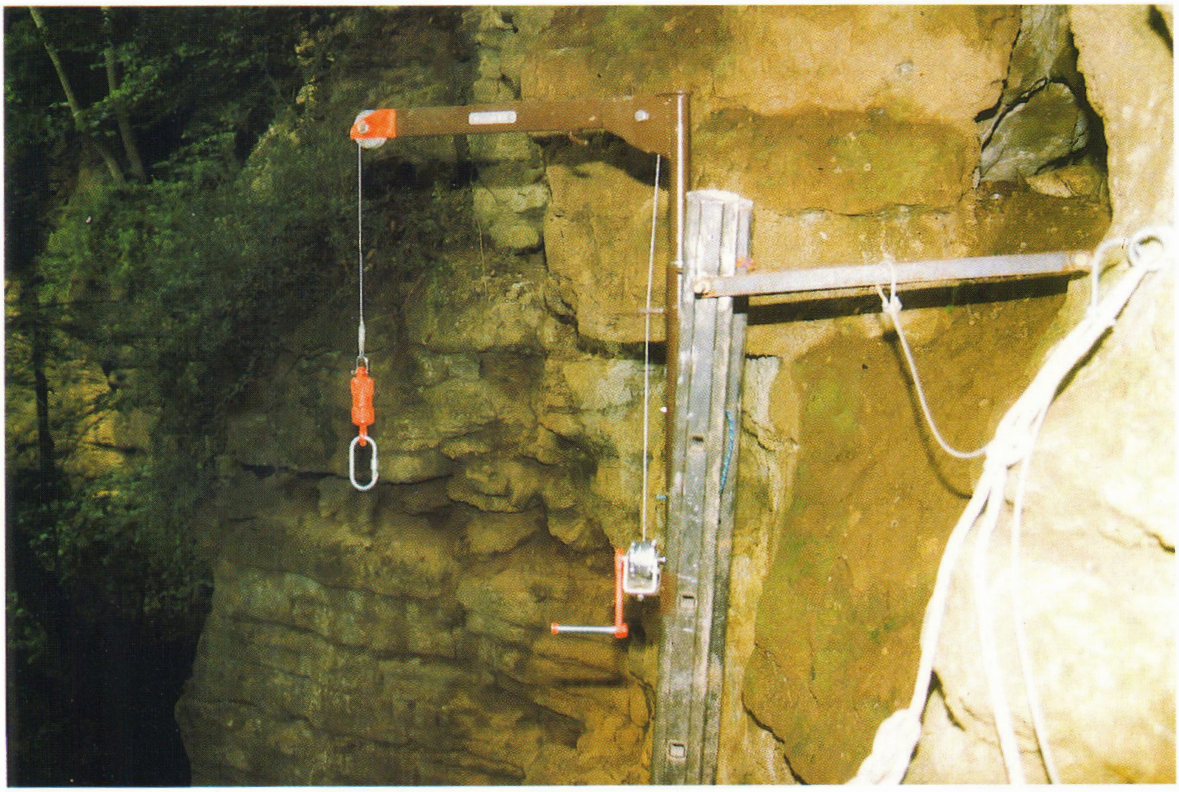

I The portable hoist mounted on top of the access ladder

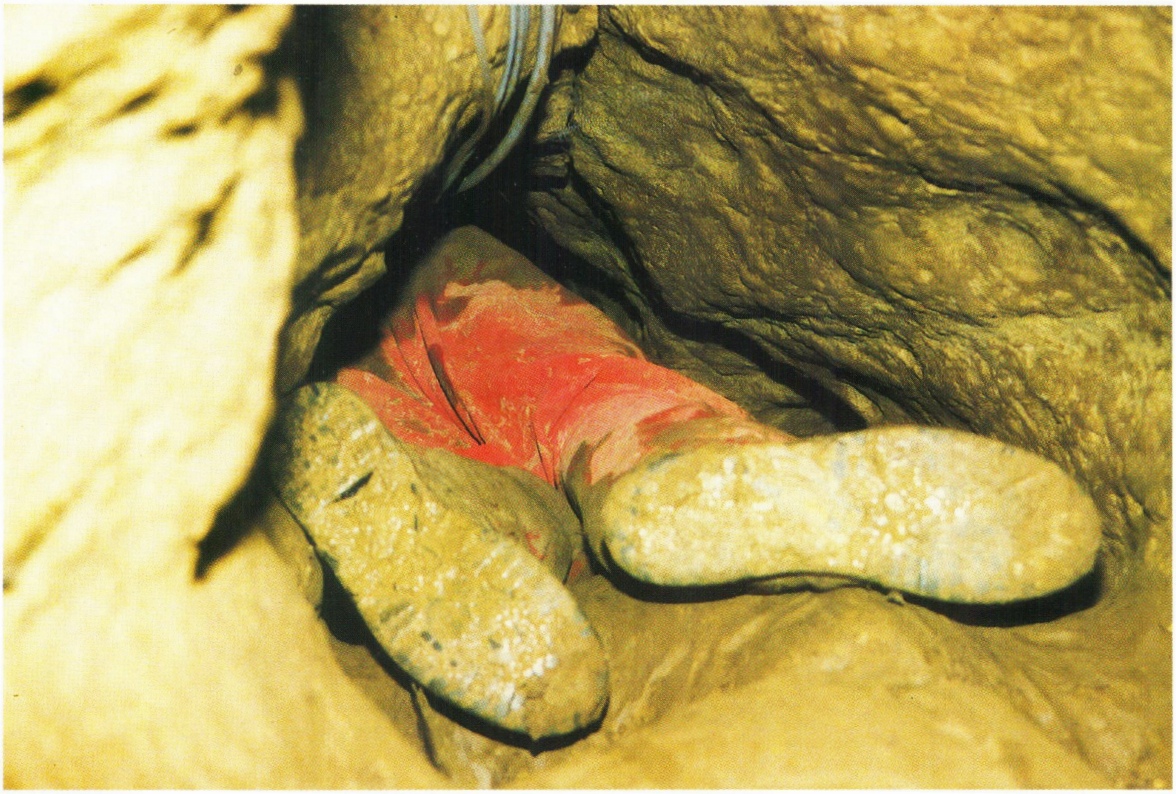

J Access to the most remote Station 4 means strenuous crawling.

K Downloading th temperature data from the stand-alone Hamster logger.

L Miscellaneous instrments at Station 4. From left to right: Dew Point Sensor, Alphaguard, Dosimeter & WL-Meter (Rn), Barometer and Temp. Logger

M Most maintenance work must be performed in lying position

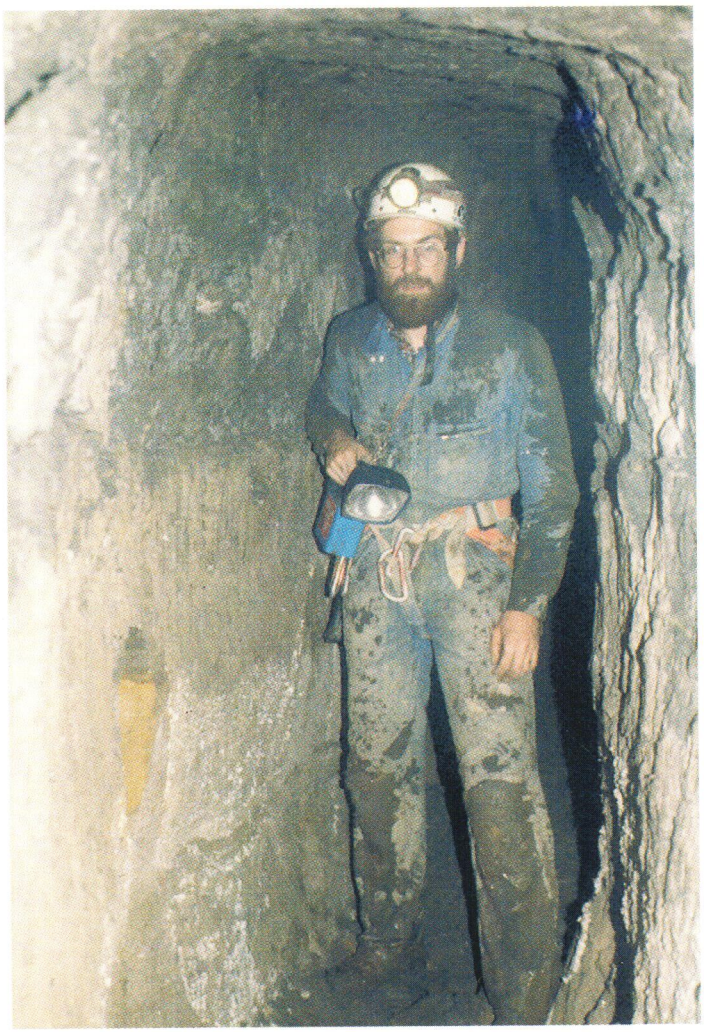

N The Phymoes team. Top left: Guy Waringo. Top right: Camille Ek (in yellow dress).
Bottom, second row: Ed Sinner, Guy Schintgen, Antoine Kies.
First row: Claude Boes, Pit Kayser, Francis Massen, Sonja Faber.

Map of the Moestroff Cave with orientation diagram of galleries (GSL 1961- 64)

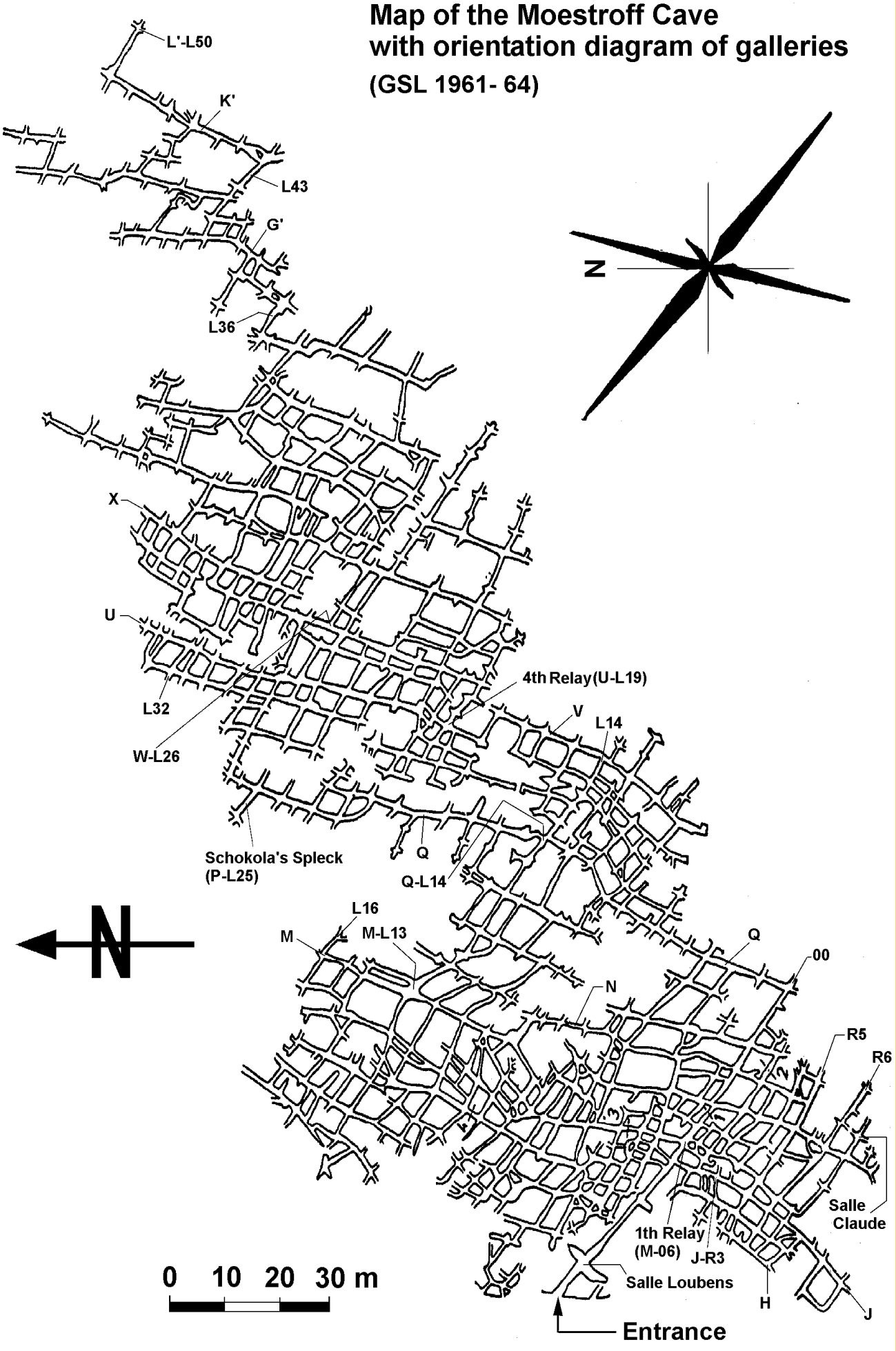

The Moestroff Cave: Errata

page 113 [eq. 3.4.9] should be: 22 october 1997

$$: \frac{1}{\sqrt{f}} = -2\log\left[\frac{\frac{\varepsilon}{D}}{3.71}\right] \qquad \textit{[eq. 3.4.9]}$$

(minus sign was missing).

This gives **ε=0.48 m**, still an impossible high value.

Thanks to Prof. Baudouin Lismonde for reporting this error!


PHOENIX
CONTACT


Worldwide
Information
Systems
Bull